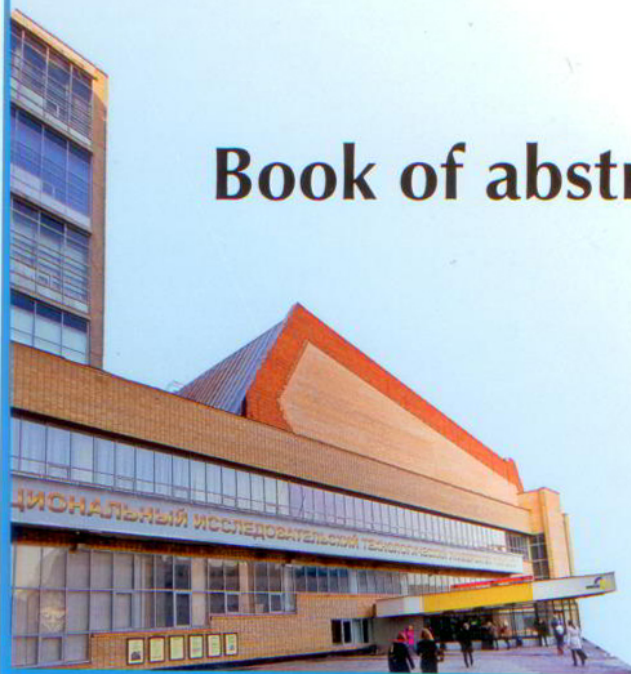


National University of Science and Technology MISiS  
Institute of Solid State Physics of the Russian Academy of Sciences  
Russian Federal Agency of Scientific Organisations  
Scientific Council on Physics  
of Condensed Matter of the Russian Academy of Sciences

XV INTERNATIONAL  
CONFERENCE ON  
INTEGRANULAR AND  
INTERPHASE BOUNDARIES  
IN MATERIALS  
NUST «MIS&S»

May 23-27, 2016, Moscow, Russia

**Book of abstracts**



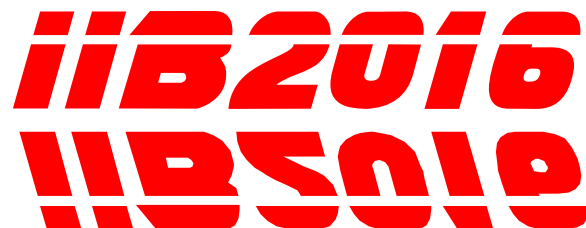
National University of Science and Technology MISiS  
Institute of Solid State Physics of the Russian Academy of Sciences  
Russian Federal Agency of Scientific Organisations  
Scientific Council on Physics of Condensed Matter of the Russian Academy of  
Sciences

**XV INTERNATIONAL  
CONFERENCE ON  
INTEGRANULAR AND  
INTERPHASE BOUNDARIES  
IN MATERIALS**

**NUST «MIS&S»  
May 23-27, 2016, Moscow, Russia**

**Book of abstracts**

Moscow, 2016





## XV INTERNATIONAL CONFERENCE ON INTEGRANULAR AND INTERPHASE BOUNDARIES IN MATERIALS (iib-2016)

*iib-2016* follows 14 conferences in this series, held in Chalkidiki, Greece (2013); Mie, Japan (2010); Barcelona, Spain (2007); Belfast, Northern Ireland, UK (2004); Haifa, Israel (2001); Praha, Czech Republic (1998); Lisboa, Portugal (1995); Thessaloniki, Greece (1992); Paris, France (1989).

The current name of *iib*-conferences was established in 1989 in Paris. Before 1989 the following “ancestor” conferences took place:

- “Grain boundary structure and related phenomena” Lake Placid, USA (1987)
- “Grain boundary structure and related phenomena” JIMIS-4, Minakami, Japan (1985)
- “International conference on the structure and properties of internal interfaces”, Irsee, West Germany (1984)
- “Computer simulation in the study of solid-solid interfaces”, Philadelphia, PA, USA (1983)
- 1<sup>st</sup> All-union conference "Structure and properties of grain boundaries", Ufa, USSR (1983)
- "Structure and properties of grain boundaries", Caen, France (1982)
- 2<sup>nd</sup> All-Union seminar "Structure and properties of grain boundaries", Chernogolovka, USSR (1982)
- “Grain boundary structure and kinetics”, ASM Materials Science Seminar, Milwaukee, WI, USA (1979)
- 1<sup>st</sup> All-Union seminar "Structure and properties of grain boundaries", Chernogolovka, USSR (1979)
- “Grain boundaries and interfaces”, Yorktown Heights, New Yor, USA (1971)
- “Properties of grain boundaries” (4e Colloque de Métallurgie), Saclay, France, 1960

The *iib* Conferences which are held every three years, represent a unique international forum bringing together the specialists working in different areas of Interface Science. Researchers that otherwise are mainly focused on their scientific domain have a unique opportunity to exchange their views and ideas with colleagues investigating the different aspects of interfacial behaviour; *iib* Conferences strongly promote an interdisciplinary approach in interface science.

**The abstracts in this book are divided in three chapters: invited, oral and posters.  
They follow in the alphabetic order of presenting authors.**

### **Chairperson**

- Boris Straumal; NUST MISiS & Institute of Solid State Physics of Russian Academy of Sciences, Russia

### **Honorary co-chairmen**

- Prof. Lasar S. Shvindlerman,  
Institut für Metallkunde und Metallphysik RWTH Aachen
- Prof. Boris S. Bokstein,  
NUST MISiS

### **International scientific committee (alphabetically)**

- Paul Bristowe, Univ. of Cambridge, UK
- Barry C. Carter, Univ. of Connecticut, USA
- Michael W. Finnis Imperial College, UK
- Olivier Hardouin Duparc, Ecole Polytechnique, France
  - James M. Howe, Univ. of Virginia, USA
- Yuichi Ikuhara , Univ. of Tokyo / JFCC/ Tohoku Univ. WPI, Japan
  - Suk-Joong L. Kang , AIST, Korea
  - Wayne D. Kaplan, Technion Univ., Israel
  - Alexander H. King, Purdue University, USA
    - Masanori Kohyama , AIST, Japan
    - Philomela Komninou, AUTH, Greece
- Sylvie Lartigue-Korinek, Institut de Chimie et des Materiaux, Paris Est, France
  - Douglas L. Medlin, Sandia Nat. Lab., USA
  - Dmitri A. Molodov, Aachen Univ., Germany
  - Vaclav Paidar, Academy of Sci., Czech Republic
  - Stephen J. Pennycook, Oak Ridge Nat. Lab., USA
    - Robert Pond, Univ. of Exeter, UK
    - Eugen Rabkin, Technion Univ., Israel
      - Manfred Rühle, MPI, Germany
    - David Seidman, Northwestern Univ., USA
    - Anna Serra, Technical Univ.of Catalonia, Spain
      - Lazar S. Shvindlerman, ISSP, Russia
      - David J. Srolovitz, IHPC, Singapore
      - Boris B. Straumal, ISSP, Russia
  - Antoni Tomsia, Lawrence Berkeley Nat. Lab., USA
    - Wenzheng Zhang, Tsinghua University, China

## Invited talks

## Recent advances in experimental investigations of grain boundary diffusion

S.V. Divinski

Institute of Materials Physics, University of Münster, Wilhelm-Klemm-Str. 10, 49149 Münster, Germany

An overview of recent advances in grain boundary diffusion and segregation in bi-crystalline, tri-crystalline, and poly-crystalline metals is presented with an emphasis on the relationship between the structure and kinetic properties. Grain boundary diffusion is strongly affected by the structural state of interfaces and segregation of residual impurities. Temperature-induced transitions in the grain boundary structure are revealed by radiotracer diffusion measurements for specific low sigma interfaces [1, 2]. The results are compared with the data obtained previously on high-purity copper [3]. The segregation of Ag at Cu Sigma 5 and Sigma 17 grain boundaries is found to be significantly stronger as compared to that at general high-angle grain boundaries as they are present in annealed polycrystalline copper. An existence of critical temperatures, which corresponds simultaneously to specific "kinks" in the temperature dependences of the grain boundary diffusivity and the disappearance of the grain boundary diffusion anisotropy, is discovered and they are related to temperature-induced phase transitions as shown in [4].

The so-called "high-energy" state of grain boundaries is introduced by severe plastic deformation of metals using different routes. These interfaces are characterized by an increased free volume, larger excess free energy and, as a result, enhanced diffusivities. The kinetic and structure properties of the "high-energy" grain boundaries are investigated for several pure metals (Cu, Ni, Ti, Ag) and Cu-based alloys severely deformed via equal channel angular pressing or high-pressure torsion. The relaxation behavior of interfaces in ultra-fine grained metals is investigated by the radiotracer diffusion measurements and differential scanning calorimetry [5-8].

- [1] H. Edelhoff, S. I. Prokofjev, S.V. Divinski, *Scr. Mater.* 64, 374-377 (2011)
- [2] S.V. Divinski, H. Edelhoff, S. Prokofjev, *Phys. Rev. B* 85 (2012) 144104
- [3] S.V. Divinski, B.S. Bokstein, *Defect Diffusion Forum* 309-310 (2011) 1-8.
- [4] T. Frolov, S.V. Divinski, M. Asta, Y. Mishin, *Phys Rev Lett* 110 (2013) 255502.
- [5] S.V. Divinski, G. Reglitz, I. Golovin, M. Peterlechner, G. Wilde, *Acta Mater* 82 (2015) 11-21.
- [6] D. Prokoshkina, L. Klinger, A. Moros, G. Wilde, E. Rabkin, S.V. Divinski, *Acta Mater* 69 (2014) 314 - 325.
- [7] J. Ribbe, G. Schmitz, D. Gunderov, Y. Estrin, Y. Amouyal, G. Wilde, S.V. Divinski, *Acta Mater* 61 (2013) 5477 - 5486.
- [8] G. Reglitz, B. Oberdorfer, N. Fleischmann, J.A. Kotzurek, S.V. Divinski, W. Sprengel, G. Wilde, R. Würschum, *Acta Mater* 103 (2016) 396-406.

**Phonon spectrum engineering in rolled-up micro- and nano-architectures**

V.M. Fomin<sup>1</sup>, A.A. Balandin<sup>2</sup>

<sup>1</sup> Institute for Integrative Nanosciences (IIN), Leibniz Institute for Solid State and Materials Research (IFW) Dresden, Helmholtzstraße 20, D-01069 Dresden, Germany

<sup>2</sup> Phonon Optimized Engineered Materials (POEM) Center, Department of Electrical and Computer Engineering, University of California – Riverside, Riverside, California 92521, USA

Spatial confinement of acoustic and optical phonons in semiconductor thin films, superlattices and nanowires dramatically changes their properties in comparison with bulk materials. In particular, the changes in the phonon dispersion due to the confinement have a great impact on the electron-phonon scattering rates, optical properties of the nanostructured materials and phonon scattering on defects and boundaries. Efficient engineering of the acoustic phonon energy spectrum is possible in multishell tubular structures produced by a novel high-tech method of self-organization of micro- and nano-architectures. The strain-driven roll-up procedure paved the way for novel classes of metamaterials such as single semiconductor radial micro- and nano-crystals and multi-layer spiral micro- and nano-superlattices. The acoustic phonon dispersion is determined by solving the equations of elastodynamics for InAs/GaAs multishell systems. It is shown that the number of shells is an important control parameter of the phonon dispersion together with the structure dimensions and acoustic impedance mismatch between the superlattice layers. In view of the well-developed interfaces in the structure, the properties of the intershell boundaries are of key significance for the phonon transport. The obtained results suggest that rolled up nano-architectures are promising for thermoelectric applications owing to a possibility of significant reduction of the thermal conductivity without degradation of the electronic transport.

Discussions with O. G. Schmidt are gratefully acknowledged. The work at the IIN IFW Dresden was partly supported by the Deutsche Forschungsgemeinschaft (DFG) under Grant # FO 956/2-1.

[1] V.M. Fomin, A.A. Balandin, *Appl. Sci.* **5**, 728-746 (2015).

## Survey of grain boundary phases in nickel superalloys

A.M. Korsunsky<sup>1,2</sup>, C. Papadaki<sup>1</sup>, P. Kontis<sup>3</sup>, R.C. Reed<sup>3</sup>

<sup>1</sup> MBLEM Multi-Beam Laboratory for Engineering Microscopy, Department of Engineering Science, University of Oxford, Parks Road, Oxford OX1 3PJ, U.K.

<sup>2</sup> CIPS Centre for In situ Processing Studies, Research Complex at Harwell (RCaH), Harwell Oxford Science Campus, Didcot OX11 0QX, U.K.

<sup>3</sup> Department of Materials, University of Oxford, Parks Road, Oxford, OX1 3PH, U.K.

Grain boundary phases play an important role in determining the mechanical performance and corrosion resistance of nickel-base superalloys. Most common alloying elements in nickel-base alloys are Al and Ti ( $\gamma'$ -forming elements, along with Nb, Ta, Hf) and Cr and Co ( $\gamma$ -forming elements, along with Mo, W, Fe). Small amounts of B, C and Zr are also present.

The phase composition of these alloys is complex: along with the fcc  $\gamma$  matrix, the strengthening  $\gamma'$  phase with the ordered  $L1_2$  structure is present in the form of coherent precipitates that are typically grown to assume the cuboidal form by processing. Important secondary influence on the strength nickel-base alloys is exerted by the minority phases that often segregate to grain boundaries. These include Topologically Close-Packed (TCP) phases (designated  $\sigma$ ,  $\mu$ , Laves, etc.) that may form during heat treatment or service, are generally brittle and adversely affect mechanical properties. The close-packed atomic planes in these phases are separated by relatively large interplanar distances responsible for their low toughness and detrimental effect on the overall strength. TCP phases also capture the elements required for forming the strengthening  $\gamma'$  phase.

The most important grain boundary phases that must be considered are carbides, borides, TCP's and secondary grain boundary  $\gamma'$  precipitates whose size and density determines the morphology and tortuosity of grain boundaries that have significant effect on the structural integrity of alloys under thermo-mechanical loading [1]. Also, a study of the effect of borides on the grain boundary structure has been recently reported [2].

The talk will survey recent reports on the morphology and properties of the grain boundary phases in nickel-base superalloys and chart some avenues towards further studies.

1. Mitchell RJ, et al. On the Formation of Serrated Grain Boundaries and Fan Type Structures in an Advanced Polycrystalline Nickel-base Superalloy. *J. Materials Processing Technology* 2009; 209:1011-17.
2. Kontis P, Yusof HAM, Pedrazzini S, Danaie M, Moore KL, Bagot PAJ, et al. On the effect of boron on grain boundary character in a new polycrystalline superalloy. *Acta Mater.* 2016;103:688–99.



## Grain boundary complexions and their influence on microstructure evolution

G.S. Rohrer

Department of Materials Science and Engineering, Carnegie Mellon University, Pittsburgh,  
Pennsylvania 15213, USA

The characteristic structure and chemical composition of a grain boundary, free surface, phase boundary, or dislocation are referred to as its complexion [1]. Extensive research has shown that grain boundary complexions can abruptly transition from one state to another in response to a change in composition or temperature and that these transitions lead to discontinuous changes in grain boundary properties such as energy or mobility. Because of the change in grain boundary properties, the evolution of microstructures during grain growth can be dramatically altered. Therefore, to control microstructures, it is necessary to understand the kinetics of complexion transitions that alter grain boundary properties. In analogy to bulk phase transformations, complexion transition kinetics can be represented on time-temperature-transformation (TTT) diagrams. In this presentation, experiments designed to test the effects of grain boundary energy on complexion transitions will be described, as will the methods for experimentally determining complexion TTT diagrams. Furthermore, recently determined complexion TTT diagrams for impurity doped alumina, yttria, and spinel will be reviewed. It will be shown how complexion TTT diagrams can be used to design heat treatments to promote solid-state single crystal growth, dense nanocrystalline ceramics, or bimodal microstructures.

- [1] P.R. Cantwell, M. Tang, S.J. Dillon, J. Luo, G.S. Rohrer, M.P. Harmer, "Grain Boundary Complexions," *Acta Materialia*, 62 (2014) 1-48.

**Grain boundaries and superior properties of ultrafine-grained materials**

R.Z. Valiev

Institute of Physics of Advanced Materials, Ufa State Aviation Technical University,  
12 K. Marx str., Ufa 450000 Russia  
Laboratory for Mechanics of Bulk Nanomaterials, Saint Petersburg State University,  
Universitetsky prospekt, 28, Peterhof, 198504, Saint Petersburg, Russia

Numerous studies in recent years show that the formation of ultrafine-grained (UFG) metals and alloys by severe plastic deformation (SPD) holds out an opportunity for a significant increase in their mechanical and functional properties. At the same time, the properties of the resulting nanomaterials are determined not only by the formation of ultrafine grains but also the structure of their boundaries. This report presents the results of complex studies of different grain boundaries (low angle and high angle ones, special and random, equilibrium and non-equilibrium with strain-distorted structure as well as with the presence of grain boundary segregations and precipitations) in the ultrafine-grained metals produced via various SPD regimes and routes. This provides the basis for grain boundary engineering of the UFG materials to improve their mechanical and functional properties, in particular strength, ductility and superplasticity. Application of grain boundary engineering towards the creation of materials with the so-called multi-functional properties, i.e. the combination of high mechanical and functional properties (corrosion and radiation resistance, electrical conductivity, etc.) is of immediate interest. Special emphasis is laid on the physical nature and the use of multifunctional nanomaterials for their innovative applications in medicine and engineering.

**A phase field crystal study of grain boundaries in single and bilayer graphene**

R.V. Zucker, R. Freitas, M.D. Asta

Department of Materials Science and Engineering, University of California, Berkeley, 475  
Hearst Memorial Mining Building, Berkeley, CA 94705 USA

Grain boundaries in graphene have electronic properties which strongly depend on the grain boundary structure. We present a phase field crystal approach for obtaining grain boundary structures in graphene which agrees with molecular dynamics simulations and experiments. We identify general trends in low energy structures, in particular the arrangement of 5-7 ring units and microfacets. Large spatial scale simulations show patterns at length scales not accessible with other atomistic simulation methods.

## Oral talks

## Specific features of amorphous-nanocrystalline structure

G. Abrosimova, A. Aronin

Institute of Solid State Physics, Russian Academy of Sciences, Chernogolovka, Ac. Ossipyan str. 2, Moscow district, 142432 Russia

Specific features of heterogeneous amorphous and amorphous – nanocrystalline structure was studied for a number of metallic alloys. The results may be divided into two groups.

1. Heterogeneous amorphous alloys. Heterogeneous amorphous structure can be formed by heat treatment or/and by deformation of metallic glasses. The structure is usually consists of the regions with different type of short range order. The materials are known as nanoglasses. Nanoglasses are a new class of non-crystalline solids. They consist of regions with a melt-quenched glassy structure connected by interfacial regions, the structure of which is characterized by a reduced (up to about 10%) density, reduced (up to about 20%) number of nearest-neighbor atoms and a different atomic structure. Due to their atomic and electronic structure, the properties of nanoglasses may be modified by controlling the size of the glassy regions (i.e., the volume fraction of the interfacial regions) and/or by varying their chemical composition. The nanoglasses were found to be more ductile, and catalytically more active than the corresponding melt-quenched glasses. The interfaces between the regions with certain type of short range order are amorphous. The main amorphous phase and the interfacial regions have different chemical composition; the interfaces are not sharp and the chemical composition changes continuously from place to place (from one amorphous region to other through the interface). Low temperature annealing may result in separation of the amorphous phase with formation of the regions characterized by different Curie temperatures (Fe-B-P amorphous alloy). The crystallization of the nanoglasses may occur by spinodal decomposition mechanism (Fe-Zr).

2. Crystallization of heterogeneous amorphous alloy can takes place by different crystallization mechanism. It is shown that heat treatment and deformation within the amorphous state leading to heterogeneous amorphous structure formation accelerate the crystallization of the amorphous phase during subsequent heating. The size of the resulting nanocrystals depends both on the pretreatment conditions and the parameters of the heat treatment or deformation level during following crystallization. A change of chemical composition of the nanocrystals near the interfaces is discussed.

This work was partially supported by the RFBR (grant № 16-03-00505, 14-42-03566, 14-43-03564).

**Interface of anorthite ( $\text{CaAl}_2\text{Si}_2\text{O}_8$ ) and aluminium: Kinetics of high-temperature reactions**

E. Adabifiroozjaei, P. Koshy, H. Ma, C. C. Sorrell

School of Materials Science and Engineering, UNSW Australia, Sydney, NSW 2052, Australia

This current research focuses on the kinetics of interfacial reactions between anorthite and molten aluminium. Very high density anorthite substrates were produced by melting a stoichiometric mixture of alumina, silica and calcia and these were then exposed with liquid aluminium for varying reaction times (0.5 to 250 h) at different temperatures (850°, 950°, 1050°, and 1150°C). The resultant ceramic-metal interface was investigated by optical microscopy (OM), scanning electron microscopy (SEM) equipped with energy dispersive spectrometry (EDS) and electron probe microanalyser (EPMA) and electron transmission microscopy (TEM). The thickness of the interfacial region showed a parabolic growth rate with increasing temperatures and this suggests that the interaction between anorthite and aluminum occurs through a diffusion controlled process. The analyses revealed that the interfacial phases from the metal to the ceramic side were alumina ( $\text{Al}_2\text{O}_3$ ), calcium hexaaluminate ( $6\text{CaO}.\text{Al}_2\text{O}_3$ ), calcium dialuminate ( $2\text{CaO}.\text{Al}_2\text{O}_3$ ), calcium monoaluminate ( $\text{CaO}.\text{Al}_2\text{O}_3$ ), gehlenite ( $2\text{CaO}.\text{Al}_2\text{O}_3.\text{SiO}_2$ ) and anorthite. The interdiffusion of  $\text{Al}^{3+}$ - $\text{Si}^{4+}$  and  $\text{Al}^{3+}$ - $\text{Ca}^{2+}$  are believed to be the major mechanisms responsible for the reactions of anorthite with Al alloys, with the activation energy for the complete corrosion reaction being 112 kJ/mol.

## **Properties of twinned structures in metallic nanomaterials**

R.A. Andrievski

Institute of Problems of Chemical Physics, Russian Academy of Sciences  
Semenov Prospect, 1, Chernogolovka, Moscow Region, 142432, Russia

This overview outlines the current state of the nanotwinned structures studies in metallic nanomaterials. The various processes of twin generation, such as the pulse electrodeposition technique, magnetron sputtering and different variants of severe plastic deformation (equal channel angular pressing, high pressure torsion, accumulative roll bonding, and surface mechanical grinding/rolling treatment, etc.), are described. The structural characterization of the growth/deformation twins by transmission electron microscopy methods, including high-resolution one, is discussed. Special attention is given to a surface mechanical grinding/rolling treatment for the gradient structure formation with a high content of low-angle twinned boundaries. The influence of nanotwinned structure on the nanomaterials strength, ductility, fatigue properties, electrical conductivity, especially under extreme conditions (such as high temperatures, irradiation and corrosion actions) is discussed in details. A significant increase of these properties as compared with conventional nanomaterials is underlined. In many cases, the nanomaterials with the nanotwinned and gradient structure remain tolerant to the various extreme conditions, such as high temperature heating, irradiation, deformation and corrosion actions. Some poorly researched aspects are also put into considerations.

## **Structure of amorphous Al-based alloys at deformation and heat treatment**

A. Aronin, G. Abrosimova, E. Pershina, D. Matveev

Institute of Solid State Physics, Russian Academy of Sciences, Chernogolovka, Ac. Ossipyan str. 2, Moscow district, 142432 Russia

Amorphous and amorphous-nanocrystalline alloys prepared by heat treatment and deformation of amorphous alloys ( $\text{Al}_{90}\text{Y}_{10}$ ,  $\text{Al}_{87}\text{Ni}_8\text{Gd}_5$ ,  $\text{Al}_{87}\text{Ni}_8\text{La}_5$ ,  $\text{Al}_{88}\text{Ni}_6\text{Y}_6$  and  $\text{Al}_{87}\text{Ni}_8\text{La}_5$ ) were studied by X-ray diffraction, transmission and high resolution electron microscopy and DSC methods. The deformation was carried out by multiply rolling and high pressure torsion methods. The deformation by cold-rolling was 60-70%, and 1-5 rotations were used for high pressure torsion at room temperature. Amorphous phase decomposition was observed at both heating and deformation of amorphous alloys. The degree of decomposition increased with increasing duration of annealing or deformation.

The deformation occurs by formation and propagation of shear bands. The system of shear bands with high free volume formed in the alloy, these shear bands separate the nanometer amorphous regions, ie specific structures similar to the nanoglass structure form. In this way amorphous alloys after the deformation have a heterogeneous structure in which nanometer-sized amorphous clusters are separated by the "boundaries" with the increased free volume and the another atomic structure. In such "boundaries" the parameters of diffusion mass transfer are increased, which leads to facilitate the formation of nanocrystals. The processes of formation of nanocrystals near these interfaces are studied. The diffusion coefficient in the shear bands at room temperature is determined. The difference in the diffusion coefficients in deformation bands and the surrounding amorphous matrix is estimated. The diffusion coefficient in the shear bands at room temperature was found to be in the  $10^5$  -  $10^6$  times higher than that in the surrounding amorphous matrix. The values of the activation energy and pre-exponential factor were obtained for the effective diffusion coefficient that determines the growth of aluminum nanocrystals.

Nanocrystalline Al-based alloys containing amorphous phase and Al nanocrystals after first stage of crystallization exhibit high strength at low specific weight.

This research was partially supported by RFBR (14-43-03564, 14-42-03566, 16-03-00505, 16-32-00786)



**Hydrogen-assisted homophase and heterophase boundaries in austenitic stainless steel processed by rolling**

E.G. Astafurova, E.V. Melnikov, G.G. Maier

Institute of Strength Physics and Materials Science, Russian Academy of Sciences, Tomsk,  
Akademichesky av. 2/4, 634055 Russia

A stable Fe-17Cr-14Ni-2Mo and metastable Fe-17Cr-9Ni-Ti stainless steels were subjected to plain rolling (room temperature and liquid nitrogen atmosphere) in as-quenched state and after electrolytic hydrogen charging at different current densities  $j=10-200 \text{ mA/cm}^2$  (for 5 hours). Deformation of austenitic Cr-Ni steels by plain rolling was accompanied by refinement of a structure due to accumulation of deformation defects (slip, twinning, shear bands) and, in case of metastable steel, by strain-induced  $\gamma-\alpha'$  transformation. Hydrogenation affected the peculiarities of grain boundary ensemble, increased the frequency of homophase twin and heterophase  $\gamma-\varepsilon$ ,  $\gamma-\alpha'$  phase boundaries under rolling. The rolling changed strength and plastic properties of the steels drastically, but hydrogen saturation prior to rolling also increased mechanical properties of the specimens.

This research was supported by the Russian President Scholarship (project No. SP-419.2015.1). Instrumental analysis was taken with the use of the equipment of Scientific Research Center «Nanotech» (ISPMS TSC RAS).

**Evolution of grain boundary assembles in austenitic stainless steels during recrystallization and grain growth**

A. Belyakov, M. Odnobokova, M. Tikhonova, R. Kaibyshev

Belgorod State University, Pobeda 85, Belgorod, 308015, Russia

The grain boundary assembles that developed in cold worked or dynamically recrystallized austenitic stainless steels by annealing at elevated temperatures were studied. The steel types 304 and 316 were selected in the present study as typical representatives of widely used austenitic stainless steels. The steel samples were subjected to various strains under conditions of warm or cold working. The deformation microstructures depended substantially on the total strains. The work hardened structures with high dislocation densities arranged in cell blocks subdivided by dense dislocation walls and microbands were evolved at relatively small strains of around 1 irrespective of deformation temperature. On the other hand, the warm deformation to rather large strains of  $\epsilon \geq 3$  resulted in the development of continuous dynamic recrystallization leading to the evolution of ultrafine grained microstructure with grain size of 200 to 900 nm, depending on the deformation temperature; whereas the cold worked samples were characterized by lamellar microstructures consisting of austenite and martensite grain with the almost the same transverse grain size of about 100 nm. The annealing behavior of dynamically recrystallized structures was associated with the development of continuous post-dynamic recrystallization, which was accompanied by an increase in the fraction of  $\Sigma 3^n$  CSL boundaries. The latter could be defined by a relative change in the grain size, i.e., a ratio of the annealed grain size to initially dynamically recrystallized one. Similar variations in grain boundary misorientation distributions were observed in work hardened and severely strained samples. Therefore, the fraction of  $\Sigma 3^n$  CSL boundaries that developed during recrystallization and grain growth could be generally expressed by the change in the grain size, taking appropriate parameters for initial deformation microstructures.

## **Atomic complexes in grain boundaries as a phenomenon which precedes the formation of Guinier-Preston zones**

B. Bokstein, A. Rodin, A. Itckovich

National University of Science and Technology “MISIS”, Department of Physical Chemistry, 4, Leninsky pr-t, Moscow, 119049, Russia.

Atomic interaction in grain boundaries (GB) leads to complexes formation of  $B_2$  and  $A_mB_n$  type. Usually, such effect is observed in systems with restricted solubility and intermediate phases and precedes the formation of a fine scale Guinier-Preston zones [1], which in turn precede the precipitation of a new phase. Direct experimental investigation of atomic complexes is almost impossible due to their dimensions (several atoms). Nevertheless, the data of computer simulation demonstrated the existence of complexes.

According to the pioneer work of Guttmann [2], the complex is a two-dimensional aggregate. Its electronic structure and chemical bonds resemble that in a nearest bulk phase according to phase diagram [3-6]. Recently, it was also shown [7] that Fe atoms in Al+2.5% Fe system form complexes  $Fe_2$  in the symmetric GB (100) and that the Fe-Fe coordination number is close to unity, which is much more than in random solution.

Thermodynamic study of the complexes formation in GB's, based on the model of ideal association solutions [8], showed that it leads to the change of GB segregation isotherms [9] and decreases GB diffusion flux and the mean-layer concentration of diffusant [10].

At the present paper we studied mobility of the noted atomic pairs in copper using a semi-empirical potential designed for copper [11, 12] with addition the energy of interaction between the atoms in pair. Earlier, it was shown [13] that the complexes formation leads to decrease of mean-square atomic displacements. New results involve dependence the number of the stable pairs on time and temperature (from 825 to 1200K) and show the possibility of pairs to condense into ternary, quarterly and more numerous complexes.

- [1]. Guinier A. X-ray analysis of crystals. Theory and applications. Moscow, Nauka, 1961.
- [2]. Guttmann M. Met.Trans. 8A (1977) 1383.
- [3]. Briant C.L. Met.Trans. 21A (1990) 2339.
- [4]. Hashimoto M., Wakayama S., Yamamoto R., Doyama R. Acta Met. 32 (1984) 13.
- [5]. Losch W. Acta Met. 27 (1979) 1885.
- [6]. Briant C.L., Banerji S.K. Met.Trans. 10A (1979) 1729.
- [7]. Mendelev M.I., Rodin A.O., Bokstein B.S. Def. and Dif. Forum 309-310 (2011) 223/
- [8]. Prigogine I., Defay R. Chem. Thermodynamics. Longmans, Green and Co., 1954.
- [9]. Bokst5ein B.S., Esin V.A., Rodin A.O. Phys. Met. and Metallography 109 (2010) 1.
- [10]. Esin V.A., Bokstein B.S. Acta Mat. 60 (2012) 5109.
- [11]. Mendelev M.I., Cramer M.J., Becker C.A., Asta M. Phil. Mag. 88(2008)1723.
- [12]. Mendelev M.I., King A.H. Phil.Mag. 93(2013)1268.
- [13]. Itckovich A., Mendelev M., Bokstein B., to be published.

## **Influence of structure of grain boundaries and size distribution of grains on the yield strength at quasistatic and dynamical loading**

E.N. Borodin<sup>1-3</sup>, A.E. Mayer<sup>2</sup>

<sup>1</sup>Institute of Problems of Mechanical Engineering, Russian Academy of Sciences, St. Petersburg, V.O., Bolshoj pr. 61, 199178 Russia

<sup>2</sup>Department of Physics, Chelyabinsk State University, Chelyabinsk, Br. Kashirinykh str. 129, 454001 Russia

<sup>3</sup> Institute of Natural Sciences, Ural Federal University, Ekaterinburg, Mira str. 19, 620002 Russia

Two main mechanisms, the dislocation slip [1,2] and the grain boundary sliding [3], determine the plastic properties of different metals and alloys in a wide range of grain sizes and strain rates. Both mechanisms are characterized by threshold stresses and relaxation times, which determine the yield stress of the material at quasistatic and dynamic conditions of loading, correspondingly. According to our analyses, the structure and state of the grain boundaries is significant both for the coarse-grained metals in the quasistatic conditions and the nanocrystalline metals in the dynamic conditions at moderate temperatures.

At describing of mechanical properties of the fine-grained metals, the proposed model of the grain boundary sliding takes into account, in explicit form, the influence of dispersion of the grain size distribution. This influence can explain partially the observed scattering of the experimental data in the area of small grains. Dependence of the yield strength of metals on the grain size and the dispersion of the grain size are discussed for quasistatic and dynamic conditions of loading. In these two cases, the size distribution of grains influences differently on the slope of the Hall-Petch curve. Calculations show that, at the high strain rates in nanocrystalline materials, the dispersion has almost no influence on the slope of the inverse Hall-Petch curves, while the maximum of the dynamic yield strength shifts into the area of smaller grains with the increase of the dispersion. The last is important for analyses of the experimental and molecular dynamics data, where, due to this shift, the inverse Hall-Petch effect can be unobservable in the usual range of the mean grain sizes of 10-20 nm, which can be inaccurately interpreted as a total absence of the inverse effect.

The work is supported by the Russian Science Foundation (Project No. 14-11-00538), the Ministry of Education and Science of the Russian Federation (project No. 3.1334.2014/K) and the Russian Foundation for Basic Research (Project No. 16-31-6005) in the part of plasticity models.

[1] E.N. Borodin, A.E. Mayer. *Int. J. Plast.* **74** (2015) 141-157

[2] A.E. Mayer, K.V. Khishchenko, P.R. Levashov, P.N. Mayer. *J. Appl. Phys.* **113** (2013) 193508

[3] E.N. Borodin, A.E. Mayer. *Mater. Sci. Eng. A.* **532** (2012) 245-248

## **In Situ Investigation of Grain Boundaries in the Vicinity of the Special $\Sigma$ 3-CSL Misorientation in Al Bicrystals**

J.-E. Brandenburg, L.A. Barrales-Mora, D.A. Molodov

Institute of Physical Metallurgy and Metal Physics, RWTH Aachen University

The migration of twin boundaries plays an important role for the microstructural evolution of (ultrafine grained) crystalline materials, e.g. during recrystallization or deformation.

In this study, the faceting and migration behavior of high angle grain boundaries with misorientations close to the  $\Sigma$ 3-CSL relationship have been experimentally investigated using in situ electron microscopy at elevated temperatures and analysed by means of simulations.

Grain boundaries close to specific crystallographic planes, which correspond to the geometry of coherent ( $\{111\}$ -plane) and incoherent ( $\{110\}$  and  $\{112\}$ ) twin boundaries, showed a pronounced faceting, i.e. did not assumed a curved shape, and thus did not move under capillary driving force. Changing the character of the grain boundaries, either by a deviation from the  $\Sigma$ 3-CSL relationship or by introducing a twist component, reduced the faceting in most cases; such boundaries assumed a curved shape and moved under curvature driving force. The observed behavior was interpreted in terms of the inclination dependency of the grain boundary energy obtained from molecular statics simulations.

The behavior of the same grain boundaries have been investigated under the influence of an applied mechanical stress. While boundaries close to coherent and incoherent twin boundaries did not migrate well in this case, which has been explained by the lack of dislocations to interact with the stress field, the boundaries with deviation from  $\Sigma$ 3 character exhibited migration and their kinetics were compared with the curvature driven boundary migration.

## Comparative study between grain boundaries in hafnia and in silicon

N. Capron<sup>1,2</sup>, E. Degoli<sup>3</sup>, E. Luppi<sup>4,5</sup>

<sup>1</sup>Sorbonne Universités, UPMC, Univ Paris 06, UMR 7614, Laboratoire de Chimie Physique Matière et Rayonnement, F-75005 Paris, France

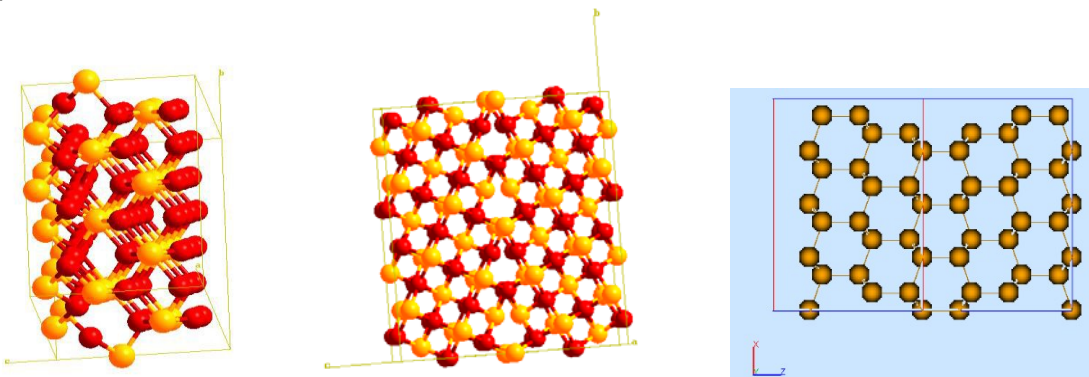
<sup>2</sup>CNRS, UMR 7614, Laboratoire de Chimie Physique Matière et Rayonnement, F-75005 Paris, France

<sup>3</sup>Dipartimento di Scienze e Metodi dell'Ingegneria, Università di Modena e Reggio Emilia, Via Amendola 2 (Padiglione Morselli) 42122 Reggio Emilia, Italy.

<sup>4</sup>Sorbonne Universités, UPMC, Univ Paris 06, UMR 7616, Laboratoire de Chimie Théorique, F-75005 Paris, France

<sup>5</sup>CNRS, UMR 7616, Laboratoire de Chimie Théorique, F-75005 Paris, France

We present an ab-initio density-functional theory study of grain boundaries (GBs) in  $\text{HfO}_2$  insulator, whose importance as high-k material in CMOS transistors is incontestable [1], and in semiconducting Si. Our goal is to investigate the structural and electronic properties of these materials. We first studied how structural and electronic properties can be modified by changing the size and the type of GBs. Indeed, symmetric GBs can be of two types : tilt and twist and also the crystallographic systems can vary: cubic or monoclinic as in the case of  $\text{HfO}_2$ .



*From the left to the right : c-HfO<sub>2</sub>, twin, 90 atoms ; c-HfO<sub>2</sub>, tilt, 108 atoms; Si, tilt 96 atoms*

Then, we investigated the effect of an oxygen atom inserted inside the most stable GB structures, and we try to highlight possible minimum energy paths with Nudged Elastic Band method [2].

[1] R.D. Clark, “Emerging applications for high k materials in VLSI technology”, *Materials*, 2014, 7, 2913-2944

[2] H. Jönsson, G. Mills and K. W. Jacobsen, “Nudged elastic band method for finding minimum energy paths of transitions”, in « Classical and quantum dynamics in condensed phase systems », ed B. J. Berne, G. Cicotti and D.F. Coker, World Scientific, 1998

## Theory of fast ion transport on solid electrolyte/indifferent electrode heterojunctions

A.L. Despotuli, A.V. Andreeva

Institute of Microelectronics Technology and High Purity Materials RAS, Chernogolovka, Ac.  
Ossipyan street 6, Moscow Region, 142432 Russia

Earlier [1], we have shown that future integrated circuits in deep sub-voltage nanoelectronics should include devices with fast ion transport (FIT). Among them, for example, all solid state thin-film impulse supercapacitors which basic working part is a solid electrolyte (SE)-advanced superionic conductor (AdSIC)/electronic conductor (EC) heterojunction. This implies the development of the FIT-theory on nanoscale and its application for the creation of new nanodevices. However, a basic FIT- theory describing nano-object response on external dynamic influence has not been formulated until now. For the development of nanoionics (the term and conception were first introduced by one of the authors in 1992-1993 [2]) and interpretation of frequency-dependent impedance of SE (AdSIC)-nanosystems we have put forward a structure-dynamic approach (SDA) of nanoionics [3-4]. The theoretical system of SDA includes a structural layered 1D-hopping atomic model of the region with a non-uniform potential landscape, a method of “hidden” variables (excess concentrations of mobile ions induced by external influence on crystallographic planes), a physico-mathematical formalism (based on the principle of a detailed balance and the kinetic equation in the form of the particle conservation law), and a method of uniform effective field. Nanoscale dynamic modeling of ion-transport is generalized by including a new notion - the Maxwell displacement current on a potential barrier and an essential definition of effective electrostatic field  $F_{\text{eff}}$  (corrected uniform Gauss field) for model SE-nanostructures [5,6]. The objects under consideration are model SE/EC ideally polarizable blocking heterojunctions, representing the sequence of potential barriers of different height in the crystal potential relief of a “rigid” sub-lattice of SE distorted at the interface. SDA interconnects the processes of space charge formation and relaxation with local ionic and Maxwell displacement currents in the interface region. Within the framework of SDA a computer simulation of ion transport, the frequency (time) behavior of SE/EC-capacitance and impedance have been performed under external influence of a current generator (ac and galvanostatic charging).

[1] A.L. Despotuli, A.V. Andreeva. *International Journal of Nanoscience*. **8** (2009)389

[2] A.L. Despotuli, V.I. Nikolaichik. *Solid State Ionics*. **60** (1993)275

[3] A.L. Despotuli, A.V. Andreeva. *Nano and Microsystem Technique*. **9** (2012)16

[4] A.L. Despotuli, A.V. Andreeva. *Nano and Microsystem Technique*. **11**(2012)15

[5] A.L. Despotuli, A.V. Andreeva. *Ionics* **21** (2015)459

[6] A.L. Despotuli, A.V. Andreeva. *Ionics* **22** (2016)

**Interface properties and shear bond strength of Al/Cu bimetallic rods produced by equal channel angular pressing**

A.R. Eivani, H. R. Mirzakouchakshirazi, Sh. Kheirandish

School of Metallurgy and Materials Engineering, Iran University of Science and Technology (IUST), Tehran, Iran

This research was aimed at investigating the effect of number of equal channel angular deformation and annealing treatment on the interface properties and shear bond strength of Al/Cu bimetallic rods. For this purpose, the rods were fabricated using equal channel angular pressing (ECAP) followed by annealed at different temperatures. For the as-deformed samples, the one with two passes of ECAP indicated higher shear bond strength. Formation of a layer of intermetallic compounds during annealing treatment is confirmed. In general, by increasing annealing temperature, thickness of intermetallic compounds at the interface increases. Shear bond strength was initially reduced by annealing at 200, 250 and 300°C and increased at 350°C. With further increase in annealing temperature to 400°C, shear bond strength slightly decreased which is correlated to the increased thickness of the intermetallic compounds.



## **Grain boundary segregation impacts strength of UFG stainless steel**

N.A. Enikeev<sup>1</sup>, M.M. Abramova<sup>1</sup>, X. Sauvage<sup>2</sup>, R.Z. Valiev<sup>1</sup>

<sup>1</sup>Institute of Physics of Advanced Materials, Ufa State Aviation Technical University,  
12 K. Marx str., Ufa 450000 Russia

<sup>2</sup>University of Rouen, CNRS UMR 6634, Groupe de Physique des Matériaux, Faculté des  
Sciences, BP12, 76801 Saint-Etienne du Rouvray, France

Further increasing strength of commercial alloys is a topical issue for the modern materials science. One of the effective means for this purpose is modification of the microstructure – for example, severe plastic deformation can lead to significant reduction in grain size of metallic materials and provide the corresponding hardening.

In this study we report that yield stress of austenite stainless Cr-Ni steel can be affected not only by grain boundary strengthening (thanks to grain refinement) but also by grain boundary segregations. Ultrafine-grained (UFG) 316 steel was produced by high pressure torsion (HPT) at room and elevated (400°C) temperatures. Yield strength of the steel in both UFG states was found to be increased up to the extra-high level exceeding 1800MPa despite a considerable difference in grain size. It was shown that the UFG steel processed by HPT at elevated temperature exhibited strength notably exceeding the Hall–Petch prediction. In contrast, 316 steel processed by HPT at room temperature demonstrated impressive increasing of strength (exceeding 2000 MPa) after annealing in the range of 450-600°C while dislocation density decreased and no precipitation was observed.

Analyses by 3D atom probe tomography allowed revealing unusual segregations of Mo, Cr and Si at grain boundaries in UFG steel produced by HPT at 400°C, while in the UFG steel, produced by HPT at 20°C the segregations were absent and appeared only after annealing.

The nature of the revealed extra–strength manifestation is discussed. We show that the additional strengthening can be linked to grain boundary segregations formed due to HPT at elevated temperature as well as due to annealing after HPT at room temperature. The results obtained clearly illustrate application of grain boundary engineering to UFG materials to control their properties.

**Study of grain rotations in austenitic steel subjected to hot uniaxial compression using EBSD analysis of misorientations at twin boundaries**

N.Yu. Zolotarevsky<sup>1,2</sup>, N.Yu. Ermakova<sup>1,2</sup>, V.S. Sizova<sup>1</sup>, E.A. Ushanova<sup>2,3</sup>, V.V. Rybin<sup>1,2</sup>

<sup>1</sup>Institute of Applied Mathematics and Mechanics, Saint-Petersburg Polytechnic University, Saint-Petersburg, 195251 Russia

<sup>2</sup>Mechanical Engineering Research Institute of the Russian Academy of Sciences, Nizhnii Novgorod, 603024 Russia

<sup>3</sup>Central Research Institute of Structural Materials “Prometey”, Saint-Petersburg, 191015 Russia

It is well known that grains of polycrystalline material lose their initial orientation uniformity and become fragmented during plastic deformation. However, until the present time the mechanisms of deformation-induced grain refinement as well as deformation texture development remain under discussion. In this connection the twin boundaries being natural references when examining local lattice rotations provide unique opportunity to study phenomena mentioned above. In the present EBSD study the austenitic steel having more than 50% twin boundaries in the non-deformed condition was used.

The misorientations at originally twin boundaries evolve under deformation. As this takes place, their variation proceeds differently at different boundaries, depending of orientations of the neighboring grains, and non-uniformly along an individual boundary, that reflects non-uniformity of grains deformation and reorientation. Based on measurements made on a large set of twin boundaries after true strains of 0.36 and 0.7, the distributions of additional misorientations induced by plastic strain has been obtained. Then, the experimental distributions were compared with theoretical ones computed using Taylor model of polycrystal deformation. It turned out that there is a considerable fraction of boundaries, at which the angular deviations from the strict twin misorientation is lower than it was predicted by modeling. Subsequent analysis showed that at some boundaries the misorientation measured immediately at the boundary is less deviated from twin misorientation as compared with the misorientation measured between the points remote from the boundary. In such cases the grain regions remote from the boundary were shown to undergo larger rotation to the stable orientation  $\langle 110 \rangle$  than the near-boundary regions. The results obtained are discussed in connection with the mechanism of the impact of grain boundaries on the grains deformation.

**Atomistic investigation of grain boundary solute segregation behavior in yttria-stabilized zirconia**

B. Feng<sup>1</sup>, T. Yokoi<sup>2</sup>, A. Kumamoto<sup>1</sup>, M. Yoshiya<sup>2,3</sup>, Y. Ikuhara<sup>1,3,4</sup>, N. Shibata<sup>1</sup>

<sup>1</sup>Institute of Engineering Innovation, The University of Tokyo, Tokyo, 113-8656 Japan

<sup>2</sup>Department of Adaptive Machine System, Osaka University, Osaka 565-0781, Japan

<sup>3</sup>Nanostructures Research Laboratory, Japan Fine Ceramics Center, Nagoya 456-8587, Japan

<sup>4</sup>WPI advanced Institute for materials research, Tohoku University, Sendai 980-8577, Japan

Grain boundary segregation is known to strongly alter the local structures of grain boundaries, and thus the resultant properties of polycrystalline materials. Although the advanced aberration-corrected scanning transmission electron microscopy (STEM) has greatly improved our understanding of grain boundary segregation even down to the atomic dimensions [1], most of these studies have been focused on the non-solute segregation, of which the dopant atoms only reside at grain boundary cores and thus the experimental identification is rather straightforward [2]. For solute segregation, of which the dopant atoms can reside both at the grain interiors and grain boundaries, it is still challenging to experimentally identify such phenomena at atomic resolution.

Using yttria-stabilized zirconia (YSZ) as a model material, we tried to investigate such solute segregation phenomenon at atomic scale in this study. In YSZ, Y is soluble inside bulk  $ZrO_2$ , and meanwhile Y segregation occurs in grain boundaries [3]. However, the atomistic mechanisms of how Y atoms segregate in the grain boundaries are still unclear. In the present study, the local Y distributions near a  $\Sigma 3$  [110]/(111) YSZ GB was directly determined by atomic-resolution elemental mapping using STEM-EDS, equipped with double high-sensitivity silicon drift detectors (SDD).

YSZ (10 mol%  $Y_2O_3$  doped  $ZrO_2$ ) bicrystal containing  $\Sigma 3$  [110]/(111) GB was first fabricated by diffusion bonding of two single crystals at 1600 °C for 15 h [3]. The STEM-EDS system used in our study is equipped with double SDD-EDS detectors and the solid angle for the whole collection system is about 1.7 sr. Our results demonstrate that Y atoms indeed segregate to the grain boundary, but occupy some specific atomic sites, forming a characteristic ordered grain boundary structure [4]. Combined with the large-scale Monte Carlo simulations, we demonstrated that such solute segregation structure is formed to stabilize the interactions between several point defects at the grain boundary core. The detailed mechanisms will be discussed in the presentation.

#### References

- [1] Y. Ikuhara, *J Electron Microsc.* **60** (2011) p. 173-188
- [2] N. Shibata *et al*, *Nature Mater.* **8** (2009) p. 654-658
- [3] N. Shibata *et al*, *Philos Mag.* **84** (2004), p. 2381-2415.
- [4] B. Feng *et al*, *Nature Commun.* in press.

## Grain boundary diffusion of cobalt in high-purity copper

D. Gaertner, S.V. Divinski

Institute of Materials Physics, Westfälische Wilhelms-Universität Münster, Wilhelm-Klemm-Str. 10, 48149 Münster, Germany

Grain boundary diffusion of cobalt in high-purity polycrystalline copper was measured using the radiotracer method and applying the  $^{57}\text{Co}$  isotope. At temperatures lower than 950 K, the measurements were performed under Harrison's C kinetic regime and the grain boundary diffusion coefficient of Co in Cu,  $D_{gb}$ , was determined,  $D_{gb} = 3.7 \cdot 10^{-9} \times \exp(-93.5 \text{ kJmol}^{-1} / RT) \text{ m}^2\text{s}^{-1}$ . Penetration profiles were measured for Co grain boundary diffusion in Cu at temperatures above 850 K under the intended B-type kinetic regime and the so-called triple product  $P = s \delta D_{gb}$  was determined,  $P = 1.7 \cdot 10^{-1} \times \exp(-72.6 \text{ kJmol}^{-1} / RT) \text{ m}^3\text{s}^{-1}$ . The grain boundary diffusion measurements in both B-type and C-type conditions after Harrison and the determined value,  $s \cdot \delta$ , i.e. the product of the solute segregation factor  $s$  and the diffusional GB width  $\delta$ , were compared with the results on grain boundary diffusion of Fe [1], Ni [2], Bi [3] and Ag [4] in the same polycrystalline Cu.

- [1] S.V. Divinski, J. Ribbe, G. Schmitz. *Defect and Diffusion Forum.* **289 - 292** (2009) 211-217
- [2] S.V. Divinski, J. Ribbe, G. Schmitz, Chr. Herzig. *Acta Mater.* **55** (2007) 3337-3346
- [3] S.V. Divinski, M. Lohmann, Chr. Herzig. *Acta Mater.* **52** (2004) 3973
- [4] S.V. Divinski, M. Lohmann, Chr. Herzig. *Defect and Diffusion Forum.* **194 - 199** (2001) 1127

**The grain-boundary precipitates in ultrafine-grained carbon steels produced by HPT**

A.V. Ganeev<sup>1</sup>, M.V. Karavaeva<sup>1</sup>, X. Sauvage<sup>2</sup>, Yu. Ivanisenko<sup>3</sup>, R.Z. Valiev<sup>1</sup>

<sup>1</sup>Institute of Physics of Advanced Materials, Ufa State Aviation Technical University,  
12 K. Marx str., Ufa 450000 Russia

<sup>2</sup>University of Rouen, CNRS UMR 6634, Groupe de Physique des Matériaux, Faculté des  
Sciences, BP12, 76801 Saint-Etienne du Rouvray, France

<sup>3</sup>Institute of Nanotechnology (INT), Karlsruhe Institute of Technology (KIT), Hermann-von-  
Helmholtz-Platz 1, 76344 Eggenstein-Leopoldshafen, Germany

Formation of nanostructured state in steels and alloys produces a unique combination of mechanical properties. One of the effective methods for the preparation of bulk nanostructured materials is high-pressure torsion (HPT) - severe plastic deformation (SPD) by torsion under high quasi-hydrostatic pressure. In carbon steels there occur the dissolution of cementite phase, formation of segregates at grain boundaries, and the precipitation of dispersed phases after a large strain and deformation-induced redistribution of carbon atoms. These processes play a great role in the formation of microstructure in steels during SPD processing. New methods of structure study have been widely developing in recent years, such as automatic crystallographic orientation mapping (ACOM) and 3D atom probe tomography (3D ATP), allowing to obtain data on the nano- and atomic level. The combination of these methods makes it possible to obtain new information about the mechanisms of pattern formation in carbon steels by SPD.

Ultrafine-grained ARMCO iron, low-carbon steel C10 and medium-carbon steel C45 produced by HPT were investigated in this paper. The structure and condition of grain boundaries were analysed with the help of conventional methods of electron microscopy, ACOM and 3D APT. It was shown that along the grain boundaries there were formed carbon segregations in the investigated materials, and in carbon steels at the grain boundaries there were detected nano-sized (3-5 nm) carbides. The correlation between the precipitates and the form of grains produced by severe plastic deformation was established. Based on the results of structural analysis, the contribution of various hardening mechanisms was calculated, and the theoretical data were compared with the experimental data.

**Nucleation, evolution and stability of nano voids in steels under plastic deformation**

G. Gerstein<sup>1</sup>, H.J. Maier<sup>1</sup>, G.G. Gottstein<sup>2</sup>, L.S. Shvindlerman<sup>2,3</sup>,  
L.A. Barrales-Mora<sup>2</sup>, Y. Estrin<sup>4,5</sup>

<sup>1</sup>Institute of Materials Science, Leibniz University Hanover,  
An der Universität 2, 30823 Garbsen, Germany

<sup>2</sup>IMM, RWTH Aachen University, Kopernikusstraße 14, 52074 Aachen, Germany

<sup>3</sup>Institute of Solid State Physics, Russian Academy of Sciences,  
142432 Chernogolovka, District Moscow, Russia

<sup>4</sup>Department of Materials Science and Engineering, Monash University,  
Clayton 3800 Victoria, Australia

<sup>5</sup>Laboratory of Hybrid Nanostructured Materials NUST MISIS, Leninsky prospect 4, 119049  
Moscow, Russia

We present the results of a study of nucleation and evolution of nano voids in steels subjected to plastic straining. A special technique of ion slope cutting was employed for layer-by layer removal of atoms from the surface that preserves the inner microstructure of the material. Subsequent observation of emerging and growing voids and microcracks in a size range of 8 to 200 nm and beyond by scanning electron microscopy is thus enabled.

The dependence of the character of void distribution in single-phase (DC04) and dual-phase (DP600) steels on the amount of strain was investigated. It was shown that the number density and the average size of nano voids is a function of strain. It was also found that the kinetics of growth and the shape of the voids is related to the slip geometry in the material. The void nucleation sites were found to be associated with the intersections of slip bands aligned with close packed lattice planes, as well as grain boundaries and triple junctions. The contribution of each of these mechanisms varied with the type of material and the amount of strain it underwent. Additional information on the genesis of nano voids and microcracks obtained by *in situ* investigation of deformation of steels in the scanning electron microscope will also be presented.

We shall also discuss theoretical considerations on stability and growth of nano voids formed at grain boundaries and triple junctions.

## Re-partitioning of grain boundary segregation to initiate abnormal grain growth in ceramics

H. Gu

Materials Genome Institute and School of Materials Science and Engineering, Shanghai University, 99 Shangda Road, Shanghai, 200444 China

From ceramics to metal systems, facet-roughening transition recently becomes a leading topic for grain boundary study, thanks largely to the establishment of grain boundary complexions (GBCs) scheme to correlate such transition directly with the abnormal grain growth (AGG) in ceramics. However, this scheme raises several concerns: (a) the intergranular glassy films (IGFs) at roughened GBs are much more common in ceramics than in metals, hence the generalization of GBC especially their transitions are questionable; (b) such transitions were observed only in  $\text{Al}_2\text{O}_3$  systems, but not even in the model  $\text{Si}_3\text{N}_4$  systems; (c) the triple-grain pockets (TPs) accommodating much more dopants should affect IGFs or GB transitions, and should play a much more active role in AGG. Here we report an analytical TEM study for partition and re-partition behaviors of dopant segregation to IGF at different GB facets, in both  $\text{Si}_3\text{N}_4$  and  $\text{Al}_2\text{O}_3$  systems, before or during AGG. These results indicate: (i) the equilibrium IGF structure independent to different GB facets, in a given ceramic system, is never true [1,2]; (ii) similar IGF partitions or structural transitions occur with and without AGG [2-4]; (iii) TP phases interact with IGFs, especially before the start of AGG [5-7].

- [1] M.F. Chi, H. Gu, *Interf. Sci.* **12** (2004) 335
- [2] H. Gu, I. Tanaka, R.M. Cannon, X.Q. Pan, M. Rühle. *Int. J. Mater. Res.* **101** (2010) 66
- [3] P.X. Qian, H. Gu, F. Aldinger, *Int. J. Mater. Res.* **99** (2008) 240
- [4] J.J. Xing, H. Gu, Y. Heo, M. Takeguchi, *J. Mater. Sci.* **46** (2011) 4361
- [5] R. Huang, H. Gu, J.X. Zhang, D.L. Jiang, *Acta Mater.* **53** (2005) 2521
- [6] H. Gu, R.M. Cannon, I. Tanaka, M. Rühle, *Mater. Sci. Engin.* **A422** (2006) 51
- [7] P.X. Qian, H. Gu, M.F. Chi, *J. Am. Ceram. Soc.* **93** (2010) 326

## The atomic origin of unique properties of graphene

J.J. Guo<sup>1</sup>, B.S. Xu<sup>1</sup>, P.Z. Liu<sup>1</sup>, M.F. Chisholm<sup>2</sup>, S.J. Pennycook<sup>3</sup>

<sup>1</sup>Key Laboratory of Interface Science and Engineering in Advanced Materials of Ministry of Education, Taiyuan University of Technology, Taiyuan 030024, P.R.China

<sup>2</sup>Materials Science and Technology Division, Oak Ridge National Laboratory, Oak Ridge, TN 37831-6065, USA

<sup>3</sup>Department of Materials Science and Engineering, National University of Singapore, Singapore 117576, Singapore

Atomic-scale defects in graphene layers alter the physical and chemical properties of graphene based carbon nanostructures. Pentagon–heptagon pairs, vacancies and adatoms are typical stable graphene defects that have been observed and widely studied.

In this study, the atomic configurations of graphene, graphene oxide and nanoporous carbon were analyzed by using the gentle aberration-corrected scanning transmission electron microscopy operated at 60kV to study the atomic origin of their unique properties.

Atomic-resolution images demonstrate the nanoporous carbon materials comprise isotropic, three-dimensional networks of wrinkled one-atom-thick graphene sheets. The topological defects graphene induce localized rippling of graphene sheets, which interferes with their graphitic stacking[1]. We introduced a large number of single niobium atoms in graphitic layers, which suppresses the chemical/thermal coarsening of the active metal atoms. It presents a new approach for stabilizing metallic single atoms, and thus opens up the possibility for developing highly efficient and durable electrocatalysts[2]. We also directly observed that residual oxygen atoms in oxidized graphene formed highly stable crown ether configurations, exhibited better selectivity for different cations[3].

- [1] Guo J J, Morris J R, Ihm Y, Contescu C I, Gallego N C, Duscher G, et al. Topological Defects: Origin of Nanopores and Enhanced Adsorption Performance in Nanoporous Carbon. *Small*, **8(21)** (2012) 3283-3288.
- [2] Zhang X F, Guo J J, Guan P F, Liu C J, Huang H, Dong X L, et al. Catalytically active single-atom niobium carbide in graphitic layers, *Nature Commun.* **4** (2013) 1924.
- [3] Guo J J, Lee J, Contescu C I, Gallego N C, Pantelides S T, Pennycook S J, et al. Crown ethers in graphene, *Nature Commun.* **5** (2014) 5389.



## **Atomistic investigations on the mechanisms of hydrogen diffusion in Ni $\Sigma 3$ grain boundaries**

A. Hallil, A. Metsue, A. Oudriss, J. Bouhattate, X. Feaugas

Laboratoire des Sciences de l'Ingénieur pour l'Environnement, LaSIE-CNRS UMR 7356,  
Université de La Rochelle, Avenue Michel Crépeau, 17000 La Rochelle, France

The context of this work falls within an approach to understand the mechanisms of diffusion and trapping of hydrogen in fcc grain boundaries (GB) and their influence on the GB microstructure. Recently, it has been shown experimentally [1] that the grain boundary character plays an important role in hydrogen diffusion and segregation processes. In this present study, atomistic simulations based on energy minimization method were employed to compute the structural and defect properties of four Ni  $\Sigma 3$   $\langle 110 \rangle$  tilt grain boundaries (GBs). The GB properties (energy, excess volume) are treated by the notion of the inclination angle between the two symmetric tilt grain boundaries (STGB): coherent twin boundary (CTB) and incoherent twin boundary (SITB) configurations, including two other asymmetric GBs:  $\Sigma 3$  (110)/(114) and  $\Sigma 3$  (221)/(001).

In order to assess the H absorption efficiency at grain boundaries, the distribution of the H segregation energy as a function of the direction normal to the GB plane will be presented for each GB configuration. Relatively, the hydrogen segregation profile displays a tiny width compared to the energetic distribution of the Ni vacancies within the GB core region. A linear correlation between the atomic volume and the segregation energy of the H interstitial site was established for all the GBs treated in this work, suggesting that GB interstitial sites with large local volume facilitate the hydrogen segregation. However, this linear relationship presents some limits for the H segregation when the interstitial site reaches a certain critical atomic volume. Beside this relevant result, more investigations on the mechanisms of H diffusion in Ni  $\Sigma 3$  GBs will also be explored by giving an example of static jump events and by quantifying barrier and activation energies between the relative stable GB interstitial sites.

[1] A. Oudriss, J. Creus, J. Bouhattate, E. Conforto, C. Berziou, C. Savall, X. Feaugas. Acta Mater. 60 (2012) 6814.

## On the origins of Otto Mügge's classical notations for mechanical twinning

O.B.M. Hardouin Duparc

École Polytechnique, LSI, CNRS, CEA, Université Paris-Saclay, 91128 Palaiseau, France

Independently from the coincidence lattice concept and the famous inverse coincidence index  $\Sigma$  developed by Georges Friedel at the very beginning of the XXth century to describe twins (see [1] for a review), there exists a specific nomenclature for the so-called mechanical twins, or twins obtained by mechanical deformation. This nomenclature,  $(K_1, \eta_1, K_2, \eta_2)$ , is due to Otto Mügge in 1889 [2]. The German mineralogist and crystallographer Mügge (1852-1932) rationalized twinning observations made by himself and by other German scientists since 1859 (Pfaff, Dove, Reusch). These twinning observations came from deformations carried out on transparent crystals and analysed via birefringence, naturally following observations of birefringence induced by deformation of glasses by Seebeck, Brewster and Biot. Mügge found that the observed twins could be systemized into two types that he named  $\alpha$  et  $\beta$  to which he associated descriptive crystallographic elements, viz. a first circle cutting plane (the twin surface)  $k_1$  and a second cutting plane  $k_2$ , because he geometrically considered the shear deformation of a circle, hence the  $k$  letter, from the German word Kreis which means circle. Mügge also defined a slipping vectors  $\sigma_1$  and another vector  $\sigma_2$  with the Greek letter  $\sigma$  reminiscent of the 's' of Schiebung which means shear in German.  $k_1$  et  $k_2$  became  $K_1$  and  $K_2$ , and  $\sigma_1$  and  $\sigma_2$  became  $\eta_1$  and  $\eta_2$ , at least since 1914 in a review by Arrien Johnsen [3], one of Mügge's pupils. The  $\alpha$  et  $\beta$  deformations became deformations of the first and of the second kind, probably because of Frédéric Wallerant (Friedel's *bête noire*) in 1904, then type I and II with Johnsen. It is worth noting that Georges Friedel abundantly mentioned Mügge in the chapter devoted to the Mechanical Twins of his 1926 *Leçons de Cristallographie* [4] where he otherwise never missed an opportunity to denigrate German scientists. This description is also the one used by Marina Viktorovna Klassen-Neklyudova in her classical book *Mechanical Twinning of Crystals* [5] (1960 in Russian, 1964 in the revised and expanded US-English translation). It is still very much used today in studies of *twinning* at the atomistic level involving *twinning* dislocations.

- [1] O. Hardouin Duparc, A review of some elements in the history of grain boundaries, centered on Georges Friedel, the coincident site lattice and the twin index, *Journal of Materials Science* 46 (2011) 4116
- [2] O. Mügge. *N. Jahrb. Miner. Geol. Pal.* BB6 (1889) 274
- [3] A. Johnsen. *Jahrb. der Radioaktivität und Elektronik* 11 (1914) 226
- [4] G. Friedel, *Leçons de cristallographie*, Berger-Levrault, Paris, 1926
- [5] M.V. Klassen-Neklyudova, *Mechanical Twinning of Crystals*, Consultants Bureau, 1964

**Atomistic modeling of pre-melted grain boundaries**

J. Hickman, Y. Mishin

Department of Physics and Astronomy, George Mason University, MSN 3F3, Fairfax, VA  
22030, USA

In binary systems with temperatures and chemical compositions approaching the solidus line, many grain boundaries (GB's) become increasingly disordered and may even pre-melt by forming a thin liquid layer at the interface [1][2]. The phenomenon can be modeled using a temperature and composition dependent disjoining potential which describes the interaction forces between the two solid-liquid interfaces bounding the liquid layer. This disjoining potential has been previously extracted using molecular dynamic simulations for a single component Ni system [3]. However, no studies have used atomistic simulations to compute the disjoining potential in an alloy. To this end, we present a theory which provides an expression for the probability distribution for the width of a pre-melted GB in a binary solid. This distribution describes width fluctuations arising as a result of both thermal and compositional fluctuations occurring at the interface. It is demonstrated that critical information, including the disjoining potential, can be extracted from the fluctuation analysis [4]. The proposed theory is applied to semi-grand-canonical Monte Carlo simulations of GB pre-melting in Cu-rich alloys in the eutectic Cu-Ag system modeled with an embedded-atom potential. The simulations are carried out for various GB misorientation angles. Several forms of the disjoining potential are observed, including attractive, repulsive, and even a mixed (bimodal) form depending on the alloy composition, temperature and the GB misorientation angle.

- [1] P. Williams, Y. Mishin. *Acta Materialia* **57**, (2009) 3786–3794
- [2] J. Hoyt, D. Olmsted, S. Jindal, M. Asta, A. Karma. *Physical Review E* **79** (2009) 020601
- [3] S. Fensin, D. Olmsted, D. Buta, M. Asta, A. Karma, J. Hoyt. *Physical Review E* **81** (2010) 031601
- [4] Y. Mishin. *Annals of Physics* **363** (2015) 48–97

**Phase transition kinetics in nanostructured alloy: experiments and modeling**

L. K. Huang, F. Liu

State Key Laboratory of Solidification Processing, Northwestern Polytechnical University,  
Xi'an, Shaanxi 710072, P.R. China

Experimental observation and theoretical interpretation on the concurring kinetics of grain growth and phase transition in nanostructured Fe<sub>91</sub>Ni<sub>8</sub>Zr<sub>1</sub> alloy were first presented. From *in situ* high temperature X-ray diffraction and differential scanning calorimetry, it can be confirmed that concomitant grain growth occurs and comes to a halt before phase transition is fully completed. On this basis, a kinetic mode describing the phase transition process in nanocrystalline materials is developed. From the currently kinetic description, grain growth not only adjusts the constitution of enthalpy change, but also influences the kinetics of phase transition. The present findings, offer a new behavior of phase transition owing to the size effect, and further, extend the understanding of the role grain boundary played in solid-state phase transition.

**Computer modeling of atomic complexes formation in grain boundaries. Effect on grain boundary diffusion**

A. Itckovich<sup>1</sup>, M. Mendeleev<sup>2</sup>, B. Bokstein<sup>1</sup> A.Rodin<sup>1</sup>

<sup>1</sup>National University of Science and Technology MISiS, Moscow, Russia

<sup>2</sup>Ames Laboratory, Ames, IA, USA

At the present paper we studied the peculiarities of grain boundary diffusion (GBD) in copper connected with the effect of atomic pairs formation in grain boundaries (GB). Our choice is based on the results of thermodynamic study of the complexes formation in GB's [1,2] and pioneer results of computer simulation [3-5] which showed the formation of the complexes of B<sub>2</sub> and AB type, a deviation of solute-solute coordination number from random distribution [6] and decrease of mean-square atomic displacements [7].

We used the molecular dynamics simulation taking semi-empirical potential designed for copper [8,9] with addition the energy of interaction between the atoms in the pair. To obtain reliable data of the mean-square displacement at comparatively low temperatures we used the simulation cell consisted of three hundred thousand of atoms, two symmetrical GB's Sigma 5(001)(012) and 70 pairs of identical random atoms Cu in GB's. We required also that MD should run at least 100 ns. The data were obtained for the temperature interval from 825 to 1200 K.

It was confirmed that the complexes formation leads to decrease of mean-square displacement at atomic pairs compared with free atoms. The activation energy of GBD was obtained, close to experimental data for "free" atoms, but growing at displacement of atomic pairs. New results involve dependence the number of the stable pairs on time and temperature and show the possibility of pairs to condense into ternary, quarterly and more numerous complexes.

- [1] Bokstein B.S., Esin V.A., Rodin A.O. Phys.Met. and Metallogra phy, 109 (2010) 1
- [2] Esin V.A., Bokstein B.S., Acta Mat. 60 (2012) 5109
- [3] Briant C.L. Met.Trans. 21A (1990) 2339
- [4] Hashimoto M., Wakayama S., Yamamoto R., Doyama R. Acta Met., 32 (1984) 13
- [5] Losch W., Acta Mat., 27 (1979) 1885
- [6] Mendeleev M.I., Rodin A.O., Bokstein B.S. Def. and Dif. Forum, vol 309-310 (2011) 223
- [7] Itckovich A., Mendeleev M., Bokstein B., to be published
- [8] Mendeleev M.I., Kramer M.J., Becker C.A. and Asta M., Phil. Mag. 88, (2008) 1723
- [9] Mendeleev M. I., King A.H., Phil. Mag 93 (2013) 1268

## High temperature plasticity of the $\gamma'$ rafts of a single crystal superalloy: Dislocation transmission through the $\gamma/\gamma'$ interface

R. Trehorel<sup>1</sup>, T. Schenk<sup>1</sup>, A. Jacques<sup>1</sup>, J. B. Le Graverend<sup>2,3</sup>, J. Cormier<sup>3</sup>

<sup>1</sup>IJL/SI2M, Labex DAMAS, Parc de Saurupt, CS 50840, 54011 Nancy cedex, France

<sup>2</sup>Texas A&M University, Department of Aerospace, College Station., TX 77843, USA

<sup>3</sup>Institut P', 1 avenue Clément Ader, BP 40109, 86961 Futuroscope - Chasseneuil Cedex, France

During Stage II of the high temperature creep curve of a single crystal superalloy, the plastic strain of the  $\gamma'$  rafts is believed to take place by climb of dislocations from different systems exchanging vacancies. However, several physical processes involved in climb might limit the strain rate of these rafts: the intrinsic mobility or the density of dislocations, the diffusion of vacancies...

We may get some insight on these mechanisms by determining the actual plastic strain rate of the rafts as a function of the different components of the stress tensor for the  $\gamma'$  phase. This can be achieved by in situ high resolution synchrotron X-Ray diffraction during creep tests, which provide a way of measuring the lattice parameters in the direction perpendicular to the tensile axis (and the lattice mismatch in the interface plane) with a precision of a few  $10^{-5}$  at 5 minutes intervals. From this data and the plastic strain of the specimen, it is possible to deduce the plastic strain of the rafts and the stress components  $\sigma'_{xx} = \sigma'_{yy}$  perpendicular to the tensile axis.

This method was used during creep tests involving either stress jumps or temperature jumps. During a stress jump, as the applied stress  $\sigma_a = \sigma'_{zz}$  is changed, plasticity within the  $\gamma$  corridors results in a proportional variation  $\sigma'_{xx}$ . During a temperature jump, as the volume fraction of the  $\gamma'$  phase decreases, the Orowan stress for the corridors also decreases. The subsequent deformation of the corridors results in a change of  $\sigma'_{xx}$  under a constant applied stress.

A comparison of the tests results suggests that the main factor for raft plasticity is not the applied stress but the internal stress  $\sigma'_{xx}$ . The rate limiting factor for plasticity might be the entry of a'.[100] dislocations into the  $\gamma'$  rafts or their multiplication.

**Microstructure and mechanical properties evolution during reverse martensite transformation through grain boundary engineering**

M. Falaki<sup>1</sup>, H. Jafarian<sup>1</sup>, H. Shirazi<sup>2</sup>, M. Nili Ahmadabadi<sup>2</sup>

<sup>1</sup>School of metallurgy and materials engineering, Iran University of science and technology, Tehran, Iran

<sup>2</sup>School of metallurgy and materials engineering, University of Tehran, Tehran, Iran

Grain refinement is known as effective way to obtain outstanding combination of strength and ductility. Among grain refinement techniques, reverse transformation is highly interested in ferrous alloys. This study is aimed to study the different cycle of reverse martensite transformation in Fe-18Ni martensitic steel for both as pre-deformed and non-deformed states with respect to microstructure engineering and mechanical properties. Microstructure was characterized by scanning electron microscope equipped with electron backscattered diffraction (EBSD) system. The EBSD results demonstrated that the fraction of high angle boundaries increased significantly by even 1-cycle of the reverse transformation, i.e., each martensite variant transformed to different austenite grains. As a result, grain refinement occurred during reverse transformation. Furthermore, tensile strength besides uniform elongation considerably enhanced in both pre-deformed and non-deformed specimens by reverse transformation. However, it should be noted that pre-deformed specimen exhibited larger yield strength comparing to the non-deformed specimen in the same cycle of the reverse transformation.

## **Effect of grain boundary, columnar boundary, and hydrogen in weld hot cracking**

S. Jothi<sup>1</sup>, T. Sebal<sup>2</sup>, E.D. Reese<sup>3</sup>

<sup>1</sup>Material Research Centre, College of Engineering, Swansea University, Bay Campus, Fabian Way, Swansea SA1 8EN, UK

<sup>2</sup>Airbus Defence and Space, 81663 Munich, Germany

<sup>3</sup>Airbus Group Innovations, 81663 Munich, Germany

Electrodeposited metallic metals are widely used as metallic structural materials in aerospace rockets due to their good thermal conductivity and corrosion resistance in high temperatures. However it is often accompanied by a limited weldability due to high hot cracking sensitivity. This paper presents a comparative overview of the susceptibility of Hot Cracking (HC) and weldability are influenced by the microstructure morphology including grain boundary (GB) and column boundary. HC are known to cause failures in aerospace components and it is vitally important to investigate the effect of microstructure morphology and GBC and column boundary in order to assess the resistance of weldability to these phenomena. In this investigation, Varcstraint hot ductility weldability test was conducted to evaluate this susceptibility on electrodeposited metal with complex microstructure. Scanning electron microscopy (SEM) in combination with electron backscatter diffraction (EBSD) and focus ion beam (FIB) was then performed to investigate the complex microstructure in electrodeposited metallic material. Then the welding was performed using gas tungsten arc welding (GTAW) on hydrogen charged and uncharged metallic material. The average value of total crack length (i.e the total length of all cracks occurs in both HAZ and FZ) was measured and used to represent the materials weldability. Optical microscopy was used to measure hot cracking. SEM in combination with EBSD was then performed to investigate the hot cracking associated with the columnar grain orientation distribution, grain boundary characteristics, residual plastic strain, and weldability. It reveals that columnar boundaries are the preferential path for hydrogen segregation and more susceptible to hydrogen induced hot cracking when compared to grain boundary. Grain boundary characteristic related to hot cracking are discussed.



**Kinetic models of impurity segregation in the grain boundaries of steels and the problem of quantitative AES measurements**

A.N. Khodan<sup>1</sup>, M.V. Sorokin<sup>1</sup>, A. Khvan<sup>2</sup>, E.A. Syutkin<sup>2</sup>, Z.V. Lavrukina<sup>1</sup>, D.A. Maltsev<sup>1</sup>,  
M.A. Saltykov<sup>1</sup>, A.I. Ryazanov<sup>1</sup>, B.A. Gurovich<sup>1</sup>

<sup>1</sup> Kurchatov Nuclear Technological Complex NRC "Kurchatov Institute", 1 Akademika  
Kurchatova Sq, 123182 Moscow, Russia

<sup>2</sup> Thermochemistry of materials SRC, NUST MISIS 4, Leninsky pr. 119049 Moscow, Russia

The temper embrittlement of steels remains an actual problem, and becomes particularly acute for the safety of nuclear reactors after prolonged operation. AES analysis of the grain boundaries (GB) in the test samples of reactor steels is an efficient method to control the content of impurity and kinetics of segregation. Quantitative description of the segregation kinetics in GB can be obtained if: (1) local AES analysis providing reliable data about the composition of the surfaces cleaved along GB, (2) changes of the chemical composition in GB may be measured during sufficiently long operation period, and (3) there is a physical model of segregation process that takes into account the influence of chemical and structural factors on the transport of impurities to the GB.

The use of standard AES techniques for the cleaved surfaces of GB gives results that are generally distorted by the presence in analysis zone  $\text{Me}_{23}\text{C}_6$  type precipitates with the average size  $\sim 100$  nm and the surface density of particles  $\sim 4 \cdot 10^{12} \text{ m}^{-2}$ . AES results can be corrected, if the average composition of carbide precipitates is known: for WWER-1000 vessel steel we obtained  $\sim (\text{Cr}_{0.9}\text{Mo}_{0.1})_{23}\text{C}_6$  by TEM and SEM techniques.

The effect of transgranular cleavage, existing on the GB surface, can be also estimated using morphological features of such sites and their proportion in the zone of analysis. Using SEM

methods we have obtained that for WWER-1000 vessel steel a cleaved area does not exceed 15%, and the value of AES data correction is comparable with the measurement accuracy.

We compared several physical models describing the segregation kinetics, in particular a simple [1-2] and more complex one, which takes into account the grain structure of the steel [3]. Applying the AES corrected data does not reveal the advantage of a particular model for  $t > 20$  years. However, application of the model [3] gives definitely more confidence for  $t < 10$  years results, whereas the kinetic dependencies, suggested in [1] and [2], constrains the dependence of the model [3] from above and below.

Accuracy of the impurity segregation kinetics prediction at long times ( $t > 10$  years) essentially depends on the estimation of the impurity equilibrium in the GB. Thermodynamic model was used for evaluation of the GB energy and elements concentrations in GB depending on temperature, pressure and composition in the grain volume. As a result, the value of 4.1 at.% was obtained for phosphorus equilibrium concentration in the GB, what is close to the experimental value of 3.7 at.% for WWER-1000 vessel steel 195000 hours at 315 °C [3].

- [1] D. McLean, Grain boundaries in metals (Clarendon Press, Oxford, 1957).
- [2] B.S. Bokstein, A.N. Khodan, O.O. Zabusov, D.A. Maltsev, B.A. Gurovich. Phys. Met. Metallogr. 115 (2014) 146.
- [3] M.V. Sorokin, Z.V. Lavrukhina, A.N. Khodan, D.A. Malzev, B.S. Bokstein, A.O. Rodin, A.I. Ryazanov, B.A. Gurovich. Materials Letters 158 (2015) 151–154

## Burrowing of metal particles into substrate by diffusion along interphase boundaries

L. Klinger, E. Rabkin

Department of the Material Science and Engineering, Technion-Israel Institute of Technology,  
Haifa, Israel

We simulated chemical interdiffusion of two components along an interphase boundary between two immiscible solids occurring simultaneously with an evaporation of one of the solids. We employed a general variation-based method for treating the morphology and microstructure evolution in heterophase solids controlled by surface and interphase boundary diffusion [1].

We demonstrated that depending on kinetic and thermodynamic parameters of the system the morphology evolution can be very different. Particularly, when diffusion along the interphase boundary is much faster than surface diffusion, the evaporating particles burrow into substrate and form long and narrow channels. The depth of these channels is much larger than initial dimensions of the particles.

Simulation results were in a good agreement with the results of recent experiments in which evaporating gold particles produced long and narrow pores in amorphous silica substrate [2].

[1] L. Klinger, E. Rabkin “Capillary-driven interdiffusion along interphase boundaries in solids” *Philosophical Magazine* **93** (2013) 2033-2043

[2] Lennart J. de Vreede, Albert van den Berg, Jan C. T. Eijkel “Nanopore Fabrication by Heating Au Particles on Ceramic Substrates” *Nano Letters* 2015 **15**, 727-731

## Layered epitaxial selenides grown on (0001) AlN: hetero-interfaces and defects

C. Bazioti<sup>1</sup>, G. P. Dimitrakopoulos<sup>1</sup>, P. Tsipas<sup>2</sup>, E. Xenogiannopoulou<sup>2</sup>,  
A. Dimoulas<sup>2</sup>, Ph. Komninou<sup>1</sup>

<sup>1</sup>Physics Department, Aristotle University of Thessaloniki, 54124 Thessaloniki, Greece

<sup>2</sup>Institute of Nanoscience and Nanotechnology, NCSR DEMOKRITOS, 15310, Athens, Greece

Successful epitaxial deposition of ultra-thin films by molecular beam epitaxy constitutes a significant advancement in the field of selenide compounds. The substrate of choice was (0001) AlN which, contrary to previous efforts on (111) Si epilayers, ensured a crystalline epitaxial interface as shown by high resolution transmission electron microscopy observations (HRTEM). This has been verified for Bi<sub>2</sub>Se<sub>3</sub>, MoSe<sub>2</sub>, and HfSe<sub>2</sub> epilayers that could be grown on wafer scale without interfacial amorphization, interdiffusion or chemical reaction. In the case of Bi<sub>2</sub>Se<sub>3</sub>, a topological insulator, angle-resolved photoelectron spectroscopy measurements verified a surface Dirac cone, whereas HRTEM, combined with geometrical phase analysis (GPA), showed an ordering Bi<sub>2</sub>Se<sub>3</sub>/AlN interface with 3:4 plane matching periodicity. Such two-dimensional (2D) behavior was exhibited for films with thicknesses of 3 and 5 quintuple layers (QLs) [1]. The films contained vertical and in-plane 180° rotational domain boundaries. Furthermore, ultra-thin films of MoSe<sub>2</sub> and HfSe<sub>2</sub> semiconductors comprising only a few monolayers (MLs) exhibited device quality suitable for nanoelectronics applications mediated by the van der Waals bonding [2]. The next forward was the combination of 2D selenide films in heterostructures in order to obtain additional benefits. One structurally successful approach was to employ Bi<sub>2</sub>Se<sub>3</sub> as a buffer layer in order to achieve a reduction of the deposition temperature. We have also studied multiple other heterostructures of the aforementioned compounds that demonstrate the attainable versatility towards advanced nanodevices e.g. for combined 2D semiconductor/TI applications. HRTEM image simulations were employed in conjunction with GPA order to localize the interfaces of the ultra-thin dissimilar materials.

[1]P. Tsipas, E. Xenogiannopoulou, S. Kassavetis, D. Tsoutsou, E. Golias, C. Bazioti, G.P. Dimitrakopoulos, Ph. Komninou, H. Liang, M. Caymax, A. Dimoulas. *ACS Nano* **8** (2014) 6614

[2]E. Xenogiannopoulou, P. Tsipas, K. E. Aretouli, D. Tsoutsou, S. A. Giamini, C. Bazioti, G.P. Dimitrakopoulos, Ph. Komninou, S. Brems, C. Hughebaert, I. P. Radu, A. Dimoulas. *Nanoscale* **7** (2015) 7896

**Acknowledgement:** Work supported by the ERC Advanced Grant SMARTGATE-291260- and the National program of excellence (ARISTEIA-745) through the project TOP-ELECTRONICS.

**Phase-field model of contact-line dynamics and interface migration  
in additive manufacturing of metals**

M.D. Krivilyov<sup>1</sup>, S.Dj. Mesarovic<sup>2</sup>, D.P. Sekulic<sup>3</sup>

<sup>1</sup>Institute of Mathematics, Informatics and Physics, Udmurt State University,  
Universitetskaya 1, 426034 Izhevsk, Russia

<sup>2</sup>School of Mechanical and Materials Engineering, Washington State University, PO Box  
642920, Pullman, WA 99164-2920, USA

<sup>3</sup>Department of Mechanical Engineering, University of Kentucky, Lexington, KY 40506, USA;  
School of Materials Science and Engineering, State Key Laboratory of Advanced Welding  
Technology, Harbin Institute of Technology, Harbin, 150001 China

The phase-field (PF) method based on the diffuse-interface approach [1] is suitable for an analysis of complex multiphase systems. Recently the PF model has been substantially extended to the problem of non-reactive and reactive wetting in Al brazing [2]. That model accounts for a diffusive nature of the triple “gas-liquid-solid” line kinetics. It has demonstrated (i) an excellent agreement with experimental data involving two non-reactive (water – glass, silicon oil – glass) systems and (ii) a fair agreement involving one reactive (Al-Si clad – Al substrate) system. Consequently, it was confirmed that migration of the interfaces under complex wetting conditions may quantitatively be described by PF well. In this work, a model of a multiphase flow is developed for a problem of powder consolidation in selective laser melting. The suitable PF formulation for this problem is presented and the boundary-value problem is critically analysed. The consolidation of few molten particles under conditions of laser heating is studied. The consolidation of carbonyl Fe powder with a typical particle size of 3  $\mu\text{m}$  is simulated. It is shown that the initial stage of the neck formation proceeds the time span of 0.001-0.01 ms, just at the beginning of a 1 ms laser pulse. The second stage where the molten metal - gas mixture consolidates is much slower. It consists of the migration of interfaces controlled by both system energy minimization and gas removal. As a result, the residual gas pores are observed in the compacts [3]. For inhomogeneous powders with ceramic inclusions the consolidation mechanism is even more complex due to a limited spreading velocity at triple lines. A suitability of the developed PF method for the analysis of composite powders is demonstrated as well.

- [1] D.M. Anderson, G.B. McFadden, A.A. Wheeler. *Ann. Rev. Fluid Mech.* **30**(1) (1998) 139
- [2] H. Fu, M. Dehsara, M. Krivilyov, S.Dj. Mesarovic, D.P. Sekulic. *J. Mater. Sci.* **51** (4) (2016) 1798
- [3] E.V. Kharanzhevskiy, M.D. Krivilyov. *The Physics of Metals and Metallography* **111** (1) (2011) 53

### Interfaces and defects in a steel-based composite

S. Lartigue-Korinek<sup>1</sup>, M. Walls<sup>2</sup>, W. Wang<sup>1</sup>, L. Mazerolles<sup>1</sup>,  
M. Dammak<sup>3</sup>, M. Gasperini<sup>3</sup>, F. Bonnet<sup>4</sup>

<sup>1</sup>Institut de Chimie et des Matériaux Paris-Est, UMR 7182 CNRS-Université Paris Est, 2 rue H. Dunant, 94320 Thiais, France

<sup>2</sup>Laboratoire de Physique des Solides UMR 8502 CNRS-Université Paris-Sud, Bât 510, 91405, Orsay, France

<sup>3</sup>Laboratoire des Sciences des Procédés et des Matériaux, UPR CNRS 3407, PRES Paris Sorbonne Cité, Université Paris 13, 93430 Villetaneuse, France

<sup>4</sup>ArcelorMittal Research SA, APRC, Voie Romaine, BP30320, 57283 - Maizières les Metz, France

The requirement for weight reduction in the automotive industry has led to the development of novel steel-based composites reinforced with titanium diboride ceramic particles and solidified directly from the melt through eutectic solidification route. These composites display a significant increase in specific stiffness ( $E/\rho$ ) in comparison with usual steels. The hot-rolled material shows a very limited final damage that is attributed to a strong interfacial cohesion and to the occurrence of a significant plastic deformation inside the  $TiB_2$  particles [1].

The chemistry and atomic structure of interfaces between  $TiB_2$  and Fe are investigated at the atomic level. Interfaces are mainly parallel to dense planes of the diboride, with a preferential growth of prismatic planes. Interfaces with specific orientation relationships display misfit dislocations located in the iron phase. The hot rolling operation induces a significant plastic deformation in the  $TiB_2$  particles with the activation of basal and prism plane slip systems. All these characteristics may account for the good behaviour of the composite during processing and when submitted to large deformations. Planar simple shear tests up to 50% plastic shear strain reveal that damage occurs mainly by diboride particles cracking. The deformation micro-mechanisms are analysed by transmission electron microscopy.

[1] S.Lartigue-Korinek, M.Walls, N. Haneche, L.Cha, L. Mazerolles, F. Bonnet, *Acta Materialia* **98** (2015) 297-305

## Auger electron spectroscopy study of grain boundary segregation in surveillance samples of Russian RPV steels after thermal exposure and irradiation

E.A. Kuleshova<sup>1,2</sup>, B.A. Gurovich<sup>1</sup>, Z.V. Lavrukhina<sup>1</sup>, M.A. Saltykov<sup>1</sup>, S.V. Fedotova<sup>1</sup>,  
A.N. Khodan<sup>1</sup>

<sup>1</sup>NRC "Kurchatov institute", Kurchatov sq.1, 123182, Moscow, Russia

<sup>2</sup>National Research Nuclear University "MEPhI" (Moscow Engineering Physics Institute)  
Kashirskoe highway 31, 115409, Moscow, Russia

Reactor pressure vessel (RPV) steels with bcc lattice are exposed to both operating temperature of ~300 °C and fast neutrons ( $E \geq 0.5$  MeV) irradiation. Long-term exposure to operational factors reduces the resistance of materials to brittle fracture, which is determined by ductile-to-brittle transition temperature shift ( $\Delta T_K$ ) in impact tests or fracture toughness curve shift to higher temperatures [1,2]. An increase of the ductile-to-brittle transition temperature  $T_K$  is due to both the hardening embrittlement mechanism caused by radiation-induced changes of the material phase composition, and the non-hardening one associated with the grain boundary (GB) and intragranular segregations [3]. Segregation processes in GBs start to play a special role for extending the RPV lifetime up to 60 years or more.

The most reliable information on RPV material condition can be obtained by investigation of the surveillance specimens (SS) that are subjected to operational factors simultaneously with the RPV [4, 5]. In this paper the GB composition in the SS with different thermal exposure time at RPV operating temperature as well as irradiated to different fast neutron fluences  $(20-71) \cdot 10^{22} \text{m}^{-2}$  was studied by means of Auger electron spectroscopy (AES) including both impurity and main alloying elements content.

The data obtained allowed to trace the influence of the operating temperature and radiation-stimulated diffusion on the overall segregants level in GB. The revealed differences in the concentration levels of GB segregants in different steels are due to the different chemical composition of the steels. The GB composition database revealed regularities of change in the impurities and alloying elements GB concentrations in Russian RPV steels under the influence of temperature exposure and irradiation. The experimental data allowed estimation of the GB impurity segregation kinetics for long-term operation period using both the well-known Langmuir-McLean model [6] and the one specially developed for RPV steels [7].

- [1] B. Gurovich, E. Kuleshova, Y. Shtrombakh, S. Fedotova, D. Maltsev, F. Frolov, D. Zhurko. *J. Nucl. Mater.* **456** (2015) 23
- [2] X. Bai, S. Wu, P.K. Liaw. *Mater. Des.* **89** (2016) 759
- [3] Y.I. Shtrombakh, B.A. Gurovich, E.A. Kuleshova, D.A. Maltsev, S.V. Fedotova, A.A. Chernobaeva, *J. Nucl. Mater.* **452** (2014) 348
- [4] M.K. Miller, K.F. Russell, J. Kocik, E. Keilova. *Micron.* **32(8)** (2001) 749
- [5] A. Kryukov, R.K. Nanstad, M. Brumovsky. *Nucl. Eng. Des.* **273** (2014) 175
- [6] D. McLean, Grain boundaries in metals, Clarendon Press, Oxford, (1957)
- [7] M.V. Sorokin, Z.V. Lavrukhina, A.N. Khodan, D.A. Malzev, B.S. Bokstein, A.O. Rodin, A.I. Ryazanov, B.A. Gurovich, *Mater. Lett.* **158** (2015) 151

## **Hierarchical Cr-containing high strength NiAl alloy produced by centrifugal SHS casting and vacuum induction remelting**

E.A. Levashov<sup>1</sup>, A.A. Zaitsev<sup>1</sup>, P.A. Loginov<sup>1</sup>, D.A. Sidorenko<sup>1</sup>, Yu.S. Pogozhev<sup>1</sup>, Zh.A. Sentyurina<sup>1</sup>, S.I. Rupasov<sup>1</sup>, M.I. Petrzhik<sup>1</sup>, V.N. Sanin<sup>2</sup>, V.I. Yukhvid<sup>2</sup>

<sup>1</sup>National University of Science and Technology “MISIS”, Leninsky prospect, 4, Moscow, 119049 Russia

<sup>2</sup>Institute of Structural Macrokinetics and Materials Science, Russian Academy of Sciences, ul. Academica Osipyana, 8, Chernogolovka, Moscow district, 142432 Russia

Integral technology are currently developing and include: 1- centrifugal SHS casting of a semi-product based on NiAl using oxide raw material; 2- vacuum remelting of semi-product with structure modification using nanopowder containing master alloys and electrode molding; 3- centrifugal sputtering of electrodes and classification of granules to the specified grain size. Advanced NiAl-CrCoHf alloy composition with the allowable impurity content, high strength with partial plastic deformation at the room temperature was developed. SHS under centrifugal forces including searching for the optimal modes to provide the greatest degree of phase separation from the slag phase and formation of porous free alloy was performed. Content of alloying and functional additives, crystallization conditions were optimized in order to achieve hierarchical SHS-alloy CompoNiAl-M5 with 4 levels structure: *1<sup>st</sup> level* - large sized grains consist of colonies of NiAl dendrites separated from each other by 1-2  $\mu\text{m}$  layers of Cr-base solid solution and Hf ( $\sim 1 \mu\text{m}$ ) particles; *2<sup>nd</sup> level* is a single NiAl dendrite with central part containing Co, Cr and Cr-rich periphery; *3<sup>rd</sup> level* – 50-150 nm Cr-based spherical ring shaped precipitations (81-83% Cr, 3-5% Co, 10-14 at.% Al+Ni) inside NiAl matrix; *4<sup>th</sup> level* – 3-4 nm precipitations of Cr in the body of NiAl matrix clear observed after the foil heating in a microscope column. The 4<sup>th</sup> level nanocrystal grows up from 3-4 nm to 40 nm after 30 min annealing at 700<sup>o</sup>C. Moreover, it was observed the annealing resulting in the fragmentation of 3<sup>rd</sup> level Cr-based precipitations from size 250-300 nm to 20-30 nm. Cr content in ring intermediate zone (about 50 nm thick) decrease from center to periphery that is demonstrates diffusion mechanism of precipitation's formation. Such 4 level structures were observed in SHS-alloys with relation Cr/Co $\sim$ 1-3. The high content of Cr in alloys the Cr-based layer in between the dendrites becomes thicker. This leads to increase in amounts of nanosized precipitations. It was shown that the coherent structure of interphase between NiAl phase and Cr- precipitations forms in case of its size less than 80 nm. But if precipitation size higher than 150 nm interphase has amorphous structure.

Interesting that heritage of hierarchical 4 level structures has been established after vacuum remelting of alloys. Compressive strength of SHS- alloy samples at  $T_{\text{room}}$  achieve to 2260 $\pm$ 210 MPa. However strength of alloy after remelting becomes smaller (1710 $\pm$ 90 MPa) resulting larger size of Cr-based precipitations (till 0,5  $\mu\text{m}$ ) because of less cooling rate of crystallization. Further increasing the size of Cr-based precipitations (1  $\mu\text{m}$ ) resulting recrystallization at annealing (860 C, 3 h) was observed. Effects of Cr concentration in a wide range of value Cr/Co=0,5-3 on the phase state, microstructure, hardness H, elastic recovery, elastic modulus E, strength, H/E,  $H^3/E^2$  oxidation resistance were well characterized using a combination of various techniques including SEM, TEM, HR TEM, XRD, indentation tests.

Authors gratefully acknowledge the support from the Ministry of Education and Science of the Russian Federation in the framework of Federal Target Program on Priority Directions of R&D



in 2014–2020 (agreement 14.578.21.0040, project RFMEFI57814X0040).

**Origin of size dependent concurrence of grain growth and phase transition: a deep insight from thermodynamics and kinetics**

B. Lin, L.K. Huang, W.T. Lin, F. Liu

State Key Laboratory of Solidification Processing, Northwestern Polytechnical University,  
Xi'an, Shaanxi 710072, P.R. China

Concurrence of grain growth and phase transition are ubiquitous in condensed matter physics; however, the thermodynamics and kinetics involved which is critical to understand the concurrence remains scarcely studied. Here, we performed a systematic study of probing the interaction between phase transition and grain growth by adjusting the grain size when phase transition is triggered. Our study indicates as the grain size decreases the measured enthalpy change decreases, and both transition kinetics are more strongly influenced. Furthermore, we give a full description of the thermodynamic driving force and kinetic activation energy of every individual elemental process, suggesting a reverse correlation exists for both two solid reactions. Our findings clearly provide a comprehensive picture on the size-dependent concurring kinetics of grain growth and phase transition, and show a method to tailor the interaction in between, which could be easily extent to other material system.

**Unexplored dual-phase bimodal microstructure induced by two conventionally undesirable reactions in nanostructured materials**

W.T. Lin, L.K. Huang, B. Lin, F. Liu

State Key Laboratory of Solidification Processing, Northwestern Polytechnical University,  
Xi'an, Shaanxi 710072, P.R. China

In nanostructured metals, heterogeneous and multi-scale microstructure is found to be effective in improving the low ductility, which has been the Achilles heel of their application as structural materials. To achieve the unique microstructure, generally, various strategies focus on the design of fabrication process rather than the application of inherent microstructural changes, such as phase transition and grain growth, since they are conventionally undesirable and considered as two typical reflections when nanostructured materials suffer instability. Here, we report a new kind of heterogeneous microstructure, i.e., dual-phase bimodal microstructure, induced by the concurrence of phase transition and grain growth. The physics behind the concurrence aiming to understand the formation of this kind of heterogeneous microstructure, are investigated both experimentally and computationally from macro- to micro-scale. The present finding, offers an unexplored and feasible strategy that is expected to find important applications in optimizing the mechanical properties in nanostructured materials.

**Atomistic simulations predict a second-order phase transition in grain boundaries of nanocrystalline copper**

A.G. Lipnitskii, I.V. Nelasov

Belgorod State University, 85, Pobedy St., Belgorod, 308015, Russia

Phase transformations in metallic grain boundaries (GB) and their impact on the grain boundary diffusion present significant fundamental interest in the context of properties of low-dimensional systems. We report on atomistic computer simulations of the nanocrystalline copper that provide direct evidence that a second-order phase transition, which affects the GB diffusion, can exist in a single-component GB. We calculated the average excess volume, entropy, enthalpy, Gibbs energy (the grain boundary energy) and the diffusion characteristics of the high angle grain boundaries of general type in nanocrystalline copper as functions of temperature at 0 GPa by molecular dynamics method. We found that all the above thermodynamics characteristics of the grain boundaries are continuous functions at the considered temperatures in the range from 350 to 900 K. At the same time, the temperature dependences for the volume, the entropy and the enthalpy change slope at about 600 K in contrast to the Gibbs energy, for which there is no change of slope. The established temperature dependence of the thermodynamic quantities characterizes a phase transition of second order in the grain boundaries. The calculated activation energy of the grain boundary diffusion changes from  $0.71 \pm 0.02$  eV/atom in the range 600-1200 K to  $0.38 \pm 0.04$  eV/atom in the range 350-550 K. Thus, the results of our simulations predict the existence of the second-order phase transition in the grain boundaries of general type in copper, which is accompanied by the change in the characteristics of grain boundary diffusion.

**Concurring phenomenon of phase transition and grain growth in nanostructured alloys**

F. Liu, L.K. Huang, W.T. Lin, B. Lin

State Key Laboratory of Solidification Processing, Northwestern Polytechnical University,  
Xi'an, Shaanxi 710072, P.R. China

Concurrence of grain growth and phase transition is ubiquitous in material science; however, due to the lack of kinetic evidences directly observed, the underlying physics of concurrence remains scarcely understood. Here, we report, for the first time, macro- and micro-scale observations for the concurrence in nanostructured alloys. Macroscopically, concomitant grain growth occurs to alter both the constitution of enthalpy change and the kinetics of phase transition, and ceases before the end of phase transition. And microscopically, grain boundary and phase boundary migrations are mutually affected. On this basis, a size-dependant kinetic model of phase transition in nanostructured alloys is proposed, by which the interaction of phase transition and grain growth could be tuned, and particularly dual-phase bimodal microstructure can be formed by adjusting the concurrence. The present findings, reveal a new behaviour of phase transition owing to the grain size.

## Atomic and charge state of hydrogen at low-angle grain boundaries in silicon

A.S. Loshachenko, N.V. Vysotskii, E.V. Borisov, O.F. Vyvenko

Saint-Petersburg State University, 1 Ulyanovskaya str., Saint-Petersburg, 198504 Russia

Grain boundaries (GB) are well known to be effective gettering centers for impurities in any materials. More interest impurity for silicon is hydrogen (H) due to its technological importance in photovoltaic industry. The segregation of hydrogen at the GBs leads to the reduction or even complete vanishing of excess charged carrier recombination significantly increasing multi-crystalline silicon (mc-Si) solar cell efficiency. That phenomenon is well known as “hydrogen passivation” of GBs but detailed understanding of the H-GBs interaction processes fails which, in turn, is due to experimental difficulties of mc-Si investigation.

Here we report the results of our study of the model objects which were low-angle GBs produced by direct bonding of two mutually twisted (0.5-3°) and tilted (0.5-0.8°) Si wafers combined with SmartCut technology. GBs produced in this way consist of square dislocation networks (DN) of screw and rows of edge type dislocation with the interdislocation distances in the ranges between 5 nm to 50nm. The DNs were situated at the depth of 200 nm making them an ideal model structure for studying of H influence on the GB by means of combination of diverse experimental techniques such as electro-physical characterization, transmission electron microscopy (TEM) and Raman spectroscopy. Hydrogenation was implemented by means of wet-chemical etching in buffered HF. Electro-physical investigations of schottky diodes prepared on the wafers with the DNs revealed that H did not penetrate though the GBs being captured with them in a neutral charge state [1, 2].

Atomic configuration of H captured at GBs was determined with the help of Raman spectroscopy in combination with TEM [1]. Thin plan view TEM foils prepared from the bonded wafers served as the samples under the investigations that allowed to reduce Raman background and to determine spatial localization of the detected signal. An additional broad Raman peak at 2000 cm<sup>-1</sup> was found at the GBs. Such peak is known as Si bond stretch mode indicating that H at the GB is located in Si bond center (BC) position as a single atom. That results confirmed recent theoretical prediction [3] that H<sub>2</sub> molecule in T-site which is energetically favorable in regular Si lattice dissociates in the region of shear elastic strains of dislocations making more stable monoatomic BC configuration.

The experimental data were obtained using equipment of the Interdisciplinary Recourse Center for Nanotechnology and Centre for Optical and Laser Materials Research at St. Petersburg State University, Russia.

- [1] Vysotskii N, Loshachenko A, Borisov E, Vyvenko O. *J. Phys: Conf Ser.* **690** (2016) 012004
- [2] Loshachenko A, Bondarenko A, Vyvenko O, Kononchuk O. *Physica status solidi (c)* **10** (2013) 36-39.
- [3] Matsubara M, Godet J, Pizzagalli L. *J. Phys.: Cond. Mat.* **22** (2010) 035803.

**Electroconductive properties of composite based on oxide ceramic aerogel modified with carbon nanotubes**

E.A. Lyapunova<sup>1,2,3</sup>, I.A. Morozov<sup>2,3</sup>, O.B.Naimark<sup>2,3</sup>

<sup>1</sup>Institute of natural sciences, Ural Federal University, 620000 Ekaterinburg, 48 Kuibyshev str., Russia

<sup>2</sup>Institute of continuous media mechanics, Ural Branch of RAS, 614013 Perm, 1, Ak. Korolev str., Russia

<sup>3</sup>Perm State University, 614990 Perm, 15 Bukirev str., Russia

Development of novel functional materials based on nanocarbons and inorganic compounds is one of the priorities of modern material science. Such hybrids can be used as active electrodes for photovoltaics and catalysis, new generation filters for water deionization and desalination. In order to maximize the functional properties of such materials, it is necessary to create the well-developed bulk conductive structure. Despite of significant progress in this field of material science, there are still many uncertainties associated with the optimal synthesis methods and properties of such bulk conductive systems. In the present work results of experimental investigations of the conductivity of bulk composite produced by hydrothermal synthesis and critical point drying of ceramic precursor hydrogel are reported.

Hybrid composite was made from zirconium dioxide/0.2 wt.% multiwalled carbon nanotube aerogel fragments thermally pretreated at 1000 °C and consolidated into 1.5 mm thick tablets by hot pressing in a graphite matrix in an argon atmosphere. Thermal pretreatment of aerogel fragments caused rigid fixation of carbon nanotubes arrangement formed during hydrothermal synthesis and preserved by critical point drying.

The synthesized composite exhibits bulk percolation cluster-like conductivity provided by the spatial configuration of carbon nanotubes in aerogel ceramic matrix. This bulk conductivity was spread to the macroscopic scale by hot pressing of aerogel fragments, which not only preserved their structure during treatment but also formed contact points. The presence of unclosed conductive loops in the bulk percolation cluster and the possibility of their closing by movable ions were demonstrated in the experiments on registration of I-V curves during the evacuation of the composite impregnated with distilled water. The obtained experimental data show that electric properties of the composite can be represented as the parallel connections of numerous voltage dividers constituting the bulk porous structure.

This work is supported by Russian Found for Basic Research (project № 14-01-96015).

### **Grain boundary wetting in W–Ni alloys**

A. Mazilkin<sup>1,2</sup>, B. Straumal<sup>1,2</sup>, S. Protasova<sup>1</sup>, B. Baretzky<sup>2</sup>

<sup>1</sup>Institute of Solid State Physics, Russian Academy of Sciences, 142432 Chernogolovka, Russia

<sup>3</sup>Karlsruher Institut für Technologie (KIT), Institut für Nanotechnologie, 76344 Eggenstein-Leopoldshafen, Germany

Aim of the investigation is of the wetting (covering) phase transition in the binary W –Ni system. Influence of the alloys composition and annealing temperature on the structure of grain boundaries has been studied. The study was carried out by means of high-resolution electron microscopy and analytical electron microscopy. W –Ni phase diagram contained tie lines of the liquid and solid-state wetting transition was constructed taking into account the obtained experimental results and the results of the literature search among the available published data.

Authors thank the Russian Foundation for Basic Research (contracts 14-42-03621 2014) for the financial support.



## Surface and grain boundary effects in luminescent properties of ZnO ceramics as functional material

F. Muktepavela<sup>1</sup>, E. Gorokhova<sup>2</sup>, L. Grigorjeva<sup>1</sup>, E. Tamanis<sup>3</sup>, R. Zabelis<sup>1</sup>

<sup>1</sup>Institute of Solid State Physics, University of Latvia, 8 Kengaraga str, Riga LV-1063, Latvia

<sup>2</sup>Research and Technological Institute of Optical Materials All-Russia Scientific Center “S.I. Vavilov State Optical Institute” 36 Babushkina str, St. Petersburg 192171, Russia

<sup>3</sup>Daugavpils University, 13 Vienibas str., Daugavpils, LV-5401, Latvia

Due to unique optical, electrical and piezoelectric properties Zinc oxide is a promising multifunctional wide band semiconductor material for applications in lasers, light-emitting diodes, short-wavelength optoelectronics, sensors, spintronic, etc. Taking into account the great opportunities of ZnO ceramics as a high-speed scintillators, hot pressing methods for obtaining transparent ZnO ceramics have been developed [1]. However, creating ZnO ceramic with a high-quality structure is largely determined by the initial stages of sintering due to the influence of agglomeration of ZnO grained powders leading to segregation and formation of pores on initial grain boundaries (GB) during sintering. On the other hand ZnO in form of tetrapods, due to their geometry and energy factors, cannot form aggregates and agglomerate [2]. Such a way opens up a new and quite simple possibility to control the sintering process. In this work ZnO ceramics obtained from grained powders by hot pressing (at 1100<sup>0</sup>C) and ceramic from tetrapods obtained by press-less sintering at 1200<sup>0</sup>C have been investigated using nanoindentation, SEM, AFM and photoluminescence (PL) methods. A comparative analysis of properties showed that ceramics obtained by hot pressing were composed of inhomogeneous grains (d=8-35μm) exhibiting a faceted substructure. Decreased values of elastic modulus within a grain and a wide defect-associated (“green”) PL band at 2.2-2.8 eV in conjunction with a weak excitonic band indicate on a high concentration of residual point defects. The cause for these defects is dissolution of, typical for agglomerations, initial micropores into point defects during hot pressing. Their stability is attributed to slow low-angle GB diffusion and large distance to probable sinks on the grain growth stage. Use of the powder with a uniform grain size and the addition of tetrapods led to a significant increase of excitonic band and elimination of PL defect band that is very important for fast scintillators. Ceramics obtained from tetrapods had fine-grained structure (d=1-4μm) with no signs of a substructure. PL spectrum had a narrow excitonic band with phonon replicas (1LO\_ExD<sup>0</sup>) whereas the “green” (defect associated) luminescence is negligible. This is due to the fact that during sintering tetrapod-like particles transformed into grains with randomly misorientated large-angle GBs which are efficient paths for atomic transport and densification. In work it is shown that by controlling the optimal combination of powders morphology with the structure of GBs ZnO ceramics with desired properties can be obtained for use as gas sensors, UV-emission detectors (by press-less sintering) and as transparent fast scintillators (by hot press sintering). This work has been supported by the National Research Program IMIS2

[1] E. I. Gorokhova, P. Rodnij et al **75** (2008) *J. Opt. Technol.* 66–72

[2] F. Muktepavela, V. Sursajeva, L. Grigorjeva, K. Kundzins *Mater.Sci.Eng. Conf Ser.* **38** (2012) 012016

**The influence of interfaces on mechanical and acoustic properties of titanium alloys**

E.V. Naydenkin, I.V. Ratochka, I.P. Mishin, O.N. Lykova

Institute of Strength Physics and Materials Sciences, Siberian Branch of Russian Academy of Sciences, Tomsk, pr. Akademicheskii 2/4, 634055 Russia

The interfaces (intergranular and interphase boundaries) largely determine mechanical properties, character of deformation behavior and fracture of metallic materials. In recent years polycrystalline materials with ultrafine-grained (submicro- and nanocrystalline) structure are intensively developed and investigated. The formation of such structure by methods of severe plastic deformation leads to significant increase in density of interfaces and change in physical-mechanical properties of metals and alloys. In particular, such materials can exhibit low-temperature and/or high strain rate superplasticity under certain conditions. Herewith, the mechanical behavior of such materials under superplastic deformation is determined not only by grain size but also the structural-phase state and a high degree of nonequilibrium grain boundaries with enhanced diffusivity. Meanwhile, the behavior of ultrafine-grained materials under external influences has a number of features that are currently not fully understood. In this regard, experimental studies of the effect of structural-phase state on mechanical and acoustic properties of titanium alloys are relevant.

I

In present work the influence of structure and phase composition of the ultrafine-grained (UFG)  $\alpha+\beta$  titanium alloys, obtained by method of *abc* pressing, on the features of plastic deformation was investigated. It was established that the formation of UFG structure in the investigated titanium alloys increases the yield strength at room temperature by 30-40% with a simultaneous reduction in ductility as compared with coarse-grained counterparts. Herewith the temperature of the beginning of superplastic flow realization is reduced by 150-200 degrees (up to 823K). Shift of superplasticity interval, apparently, caused by significant decrease in size of grain-subgrain

structure (less than 0.3  $\mu\text{m}$ ) and increase of the nonequilibrium of grain boundaries in the UFG alloys. The increase in volume fraction of  $\beta$ -phase and, consequently, the length of interphase boundaries in the alloys leads to enhancement of temperature interval of superplastic flow and elongation to failure ( $>1300\%$ ). It can be assumed that this effect is due to the stabilization of the ultrafine-grained state in titanium alloys by the formation of micro-duplex two-phase structure.

The increase in density of interfaces also leads to a change in the acoustic characteristics of titanium alloys. Acoustic testing in ultra-sound range with high power density (amplitude 100  $\mu\text{m}$  and above) shows that the failure of the waveguides from the titanium alloy with UFG structure occurred at a power about 1.5-2 times higher than for those from initial coarse-grained material. The work resource (multi-cycle loading) of the waveguide from UFG alloy was more than 10 hours while another one with coarse-grained structure was destroyed after a few seconds. In the case of waveguides fabricated from UFG alloy was observed the decrease of resonant frequency vibrations about 0.5%. That can be associated with corresponding decrease in density of the alloy due to the formation of UFG structure.

Thus, the increase in density of the interfaces in the UFG titanium alloys leads to grow in the strength properties and fracture resistance under conditions of ultra-sound influence, and to decrease of temperature interval of superplasticity realization. The increase in volume fraction of  $\beta$ -phase in the alloys contributes to extension of temperature range of superplasticity and increases the elongation to failure.

## Interfacial structure and contact angle of Al/sapphire system

Xiao-Shan Ning, Yang Liu

State key laboratory of new ceramics and fine processing, School of Materials Science and Engineering, Tsinghua University, Haidian district, Beijing, 100084, China

The contact angle of Al/Al<sub>2</sub>O<sub>3</sub> system is important both for manufacturing of composite and for the study of interface physics [1]. Its research has been lasted over 60 years, but there still lack a consensus relating with the value of contact angle. John et al [2] used Zr getter, and measured a value of 90° at 700°C. Levi et al [3] measured a similar value under a lower oxygen partial pressure in a temperature range from 900 to 1000°C. Naidich [4] adopted an improved sessile drop method (IM) and measured a similar value in 700-800°C, but 72° at 1100°C. Wang et al [5] used IM and Zr getter, and measured a value of 90° in 660-800°C and 74° at 850°C. Weirauch [6] found that IM cannot prevent the quick oxidation of the Al drop after being pushed out from orifice, and the contact angle of 90° measured at 800°C by IM actually reflects a wettability of Al with a 4-nm-thick oxide film. A contact angle of 50° was measured after the breaking of the oxide film. Recently, we successfully coated a layer of molten Al on sapphire, which means that the contact angle can even decrease to near zero degree at some specific conditions [7]. In the present work, we study the interface of a dip-coating sample by HRTEM. The interfacial structure of the dip coating sample is much different from the interface reported by other group, but are in consistent with a simulated non-stoichiometric Al<sub>2</sub>O<sub>3</sub>/Al interface. It is concluded that the super wetting phenomena in dip coating comes from the reconstruction of the surface of Al<sub>2</sub>O<sub>3</sub>; and the contact angle of Al/Al<sub>2</sub>O<sub>3</sub> system depends on the partial pressure of oxygen at the vicinity of the interface and the free surface of Al drop.

- [1] D. J. Siegel, L.G. Hector, Jr, J. B. Adams. *Phys. Rev. B* **65** (2002) 085415.
- [2] H. John, H. Hausner. *J. Mater. Sci. Lett.* **5**(1986)549.
- [3] G. Levi, W. D. Kaplan. *Acta Materialia* **50**(2002)75.
- [4] Y. Naidich. *Prog. Surf. Membrane Sci.* **14**(1981)353.
- [5] D. J. Wang, S. T. Wu. *Acta metal. mater.* **42**(1994)4029.
- [6] D. A. Weirauch, Jr. *Ceramic Microstructure '86*, 329. Plenum Press, New York.
- [7] X. S. Ning, S. Li, B. Wang, G. C. Li, N. Bi, Y. Liu. *Ceramic Transaction*, **249**(2014)93.

**Method of substitution of atoms - a new method for the synthesis of nanomaterials.  
First order phase transition through an intermediate state**

S.A. Kukushkin, A.V. Osipov

Institute of Problems of Mechanical Engineering RAS, V.O., Bolshoj pr. 61, St. Petersburg,  
199178 Russia

A modern state of the growth of epitaxial SiC films on Si is presented by a new method of atoms substitution. An ideology of the new method of SiC synthesis on Si is stated and a comparison of the theoretical statements with the experimental results is provided [1]. The method consists in replacing a fraction of atoms of the silicon matrix by the carbon atoms to form molecules of silicon carbide. It was experimentally discovered that the process of substitution of Si matrix occurs gradually without destroying its crystal structure. The film orientation is set therewith not only by the surface of the silicon substrate but by the crystal structure of the original silicon matrix. A comparison of the new method of growth with the classical methods of thin film growth is presented. The properties of the realized SiC layers are specified in detail.

By the example of chemical interaction of CO gas with monocrystalline Si matrix, the mechanism of behavior of a broad class of heterogeneous chemical reactions between the gas phase and solid has been revealed [1]. As a result of this has been described a new type of phase transitions in a solid phase with a chemical reaction conducted through an intermediate state [2]. This method will be illustrated by an example of the growth of SiC epitaxial layers due to the chemical interaction of CO gas with the monocrystalline silicon matrix. The theory of first order phase transitions in systems where the direct formation of nuclei of a new phase is inhibited for any reason, for example, because of the extremely high elastic energy, has been constructed using the example of the silicon–silicon carbide phase transition due to the chemical reaction with carbon monoxide. It has been shown that, in this case, the phase transition occurs through an intermediate state, which significantly promotes the formation of new phase nuclei. For the silicon–silicon carbide phase transition, such an intermediate state is the “precarbide” state of silicon saturated with dilatation dipoles, i.e., pairs formed by a carbon atom and a silicon vacancy that are strongly attracted to each other. The model dependence of the potential energy of systems with an intermediate phase on the reaction coordinates has been investigated. The kinetics of transformation of the intermediate state into a new phase has been described.

[1] S.A. Kukushkin and A.V. Osipov. *J. of Phys. D: Appl. Phys.* **47** (2014) 313001.

[2] S.A. Kukushkin and A.V. Osipov. *Physics of the Solid State.* **56** (2014) 792.

**Slip dislocation and twin nucleation mechanisms in hcp metals**

A. Ostapovets<sup>1</sup>, A. Serra<sup>2</sup>

<sup>1</sup>Central European Institute of Technology - Institute of Physics of Materials (CEITEC IPM),  
Academy of Sciences of the Czech Republic, Žitkova 22, 61662 Brno, Czech Republic

<sup>2</sup>Department of Civil & Environmental Engineering, Universitat Politecnica de Catalunya,  
Jordi Girona 1-3, 08034 Barcelona, Spain

New nucleation mechanism will be proposed for  $\{10\bar{1}1\}$  deformation twin in hcp materials. The mechanism is based on the results of atomistic computer simulations. The proposed mechanism will be described by means of different dislocation and disconnection reactions. Under certain circumstances these reactions can lead to the formation of a twin embryo from the core of the slip dislocation. The disconnections are line defects, which produce step on the twin boundaries. Such defects can be characterized by Burgers vector and step height. Geometry and crystallography of different defects taking part in twin nucleation and growth will be discussed.

### **Plasticity of martensitic Ni-Mn-Ga alloys**

R.C. Pond<sup>1</sup>, B. Muntiferling<sup>2</sup>, W.B. Knowlton<sup>2</sup>, P. Mullner<sup>2</sup>, L. Kovaric<sup>3</sup>, N.D. Browning<sup>3</sup>

<sup>1</sup>College of Engineering, Mathematics and Physical Sciences, University of Exeter, Exeter, EX4 4QF, U.K.

<sup>2</sup>Department of Materials Science and Engineering, Boise State University, ID 83725, U.S.A.

<sup>3</sup>Environmental Molecular Sciences Laboratory, Pacific Northwest National Laboratory, P.O. Box 999, Richland, WA 99352, U.S.A.

Deformation twinning (DT) is the predominant mode of plasticity in martensitic alloys with compositions near Ni<sub>2</sub>MnGa. HRTEM images are presented of non modulated tetragonal martensite, establishing the Burgers vector of twinning dislocations and the twin boundary structure: these observations are consistent with low twinning stress and rapid twin growth. During transformation from the austenitic phase, DT is the lattice-invariant deformation mode, leading to lamellar 40%twin/60%matrix composite domains in the martensitic phase. Microstructural features commonly observed in this phase, named “conjugation boundaries”, separate domains wherein the matrix lamellae are misoriented in the range 5 – 7°, while the interposed lamellae are formed by conjugate DT modes. HRTEM images are presented of stationary conjugation boundaries and also their motion in response to in-situ applied strain. As suggested by Mullner and King in 2010, one domain is converted into the other when both its matrix and twin lamellae undergo 50% secondary DT. In this process, the twinning dislocations which are generated accumulate at the primary matrix/twin interfaces in a coordinated manner, thereby increasing the misorientation by about 23°. Concomitantly, this mechanism produces a volume conserving deformation of a few %.

## Segregation in hetero-phase, semi-coherent interfaces and spinodal decomposition microstructures in AgCu

L. Luneville<sup>1,4</sup>, V. Pontikis<sup>2,3</sup>, D. Simeone<sup>1,2</sup>

<sup>1</sup>SPMS, LRC Carmen, Centralesupelec, CNRS, Châtenay-Malabry, France.

<sup>2</sup>DMN, SRMA, LRC Carmen, CEA, Gif-sur-Yvette, France.

<sup>3</sup>DSM, IRAMIS, LSI, CEA, Gif-sur-Yvette, France.

<sup>4</sup>DM2S, SERMA, LRC Carmen, CEA, Gif-sur-Yvette, France.

We study semi-coherent interfaces between the immiscible metals Ag and Cu by means of Molecular Dynamics and grand-canonical Monte Carlo simulations using adapted phenomenological n-body potentials from the literature. It is shown that unlike the prediction of the binary phase diagram, at the thermodynamic equilibrium a smooth miscibility profile establishes across Ag/Cu (100) and (110) hetero-phase interfaces, necessary for minimizing the excess free energy of the interface, thus suggesting that welds between no-miscible metals are feasible. Moreover, we demonstrate that coupling of the atomic and mesoscopic scales is possible via an appropriate Landau free energy functional. Advantage is taken from this finding for exploring the microstructures generated in the spinodal decomposition domain of a thermodynamically unstable concentrated Ag/Cu solution. Ongoing work focuses on the mechanical stability and resistance of such assemblies.



## **RIGAKU's X-ray diffractometer**

A. Puchkov

E-Globaledge Corporation (Japan)

Nowadays, X-ray analytical technique is widely used for materials characterization. It has some characteristic features, distinguishing it from those of other analytical techniques. One is that gives the three-dimensional structural information in atomic scale. The other is that gives accurate and precise quantitative data such as interatomic distances and bond angles. Properties and functions of materials are closely related with their structures. So the structural information is indispensable for understanding the structure-property/function relationship of materials.

**Taming the hollowness: synthesis of hollow nanostructures by short-circuit diffusion**

E. Rabkin<sup>1</sup>, N. Gazit<sup>1</sup>, S. Baylan<sup>2</sup>, A. Kosinova<sup>1</sup>, L. Klinger<sup>1</sup>, G. Richter<sup>2</sup>

<sup>1</sup>Department of Materials Science and Engineering, Technion-Israel Institute of Technology,  
32000 Haifa, Israel

<sup>2</sup>Max Planck Institute for Intelligent Systems, Heisenbergstr. 3, 70569 Stuttgart, Germany.

Hollow metallic nanostructures (nanotubes, nanoparticles) are at the forefront of a number of nanotechnology-related applications. We demonstrate that metal nanotubes and hollow nanoparticles can be produced at low homological temperatures employing a combination of surface, interface, and grain boundary diffusion. Silver nanowhiskers and nanoparticles were manufactured employing molecular beam epitaxy and solid state dewetting techniques [1]. A thin nanocrystalline gold overlayer was then deposited on these silver nanostructures, and the composite systems were annealed at low homological temperatures at which no bulk interdiffusion occurs. After annealing, gold nanotubes and nanoshells were formed. The hollowing process was discussed in terms of surface-diffusion assisted bulk intermixing (SDIBI). Silver atoms rejected by the hollowing structures were absorbed by a layer of silver-gold alloy forming on the gold film surface, resulting in significant thickening of the film. In another process, hollow gold nanoparticles were produced by a combination of solid state dewetting of the silver-gold alloy, selective dissolution of silver, and subsequent coarsening heat treatment [2]. This process allows synthesis of porous gold nanoparticles with both open and close porosity.

[1] S. Baylan, G. Richter, M. Beregovsky, D. Amram, E. Rabkin *Acta mater.* **82** (2015) 145.

[2] A. Kosinova, D. Wang, P. Schaaf, O. Kovalenko, L. Klinger, E. Rabkin *Acta mater.* **102** (2016) 108.

## Faceting of grain boundaries in nanosilicon films

N.G. Nakhodkin, T.V. Rodionova

Taras Shevchenko National University of Kyiv, 4g, Academician Glushkov Prosp., Kyiv 03022, Ukraine

Nanosilicon films are one of the leading electronic materials for large-area application as solar cells or switching electronics used for flat-panel displays. As is known [1], the characteristics of the electronic devices that used nanosilicon films are directly connected with the structural properties of the films, in particular, their grain boundary and grain boundary joints. Some grain boundary in nanosilicon films are faceted. Faceting of grain boundary or surfaces is defined as transformation of the original surface or grain boundary into flat segments whose energy is less than that of the original surface or grain boundary [2]. As is known [3], faceted grain boundary have a low trap density. Thus, the presence of the faceted grain boundary is favorable for electronic devices, such as thin transistors and solar cells.

In this work, the grain boundary faceting in undoped nanosilicon films have been investigated by transmission electron microscopy(TEM).

Nanosilicon films were prepared by low-pressure chemical vapor deposition from a silane/argon mixture. Films were deposited on thermally oxidized (100 nm oxide thickness)(100) single-crystal silicon wafers. The deposition temperature was equal to 630<sup>0</sup>C. The film thickness was ranged from 3 to 100 nm.

TEM studies show that the following facet types are observed in undoped polysilicon films:

γ 90<sup>0</sup> facets, which are formed by twin boundaries  $S=3\{111\}_1/\{111\}_2$  (or (100)CSL) and  $\{211\}_1/\{211\}_2$  (or (010)CSL) and 124<sup>0</sup> facets, which are characterized by the following orientations:  $S=3\{111\}_1/\{111\}_2$ ,  $S=9\{122\}_1/\{122\}_3$ , and  $S=3\{111\}_2/\{111\}_3$ . The subscripts 1, 2 and 3 correspond to the grains 1, 2 and 3).

All facets that were observed in nanosilicon films are generally parallel to close-packed CSL planes and contain the  $\parallel 110 \parallel$  axis with the maximum density of coincidence sites.

In contrast to thick (500 nm) phosphorus-doped films [4,5], 109<sup>0</sup> and 140<sup>0</sup> facets are not observed in undoped nanosilicon films. It can be assumed that this difference is caused by the presence of different types of special grain boundaries in the films depending on the film thickness, doping, annealing.

[1] - S. Mukhopadhyay. *Thin Solid Films* **516** (2008) 6824

[2] - B. B. Straumal, S. A. Polyakov, E. Bischoff, and E. J. Mittemeijer *Z. Metallkd.* **95** (2004) 939

[3] - S. B. Lee, J. Moon, C.-H. Chung, Yo.-H. Kim, J. H. Lee, and D.-K. Choi, *J. Vac. Sci. Technol. B* **24** (2006) 2322

[4] - N.G. Nakhodkin, N.P. Kulish, and T.V. Rodionova *Phys. Status Solidi A* **207** (2010) 316

[5] - N.G. Nakhodkin, N.P. Kulish, and T.V. Rodionova *J. Cryst. Growth* **381** (2013) 65

## Atomistic mechanisms of nonstoichiometry-induced twin boundary structural transformation in titanium dioxide

M. Saito<sup>1,2</sup>, R. Sun<sup>1</sup>, N. Shibata<sup>1</sup>, Y. Ikuhara<sup>1,2,3</sup>

<sup>1</sup>Institute of Engineering Innovation, The University of Tokyo, Tokyo 113-8656, Japan

<sup>2</sup>Advanced Institute for Materials Research, Tohoku University, Sendai 980-8577, Japan

<sup>3</sup>Nanostructures Research Laboratory, Japan Fine Ceramics Center, Nagoya 456-8587, Japan

Polycrystalline TiO<sub>2</sub> is used for numerous technological applications where its grain boundaries (GBs) are known to influence the functionality. Light sensitive photovoltaics, oxygen transfer catalysts and host for semiconductor spintronics are just a few important examples. So far, many studies have provided convincing evidence that GBs in TiO<sub>2</sub> can act as sinks for defects and impurities and also can offer shortcut pathways for their diffusion. However, an issue that has been rarely addressed is that defects segregated to GBs *via* external stimuli such as temperature or atmosphere may induce a structural transformation of the GBs, significantly modifying their properties of TiO<sub>2</sub>. A detailed understanding of such an effect requires a spatial resolution and chemical identification of the atoms at GBs.

We perform a systematic investigation of individual  $\Sigma 3(112)[1-10]$  symmetric tilt GB of TiO<sub>2</sub>, which is subject to heat treatment at three different atmospheres (in air, in UHV, or in H<sub>2</sub>). Firstly, the (112)[1-10] symmetric tilt GBs of TiO<sub>2</sub> were fabricated using the bicrystal technique. In this case, two pristine high-purity single crystals were joined at 1773 K for 10 h in air. The other two samples were then separately annealed again at 1073 K for 4 h in UHV environment or at 1073 K for 4 h in 5% H<sub>2</sub> and 95% Ar mixed atmosphere after the first annealing in air. The high-angle annular-dark-field (HAADF) STEM and annular bright-field (ABF) STEM images for all specimens were taken with a 200 kV STEM (JEM-ARM200F) equipped with an aberration corrector, which provides a fine probe for a Sub-Å resolution. The electron energy-loss spectroscopy (EELS) spectra were recorded using a Gatan ENFINA system equipped on STEM with an energy resolution (full-width of half-maximum) of 0.7 eV.

Depending on an annealing environment, atomic arrangements were observed in the HAADF-STEM images especially (FIG. 1). The GB structure (FIG. 1(b-c)) is modified significantly from original structure (FIG. 1(a)) after annealing in both UHV and H<sub>2</sub> atmospheres. We demonstrate that structural defects which are stimulated by the heat treatment can self-assemble to form an ordered superstructure at GB, resulting in nonstoichiometric structure in the GB<sup>[1]</sup> and hence mediate their property changes.

[1] R. Sun, et al., Nat. Commun., **6**, 7120 (2015)

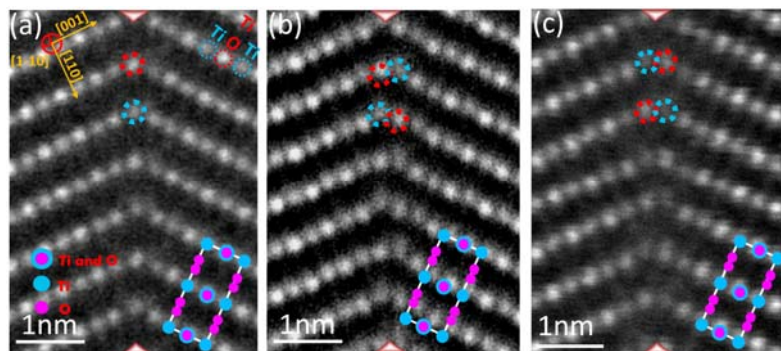


FIG. 1. HAADF-STEM images of  $\Sigma 3(112)[1-10]$  symmetric tilt GB of TiO<sub>2</sub>, which is subject to heat treatment at three different atmospheres (a) in air, (b) in UHV, and (c) in H<sub>2</sub> (+Ar).

## Solid state wetting in metal systems at nanoscale: molecular dynamics simulation

V.M. Samsonov, T.E. Samsonov, I.V. Popov, A.G. Bembel

General physics department, Tver State University, Sadovii per., 35, Tver, 170002 Russia

Solid state wetting (SSW) is an interesting phenomenon discovered and investigated about 10 years ago on metal microparticles (0.1-10  $\mu\text{m}$  in size). In [1] SSW of Cu polycrystalline substrate was investigated, and the partial wetting was observed, i.e. the equilibrium contact angle of about  $40^\circ$  (3h after the contact between spherical particles and the substrate). We have simulated the spreading of Cu solid nanoparticles consisting of 5000-1000 atoms on Cu (100) substrate and of Au particles on Au (100) substrate using molecular dynamics (MD) method (the melting temperature was preliminary found via MD experiments as well). In the Cu/Cu system the complete wetting was observed (Fig. 1). The results for Au/Au system seem to be more interesting: (i) they demonstrate the partial wetting; (ii) when the atoms of the first (upper) substrate monolayer were not fixed, SSW was accompanied by the dewetting phenomenon [2] in the substrate monolayer in question (see Fig. 2).

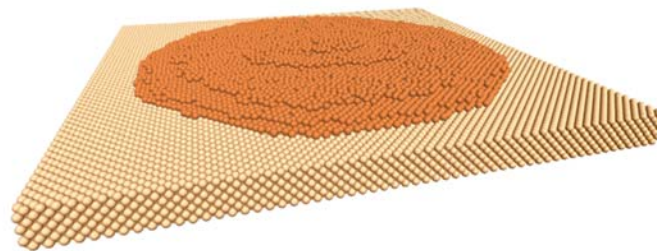


Fig.1. A final Cu/Cu (100) configuration

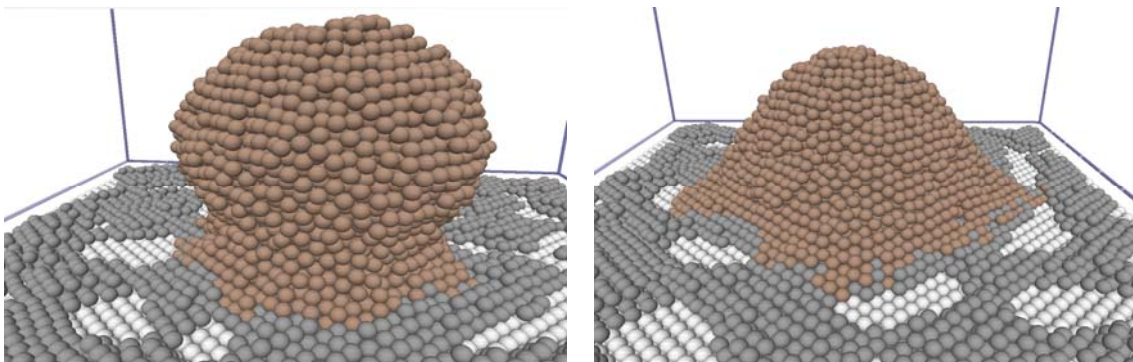


Fig.2: Two consequent configurations of a primarily spherical Au nanoparticle consisting of 5000 atoms on Au (100) face. Temperature  $T = 900\text{K}$

Support of Ministry of Education and science of RF (project No. 3.2448.2014/K) and of RFBR (grant No. 16-33-60171) is acknowledged.

[1] J.M. Missiaen, R. Vogtovych, B. Gilles and N. Eustathopoulos, *Journ. Mater. Sci.* **40** (2005) 2377.

[2] C.V.Thompson, *Annu. Rev. Mater. Res.* **42** (2012) 399-434.

**Interactions between grain boundary sliding, intragranular slip and boundary migration during high-temperature deformation**

A.D. Sheikh-Ali

Institute of Rheotechnologies LLC, 161-1 Kozhamkulova, 050026, Almaty, Republic of Kazakhstan

Grain boundary sliding (GBS), boundary migration and intragranular slip are the most visible processes during high-temperature deformation. In polycrystalline materials, they often operate simultaneously which makes difficult to understand the character of their interaction with each other. This may (and does) result in misconceptions about the real nature of GBS and stress induced boundary migration. In this report, we present the experimental results of deformation of bicrystals with predetermined crystal geometry and boundary parameters. Such approach allows to separate the effects of mutual interactions of the above processes and discover their prime causes. The following aspects are considered: coupling between boundary sliding and migration in the range of stresses and temperatures, sliding induced boundary migration, sliding induced by intragranular slip and others.

**Grain growth in thin nanocrystalline silver films**V.G. Sursaeva<sup>2</sup>, G. Gottstein<sup>1</sup>, L.S. Shvindlerman<sup>1,2</sup><sup>1</sup>Institut für Metallkunde und Metallphysik, RWTH Aachen University, Aachen, Germany<sup>2</sup>Institute of Solid State Physics, Russian Academy of Sciences, Chernogolovka, Moscow Distr.,  
Russia

The results of grain growth experiments in nanocrystalline films deposited on a substrate are discussed in the framework of a theoretical concept in which grain growth is accompanied by vacancy generation to compensate for the released excess volume. It is shown that the predicted “incubation time”, which precedes grain growth is also observed in experiment. The thermodynamic approach which permits to determine correctly the grain boundary excess free volume is considered. It was shown that the measured “incubation time” can be utilized to determine the grain boundary excess free volume. The results compare reasonably well to values obtained in experiments, where the pressure dependence of grain boundary energy was measured.

**Phenomena of interfacial spontaneous chemical reactions – trend to improve the diamond tools ability?**

D.A. Sidorenko, E.A. Levashov, P.A. Loginov, N.V. Shvyndina, E.A. Skryleva

National University of Science and Technology “MISiS”, Leninsky Prospect, 4, Moscow,  
119049 Russia

Diamond cutting tools with metal binders are widely used to machine the most difficult to work with materials, such as reinforced concrete, stone and ceramics. The working layer of the tool contains diamond grains embedded in a metal matrix (binder). The role of the matrix is to retain the diamond grains until they are completely worn out. The grain retention strength depends on the strengths of the matrix material and its interface with diamond, which is influenced by chemical interactions between the two phases. The iron triad metals (Ni, Co, Fe) are usually added to the binder composition to increase its mechanical properties. However, these metals have a negative effect on diamond retention, as they catalyze the diamond ( $sp^3$ ) – graphite ( $sp^2$ ) phase transition at elevated temperatures. As a result, a low-strength graphite layer is formed on the diamond surface when a tool is manufactured and/or used, which causes diamonds to prematurely chip off the metal matrix.

The influence of functional additives of Mo, WC,  $ZrO_2$  nanosized powders on the graphitization mechanism of diamond crystals in metal–matrix composites was studied. It was shown that Mo and  $ZrO_2$  additives intensified graphitization of the diamond surface. However, the addition of WC was found to suppress the graphitization by 25–30%. This is associated with (a) a decrease in the contact surface between diamond and metal catalysts present in the binder and (b) accelerated grain-boundary diffusion of graphite from the surface into the metal matrix. Moreover, the phenomena of spontaneous reactions of WC thin film formation on diamond surface during the sintering of composite in the presence of WC(O) nanoparticles was observed. This film was found to appear with drawing force of gas-phase transport mechanism leading to chemisorption of volatile tungsten oxide  $WO_3$  onto diamond surface followed by  $WO_3$  reduction and WC formation. The mechanism of WC film formation was proposed. The simultaneous enhancement of mechanical properties of the binder and formation of a protective WC interfacial layer on diamond crystals facilitate a synergistic effect which results in increased productivity and cutting speed of diamond tools.



**Amorphous grain boundaries and dopant segregation as source of nanograined ZnO ferromagnetism**

P.B. Straumal<sup>1,2</sup>, S.V. Stakhanova<sup>2</sup>, A.A. Mazilkin<sup>3,5</sup>, S.G. Protasova<sup>3,5</sup>, B.B. Straumal<sup>2-4</sup>, G. Schütz<sup>5</sup>, Th. Tietze<sup>5</sup>, E. Goering<sup>5</sup>, B. Baretzky<sup>4</sup>

<sup>1</sup>A.A. Baikov Institute of Metallurgy and Materials Science, Russian Academy of Sciences, Leninsky prospect 49, 117991 Moscow, Russia

<sup>2</sup>Laboratory for hybrid nanostructures, National University of Science and Technology “Moscow Institute of Steel and Alloys – MISiS”, Leninsky prospect 4, 119991 Moscow, Russia

<sup>3</sup>Institute of Solid State Physics, Russian Academy of Sciences, Chernogolovka, Moscow district, 142432 Russia

<sup>4</sup>Karlsruher Institut für Technologie, Institut für Nanotechnologie, Hermann-von-Helmholtz-Platz 1, 76344 Eggenstein-Leopoldshafen, Germany

<sup>5</sup>Max-Planck-Institut für Intelligente Systeme (former MPI Metallforschung), Heisenbergstrasse 3, 70569 Stuttgart, Germany

In order to elucidate room temperature (RT) ferromagnetism (FM) in pure ZnO and ZnO doped by Co, Mn and Fe, we have analyzed a multitude of experimental publications with respect to the ratio of grain boundary (GB) area to grain volume. FM only appears, if this ratio exceeds a certain threshold value  $s_{th}$ . Based on these important results nano-grained pure, Co-, Mn-, and Fe-doped ZnO films have been prepared, which reveal reproducible RT-FM and magnetization proportional to the film thickness, even for pure ZnO films. ZnO films consist of crystalline grains with wurzite structure separated by amorphous layers. Our findings strongly suggest that grain boundaries and related vacancies are the intrinsic origin for RT ferromagnetism. The amorphous layers form the GB wetting ferromagnetic layers – a kind of ferromagnetic foam.

The nanograined thin films of undoped ZnO and ZnO doped by Mn, Fe, Co, Cr and Ni were synthesized by the wet chemistry (“liquid ceramics”) method from butanoate precursors. Films consist of the dense equiaxial nanograins, and possess ferromagnetic properties. The ferromagnetism appears only in ZnO polycrystals with a quite high density of grain boundaries. The critical size of grains is about 20 nm for pure ZnO. It increases if nanograined ZnO is doped by Mn, Fe, Co, Cr or Ni. Most effective is the doping by iron (the critical grain size in this case is above 40  $\mu\text{m}$ ). The addition of 0.1-1 at. % of Mn, Fe, Co, Cr or Ni to pure ZnO increases the saturation magnetization 3 to 10 times. Further increase of dopant content leads to the decrease of magnetization. Total solubility of Mn, Fe, Co, Cr or Ni in ZnO drastically increases with decreasing grain size.

The financial support of Russian Foundation for Basic Research (project no. 15-33-70051-mol-a-mos) and The Ministry of Education and Science of the Russian Federation (project no.14.A12.31.0001) is greatly acknowledged.

### **Pseudopartial wetting of grain boundaries**

A.B. Straumal<sup>1</sup>, X. Sauvage<sup>3</sup>, B. Baretzky<sup>2</sup>, A.A. Mazilkin<sup>1,2</sup>, I. Konyashin<sup>4</sup>, R.Z. Valiev<sup>5</sup> B.B. Straumal<sup>1,2</sup>

<sup>1</sup>Institute of Solid State Physics, Russian Academy of Sciences, Chernogolovka, Ac. Ossipyan str. 2, Moscow district, 142432 Russia

<sup>2</sup>Karlsruher Institut für Technologie, Institut für Nanotechnologie, Hermann-von-Helmholtz-Platz 1, 76344 Eggenstein-Leopoldshafen, Germany

<sup>3</sup>Université de Rouen – GPM UMR 6634 – BP 12 – 76801 St-Etienne-du-Rouvray CEDEX, France

<sup>4</sup>Element Six GmbH, Technical Development Centre, Staedeweg 18-24, D-36151 Burghaun, Germany

<sup>5</sup>Institute of Physics of Advanced Materials, Ufa State Aviation Technical University, 12 K. Marx str., Ufa 450000 Russia

Usually one distinguishes partial and complete wetting of surfaces or interfaces. In case of partial wetting contact angle  $\theta > 0$  and the liquid droplet is surrounded by “dry” surface or interface. In the majority of cases the direct transition occurs from partial wetting into complete wetting, for example by increasing temperature or decreasing pressure. However, in some cases the state of pseudopartial wetting occurs between partial and complete wetting. In this case the contact angle  $\theta > 0$ , the liquid droplet does not spread over the substrate, but the thin (few nm) precursor film exists around the droplet and separates substrate and gas. Such precursor film is very similar for the liquid “pancake” in case of complete wetting and deficit of the liquid phase. The pseudopartial wetting has been observed before only for liquid/liquid mixtures (alcanes/water solution of salt or glucose) or Pb and Bi on the Cu surface. We observed the pseudopartial wetting on Al/Al grain boundaries (GBs) in the Al – 10 wt.% Zn ultra-fine grained polycrystals and in NdFeB-base hard magnetic alloys. The solid Zn partially wets Al/Al GBs (with non-zero contact angle). Nevertheless, the Al/Al GBs contain the 2 nm thin uniform Zn-rich layer connected with Zn grains. Such thin layers are the reason of high ductility of ultra-fine grained Al–Zn alloys at room temperature. The same phenomenon of pseudopartial wetting is found in NdFeB-base alloys. It has been shown that the thin intergranular films can exist in broad two-phase regions of phase diagrams and could be very useful for various applications. The focused usage of such thin magnetically isolating GB layers can further improve the properties of NdFeB-based hard magnetic alloys and opens the way for development of novel light-weight alloys.

## Self-organized $\alpha$ -FeSi<sub>2</sub> nanocrystals on Si(100): their origin and physical properties

I.A. Tarasov<sup>1,2</sup>, L.A. Solovyov<sup>3</sup>, M. Volochaev<sup>4</sup>, M.V. Rautskii<sup>2</sup>, I.V. Nemtsev<sup>4</sup>,  
I.A. Yakovlev<sup>1,2</sup>, S.N. Varnakov<sup>1,2</sup>, S.G. Ovchinnikov<sup>1,2</sup>.

<sup>1</sup>Siberian State Aerospace University, 31 Krasnoyarsky Rabochiy Av., Krasnoyarsk 660014  
Russia

<sup>2</sup>Kirensky Institute of Physics, Russian Academy of Sciences, Akademgorodok 50, bld. 38,  
Krasnoyarsk 660036, Russia

<sup>3</sup>Institute of Chemistry and Chemical Technology, Siberian Branch of Russian Academy  
Sciences, 660036 Krasnoyarsk, Russia

<sup>4</sup>Krasnoyarsk Scientific Centre, Russian Academy of Sciences, Akademgorodok 50,  
Krasnoyarsk 660036, Russia

Self-assembled  $\beta$ -FeSi<sub>2</sub> single-crystalline nanowires grown on silicon substrate is a prominent material for light emitting diode applications, which could enhance  $\beta$ -FeSi<sub>2</sub> IR luminescence to the suitable level for its commercial utilization. Nevertheless there are a few reports concerning their growth that is possibly caused by the poor orientation relationship (OR) between  $\beta$ -FeSi<sub>2</sub> and silicon [1]. The means to achieve such Si- $\beta$  heterostructures may be by utilizing precursors. These precursors can serve other disilicides phases,  $\alpha$ - or  $\gamma$ -FeSi<sub>2</sub>, having a better OR with silicon. In this report we discuss a new approach to form self-assembled  $\alpha$ -FeSi<sub>2</sub> nanocrystals grown on Si(100) by molecular beam epitaxy and their physical properties. Self-organized  $\alpha$ -FeSi<sub>2</sub> nanocrystals on (100) silicon substrate were synthesized by molecular beam epitaxy with Au catalyst under different rates Fe and Si flows, namely 1:2 and 3:1 (Fig.1). The microstructure and basic orientation relationship between the silicide nanocrystals and silicon substrate were analyzed in detail.  $\alpha$ -FeSi<sub>2</sub> nanocrystals appeared to be inclined trapezoid and rectangular nanoplates, polyhedral nanobars and pyramid-like ones, aligned along  $\langle 011 \rangle$  directions on (100) silicon substrate with the sizes from 30 up to 1500 nm. It has been shown that despite a very large difference in the stoichiometry of the Fe and Si flows the resulted phase leaves the same ( $\alpha$ -FeSi<sub>2</sub>) and it has effect only on the ratio of volumes occupied by differently oriented nanocrystals. As has been proposed metallic iron silicide may be used for manufacturing electric contacts on silicon. A current-voltage characteristic of the structure was measured at room temperature and showed good linearity.

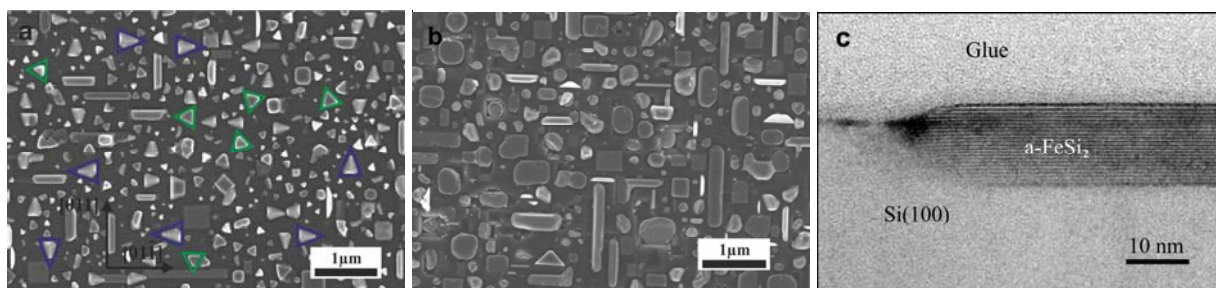


**Fig. 1.** SEM and TEM images of  $\alpha$ -FeSi<sub>2</sub> nanocrystals: large scale view of the samples with Fe and Si flows utilized stoichiometry a) 1:2 b) 3:1 c) TEM image of  $\alpha$ -FeSi<sub>2</sub> nanocrystal.

[1] I.A. Tarasov, I.A. Yakovlev, M.S. Molokeyev, et al.. *Materials Letters* **168** (2016) 90

**Atomic and electronic structure of the LaAlO<sub>3</sub>/(001)SrTiO<sub>3</sub> interfaces.**

M.P. Volkov<sup>1</sup>, Yu.A. Boikov<sup>1</sup>, I.T. Serenkov<sup>1</sup>, V.I. Sakharov<sup>1</sup>, M.A. Shakhov<sup>1</sup>, V.A. Danilov<sup>1</sup>,  
A. Kalabukhov<sup>2</sup>, T. Claeson<sup>2</sup>

<sup>1</sup>Ioffe Physico-Technical Institute, Russian Academy of Sciences, St. Petersburg, Russia

<sup>2</sup>Department of Microtechnology and Nanoscience (MC2), Chalmers University of Technology,  
Gothenburg, Sweden

Laser ablation (KrF,  $\lambda=248$  nm,  $\tau=30$  ns) was used to grow LaAlO<sub>3</sub> (LAO) films with a thickness  $d = 1-10$  unit cell (u.c.) on the TiO<sub>2</sub> terminated (001)SrTiO<sub>3</sub> (STO) substrates. Density of laser radiation at the surface of the ceramic bulk LAO target was 1.9 J/cm<sup>2</sup>. Substrate temperature and oxygen pressure during the lanthanum aluminate layer formation were 790°C and 10<sup>-4</sup> mbar respectively. Layer by layer growth of the LAO film on the STO substrate was controlled through RHEED oscillations.

Structure and composition of the interface in between the LAO film and STO substrate integrated in heterostructure were investigated by Middle Energy Ion Scattering (MEIS, He<sup>+</sup>,  $E=96$  keV). Cationic substitutions (Sr  $\leftrightarrow$  La) are traced down to the depth of 7 unit cell (u.c.) from the top of the (2 u.c.)LAO/STO heterostructure. Inter diffusion of the La atoms from the LAO film into STO substrate is inhomogeneous, as follows from comparison of experimental and simulated MEIS spectra. Large positive magnetoresistance is observed for the (6 u.c.)LAO/STO heterostructures at low temperatures (up to 70% at 4.2K). Usage of the heterostructures with small thickness ( $d = 1-2$  u.c.) of the LAO film enable to make an unambiguous conclusions on cationic substitutions near around of the LAO-STO interface.

It was clear established that electronic parameters of the LAO/STO boundary sharply respond on variations of the oxygen pressure during LAO film growth and depend on STO substrate termination. Impact of high density of oxygen vacancies, cationic substitutions and strain-induced ferroelectricity on conductance of LAO/STO interface was analyzed.

## First-principles study of Si and Mg segregation in grain boundaries in Al and Cu: application of local-energy decomposition

H. Wang<sup>1,2</sup>, M. Kohyama<sup>1</sup>, S. Tanaka<sup>1</sup>, Y. Shiihara<sup>3</sup>

<sup>1</sup>Research Institute of Electrochemical Energy, Department of Energy and Environment, National Institute of Industrial Science and Technology (AIST), 1-8-31, Midorigaoka, Ikeda, Osaka 563-8577, Japan

<sup>2</sup>School of Materials Science and Engineering, Shanghai University, 99 Shangda Road, BaoShan District, Shanghai 200444, China

<sup>3</sup>Institute of Industrial Science, The University of Tokyo, Komaba, Meguro-ku, Tokyo 153-8505, Japan

Segregation of Si and Mg at grain boundaries (GBs) in Al and Cu has been investigated using density functional theory calculations combined with recently developed local-energy and local-stress schemes. The physics behind the impurity-segregation energy is effectively analyzed by the local-energy decomposition. For the  $\Sigma 9$  tilt and  $\Sigma 5$  twist GBs in Al and Cu, Si shows large segregation-energy gains only at tighter sites, where local configuration of remarkably short Si–Al or Si–Cu bonds with high charge densities of covalent-bonding features are formed, leading to the local-energy stabilization as the final-state effects. On the other hand, Mg shows large gains only at looser sites. For Mg in the Cu GBs, the formation of stable Mg–Cu bonds or Mg states at looser sites is the origin of the preferential segregation as the final-state effects. For Mg in the Al GBs, however, the local energies of Mg–Al bonds are not so stable at looser sites, while the instability of Al atoms at looser sites in pure GBs before substitution is the origin of the preferential segregation as the initial-state effects. The behaviors of Si and Mg in Al GBs are dominated by the difference in local *sp* bonding nature among Mg, Al and Si, while Si–Cu and Mg–Cu *sp-d* hybridization interactions dominate the behaviors of Si and Mg in Cu GBs[1].

[1] Hao Wang, Masanori Kohyama, Shingo Tanaka, Yoshinori Shiihara, *J. Mater. Sci* **50** (2015) 6864

## Magnetism of Surfaces of $\alpha$ -Fe<sub>2</sub>O<sub>3</sub>

R. Yu, W. Zhan, and J. Zhu

National Center for Electron Microscopy in Beijing, School of Materials Science and Engineering, Tsinghua University, Beijing 100084, China

Surfaces of metal oxides are of crucial importance for a variety of technological applications such as heterogeneous catalysis, thin film growth, gas sensing, and corrosion prevention [1]. Due to the complexities of oxides in crystal structure and electronic structure, however, the surface science of oxides lags far behind that of metals or semiconductors. Metal oxides are usually good insulators, either band insulators or Mott insulators, making them not suitable for STM, LEED, and most of spectroscopic methods using low energy electrons as probes. On the other hand, the complex atomic structures of oxides results in too many structural parameters to be determined by spectroscopy or diffraction methods. Recent developments in both TEM and DFT provide us opportunities to overcome the above difficulties in the study of oxide surfaces. With the realization of aberration-correction on transmission electron microscopy (TEM), the point resolution of TEM has been improved into the milestone 1 Angstrom scale. In addition, the correction of the spherical aberration has almost eliminated the contrast delocalization in high-resolution images. Therefore, high resolution TEM becomes an even more powerful tool than before for materials research at a truly atomic-scale [2]. We have shown that the surface structure of oxide particles can be directly imaged and measured at the sub-angstrom scale [3]. The geometrical positions of all the atomic columns within the surface layers can be measured to an accuracy of picometers, comparable to that obtained by conventional surface science techniques on single crystals.

Mixed valence is widely found in transition metal oxides and plays an important role in determining the electronic, magnetic, and chemical properties of the materials. In this study, the atomic and electronic structures of the surfaces of  $\alpha$ -Fe<sub>2</sub>O<sub>3</sub> and the defects on them, have been investigated combining aberration-corrected transmission electron microscopy and density functional theory calculations. Enhanced covalence and reduced magnetism on the surfaces have been revealed.

[1] V.E. Henrich, and P.A. Cox, *The Surface Science of Metal Oxides* (Cambridge University Press, Cambridge, 1994).

[2] K. Urban, *Science*, 321, 506 (2008).

[3] R. Yu, L.H. Hu, Z.Y. Cheng, Y.D. Li, H.Q. Ye, J. Zhu, *Phys. Rev. Lett.*, 105, 226101 (2010).

## Faceted interfaces—row matching criterion and atomic simulation

W.-Z. Zhang, Z.-P. Sun, F.-Z. Dai, J.-Y. Zhang

Key laboratory of Advanced Materials (MOE), School of Materials Science and Engineering,  
Tsinghua University, Beijing 100084, China

Faceted interphase boundaries are often generated from solid state phase transformations. The orientation relationship (OR) between two phases usually has freedom to vary so as to permit these facets to develop either of the two types of preferred states, as classified by Bollmann [1]. While interpretations of the observed facets have achieved a certain degree of success, predictions and simulations of the development of the facets remain a challenging task. This presentation reports recent progress in predictions and simulations of the development of the facets for both preferred states.

The primary preferred state is usually taken by systems where the lattice parameters allow local coherence between lattice points. However, the orientation relationship (OR) between two phases corresponding to the primary preferred state can vary in a considerable range (~10 degrees). The orientations of facets are sensitive to the variation in OR. In order to understand what specific facet(s) and OR are preferred by a system. A simulation combining Monte Carlo and molecular statics was carried out to study the evolution of OR and morphology of a bcc phase in a Cr/Cu system at the early stage. The simulation results are in a good agreement with experimental measurements in literatures. They explain the change of the facet from a rational orientation to an irrational orientation. New methods developed for the interface simulations [2-4], which are applicable to general interfaces, will also be briefly presented.

A secondary preferred state usually occurs when the lattice parameters of two phases are significantly different, such that local coherence is physically impossible. In this case, different faceted interfaces and multiple ORs may coexist in one alloy, corresponding to different secondary preferred states. Similar to the early investigations in finding possible coincidence site lattices (CSLs) in a homophase system, 2D near CSLs corresponding to possible secondary preferred states are searched. A simple searching method to predict the candidates of facets is proposed on basis of a modified row matching condition. It is in principle different from the edge-to-edge matching method [5] that also stems from the row matching condition. Applications of the method to an Mg<sub>2</sub>Sn/Mg system will be given. Almost all experimental observed ORs in this system are covered by the searching results.

- [1] Bollmann W. *Crystal lattices, interfaces, matrices*. (1982) Geneva: Bollmann
- [2] F.-Z. Dai, W.-Z. Zhang. *Modelling Simul. Mater. Sci. Eng.* **22** (2014) 035005
- [3] F.-Z. Dai, W.-Z. Zhang. *Modelling Simul. Mater. Sci. Eng.* **21** (2013) 075002
- [4] F.-Z. Dai, W.-Z. Zhang. *Comput. Phys. Commun.* **188** (2015)103–109
- [5] P.M. Kelly, M.-X. Zhang. *Mater. Forum.* **23** (1999) 41-62

## Interface study of CrN (VN, TiN) films on MgO and Al<sub>2</sub>O<sub>3</sub> substrate using C<sub>S</sub>-corrected HRTEM

Zaoli Zhang

Erich Schmid Institute, Austrian Academy of Sciences, Leoben, Austria

In this paper, we will present some recent results on the atomic and electronic structures of the interface between metal nitride thin films (CrN, VN and TiN) on MgO and Al<sub>2</sub>O<sub>3</sub> substrate using advanced TEM techniques, such as C<sub>S</sub>-corrected HRTEM and STEM, EELS/EDXS, quantitative atomic measurement and diffraction analysis as well as theoretical calculations. Interfacial detailed atomic and electronic structures are revealed and compared. Interface induced phenomena between nitride films and substrates are unveiled [1-4].

Particular study on the effect of N defects in the metal nitride (CrN) film has led to some interesting conclusions. Combining independent image analysis and spectrum analysis some generalized conclusions are drawn, which are: (i) a relationship between the lattice constant and N vacancy concentration in CrN is established [5], (ii) the change of ionicity in CrN crystal with the N vacancy concentration is shown; (iii) Particularly, a direct relationship between electronic structure change (L<sub>3</sub>/L<sub>2</sub> ratio) and elastic deformation (lattice constants) in CrN films has been experimentally derived, revealing that the elastic deformation may lead to a noticeable change in the fine structure of Cr-L<sub>2,3</sub> edge, i.e. L<sub>3</sub>/L<sub>2</sub> ratio (shown in Fig.1). The experiment demonstrates an indirect approach to acquire electronic structure changes during the elastic deformation. The effect of randomly distributed defects in the films has been explored in a quantitative way using quantitative electron diffraction, combined with HRTEM and EELS analysis. Some quantitative relations are established [5].

[1]. Z. L. Zhang, *et al* Physical. Review B **82**(R)(2010) p060103-4

[2]. Z. L. Zhang, *et al* Journal of Applied Physics, 110(2011)p043524-4

[3]. Z.L. Zhang *et al* Physical Review B **87** (2013) p014104.

[4]. T.P. Harzer, *et al* Thin Solid Films 545 (2013) p154–160

[5]. Acknowledgement: Gabriele Moser and Herwig Felber are gratefully acknowledged for their help with sample preparation, thanks are given to Dr.Hong Li for *ab-initio* calculations. Thank are also given to Dr. Rostislav Daniel and Christian Mitterer in Montanuniversität Leoben, Leoben, Austria for delivering the materials, and to Gerhand Dehm (Max-Planck-Institut für Eisenforschung) for helpful discussion.



**Effect of interfaces on microstructure evolution in titanium alloys during deformation**

S. Zherebtsov, M. Klimova, M. Ozerov, G. Salishchev

Belgorod State University, 85 Pobeda str., Belgorod 308015 Russia

The influence of the nature of interphase boundaries in  $\alpha/\beta$  titanium alloys and Ti/TiB metal-matrix composite on microstructure evolution during deformation was analyzed in the present work. In two- or multiple phase alloys the crystal lattices of different phases usually satisfy an orientation relationship (OR) which promotes low energy and a (semi)coherent structure of the interface. The energy of interphase boundaries between  $\alpha/\beta$ ,  $\alpha/\text{TiB}$  or  $\beta/\text{TiB}$  phases in the initial undeformed condition was determined by means i) of the van der Merwe model for stepped interfaces [1] or ii) of the Liebman model [2] for the network of misfit dislocations. The subsequent loss of coherency during deformation was ascribed to the increase of interphase energy due to absorption of lattice dislocations and was quantified by a relation similar to the Read–Shockley equation for low-angle boundaries in single-phase alloys.

It was found that interphase boundaries lose their coherency by a strain of approximately 0.4-0.5 at 800°C for Ti-6Al-4V and Ti-5Al-5Mo-5V-1Cr-1Fe. For these strains, the acceleration of dynamic spheroidization of lamellar  $\alpha/\beta$  microstructure in Ti-6Al-4V was found. However in Ti-5Al-5Mo-5V-1Cr-1Fe with much larger fraction ( $\sim 0.5$  vs  $\sim 0.15$  in Ti-6Al-4V at room temperature) of the more ductile  $\beta$  phase the loss of coherency was almost not result in the acceleration of the dynamic spheroidization.

In Ti/TiB metal-matrix composite TiB whiskers in Ti matrix form during *in-situ*  $\text{Ti} + \text{TiB}_2 \rightarrow 2\text{TiB}$  reaction which can occurs both in  $\alpha$  and  $\beta$  temperature region depending on the temperature of processing ( $\alpha \leftrightarrow \beta$  transition in Ti occurs at 882°C). The interfaces  $\alpha/\text{TiB}$  and  $\beta/\text{TiB}$  obey an OR also, however the energy of the Ti/TiB interphase boundaries was found to be noticeably higher than those in the alloys. In addition it was found that formation of TiB in the  $\beta$  phase and then transformation of  $\beta$  into  $\alpha$  during cooling can also result in considerable rise of energy of some parts of interfaces. Rapid increase of interphase energy at the initial stages of deformation was found; it likely promotes the formation of cracks in the vicinity of interfaces.

[1] J.H. van der Merwe. *Proc. Phys. Soc. A* **63** (1950) 616.

[2] W.K. Liebmann, E.A. Miller. *J. Appl. Phys.* **34** (1963) 2653.

**Interfacial free energy and viscosity of Cu(Ag) solid solutions**

S.N. Zhevnenko, A.K. Khayrullin

National University of Science and Technology “MISIS”, Leninsky pr. 4, Moscow, 119049,  
Russia

We conducted experiments on direct measurements of interfacial free energies in Cu(Ag) solid solutions. The experiments were performed by the modified zero-creep method in situ [1] at high temperatures in dry H<sub>2</sub>+Ar atmosphere. As a result we obtained temperature dependences of interfacial free energies of Cu(Ag) alloys and their viscosities. Ag concentrations were up to solubility limit. In general, the energy decreases with the increase of Ag concentration, but isotherms have singularities. We propose that the singularities correspond to the surface transitions which have been predicted by calculations [2] and confirmed experimentally [3, 4].

The viscosity increases with the addition of a small amount of silver (up to about 0.5 at % Ag). At relatively high concentrations of silver the viscosity decreases. The activation energy of creep has complicated concentration dependence. At concentrations close to solubility limit the viscosity of alloys has non-Arrhenius temperature dependence. We propose all these experimental results can be explained by grain-boundary phase transformations.

[1] S. Zhevnenko. *Met. Mat. Trans. A*, 44 (2013) 2533

[2] G. Treglia, B. Legrand, F. Ducastelle, et.al. *Comput. Mater. Sci.*, 15 (1999) 196

[3] Y. Liu, P. Wynblatt, *Surf. Sci.* 290 (1993) 335

[4] J. Y. Wang, J. du Plessis, J. J. Terblans and G. N. van Wyk. *Surf. Interface Anal.* 28 (1999)

73

## Posters

**The combustion synthesis of Co-Al intermetallic compounds in the thermal explosion mode**

M. Adeli, Q. Aghelan

School of Metallurgy and Materials Engineering, Iran University of Science and Technology,  
Narmak, 1684613114 Tehran, Iran

Combustion synthesis has been known as a rapid, low-cost and effective method for producing various compounds, namely, ceramics, composites, and intermetallics. In this research, the possibility of synthesis of cobalt aluminides via the thermal explosion mode of combustion synthesis has been investigated. The Co-Al intermetallic compounds were successfully produced by rapid heating and igniting cylindrical compacts made of compressed powder mixture of Co:Al=1:1. The effect of such parameters as the green density of compacts as well as ball milling of powder mixtures prior to heating on the phases and microstructure of products was investigated. It was found out that changing the process parameter had little or no effect on the formed phases, as shown by XRD and SEM. Ball-milling of mixed starting powders resulted in a decrease in the particle size of reacting powders, yielding a CoAl product with finer grains as well.

## **Polymer processing and chemical engineering in a developing economy**

S. Adeleye

University of Ilorin, Nigeria

The uniqueness of Chemical Engineering profession to other Engineering professions has been of great interest to all experts because of its major role in the life sciences revolution. Chemical Engineering has been described as an important “Liberal Engineering Profession” because of its relevancy to many fields of studies. Chemical engineering is the branch of engineering that is concerned with the design, construction and operation of the plants and machinery used in industrial chemical processes. The emerging Chemical Engineering field is a relatively new one; it is currently one of the most dynamic career choices available, with constantly changing technology, new innovations, and design changes daily being made. Recognizing the need for Technological Education, with respect to the industrial development envisaged in Nigeria, University of Ife now Obafemi Awolowo University took the pioneering step of establishing the first Department of Chemical Technology in this country and indeed in Black Africa. The name of the Department was later changed to Department of Chemical Engineering in 1972 to come in line with curriculum and detailed syllabuses. The developing economy refers to countries with low level of material. They are usually classified based on per capital income, life expectancy, rate of literacy, human development index, etc. The key characteristic of a developing economy is the lack of significant industrialization relative to the population in addition to poor standards of living. The Nigerian economy is being defined as one way traffic relying mainly on Petroleum production and export accounting for about 95% of the country gross earnings. More recently, incorporation of the principles of the biological and life sciences, particularly molecular and cellular biology, has provided chemical engineers the opportunity to contribute to biotechnology and related industries and to the medical field through both biochemical engineering and biomedical engineering. The emphasis of chemical engineering on the molecular basis of materials and biomaterials provides chemical engineers with the skills necessary to tackle problems from the very small scale in cells and biological tissues to the very large scale in industry and the environment. The problems associated with the development of Chemical Engineering in most Developing Economies include unstable political situation, inadequate skilled personnel, economic conditions, lack of adequate funding, legal conditions, lack of equipment, irregular power supply, societal influence and inadequate information.

### **The enhancement of fatigue life of Al-Si alloy by electron-beam processing**

K.V. Aksenova<sup>1</sup>, V.E. Gromov<sup>1</sup>, S.V. Konovalov<sup>1</sup>, Yu.F. Ivanov<sup>2,3</sup>, O.A. Semina<sup>1</sup>

<sup>1</sup>Siberian State Industrial University, Kirov str. 42, Novokuznetsk, 654007, Russia,  
e-mail: gromov@physics.sibsiu.ru

<sup>2</sup>Institute of high-current electronics SB RAS, Akademicheskii av. 2/3, Tomsk, 634055, Russia,  
e-mail: yufi55@mail.ru

<sup>3</sup>National Research Tomsk Polytechnic University, Lenin av. 30, Tomsk, 634050, Russia

The pulsed-periodic electron beams are the surface source of dynamic thermal effect on materials [1, 2]. Surface modification of Al-Si alloy by high intensity pulsed electron beam has been done and the multicycle fatigue tests have been carried out. The aim of this work is to analyze the regularities of structure modification of Al-Si alloy by high-intensity pulsed electron beam, to identify the mechanisms responsible for Al-Si alloy failure subjected to multicycle fatigue tests. Investigations of structure and surface modified layer destruction of Al-Si alloy subjected to high-cycle fatigue tests to fracture have been carried out by methods of scanning electron microscopy. On the irradiation surface of specimen showing the maximum fatigue life in tests the homogeneous structure of the grain (cellular) type (the grains size of the eutectic ranges from 30 to 50  $\mu\text{m}$ ) is formed. Grains are separated by silicon interlayers the transverse sizes of which do not exceed 20  $\mu\text{m}$ . Stress concentrators that can be sources of specimen failure are not detected on the edge of the fracture. The cracks parallel to the fracture surface are located at some distance from it. It, evidently, indicates that the concentrator being the cause of the specimen failure was located under the surface, most probably, on the interface of the liquid and solid phases. The analysis of Al-Si alloy surface irradiated by high-intensity pulsed electron beam has shown that high-speed melting and subsequent surface layer crystallization with the formation of a cellular type structure with distributed interlayers of redundant silicon along the cell boundaries, make possible to increase fatigue life of Al-Si alloy on average by more than 3.5 times relative to the initial state. The factors responsible for the increase of fatigue life of Al-Si alloy have been revealed and analyzed. It has been shown that the main reasons for Al-Si alloy fatigue life increase are: the considerable increase of the critical crack length, the safety coefficient, the reduction of average distance between fatigue striations (cracks for cycle loading), the formation of submicro- and nanosize structure.

- [1] V. E. Gromov, Yu. F. Ivanov, S. V. Vorobiev, and S. V. Konovalov, *Fatigue of Steels Modified by High Intensity Electron Beams* (Cambridge International Science Publishing Ltd, Cambridge, 2015).
- [2] J. J. Hu, G. B. Zhang, H. B. Xu, and Y. F. Chen, *Mater. Sci. Technol.* **27** (2012) 300–303.

**The spatial distribution of residual strains and stresses in multilayer step-graded buffers based on  $\text{In}_x\text{Al}_{1-x}\text{As}$  ternary solutions**

A.N. Aleshin<sup>1</sup>, A.S. Bugaev<sup>1</sup>, O.A. Ruban<sup>1</sup>, I.V. Shchetinin<sup>2</sup>

<sup>1</sup>Institute of Ultrahigh Frequency Semiconductors Electronics, Russian Academy of Sciences, 117105 Moscow, Nagorny Drive 7, build. 5, Russia

<sup>2</sup>National University of Science and Technology “MISiS”, 119049 Moscow, Lenin Avenue 4, Russia

Heterostructures applied to ultrahigh frequency (UHF) electronics devices (for example, high electron mobility transistors – HEMTs) created, as a rule, on a single substrate GaAs of (001) orientation include a metamorphic (MM) buffer to remove a mismatch between a substrate and device active layers including a quantum well (QW). MM-buffer may have a different design, for example, it may be step-graded or linearly graded. MM-buffer has very often such additional elements as an inverse step or a healing layer. During the successive growth of layers the strain release occurs accompanied by the generation of misfit dislocations and the propagation of threading dislocations into heterostructure upper layers. The MM-buffer of correct design should prevent the penetration of threading dislocations. There are some technological receptions allowing us to minimize the penetration of threading dislocation into the device active layers. MM-buffer philosophy is to create a dislocation free layer, which is, in turn, a basis for following an inverse step or a healing layer. The aim of this paper is to obtain the spatial distribution of reduced strains and stresses over a total thickness of MM-buffers of different design and reveal different and common features in them. The step-graded buffers based on  $\text{In}_x\text{Al}_{1-x}\text{As}$  ternary solutions were grown by molecular beam epitaxy (MBE) on a GaAs (001) substrate. The difference in their design was in the different terminations of MM-buffers, first buffer was terminated with an inverse step and second one had as a termination a healing layer. Both heterostructures had a high temperature buffer layer of permanent composition between MM-buffers and active layers. The determination of the spatial distribution of residual strains and stresses was done using reciprocal space mapping performed with a triple-axes X-ray diffractometer SmartLab 9kW and following processing of data obtained within the linear theory of elasticity. Two reflexes, 004 and 224, were recorded, and, consequently, the vertical and lateral parameters of lattice were determined for all epi-layers. It was established that despite the different design of the MM-buffers the character of the spatial distribution of residual strains and stresses in them was practically the same. Main difference between the buffers concluded in values of strains and stresses of terminating layers. So the inverse step and the following high temperature buffer of permanent composition had practically no strains and stresses. It was also shown that the process of residual strain release in both MM-buffers is governed by common laws and characterized by the same value of the so-called phenomenological constant  $K_2$ , which establishes the relation between a reduced strain and a thickness of epi-layer. A value of  $K_2$  equals to  $0.0013 \pm 0.0002$  nm. This value is less than that for epi-layers of  $\text{In}_x\text{Ga}_{1-x}\text{As}$  composition and indicates more intensive character of strain release in the epi-layers of  $\text{In}_x\text{Al}_{1-x}\text{As}$  system.

## **Quantitative parameters of abnormal grain growth in nanocrystalline nickel electrodeposits**

A.N. Aleshin<sup>1</sup>, R.G. Faulkner<sup>2</sup>

<sup>1</sup>Institute of Ultrahigh Frequency Semiconductors Electronics, Russian Academy of Sciences, 117105 Moscow, Nagorny Drive 7, build. 5, Russia

<sup>2</sup>Department of Materials, Loughborough University, Loughborough, Leicestershire LE11 3TU, UK

The grain growth in nanocrystalline nickel with a purity of 99.5 at % during non-isothermal annealing was experimentally investigated using differential scanning calorimetry (DSC) and transmission electron microscopy. Nanocrystalline nickel was prepared by electrodeposition at a pulsed voltage and had an average grain size of approximately 20 nm. It was established that, at a temperature corresponding to a DSC signal peak, abnormal grain growth occurs with the formation of a bimodal grain microstructure. DSC signals were processed within the Johnson – Mehl – Avrami formalism. The formal justification for the use of the Johnson – Mehl – Avrami formalism in the description of the abnormal grain growth is the fact that, at any given time, the fine-grained and coarse-grained fractions with sharp difference in grain size coexist in the material. Consequently, these fractions may be considered as two different phases, and, hence, their amounts can be determined separately. The use of the DSC method, as applied to the study of the abnormal grain growth in nanocrystalline materials, is based on the possibility of measuring the heat released due to the decrease in the area of grain boundaries during the evolution of the microstructure of the nanocrystal. The comparison of heat release with the fraction of newly formed coarse grains gives a basis for the Johnson – Mehl – Avrami formalism use when it is fitted to non-isothermal annealing. This made it possible to determine the exponent of the corresponding equation, the frequency factor, and the activation energy for grain growth, which was found to be equal to the activation energy for vacancy migration. The reasons for the abnormal grain growth in nanocrystalline nickel are discussed.



## Structure and ion-transport properties of coherent homo- and hetero-phase boundaries in nanosystems of advanced superionic conductors

A.V. Andreeva, A.L. Despotuli

Institute of Microelectronics Technology and High Purity Materials RAS, Chernogolovka,  
Ac. Ossipyan street 6, Moscow Region, 142432 Russia

Among all solid ionic conductors, we distinguished a new class of advanced superionic conductors (AdSICs) whose crystal structure is close to the optimum for fast ion-transport (FIT) and determines a record-high level of ion-transport characteristics (ionic conductivity  $\sigma_i \approx 0.3 \Omega^{-1} \text{cm}^{-1}$  at 300 K, activation energy  $E_a \approx 4 k_B T_{300} \approx 0.1 \text{ eV}$ ). The design of functional AdSIC-nanosystems essentially differs from the design of other solid-electrolyte (SE) - nanosystems [1]. This difference is due to existence continuous 3D-net of crystallographic tunnels (minimum energy paths for mobile ions) where the heights of potential barriers are  $\approx 0.1 \text{ eV}$  in the AdSIC structure. Disorder of the crystal structure affects the values of  $\sigma_i$  and  $E_a$  of AdSICs and SEs in two opposite ways. For SE –nanocomposites integral values of  $\sigma_i$  can be much larger than in the component bulks, the effect resulting from a great density of boundaries with higher ionic conductivity. However, the integral ion-transport characteristics are much worse ( $E_a$  is by 4-8 times larger) than in AdSIC ( $\alpha\text{-AgI}$ ,  $\alpha\text{-RbAg}_4\text{I}_5$ , etc.) where structure defects, e.g. boundaries, usually violate FIT conditions. In 2005 a new direction of solid state ionics, namely, “Nanoionics of advanced superionic conductors” was introduced to develop nanoionics further [2]. The central challenge in nanoionics of AdSICs is the influence of atomic structure on the ion-transport and polarization processes in the space charge region of a AdSIC/electronic conductor heterojunction, which is the key functional element of nanoionic devices.

In the present work the interrelated topological, crystal-chemical and ion-transport properties of coherent homo- and heterophase boundaries in AdSIC-nanosystems are considered. Some interface models with FIT-tunnels are presented. To explain available experimental data the FIT-theory on nanoscale was used, which was developed within the framework of the structure-dynamic approach of nanoionics [3]. In the frame of new nanoionic fundamentals, ways of creating coherent and semi-coherent interfaces in supercapacitors with carbon based composite electrodes and high quantum capacitance are discussed. The atomic structure models of interfaces between AdSIC and composite electrode, including electronic conductor and advanced carbon nanostructures such as graphene and/or ropes of single wall carbon nanotubes are presented. We think these findings provide important insight into ion-transport in AdSICs and serve as design principles of new nanoionics devices.

[1] A.V. Andreeva, A.L. Despotuli. Interface design in nanosystems of advanced superionic conductors. *Ionics* 11 (2005) 152–160. doi:10.1007/BF02430415

[2] A.L. Despotuli, A.V. Andreeva, B. Rambabu. Nanoionics of advanced superionic conductors. *Ionics* 11 (2005) 306–314. doi:10.1007/BF02430394 .

[3] A.L. Despotuli, A.V. Andreeva. Structure-dynamic approach in nanoionics. Modeling of ion transport on blocking electrode (2013) <http://arxiv.org/ftp/arxiv/papers/1311/1311.3480.pdf>

**Atomic density functional and structure phase diagram in  
Phase Field Crystal model of iron.**

V.E. Ankudinov<sup>1</sup>, P.K Galenko<sup>2,3</sup>, M.D. Krivilyov<sup>1</sup>, N.V. Kropotin<sup>1</sup>

<sup>1</sup>Udmurt State University, 426034 Russia, Izhevsk Universitetskaya str., 1

<sup>2</sup>Ural Federal University, 620002 Russia, Yekaterinburg

<sup>3</sup>Friedrich-Schiller-Universität Jena, Physikalisch-Astronomische Fakultät, D-07743 Germany,  
Jena

The phase-field crystal method is suitable for simulations of the atomic densities on the diffusion time scales. We can use this approach to calculate the structure phase diagrams for different crystal lattices and to model the wide spectrum of processes such as epitaxial grow, high speed crystal front propagation and so on [1]. The amplitude expansion approximation is based on the 'limitation' of the phase-field crystal model by the amplitude envelope. For example a liquid/solid interface can be described by the envelope that is constant-limited for the solid phase and decreases to zero in the liquid phase. Using this approximation we can construct the set of the free energy functionals for the given phases in the equilibrium state. To evaluate the various properties of the different crystal states it is useful to use two-mode approximation instead of one mode, which means to account second coordination sphere. This approach lead to the more accurate and strict calculations for more complex crystal structures. The ideal periodic BCC crystal, homogeneous phase (liquid) and set of 2D systems analyzed with the amplitude expansion of PFC method in the [2]. The method of analysis and construction developed earlier, in this work appeared as a new approach for construction the structure diagrams of 3-dimensional crystal structures. In present the developed method has been applied for construction of diagram of coexistence of homogeneous liquid phase, body-centered cubic, face-centered cubic crystal lattices of iron. The dimensionless Homogeneous-BCC-FCC phase diagram was constructed for the case of large  $\epsilon$  – dimensionless temperature as a driving force depending on the dimensionless atomic density. These structure diagrams have been recalculated for the case of real system, pure Fe, using the direct variable substitution. The proposed method is extends the current investigations in the phase transformation field.

This work was supported financially by the Russian Foundation for Basic Research (project no. 14-29-10282-ofi\_m).

- [1] N. Provatas and K. Elder, Phase-Field Methods in Materials Science and Engineering, Wiley, VCH, 2010, p. 312.
- [2] V. E. Ankudinov, P. K. Galenko, N. V. Kropotin and M. D. Krivilyov, "Atomic density functional and structure diagram in the phase-field-crystal model approach," Journal of Experimental and Theoretical Physics, vol. 142, no. 2, 2016.

**Microstructure and strength of AlN-SiC interface studied by synchrotron x-rays**

T. Argunova<sup>1</sup>, M. Gutkin<sup>2-4</sup>, K. Shcherbachev<sup>5</sup>, O. Kazarova<sup>1</sup>, E. Mokhov<sup>1</sup>

<sup>1</sup>Ioffe Institute, RAS, St. Petersburg, 26 Polytekhnicheskaya st., 194021, Russia

<sup>2</sup>Institute of Problems of Mechanical Engineering, RAS, St. Petersburg, 61 Bolshoi Ave., 199178, Russia

<sup>3</sup>St. Petersburg Polytechnic University, St. Petersburg, 29 Polytekhnicheskaya st., 195251, Russia

<sup>4</sup>ITMO University, St. Petersburg, 49 Kronverkskii Ave., 197101, Russia

<sup>5</sup>National University of Science and Technology MISiS, Moscow, 4 Leninsky Ave, 119991, Russia

Crystalline aluminum nitride (AlN) is ideal material for substrates used for epitaxial growth of layers of III-nitrides. The promising method of production of bulk AlN crystals is physical vapor transport (PVT) growth on large-area SiC substrates. The problem is that during cooling of AlN/SiC structures AlN layers are cracking because of a great difference between thermal expansion coefficients of AlN and SiC. Crystals without cracks can be obtained if a substrate is gradually evaporated during growth [1]. In this work it is shown how the growth of AlN layers and evaporation of SiC substrates can be realized in one process, so as to prevent cracking of AlN layers. Crystallinity, homogeneity, and structural perfection of AlN plates free of SiC substrates are studied by synchrotron radiation (SR) X-ray micro-imaging and by diffractometry.

Theoretical analysis of distribution of thermoelastic stresses in the AlN/SiC structure showed that, by increasing  $h_2/h_1$  ratio of the AlN layer thickness ( $h_2$ ) and the SiC substrate thickness ( $h_1$ ), a possibility of cracking of the AlN layer is reduced. The critical value of the ratio, beginning from which cracking will be suppressed, can be estimated as  $(h_2/h_1)_{cr.} \approx 15$ . Complete evaporation of a substrate during the layer growth entirely prevents AlN layer from cracking. As a result, thin freestanding AlN plates (0.2-0.8 mm thick) can be produced. Since they have no cracks, they are very strong and endure mechanical treatment.

Synchrotron x-ray imaging confirmed the absence of cracks as well as high-angle boundaries and displayed subgrains and dislocations with the density  $\geq 10^5 \text{ cm}^{-2}$ . Reciprocal space maps as well as diffraction peak widths and shapes confirmed a random distribution of dislocations. The spread of the mosaicity and strain were by an order of magnitude less than those which were obtained for nitride films grown on foreign substrates (e.g., sapphire and silicon).

[1] T. S. Argunova, M. Yu. Gutkin, O. P. Kazarova, *et al. Mater. Sci. Forum* **821-823** (2015) 1011.

### Alloys and glasses of the $\text{Li}_2\text{O}-\text{B}_2\text{O}_3-\text{Yb}_2\text{O}_3$ system

M.M. Asadov, N.A. Akhmedova

Institute of Catalysis and Inorganic Chemistry named after M. Nagiyev, Azerbaijan National Academy of Sciences, pr. H. Javid 113, Baku, AZ1143 Azerbaijan

Materials based on complex oxides of rare earth metals can be used as optical materials, oxygen sensors, ionic conductors, catalysts, etc. [1]. The selection of the  $\text{Li}_2\text{O}-\text{B}_2\text{O}_3-\text{Yb}_2\text{O}_3$  system was based, on the one hand, on the fact that it has been poorly studied up to now, and, on the other hand, on the presence in its constituent binary systems of crystalline oxides and glasses with special optical and electrical properties. Borates, for example, have nonlinear optical properties, high refractive index, dielectric constant and low dielectric loss. According to this phase diagram, solid solutions based on  $\text{Li}_2\text{O}\cdot 2\text{B}_2\text{O}_3$  ( $\alpha$ ) and  $\text{YbBO}_3$  ( $\gamma$ ) crystallize simultaneously at 800 °C (~0.2 mole fraction  $\text{Yb}_2\text{O}_3\cdot\text{B}_2\text{O}_3$ ). The polymorphic transformations of the  $\text{Yb}_2\text{O}_3\cdot\text{B}_2\text{O}_3$  compound, progressing through an eutectoid reaction at 460 °C and a metatectic reaction at 925 °C, are detected on the thermograms. According to the physico-chemical analysis, the  $\text{Li}_2\text{O}\cdot 2\text{B}_2\text{O}_3-\text{Yb}_2\text{O}_3\cdot\text{B}_2\text{O}_3$  polythermal section is quasi-binary and it allows us to partially triangulate the  $\text{Li}_2\text{O}-\text{B}_2\text{O}_3-\text{Yb}_2\text{O}_3$  system. In the  $\text{Li}_2\text{O}\cdot 2\text{B}_2\text{O}_3-\text{Yb}_2\text{O}_3\cdot\text{B}_2\text{O}_3$  system one of the components,  $\text{YbBO}_3$ , has polymorphism.  $\text{YbBO}_3$  has two polymorphs at temperatures of 577 °C and 1041 °C. Polymorphism of the  $\text{YbBO}_3$  compound is also evident in alloys of the  $\text{Li}_2\text{O}\cdot 2\text{B}_2\text{O}_3-\text{Yb}_2\text{O}_3\cdot\text{B}_2\text{O}_3$  polythermal section. The polymorphic transformation temperature is lowered by the addition of  $\text{Li}_2\text{O}\cdot 2\text{B}_2\text{O}_3$  to  $\text{YbBO}_3$ . Alloys and glasses of the  $\text{Li}_2\text{O}\cdot 2\text{B}_2\text{O}_3-\text{B}_2\text{O}_3-\text{Yb}_2\text{O}_3\cdot\text{B}_2\text{O}_3$  system studied by us have potential applications as high-temperature dielectric and semiconducting materials. The electrical conductivity of the  $\text{Li}_2\text{O}\cdot 2\text{B}_2\text{O}_3-\text{B}_2\text{O}_3-\text{Yb}_2\text{O}_3\cdot\text{B}_2\text{O}_3$  glass system exhibits semiconducting nature.

- [1] M.M. Asadov, A.N. Mammadov, D.B. Tagiev, N.A. Akhmedova. *Cambridge MRS Online Proc. Library*, **1765** (2015) imrc2014 s4a-p020. doi: 10.1557/ opl.2015.816.

### **The effect of hydrogenation on mechanical properties of high-nitrogen steel**

E.G. Astafurova<sup>1</sup>, G.G. Maier<sup>1</sup>, E.V. Melnikov<sup>1</sup>, G.N. Zakharov<sup>1</sup>, S.V. Astafurov<sup>1</sup>,  
V.A. Moskvina<sup>2</sup>, V.F. Vojtsik<sup>2</sup>

<sup>1</sup>Institute of Strength Physics and Materials Science, Russian Academy of Sciences, Tomsk,  
Akademichesky av. 2/4, 634055 Russia

<sup>2</sup>National Research Tomsk Polytechnic University, Tomsk, Lenin av. 30, 634050 Russia

Austenitic stainless steels are frequently used for hydrogen applications due to their high ductility at low temperatures and lower hydrogen environment embrittlement compared to ferritic steels. We study the effect of electrochemical hydrogen saturation on peculiarities of plastic deformation and fracture mechanisms in high-nitrogen austenitic steel Fe-24Mn-17Cr-1.3V-1.3N-0.2C (HNS). After hot rolling steel has fully austenitic structure with coarse vanadium nitrides (~200 nm), it possesses high yield stress (1300 MPa) and good uniform elongation to fracture (20%). Hydrogen saturation weakly influences the character of stress-strain curves and strain hardening of steel. Hydrogenation for 40 hours provides a change in HNS fracture mechanism from intragranular to transgranular one and decreases a value of strain to fracture. A brittle surface layer forms under hydrogen saturation of HNS specimens. As a result, numerous brittle cracks nucleate on the specimen surface from the beginning of plastic flow in tension and provoke the embrittlement of HNS specimens.

This research was supported by the Russian Foundation for Basic Researches (project No. 15-38-20056). The experimental results were obtained using equipment of Center «Nanotech» of Institute of Strength Physics and Materials Science.

**Grain growth simulation in an IF steel - Effect of CSL boundaries energy and mobility**

A. Ayad<sup>1,2</sup>, N. Rouag<sup>2</sup>, F. Wagner<sup>3</sup>

<sup>1</sup>Département de Pharmacie, Faculté de Médecine, Université Constantine 3, Algérie

<sup>2</sup>Laboratoire de microstructures et défauts dans les matériaux, Université Frères Mentouri Constantine, Algérie.

<sup>3</sup>LEM3, (CNRS-UMR 7239), Université de Lorraine, Ile du Sauley, 57045 Metz, France

In our recent papers, an original concept is proposed for the simulation of the normal grain growth stage in an IF steel by the Monte Carlo technique [1,2]. It is based on a modular consideration of the grain size effect. This allowed both better reflect the pressure at the grain boundaries and significantly speed up the calculations. This model was used to reproduce the main features of the microstructure and texture. Improvement of texture behavior, especially of the component  $\{111\}\langle 112\rangle$ , which differs slightly from the experiment, requires the introduction of strong assumptions on energy and mobility of grain boundaries. The objective of this study is to verify the ability of this model to give satisfactory results for grain growth, by considering various assumptions on energy and mobility of CSL boundaries. The validity of such assumptions and their impact on the simulation results are analyzed and discussed.

[1] A. Ayad, F. Wagner, N. Rouag, A.D. Rollett. *Comp. Mater. Sci.* **68** (2013) 189-197

[2] A. Ayad, F. Wagner, N. Rouag. *IOP Conf. Ser.: Mater. Sci. Eng.* **82**(2015) 012051

**Microstructure of binary aluminum systems Al-Zn with various Zn-content after high pressure torsion**

E.V. Bobruk<sup>1,2</sup>, X. Sauvage<sup>3</sup>, B.B. Straumal<sup>4,5</sup>, R.Z. Valiev<sup>1,2</sup>

<sup>1</sup> Laboratory for Mechanics of Bulk Nanostructured Materials, Saint Petersburg State University, 28 Universitetsky pr., Peterhof, Saint Petersburg, 198504, Russia

<sup>2</sup> Institute of Physics of Advanced Materials, Ufa State Aviation Technical University, K. Marx str. 12, Ufa, 45000, Russia

<sup>3</sup> Groupe de Physique des Matériaux, UMR CNRS 6634, Université et INSA de Rouen, 76801 Saint Etienne du Rouvray, France

<sup>4</sup> Institute of Solid State Physics, Russian Academy of Sciences, Chernogolovka, Ac. Ossipyan str. 2, Moscow district, 142432 Russia

<sup>5</sup> Karlsruher Institut für Technologie, Institut für Nanotechnologie, Hermann-von-Helmholtz-Platz 1, 76344 Eggenstein-Leopoldshafen, Germany

It has been shown in this work that processing by severe plastic deformation leads to the formation of a UFG structure with a grain size of below 500 nm in aluminium alloys of the systems Al - 2, 5, 10, 30 %Zn. The supersaturated solid solution in Al alloys is decomposed during HPT processing resulting in nucleation and growth of a secondary phase precipitates and/or formation of segregations of alloying element Zn. It is proposed that the atomic mobility could be significantly enhanced during SPD especially thanks to the high vacancy concentration, solute drag by dislocations, pipe diffusion along dislocations or grain boundary diffusion.

In the present work, we have systematically investigated such dynamic precipitation phenomena in a series of Al-Zn alloys at different HPT processing regimes.

We have demonstrated that evolution and formation of UFG microstructure in these alloys strongly depends on both the concentration of zinc and HPT processing parameters.

## **Prismatic loop of misfit dislocation around a cylindrical inclusion of finite length in a composite nanowire**

E.A. Bobyl<sup>1</sup> M.Yu. Gutkin,<sup>1-3</sup> A.L. Kolesnikova,<sup>2,3</sup> A.E. Romanov<sup>3-5</sup>

<sup>1</sup> Department of Mechanics and Control Processes, Peter the Great St. Petersburg Polytechnic University, Polytekhnicheskaya 29, St. Petersburg, 195251, Russia

<sup>2</sup> Institute of Problems of Mechanical Engineering, Russian Academy of Sciences, Bolshoj 61, Vasil. Ostrov, St. Petersburg, 199178, Russia

<sup>3</sup> ITMO University, Kronverkskiy pr. 49, St. Petersburg, 197101, Russia

<sup>4</sup> Ioffe Physical Technical Institute, Russian Academy of Sciences, Polytekhnicheskaya 26, St. Petersburg, 194021, Russia

<sup>5</sup> Togliatti State University, Belorusskaya st., 14, Togliatti, 445667, Russia

Nowadays much attention is attracted to various composite nanowires which contain discrete inclusions (quantum dots). Functional characteristics of such composite nanostructures strongly depend on residual elastic strains caused by the atomic misfit of material components. To study these effects, theoretical modeling of misfit strains and misfit defects seems to be rather useful. The first step in this modeling is the posing and solution of an appropriate boundary value elastic problem for a misfitting inclusion. The second step is the modeling of possible mechanisms of misfit strain relaxation. The aim of the present work is to develop a model for the formation of a prismatic loop of misfit dislocation in a nanowire with a finite-length cylindrical inclusion and to calculate the critical parameters for the formation of this defect in such a nanowire. Earlier, a similar model was considered in the case of an axial dilatation eigenstrain of the inclusion [1], and the results were applied to theoretical description of stress relaxation in pentagonal nanowires of inhomogeneous atomic cast [2,3]. Here we extend this solution to the general case of an axial-and-radial dilatation eigenstrain of the inclusion. First, we solve a boundary value problem in the theory of elasticity for a circular radial disclination loop (Somogiana dislocation) [4-6] coaxial with a long elastic cylinder. Then the dipole of such loops gives us a solution for a cylindrical inclusion of finite length with radial eigenstrain in the cylinder. Superposition of this solution with that found in [1] results in a solution for the inclusion problem in the general case of axial-and-radial eigenstrain. We discuss the peculiarities of stress fields with the help of corresponding stress maps and consider the misfit stress relaxation through generation of a circular prismatic loop of misfit dislocation around the inclusion.

- [1] M.Yu. Gutkin, K.V. Kuzmin, A.G. Sheinerman, *Phys. Stat. Sol. B* 248 (2011) 1651.
- [2] M.Yu. Gutkin, S.N. Panpurin, *J. Macromolecular Science B: Physics* 52 (2013) 1756.
- [3] M.Yu. Gutkin, S.N. Panpurin, *Phys. Solid State* 56 (2014) 1187.
- [4] A.L. Kolesnikova, A.E. Romanov, *Phys. Solid State* 45 (2003) 1706.
- [5] A.L. Kolesnikova, A.E. Romanov, *J. Appl. Mech.* 71 (2004) 409.
- [6] R.J.H. Paynter, D.A. Hills, A.M. Korsunsky, *Int. J. Solids Struct.* 44 (2007) 6653.



**Study of Cu/Nb interface diffusion by molecular dynamics simulation**I.V. Nelasov, A.O. Boev, A.G. Lipnitskii

Belgorod State University, Belgorod, Pobedy str. 85, 308015 Russia

Nanolayered composites, such as Cu/Nb, have a high radiation damage tolerance which increases with decreasing of component thickness [1]. When the thickness of the layers is about several tens of nanometers, a leading role is played by the processes occurring at interfaces. The interface diffusion is significant in such structures, because the interfaces serve as effective sinks for radiation-induced defects. Therefore it is important to establish the mechanisms of interface diffusion.

In this work, we carried out a molecular-dynamic simulation of diffusion in the Cu/Nb nanolayered composite sample with the Kurdjumov-Sachs orientation relationship observed experimentally [2]. We obtained that niobium diffusion at the copper-niobium interface occurs by displacement of atoms along dislocations of mismatch. Diffusion processes in niobium are activated by the introduction of a number of copper atoms in the rows of niobium atoms near the dislocations of mismatch. The activation energy of the process corresponds to the activation energy of the copper diffusion along the high angle grain boundary of niobium. Up to the temperature of 1200 K, the vacancy mechanism of diffusion at the Cu/Nb interface does not play a significant role.

[1] Misra A. et al. The radiation damage tolerance of ultra-high strength nanolayered composites //Jom. – 2007. – T. 59. – №. 9. – C. 62-65.

[2] Demkowicz M. J., Hoagland R. G. Structure of Kurdjumov–Sachs interfaces in simulations of a copper–niobium bilayer //Journal of Nuclear Materials. – 2008. – T. 372. – №. 1. – C. 45-52.

**Structural and magnetic ordering of CrNb<sub>3</sub>S<sub>6</sub> single crystals grown by gas transport method**

E.B. Borisenko<sup>1</sup>, V.A. Berezin<sup>2</sup>, V.K. Gartman<sup>1</sup>, D.V. Matveev<sup>1,2</sup>, O.F. Shakhlevich<sup>1</sup>,  
N.N. Kolesnikov<sup>1</sup>

<sup>1</sup>Institute of Solid State Physics, Russian Academy of Sciences, Ac. Ossipyan str. 2,  
Chernogolovka, Moscow district, 142432 Russia

<sup>2</sup>Institute of Microelectronics Problems, Russian Academy of Sciences, Ac. Ossipyan str. 5,  
Chernogolovka, Moscow district, 142432, Russia

The CrNb<sub>3</sub>S<sub>6</sub> single crystals with hexagonal superlattice have been grown by gas transport method. These ferromagnetic semiconductors obtained via doping layered NbS<sub>2</sub> crystals with transition metals would provide spin polarization far higher than that of ferromagnetic metals, which is important for spintronics and other fields of magnetic materials applications. Two-stage crystal growth using iodine transport is developed to produce a single-phased CrNb<sub>3</sub>S<sub>6</sub>. The X-ray diffractometry on a Gemini-R set up designed for analysis of single crystals has shown that *as grown* samples are single crystals with almost completely ordered CrNb<sub>3</sub>S<sub>6</sub> superlattice with [0001] orientation and the unit cell parameters  $a = 5.744\text{\AA}$ ,  $c = 12.132\text{\AA}$ , which are in good correlation with the XRD data. The HF absorption in CrNb<sub>3</sub>S<sub>6</sub> single crystals was measured using helical resonator with a sample in periodically switched magnetic field. Temperature dependence of HF absorption at periodical sweep of external magnetic field was measured to estimate Curie temperature of the CrNb<sub>3</sub>S<sub>6</sub> single crystal. Each period of the magnetic field sweep proceeds almost at a constant temperature, while, on the whole, HF absorption curve shows a descriptive picture of amplitude changing with field as temperature gradually changes. Sharp increase in HF absorption was detected below 115 K, which was indicated as lower Curie temperature limit of the crystals. This result is in good agreement with the value of ferromagnetic transition temperature in this semiconductor obtained by other magnetoelectric measurements [1, 2].

- [1] T. Miyadi, K. Kikuchi, H. Kondo, S. Sakka, M. Arai, and Y. Ishikawa, J. Phys. Soc. Jpn., **52** (4) (1983) 1394-1401;  
[2] Y. Togawa, Y. Kousaka, S. Nishihara, K. Inoue, J. Akimitsu, A. S. Ovchinnikov, and J. Kishine, Phys. Rev. Lett., **111** (19) (2013) 197204\_1-197204\_5.

**Formation of thermally grown oxide layer in  $Gd_2Zr_2O_7$ /YSZ underwent to thermal cycles**

P. Carpio<sup>1</sup>, M.D. Salvador<sup>1</sup>, A. Borrell<sup>1</sup>, D. Busquets<sup>1</sup>, E. Klyatskina<sup>1,3</sup>, E. Sanchez<sup>2</sup>

<sup>1</sup> Instituto de Tecnología de Materiales (ITM), Universitat Politècnica de València. Camino de Vera sn/, 46022 Valencia, Spain

<sup>2</sup> Instituto de Tecnología Cerámica (ITC), Universitat Jaume I. Campus Universitario Riu Sec, Av. Sos Baynat s/n, 12006 Castellón, Spain

<sup>3</sup> Institute of new metallurgical technologies JSC «Kompozit», Korolev, Russia

Thermal barrier coatings (TBC) are used to protect metallic parts of gas turbines against extremely high temperature environments. These coatings usually consist of a NiCrAlY bond coat and a ceramic top coat. Besides, a thermally grown oxide (TGO) layer between bond coat and top layer is formed during thermal exposition.  $Gd_2Zr_2O_7$  is an interesting material applied as a top coat because of its very low thermal conductivity and high corrosion resistance. However, the coefficient of thermal expansion mismatch between metallic parts and the  $Gd_2Zr_2O_7$  layer is too high so significant stresses are formed during thermal cycles. In order to avoid this problem, an yttria-stabilized zirconia (YSZ) layer is deposited between the bond coat and the  $Gd_2Zr_2O_7$  layer.

In this work, YSZ and  $Gd_2Zr_2O_7$  coatings were prepared by atmospheric plasma spraying. On one hand, both materials were sprayed separately to obtain monolayer coatings. In addition, the  $Gd_2Zr_2O_7$  layer was deposited onto the YSZ layer to obtain a multilayer coating. Finally, YSZ and  $Gd_2Zr_2O_7$  were sprayed simultaneously to obtain a functionally graded coating with composition variations along its thickness.

The aim of this work deals with the evaluation of the thermal fatigue resistance of the described coatings. For this purpose, the samples underwent thermal cycles until the coating failed. In addition, microstructural and mechanical characterization was performed on coatings treated at a different number of thermal cycles. TGO layer growth and crack formation between grains have been recorded and related with the thermal fatigue resistance.

The  $Gd_2Zr_2O_7$  monolayer coating displayed a thermal fatigue resistance considerably worse than the YSZ monolayer coating, although the latter showed a higher thermal conductivity. Regarding multilayer and functionally graded coatings, their thermal fatigue resistance resulted in an intermediate resistance from those observed in the monolayer coatings. Functionally graded coatings exhibited an improved resistance with respect to multilayer coatings because TGO and cracks formations were constrained. For this same reason, mechanical properties of functionally graded coatings were enhanced for a specific number of thermal cycles. In conclusion, functionally graded TBC's are a great design to optimize the properties of  $Gd_2Zr_2O_7$  and YSZ materials.

**Effect of chemo-mechanical coupling on the formation of core-shell structures in Al-Sc-Zr system**

Y. Buranova, A. Gupta, V. Kulitckii, T. Hickel, S.V. Divinski, K. Li, Y. Du, G. Wilde

Institute of Materials Physics, University of Münster, Wilhelm-Klemm-Str. 10, 49149 Münster, Germany

Aluminum alloys containing scandium show excellent mechanical properties due to the presence of  $\text{Al}_3\text{Sc}$  precipitates, which control the dislocation and grain boundary motion during the recrystallization processes. An addition of Zr can further improve the properties due to formation of  $\text{Al}_3(\text{Sc,Zr})$  dispersoids with a core-shell structure, which are more stable at elevated temperatures.

In this work we investigate a commercial aluminum alloy AA5024, containing Sc, Zr, Ti and Mg additions. The particles size, chemistry and distribution were investigated by analytical transmission electron microscopy and geometric phase analysis was applied to map local strains. It is found that the  $\text{Al}(\text{Sc,Zr,Ti})$ -precipitates reveal complex core-shell structures which are strongly affected by mechanical deformation and heat treatment. Changing of precipitates structure during the severe plastic deformation process caused the formation of principally different precipitates, which can differently affect the alloy microstructure.

The financial support of DFG within SPP 1713 is gratefully acknowledged.

### **Hall-Petch strengthening of multilayer Ti/Al coatings**

M.Ya. Bychkova, M.I. Petrzhik, Ph.V. Kiryukhantsev-Korneev, E.A. Levashov

National University of Science and Technology «MISiS», Leninskiy pr. 4  
Moscow 119049 Russia

Multilayer Ti/Al coatings consist of alternating nanosize layers of titanium and aluminium. In order to study the effect of layer thickness on mechanical properties binary Ti/Al coatings were deposited on silicon, fused silica and some other substrates by magnetron sputtering of pure metallic targets. Prepared coatings consisted of a different number (from 8 to 280) of alternating layers, and the thickness of each layer was 3.8, 7.5, 15, 35 and 125 nm for different samples [1]. According to nanoindentation data all samples shown relatively low values of hardness ( $\leq 5.0$  GPa), which corresponded to an indenter penetration depth less than 100 nm. With an increase in load in the range of penetration depth ( $\approx 130\text{--}300$  nm) the hardness of each specimen was almost unchanged. With a further increase in load (consequently the depth of indenter penetration), there was an increase in hardness, connected with the effect of harder substrates like fused silica, which hardness was 9.8 GPa. The effect of the substrate became less marked with a reduction in coating layer thickness. Besides, it was found that hardness of multilayer Ti/Al coatings depended on layer thickness according to the Hall–Petch relationship, i.e. with a reduction in thickness of individual layer the hardness of multilayer Ti/Al coatings increased.

[1] E.A. Levashov, et al. Metallurgist, Vol. 54, №. 9–10, 2011, pp.623-634.

## Effect of copper on interfacial free energy of solid silver

S.V. Chernyshikhin, S.N. Zhevnenko

National University of Science and Technology “MISIS”, Leninsky pr. 4, Moscow, 119049, Russia

Currently, there are several ways to evaluate the effect of concentration on the interfacial free energy of the solid solution. The influence of copper on the silver surface energy can be estimated by phase diagram [1, 2] or thermodynamic models [3,4]. However, the estimates contradict each other. Experimental data on surface energy and adsorption (segregation) are absent. In our work we have carried out experiments on the direct measurements of the surface free energy of pure silver and Ag (Cu) solid solutions. The experiments were conducted in Ar-10%H<sub>2</sub> atmosphere at high temperature range 760-900 °C. Copper in silver was introduced by electrolytic deposition and annealing. Before alloying the silver foil samples were used to measure the surface energy of pure silver. The obtained results are analyzed in comparison with the experimental data on interfacial free energy of Cu (Ag) solid solutions.

This study was carried out with financial support of Russian Foundation for Basic Research under Grant No. 14-03-00809 A.

1. Burton, J.J.; Machlin, E.S. Prediction of Segregation to Alloy Surfaces from Bulk Phase Diagrams. *Phys. Rev. Lett.* **1976**, *37*, 1433-1435
2. Zhevnenko, S.N. Surface Free Energy of Copper-Based Solid Solutions. *J. Phys. Chem. C*, **2015**, *119* (5), 2566–2571
3. Wynblatt, P.; Ku, R.C. Surface Energy and Solute Strain Energy Effects in Surface Segregation. *Surf. Sci.*, **1977**, *65*, 511-531
4. Jeurgens, L.; Wang, Z.; Mittemeijer, E. Thermodynamics of Reactions and Phase Transformations at Interfaces and Surfaces. *Int. J. Mater. Res.*, 2009, *100*, 1281-1307

**Nanowhiskers: fabrication technique, structural features and properties**

M.V. Dorogov<sup>1</sup>, A.Yu. Kozlov<sup>1</sup>, A.E. Kalmykov<sup>2</sup>, A.A. Vikarchuk<sup>1</sup>, A.E. Romanov<sup>1,2,3</sup>,

<sup>1</sup>Togliatti State University, 14 Belorusskaya str., Togliatti, 445667 Russia

<sup>2</sup>Ioffe Physical-Technical Institute, 26 Polytekhnicheskaya str., St. Petersburg, 194021 Russia

<sup>3</sup>University ITMO, 49 Kronverksky pr., St. Petersburg, 197101 Russia

Chemical and petrochemical industries, ecology and water cleaning have a strong need in new functional materials with developed surface and high catalytic activity. The present work is devoted to the fabrication and the analysis of structure and properties of such materials in the form of copper oxide nanowhiskers.

The stainless 12X18H10T steel mesh with cell size of 40 μm was used as a substrate for nanowhisker growth with the following procedure. As the first step, individual copper nanoparticles or copper continuous coatings were electrochemically deposited on the mesh. As the second step, the samples were annealed at 400 °C for 4 hours in air. After such treatment, "forest" of nanowhiskers covers the surface of the substrate.

Transmission and scanning electron microscopy show an almost perfect form of as grown whiskers with a pointed apex. A typical TEM image of cross-section of an individual CuO nanowhisker show that the nanowhisker is divided by a twin boundary along its length direction. Oxide nanowhiskers have a multicrystal structure (i.e., no hollow pipe present along the axial core of nanowhiskers). Using electron microscopy and X-ray microanalysis it has been shown that whiskers have chemical composition of copper oxide CuO. To study the structure of whiskers, electron diffraction patterns for single crystals were obtained and energy dispersive X-ray spectral analysis was performed. Analysis of the elemental composition of whiskers was performed at high resolution scanning electron microscope CarlZeiss Sigma.

The photocatalytic activity was evaluated by the degradation of dye (methylene blue - MB) at a concentration of 10 mg/l under the visible and UV light. During the test, the degradation rate of MB was monitored by the UV-vis absorption spectrum. The result indicates that nanowhiskers have high photocatalytic activity.

Thus, we have determined the optimal conditions to grow nanowhiskers by heat treatment of electrolytic copper. The obtained results open a wide field for possible applications of nanowhiskers.

This work has been performed under the support by the grant № 14.B25.31.0011 from the Ministry of Education and Science of Russian Federation (resolution # 220) at the Togliatti State University.

**Grain boundary self-diffusion in aluminum. Molecular dynamic calculation**A.V. Weckman , A.S. Dragunov, B.F. Demyanov

Altai State Technical University, Russia, Altai Region, Barnaul, Lenina st., 46

The article studies the process of self-diffusion in symmetric tilt grain boundaries (GBs) with the misorientation axes [100], [110] and [111]. To carry out the research, the computer simulation method has been applied. The simulation has been performed by the method of molecular dynamics in the temperature range 600÷1000 K in increments of 50 K. The calculations have resulted in the fact that all GBs are characterized by a pronounced anisotropy of the atom jumps at low temperatures (< 700 K). At temperatures approaching the melting point, the jump directions are isotropic for the three GBs ( $\Theta = 30^\circ$  [100],  $\Theta = 50^\circ$  [100] and  $\Sigma 5(013)[100]$ ) only. The Arrhenius plots have from one to three linear portions of different tilts. Change in the tilt of the Arrhenius plots is proof of the change in the self-diffusion mechanism. The parameters of grain boundary self-diffusion have been determined. The activation energy of grain boundary diffusion is 4-5 times lower than of volume self-diffusion in aluminum (approximately 200 kJ/mol). The GB  $\Theta = 10^\circ$  [100] has the minimum value of activation energy (10.15 kJ/mol), while the special GB  $\Sigma 11(113)[110]$  has the maximum value (104.12 kJ/mol).



**Origin of low angle boundaries and stability of tempered martensite lath structure under creep and fatigue**

N. Dudova, R. Mishnev, R. Kaibyshev

Belgorod State University, 85 Pobeda str., Belgorod 308015 Russia

The stability of tempered martensite lath structure (TMLS) of 9-12% Cr martensitic steels is considered as a key factor for attaining the superior creep strength and low cycle fatigue (LCF) resistance. This stability is attributed to low-angle lath boundaries with irregular internal structure exerting a long-range elastic stress field. These features of lath boundaries provide effective strengthening and low mobility under creep and cyclic loading conditions. Superior creep resistance and ability to withstand LCF are attributed to origin of lath boundaries.

It was revealed that TMLS remained during creep at 650°C at applied stresses ranging from 180 to 120 MPa with rupture time from 18 to  $\sim 4 \times 10^4$  h. The migration of lath boundaries and their transformation to subboundaries having regular dislocation structure were not observed. Therefore, rather stable irregular dislocation substructures retained the long-range internal stress fields. Nano-scale M(C,N) carbonitrides played a key role in hindering the knitting reaction between mobile lattice dislocations and lath boundaries by the pinning of mobile dislocations within the lath interiors. Under cyclic loading at constant strain amplitude from  $\pm 0.2\%$  to  $\pm 1.0\%$  the TMLS remained stable if the contribution of plastic strain to overall strain amplitude was not dominant. At these conditions no significant cyclic softening took place. In contrast, pronounced cyclic softening was associated with a transformation of the lath boundaries to subboundaries if the plastic strain amplitude exceeded the elastic one. Therefore, a dispersion of M(C,N) carbonitrides could not prevent the knitting reaction if rearrangement of intrinsic dislocations was promoted by high amplitude cyclic reversions. This process was responsible for relieving the long-range elastic stress field originated from lath boundaries. Approaches to increase the stability of TMLS in 9-12%Cr steel are discussed.

This study was supported by the Russian Science Foundation, Project no.14-29-00173.

**Nanostructured bulk aluminum smaller than 100 nm with severe plastic deformation**

A.R. Eivani, S. Najafi, H.R. Jafarian

School of Metallurgy and Materials Engineering, Iran University of Science and Technology (IUST), Tehran, Iran.

By means of severe plastic deformation, acquiring nanoscale within size range of less than 500 nm has hardly been reported in the literature. In this paper, a novel approach is proposed to acquire nanostructured AA6063 alloy within a size range of less than 100 nm using equal channel angular pressing (ECAP). This includes application of a specially designed pre-deformation thermomechanical processing after initial solution treatment. The pre-deformation treatment starts with two passes deformation in ECAP followed by annealing at 500 °C for 10 sec and quenching in water. An equiaxed nanostructured AA6063 alloy within the size range of less than 100 nm is obtained after 6 passes ECAP while more than 69 % of boundaries are high angle ones.

**Re-strengthening in AA6063 alloy during equal channel angular pressing with choked exit channel**

A.R. Eivani, M. Torabi, H.R. Jafarian, M.T. Salehi

School of Metallurgy and Materials Engineering, Iran University of Science and Technology (IUST), Tehran, Iran.

In this investigation, a new approach is proposed which can help to overcome the routine phenomenon of saturation during equal channel angular pressing (ECAP). This helps to activate re-strengthening in a sample which has already been deformed for several passes and has reached a saturated level the grain refinement and strength. For this purpose, equal channel angular pressing (ECAP) is carried out using two different configurations for the exit channel of the ECAP die, i.e., relieved and choked, with angles of  $0.2^\circ$ . It is found that in the die with relieved exit channel, the sample was extruded for 6 passes with no surface cracks. Therefore, the deformation was stopped at this stage after which an average cell size of 727 nm and a fraction of high angle grain boundaries of 54 % were achieved. Measured values of yield strength (YS) and ultimate tensile strength (UTS) were reported to be 201.1 and 259.5, respectively. Hardness was increased to 55 HBN which indicate a saturated level as already had been achieved after 4 passes ECAP. By using the die with choked exit channel, it was possible to deform the sample for up to 14 passes with no sign of surface cracking. A relatively finer cell structure around 530 nm was achieved and the fraction of HAGBs increased to 64 %. Relative increases in YS and UTS were as well observed indicating that re-strengthening has been activated in the material after saturation at the 4<sup>th</sup> pass. In addition, the mechanism of grain refinement seemed to change to progressive lattice rotation evidenced by formation of trapped single grains within the size range of less than 100 nm.

## **Non-applicability of the classic hydrodynamic approach to analyse the processes in amorphous metallic alloys**

V.A. Fedorov, A.D. Berezner, T.N. Pluzhnikova

Tambov state university named after G.R. Derzhavin, 392000 Internatsionalnaya str., 33,  
Tambov, Russia

Nowadays there are three general models to be applied for explanation of processes proceeding in amorphous metallic alloys: the model of structural relaxation [1], the model of free volume [2], and the hydrodynamic (liquid) model as well. Depending on a scope of phenomena under analysis relevant approaches are to be applied. The “liquid” approach is based on conformity of topologically disordered initial state of liquids and metallic glasses. All liquid models are described with classic hydrodynamics of laminar flow. A viscosity function is frequently determined separately within the framework of these models, the function being described with Fraenkel type exponential relationships; the function, as may be supposed, allows considering collective molecular-scale processes in their macro scope. Papers [3] and [4] are the examples of researches where a viscosity analysis in various disordered amorphous media is applied. [4] at first considered hypothetically amorphous materials under analysis as a Newtonian solution of various components having sufficiently high viscosity ( $\sim 10^{15}$  Pa s) and proposed using this value as one of reference characteristics of amorphous state endogenous processes. Still at present there are no direct results indicating fulfillment of Newtonian flow conditions for amorphous metallic alloys. This circumstance does not allow further reasonable application of the equations system for Newtonian liquid classic hydrodynamics in order to explain amorphous alloys properties.

In this context, the aims of this work are: 1) a check of Newtonian flow condition fulfillment in metallic glasses (MG) at creep testing. 2) measurement of specimens’ strain resistivity.

The deformation flow of amorphous Co-based alloys in creep tests in a temperature interval of 300 to 1200 K° has been studied. When the processes in the amorphous bands are analysed in the context of a hydrodynamic approach, difficulties emerge in the interpretation of the alloy flow from the standpoint of Newtonian fluid. The absence of Newtonian and pseudo-plastic flow characteristics of amorphous bands has been analytically proven. An explicit form of the creep function of amorphous specimens in a variable temperature field has been determined. The creep flow resistivity  $\rho(\epsilon, S, T)$  of amorphous alloys has been measured.

- [1] D. Turnbull, M.H. Cohen, J. Chem. Phys. 52 (1970) 3038.
- [2] S.S. Tsao, F. Spaepen, Acta Metall. 33, 881 (1985).
- [3] K. Csach, J. Miskuf, A. Jurikova and P. Vojtanik. Kosice, 9 July – 12 July 2007, pp. 91-94.
- [4] G. Vlasák, P. Švec, P. Duhaj. Materials Science and Engineering A. 304–306, (2001), pp. 472–475.

## Effect of alloying on interfacial energy of precipitation/matrix in high-chromium martensitic steels

A. Fedoseeva, N. Dudova, R. Kaibyshev

Belgorod State University, 85 Pobeda str., Belgorod 308015 Russia

9-12% Cr martensitic steels are used as materials for fossil power plants with steam temperature more than 600°C [1]. Superior creep strength of these steels is attributed to a dispersion of nanoscale  $M_{23}C_6$  carbides and M(C,N) carbonitrides, precipitated under tempering conditions, and Laves phase particles, precipitated during creep at 650°C.  $M_{23}C_6$  carbides and Laves phase particles precipitate along the boundaries of prior austenite grains (PAG), packets, blocks and laths of tempered martensite lath structure (TMLS). These carbides restrain migration of PAG and lath boundaries under long-term aging and creep [2,3]. M(C,N) carbonitrides located randomly within martensitic laths play a role of effective pinning agents for mobile lattice dislocations preventing their rearrangement to subgrain boundaries and the knitting reaction between them and lath boundary dislocations [4]. Coarsening resistance of these particles controls creep strength. Ability to withstand Ostwald ripening depends on coherence of their interfaces. Interfacial energy  $\gamma$  of these interfaces lies between 0.1 J/m<sup>2</sup> (coherent interface) to 1 J/m<sup>2</sup> (incoherent interface) [5]. Calculation of particle growth kinetic using Prisma-software and comparison of experimental data with theoretically predicted coarsening behavior allows determining the value of interfacial energy. In addition, effect of cobalt and tungsten solutes on the coarsening resistance of  $M_{23}C_6$  carbides, Laves phase particle and M(C,N) carbonitrides in P92-type steel was evaluated.

### Acknowledgements

This study was supported by the Russian Science Foundation, Project no.14-29-00173.

- [1] F. Abe, T.-U. Kern and R. Viswanathan, Creep-resistant steels. Cambridge: Woodhead Publishing; 2008.
- [2] V. Dudko, A. Belyakov, D. Molodov, R. Kaibyshev, *Metall.Mater.Trans. A*, Vol. 44A (2013), pp.S162-S172.
- [3] N. Dudova, A. Plotnikova, D. Molodov, A. Belyakov, R. Kaibyshev, *Mater. Sci. Eng. A* 534 (2012) 632-9.
- [4] Hald, J., *Int. J. Pres. Ves. Pip.*, Vol. 85 (2008), pp. 30–37.
- [5] J. Hald, L.Korcakova., *ISIJ International* 43 (3) (2003) 420-427.

**Resonant behaviour of Sn diffusion coefficient in alpha-iron  
in pulsed magnetic field at 730 °C**

A.V. Pokoev, A.A. Fedotov

Samara State Aerospace University, Moscow Highway, 34, Samara, 443086, Russian Federation

In the present research the diffusion volume coefficients of Sn in polycrystalline  $\alpha$ -Fe in the pulsed magnetic field (PMF) in frequencies interval of 1-21 Hz with impulses amplitudes of 39.8-557,2 kA/m at 730 °C by X-ray method are measured for the first time. The magneto-diffusive effect (MDE), i.e. the effect of appreciable PMF influence on the measured diffusion coefficient (DC) Sn in  $\alpha$ -Fe, is revealed and established by the authors. In particular, the "resonance behaviour" of DC for frequencies of ~5, 13 and 17 Hz is found out within the measured frequency spectrum. The DC resonance value depends in some complex way on the amplitude of the PMF intensity.

The character of the PMF influence on the DC behaviour of Sn in  $\alpha$ -Fe and possible MDE mechanisms are discussed. A conclusion is made, that the observed process of relaxation is realized by Zener's relaxation mechanism when elastic stresses of impurity atoms, vacancies and their complexes in diffusion zone interact with pulsed magnetostriction stresses of  $\alpha$ -Fe ferromagnetic lattice [1]. The role of the dimensional atomic factor [1] and type of the interatomic bond in the MDE formation of the mentioned diffusion pairs is defined.

- [1] A.V. Pokoev, A.A. Fedotov. Magneto-diffusive Effect in Ferromagnetic  $\alpha$ -Fe Placed in Pulsed Magnetic Field. Diffusion, Stress, Segregation and Reactions. International Workshop, DSSR-2012, Svitank, Ukraine, June 1-7, 2012, p. 212-215.

## Competition between elements solving in the volume and the segregations forming in the surface in dependence on heating temperature of $\alpha$ -Fe alloys

V.P. Filippova, R.V. Sundeev, A.A. Tomchuk

I. P. Bardin Central Research Institute for Ferrous Metallurgy, Moscow 105005, Russia

The equation (1) proposed by M.P. Seah [1] was analyzed in this work and developed for multi-component systems, where the equilibrium concentration of the  $i$ -th component was represented as the temperature function  $X_b^{\infty i}(T)$ :

$$\frac{X_b^{\infty i}(T)}{X_{bo} - \sum_{i=1}^N X_b^{\infty i}(T)} = \frac{X_v^i}{X_{vo}^i(T)} \exp\left[\frac{-\Delta G_{seg}^i}{RT}\right] \quad (1).$$

Here,  $(X_b^{\infty i}(T))$  is the segregation concentration;  $(X_{vo}^i(T))$  is the limiting volume solubility;  $X_v^i$  is the volume concentration of a solved element in a considered alloy;  $R$  is the universal gas constant;  $T$  is the absolute temperature. According to the above relationship (1), the segregation rapidly reaches equilibrium level under higher exposing temperatures, but its value is lower at higher temperatures than that one could be under lower temperatures. The latter was proposed in work [1] as to be tied with the volume solubility increasing, as rule, under exposing temperature growth and being an opposite competitive process to equilibrium surface (interface) segregations formation. A certain temperature ( $T_{seg}^i$ ) of observing a maximum segregation level for a solved element was proposed to exist. The latter should experimentally observed as the temperature interval of preferential surface enrichment. The value  $T_{seg}^i$  in this work was determined mathematically from the maximum condition for relationship (1):  $\partial X_b^{\infty i}(T)/\partial T=0$ . Obviously, the precise solution of the latter does not exist, because  $X_b^{\infty i}(T)$  in (1) is a monotonic one. We believe the following to be true at rather low temperatures and enough long time period of the isothermal exposing:  $X_b^i(T) \cong X_b^{\infty i}(T) = const$ . The segregation concentration ( $X_b^{\infty i}(T)$ ) and the limiting volume solubility ( $X_{vo}^i(T)$ ) in (1) are functions on the temperature. Other parameters in

(1) assumed to be independent on the temperature. So, it was possible to find an approximate solution:  $\partial X_b^i(T)/\partial T \cong 0$ .

From the above, we obtained the following expression for the temperature interval of preferential surface enrichment by a certain solved element:

$$(T_{seg}^i)^2 = \frac{\Delta G_{seg}}{R} \left[ X_{vo}^i(T) / \left( \frac{\partial X_{vo}^i(T)}{\partial T} \right) \right] \quad (2).$$

It was experimentally shown in [2], using Auger-spectroscopy method, that there is the certain temperature interval of forming the surface segregation of an element  $i$  solved in  $\alpha$ -Fe ( $i=C, N, B, P, Mo, Ti, Al, S, Sn, Cu$ ). The values of  $(T_{seg}^i)$  simulated with (2) are in rather good agreement with obtained experimentally in [2].

This work was financially supported by the RFBR (Project #16-08-00599).

- [1] M. P. Seah. Auger Spectroscopy in Metallurgy. In book: Practical Surface Analysis by Auger and X-ray Photoelectron Spectroscopy, edited by D. Briggs and M. P. Seah, -John Wiley & Sons, (1983).
- [2] A.I. Kovalev, D.L. Wainstein. Design Simulation of Kinetics of Multi-Component Grain Boundary Segregations in the Engineering Steels under Quenching and Tempering. In book: Handbook of Metallurgical Design, ed. by G. Totten, Lin Xie and Kiyoshi Funatani, pp.57-123; Marcel Dekker Inc. N.Y. U.S.A.(2004).



### **Ag/BN nanoparticle hybrids obtained by Ag ion implantation**

K.L. Firestein<sup>1</sup>, A. E. Steinman<sup>1</sup>, D.G. Kvashnin<sup>1</sup>, A.N. Sheveyko<sup>1</sup>, I.V. Sukhorukova<sup>1</sup>, A.M. Kovalskii<sup>1</sup>, A.T. Matveev<sup>1</sup>, O.I. Lebedev<sup>2</sup>, P.B. Sorokin<sup>1</sup>, D. Golberg<sup>3</sup>, D.V. Shtansky<sup>1</sup>.

<sup>1</sup>National University of Science and Technology “MISIS”, Leninsky prospect 4, Moscow, 119049, Russian Federation

<sup>2</sup>CRISMAT, UMR 6508, CNRS-ENSICAEN, 6Bd Marechal Juin, Caen, 14050, France

<sup>3</sup>National Institute for Materials Science (NIMS), Namiki 1, Ibaraki, Tsukuba, 3050044, Japan

Synthesis and application of boron nitride (BN) nanomaterials is an exciting and rapidly developing area. BN nanostructures have attracted significant attention due to their rich functionality in reinforcement ultralight metals and ceramics, improvement thermal conductivity and mechanical strength of polymers, making transparent superhydrophobic films, creating drug delivery systems, and many other applications.

For some important applications including quantum electronic devices, catalyst supports, drug delivery systems, photocatalysts, molecular probe sensors, pollutant capturing surface enhanced Raman spectroscopy substrates, and antibacterial agents BN/noble metal composites are envisaged to be highly prospective. Thus our work has been focused on the fabrication of Ag/BNNP nanohybrids by means of Ag ion implantation into the hollow BN nanoparticles (BNNPs) with a petal-like surface. The structural transformations occurring during Ag ion implantation into BNNPs have been studied by low- and high-resolution transmission electron microscopy (TEM), and high angle annular dark field scanning TEM (HAADF-STEM) paired with energy-dispersive X-ray (EDX) spectroscopy mapping. Our results have demonstrated that by changing Ag ion energy in the range of 2–20 kV it is possible to selectively fabricate Ag/BNNP nanohybrids with crystalline or amorphous BNNP structures and various Ag NPs distributions over the BNNP thicknesses.

Variation of the implantation parameters has led to the formation of Ag/BNNP nanoparticle hybrids with varying degrees of BNNPs inner shells amorphization and Ag NPs distribution through them. Thin surface petals have easily been destroyed even by low energy ion flux. We are confident that these novel Ag/BNNP composite nanomaterials are of interest for many novel emerging structural, functional, and medical applications.

## Mass transfer during surface alloying of metals in powders with nanostructured surface of particles

R.G. Galin<sup>1</sup>, N.A. Shaburova<sup>2</sup>, N.A. Zaharyevich<sup>3</sup>, B.B. Khina<sup>4</sup>

<sup>1</sup>VIKA-GAL Company, 7 Molodogvardeytsev str., Chelyabinsk 454138, Russia

<sup>2</sup>South Urals State University, 76 Lenin avenue, Chelyabinsk 454080, Russia

<sup>3</sup>Chelyabinsk State University, 129 Brat'ev Kashirinyh str., Chelyabinsk 454001, Russia

<sup>4</sup>Physico-Technical Institute, National Academy of Sciences of Belarus, 10 Kuprevich str., Minsk 220141, Belarus

A novel method of pack galvanizing in zinc powders whose particles are covered with a thin layer of ZnO, which has urchin-like nanostructure [1], was used to produce corrosion-resistant diffusion coatings on a low-carbon steel (0.2 wt.% C) at temperatures both below and above the zinc melting point,  $T_m(\text{Zn})=419\text{ }^\circ\text{C}$ , during 30 to 120 min. The content of ZnO in the powders was 8 wt.%, certain zinc powders contained up to 2 wt.% Fe. Microstructure, phase composition and growth kinetics of the obtained coatings were studied along with the zinc concentration profile across the coatings. It is found that the phase composition corresponds to the equilibrium Fe-Zn diagram:  $\alpha$ -solid solution of Zn in bcc iron,  $\Gamma$  ( $\text{Fe}_3\text{Zn}_{10}$ ) and  $\Gamma_1$  ( $\text{Fe}_{11}\text{Zn}_{40}$ ) phases, and  $\delta_1$  phase ( $\text{FeZn}_{10}$ ) on the outer surface of steel. The thickness of  $\alpha$ -phase is observed to rise substantially with increasing the content of iron in the zinc powder: from 14  $\mu\text{m}$  without iron to about 80  $\mu\text{m}$  at 2 wt.% Fe for pack galvanizing at 430  $^\circ\text{C}$  during 110 min, whereas the total thickness in intermetallic phases remained constant, about 50  $\mu\text{m}$ . According to the Einstein-Smoluchowski relationship  $D \sim h^2/2t$ , the apparent interdiffusion coefficient in  $\alpha$ -Fe at this temperature is  $4.8 \cdot 10^{-9}\text{ cm}^2/\text{s}$  while the grain boundary diffusion coefficient of Zn is  $3 \cdot 10^{-11}\text{ cm}^2/\text{s}$  [2]. Fast growth of  $\alpha$ -phase during the initial stage of pack galvanizing can be attributed to the presence of holes in the ZnO layer on the surface of Fe-containing Zn particles. This provides partial adhesion of the particles to the steel surface, thus not only gas-phase saturation of iron with zinc occurs but contact diffusion as well.

[1] R.G. Galin. Modified zinc powder. *Russian patent* 2170643. B22F1/02, C23C10/28. Published 20.07.2001.

[2] J.S. Dohie, J.R.Cahoon, W.F.Caley. *J. Phase Equil. Diffus.* **28** (2007) 322-327.

## **Nanocomposites for restoration of tissues by concentrated flow of energy**

A.Yu. Gerasimenko

National Research University of Electronic Technology - MIET, bld. 1, Shokin Square,  
Zelenograd, Moscow, Russia, 124498

One of the main areas in tissue bioengineering is searching for designing new imitative 3D structures-synthetic implants, which should stimulate growth and differentiation of cells during tissue formation. The characteristics of artificial implants (biocompatibility, biodegradability, porosity, size and connectivity of pores, immune response etc.) must be no worse than those of the natural intercellular matrix. At the same time, wide application of high-strength metal (for example, titanium and its alloys) implants in tissue bioengineering is hindered by their low biodegradability and insufficiently high biocompatibility. Hydroxyapatite, calcium phosphate, and composites based on them, which have a developed porous structure and are good bone substituents, are often used. However, these materials are low-tech and brittle. A new potential in this field, which is traditionally oriented toward two-dimensional nanostructures, is related to the technology of bulk nanocomposites with functional properties similar to those of an intercellular matrix. The main elements of the nanocomposites are water-albumen dispersion medium (25 wt.%) with multi- or single-walled carbon nanotubes (0.1 wt.%). The electric field of laser radiation may facilitate formation of the framework of carbon nanotubes in the nanocomposite compound. The presence of this framework forms conditions for self-organization of biological tissues, which occurs without human interference, being supported by weak noncovalent (hydrogen, ion) bonds upon hydrophobic interaction of tissues. A similar organization of biological macromolecules in nature occurs, for example, in phospholipids, which are the main components of plasma cellular membranes. Study of the composition was conducted and framework structure of nanocomposites was proved using methods of Raman and infrared spectroscopy, X-ray analysis, atomic force and scanning electron microscopy. Mechanical properties of nanocomposites were also studied. Biological experiments of laboratory animals showed the absence of allergic reactions when laser prepared nanocomposite samples were introduced into rabbit perichondrium. Replacement of a cartilaginous tissue segment with an implanted nanocomposite sample caused its regeneration upon stimulation of active division of cartilaginous cells (chondrocytes), which are generally passive. Thus, using the afore mentioned nanocomposites, one can implement conditions for growing functional biological tissues, similar to those provided by biological matrix. As result of this work, it can be assumed that nanocomposites will contribute to self-organization, cultivation, reproduction and branching of bone osteoblasts, nerve neurite, endothelial cells and stem cells and are suitable for restoring the system of blood vessels avoiding thrombus formation. Thus, these nanocomposites may be used not only to provide for the regeneration of different tissues of human body, but also for coating of implants of different materials.

This work was financially supported by Ministry of Education and Science (Agreement 14.575.21.0089, RFMEFI57514X0089).

**Formation of supersaturated near diffusant/matrix interface.**

N. Goreslavetz, A. Rodin

National University of Science and Technology "MISiS", Department of Physical Chemistry, 4,  
Leninsky pr-t, Moscow, 119049, Russia

It is generally believed that during the diffusion process the concentration of diffusing elements does not exceed the solubility limit. It gives possibility to simplify the mathematical description of diffusion problem for multiphase system e.g. for the system with restricted solubility. In this case the assumption that at the interface the concentration of the elements will be equal to equilibrium concentration at the both side of the interface can be done. Thus, the solution for diffusion equation with constant source as a boundary condition can be used if the annealing is long. At shorter time the concentration of diffusing elements is less than solubility at this temperature.

For some systems (Fe diffusion in Cu, Co in Cu, Cu in Al) it was shown that after very long diffusion annealing at moderate temperatures the concentration exceed the solubility limit in several times. Systematic study of this effect was made for the system Cu-Al at different temperatures in 300-400 °C range. It was shown that annealing at higher temperatures do leads to formation of solution with concentration equal to saturation at the interphase. But in this temperature region the concentration increases with time and after some moment exceeds the saturation. It is important to note that this effect can be seen only if intermediate phase (which must appear according to phase diagram) does not form.

### **Morphology of ( $\beta$ Ti) in the ( $\alpha$ Ti)/ ( $\alpha$ Ti) grain boundaries of VT6 alloy**

A.S. Gornakova, S.I. Prokofjev, B.B. Straumal

Institute of Solid State Physics Russian Academy of Sciences, Chernogolovka, 2 Academician  
Ossipyan str., Moscow district, 142432, Russia

Broad application of the VT6 titanium-based alloy is determined by the exceptional mechanical properties, which allows its use in the aircraft industry, machinery, medicine, etc. The aim of this study was to investigate the nature of the distribution and morphology of ( $\beta$ Ti) phase at the grain boundaries (GBs) in the ( $\alpha$ Ti) phase in the VT6 alloy.

The study was performed using the industrial titanium alloy VT6 (6.22 wt.% Al and 3.7 wt.% V). The annealings were conducted in the temperature range from 670 to 820°C (in the two-phase ( $\alpha+\beta$ ) region of phase diagram), duration of each series was 720 hours. Analysis of the microstructure of annealed samples was conducted using the scanning electron (SEM) and light (LM) microscopy. Figure 1 shows the SEM micrographs of: (a) initial and (b) annealed samples. Initial microstructure (before annealing) contains lamellar colonies of ( $\alpha$ Ti) and ( $\beta$ Ti) phases. After annealing, the microstructure consists of a grid of grain boundary layers of ( $\beta$ Ti) phase. The origin of grain boundary layers is associated with a GB wetting supported by the high rate of grain boundary diffusion and volume diffusion. We observed that at each annealing temperature the grain boundaries in ( $\alpha$ Ti) phase exist which are completely covered by the layers of ( $\beta$ Ti) phase.

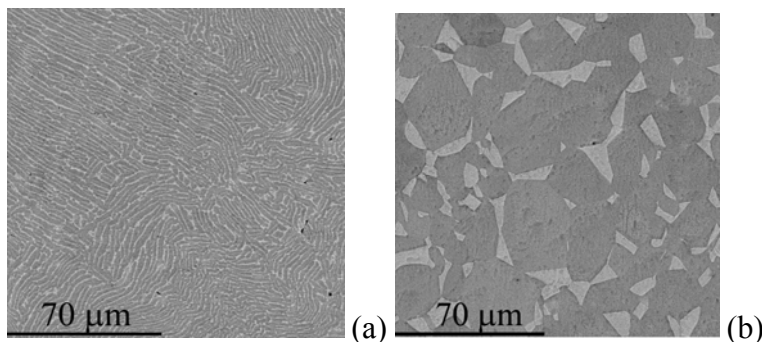


Fig. 1. SEM micrographs of titanium alloy VT6: (a) the initial microstructure, (b) the sample annealed at a temperature 800°C. Light areas are the cubic phase ( $\beta$ Ti), dark areas are the hexagonal phase ( $\alpha$ Ti).

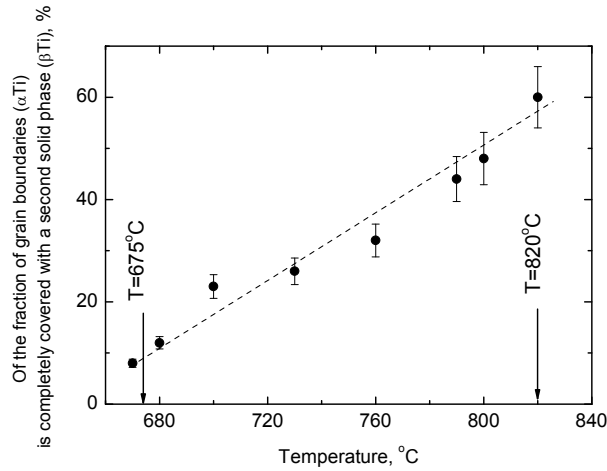


Fig. 2. Temperature dependence of the fraction of grain boundaries ( $\alpha$ Ti) completely covered with a second solid phase ( $\beta$ Ti).

The measurement results are shown in Figure 2 i.e. the temperature dependence of the fraction of grain boundaries ( $\alpha$ Ti) phase completely covered with a layer ( $\beta$ Ti) phase. It can be seen that the proportion of the grain boundaries completely covered with a layer of a ( $\beta$ Ti) phase increases approximately linearly with the annealing temperature. Linear extrapolation suggests that approximately at 650°C it can be expected that all of the grain boundaries in ( $\alpha$ Ti) phase are free from continuous layer of ( $\beta$ Ti) phase.

This work was supported by RFBR (project 16-03-00285).

### Structure-phase states redistribution at deformation of bainite steel

V.E. Gromov<sup>1</sup>, E.N. Nikitina<sup>1</sup>, K.V. Aksenova<sup>1</sup>, Yu.F. Ivanov<sup>2,3</sup>, O.A. Semina<sup>1</sup>

<sup>1</sup>Siberian State Industrial University, Kirov str. 42, Novokuznetsk, 654007, Russia,

<sup>2</sup>Institute of high-current electronics SB RAS, Akademicheskii av. 2/3, Tomsk, 634055, Russia

<sup>3</sup>National Research Tomsk Polytechnic University, Lenin av. 30, Tomsk, 634050, Russia

Recently the attention of researches in the field of physical metallurgy is paid to the study of features of bainite transformation in steels [1, 2]. The investigations of structure, phase composition and defective substructure of steel with bainite structure subjected to plastic deformation were carried out. The quantitative analysis of parameters of steel structure that made it possible to follow the redistribution of carbon atoms in steel structure under plastic deformation was performed. It was established that with growth of degree of deformation the quantity of carbon atoms located in solid solution based on  $\alpha$ -iron and defects of crystal lattice as well as cementite particles lying on intraphase boundaries increased; the quantity of carbon atoms forming cementite particles lying in volume of bainite plates and those located in solid solution based on  $\gamma$ -iron decreased. It was shown that plastic deformation by uniaxial compression of steel 30Cr2Ni2MoV with bainite structure is accompanied by: first, increase in scalar density of dislocations and volume of material containing deformation microtwins, second, decrease in average transverse sizes of fragments and increase in degree of their disorientation, third, increase in quantity of stress concentrators and curvature-torsion amplitude of crystal lattice of the material. The stages of changes of steel structure parameters were revealed. The proposal was made about the changing in steel deformation mechanism: at the first stage of loading ( $0\% < \varepsilon < 18\%$ ) deformation was done predominantly by motion of dislocations; at the second stage ( $18\% < \varepsilon < 36\%$ ) – it was done by motion of dislocations and twinning. It was shown that steel hardening had a multifactor character. The estimates of mechanisms of hardening by boundaries of bainite plates and fragments, scalar density of dislocations, long-range stress fields, cementite particles, and interstitial atoms were carried out. The largest contribution to the value of work hardening of steel under study was made by substructural hardening (hardening caused by long-range internal fields of stresses and fragmentation of structure) and solid solution hardening caused by penetration of carbon atoms into crystal lattice of ferrite. At degree of deformation  $\varepsilon > 36\%$  the formation of channels of localized deformation – particular structural states of material being localized along the interfaces of adjacent plates of bainite or grain boundaries was revealed.

[1] T. Sourmail, V. Smanio, *Acta Materialia* **61** (2013) 2639-2648.

[2] A. Borgentam, M. Hillert, J. Agren, *Acta Materialia* **57** (2009) 3242-3252.

***Ab initio* simulation of four mechanical twins  $\alpha$ -Ti in presence of H & O**

O.B.M. Hardouin Duparc, L. Liang

École Polytechnique, LSI, CNRS, CEA, Université Paris-Saclay, 91128 Palaiseau, France

$\alpha$ -Titanium plasticity at room temperature implies gliding of dislocations and twinning. Impurities like hydrogen and oxygen play a complex rôle in creep and dynamic ageing.

With a unified set of up to date *ab initio* density functional theory parameters, we get the structures and energies of the four most relevant twin boundaries (TB) in the hexagonal close packed  $\alpha$ -Ti metal, namely {10-12}, {11-21}, {11-22} and {10-11}. Then, considering one side of the TBs as the matrix part, sets of *c*-axis deformations of these TBs in pure  $\alpha$ -Ti and in presence of these segregated O/H are examined and compared, allowing for all atom relaxation and taking the Poisson effect into account. The presence of a twin weakens the theoretical ultimate tensile stress under *c*-axis tensile test. The {10-12} and {11-22} twin boundaries (TB) structures are shown to fail for deformations as low as 1% or 2% along the *c*-axis. The {11-21} and {10-11} TBs are much more resistant. Oxygen and hydrogen segregate to all four TBs, except O to {11-22}. The presence of segregated H and O enhances the {10-12} TB limited stability and so does H for the {11-22} TB. They decrease the {10-11} TB stability under high deformation and so does O for the {11-21} TB.

We also study the segregation of these impurities at the twin dislocation (TD, or disconnection) of the experimentally most commonly observed {10-12} mechanical twin. H and O should distribute more or less homogeneously to the TD core and the TB, with only a slight preference to the TD core although not at the interstitial sites of the atomic layer related to the disconnection step itself.



**Dielectric permittivity of aluminium nitride thin films deposited by pulsed DC magnetron sputtering**

M. Hasheminasari<sup>1</sup>, R. Rahman<sup>2</sup>

<sup>1</sup> School of Metallurgy and Materials Engineering, Iran University of Science and Technology (IUST), Tehran, Iran

<sup>2</sup> Department of Physics, Colorado School of Mines, Golden, CO 80401-1887, USA

Aluminum nitride (AlN) is a high-k (thermal conductivity) material with a large band gap, ~6.2 eV. This (AlN) wide band gap semiconductor has an important application to deep (down to 200 - 250 nm) ultraviolet optoelectronics. We study two batches of AlN thin films containing three in each of them; the pressures are maintained at 3 mtorr (batch 1) and 5 mtorr (batch 2) during film deposition. Nitrogen (N<sub>2</sub>) exposure is varied for both batches. We measure dielectric permittivity,  $\epsilon_{re}$ , which is the real part of the complex dielectric constant, of AlN thin films, with thicknesses of about 1  $\mu\text{m}$  deposited on 1 mm thick-glass substrates. We observe, for the first time, the dispersion of  $\epsilon_{re}$  of all AlN films in sub THz regime (100 - 160 GHz). We report that  $\epsilon_{re}$  show higher values for the AlN films deposited under higher pressure than those under lower pressure. Nitrogen (N<sub>2</sub>) to argon (Ar) ratio controls the properties such as texture, surface defects and preferred c-axis orientation, affecting the dielectric permittivity of AlN thin films as well.

**Photocatalytic activity of La substituted  $ZnFe_2O_4$  nanoparticles synthesized by sol gel autocombustion method**

S.M. Masoudpanah, M. Hasheminisari

School of Metallurgy & Materials Engineering, Iran University of Science and Technology (IUST), Tehran, Iran

Sol-gel autocombustion technique was employed to synthesize  $ZnFe_{2-x}La_xO_4$  ( $0 < x < 0.2$ ) nanoparticles. Cation distribution amongst the tetrahedral and octahedral sites and optical properties are highly dependent on La ion substitution in the spinel structure which were examined by X-ray diffraction, Raman spectroscopy and diffuse reflectance spectroscopy. Furthermore, the effects of La substitution on the photodegradation of the methyl orange (MO) under visible light were also studied. The  $ZnFe_{2-x}La_xO_4$  nanoparticles exhibited strong absorption in the visible region with the optical band gap calculated from Tauc's plot in the range of 1.93-1.98 eV. The photocatalytic activity results showed that the degradation of methyl orange dye was enhanced with increasing  $La^{3+}$  substitution from  $x=0$  to  $x=0.2$ , may be due to the octahedral site preference and higher redox potential of  $La^{3+}$  ion as compared to those of iron.

## **Reduction of the number of cracks in albumin using carbon nanotubes**

L.P. Ickitidze, A.Y. Gerasimenko, V.M. Podgaetsky, S.V. Selishchev

National Research University of Electronic Technology - MIET, bld. 1, Shokin Square,  
Zelenograd, Moscow, Russia, 124498

We investigated cracks in a bulk nanomaterial (BNM) formed from a bovine serum albumin (BSA) matrix filled with multiwall carbon nanotubes (MWCNTs) using a laser technique. The water dispersion consisting of 25 mass% BSA and 0.005–0.5 mass% MWCNTs was mixed in a magnetic stirrer and ultrasonic bath for 60 and 30 min, respectively. The dispersion with a volume of  $\sim 2 \text{ cm}^3$  was exposed to laser irradiation with a power density of  $0.1 \text{ MW/cm}^2$  and a generation wave length of 970 nm to obtain a rubbery BNM. Then, the BNM was dried under normal conditions and a  $4 \times 2 \times 10$ -mm bridge-like sample with narrowed parts was cut from it. The free sample's surface was ground and polished. Material density  $\rho$  was determined by hydrostatic weighting in benzene and Vickers microhardness  $H_v$  and breaking strength  $\sigma$  were measured. In addition, optical and scanning electron microscopy (SEM) investigations were carried out.

The obtained experimental values are  $\rho \sim 1200\text{--}1250 \text{ kg/m}^3$ ,  $H_v \sim 120\text{--}350 \text{ MPa}$ , and  $\sigma \sim 15\text{--}30 \text{ MPa}$ . The correlation between crack density  $\pi$  (the number of cracks per unit BNM surface area) and mechanical parameters of the samples was observed: as MWCNT concentration  $C$  is increased, the  $\pi$  value decreases and the  $H_v$  and  $\sigma$  values increase. Crack density  $\pi$  was determined from optical microphotographs of the sample's surface. Sometimes, the crack density was found to be  $\pi \leq 0.1 \text{ mm}^{-2}$ , whereas in the initial BSA matrix it was  $\pi \geq 100 \text{ mm}^{-2}$ . At the same time, the BSA samples exhibited the low Vickers microhardness ( $H_v \sim 50 \text{ MPa}$ ). The cracks were  $\leq 20\text{-}\mu\text{m}$  wide and  $\leq 200\text{-}\mu\text{m}$  long and formed a cellular structure on the BNM surface.

The ordering of the BSA/MWCNT bulk nanomaterial with increasing MWCNT concentration can be attributed to the reduction of the number of cracks and their ordering in the material. Indeed, in the SEM patterns one can clearly see MWCNT threads that link the crack ( $\leq 10 \mu\text{m}$ ) banks.

The investigated BSA/MWCNT bulk nanomaterial with the high mechanical hardness and breaking strength is promising for application as a surgical implant filler.

This research was done at the expense of the project of the Ministry of Education and Science of the Russian Federation (agreement 14.575.21.0044, RFMEFI57514X0044).

**Nanomaterial layers with multiwall carbon nanotubes as strain sensors**

L.P. Ickitidze<sup>1</sup>, E.V. Blagov<sup>2</sup>, A.Y. Gerasimenko<sup>1</sup>,  
A.A. Pavlov<sup>2</sup>, V.A. Petuhov<sup>1</sup>, Y.P. Shaman<sup>3</sup>

<sup>1</sup>National Research University of Electronic Technology - MIET, bld. 1, Shokin Square,  
Zelenograd, Moscow, Russia, 124498

<sup>2</sup>Institute of Nanotechnology Microelectronics of RAS, Leninsky Prospect, 32A, Moscow,  
Russia, 119991

<sup>3</sup>NPK "Technology Center", MIET, Zelenograd, Moscow, Russia, 124498

We report the data of preliminary investigations of a prototype of the strain sensor based on a nanolayer with carbon nanotubes (CNTs). The resistance was measured as a function of the bending angle and number of bending cycles of the layers consisting of a biocompatible carboxymethylcellulose (CMC) matrix filled with multiwall carbon nanotubes (MWCNTs). The layers were deposited onto different flexible substrates, including polyimide, polyester, polyethylene, cotton cloth, and office paper. In the experiments, we used a CMC matrix (~4 wt.%). The prepared matrix was filled with MWCNTs (~2 wt.%). Then, the water dispersion consisting of the CMC and MWCNTs was mixed in a magnetic stirrer and ultrasonic bath again for ~1.5 and ~1.5 h. The dispersion was deposited onto the 30-mm-square substrates of all types by silk screening under the same conditions. The obtained layers were dried at  $t \sim 30^\circ\text{C}$  for ~60 h. The measurements were performed on the prepared samples and repeated after their annealing in air at temperatures of 400–430 K for 30 min. Upon annealing, the moisture and mass of the samples decreased by a factor of about 4–5 relative to the initial values. The layer thicknesses were fixed within  $d \sim 0.3\div 10 \mu\text{m}$ . We determined conductivity  $\sigma_{\text{sq}}$  reduced to the squared area and bulk specific conductivity  $\sigma$ . They were found to be  $\sigma_{\text{sq}} \sim 0.1\div 1 \text{ S}$  and  $\sigma \sim 1\div 10 \text{ kS/m}$ . The strain investigations were carried out on an automatic setup, which allowed controlling bending angle  $\theta$  of a sample, sample resistance, temperature, and number of measuring cycles. The bending angle changed within  $\pm 90^\circ$  with a pitch of  $2^\circ$ . At  $\theta = 0$ , the  $5\times 10\text{-mm}^2$  strip sample was at the initial (unstrained) position. Resistance  $R$  depends on angle  $\theta$  for all the investigated layers as follows: when the sample was bent so as to the layers on the substrate approached one another, the resistance decreased; when, on the contrary, the layers separated, the resistance increased. In the angle range of  $\pm 30^\circ$ , the  $R(\theta)$  dependences were approximately linear (with an error of  $\leq 10\%$ ), while beyond this range, they became nonlinear. For the minimum bending radius ( $\sim 5 \text{ mm}$ ) and  $d \leq 1 \mu\text{m}$ , we obtained the estimated strain sensitivity of  $\sim 150\div 300$ , which is of the same order of magnitude as the available values or higher. In the temperature interval of 290–400 K, the investigated layers exhibited the thermal resistance of  $\leq 0.0005 \text{ K}^{-1}$ , which is lower than the value for the strain sensors based on metal and semiconductor materials by an order of magnitude and more. Thus, the investigated layers of a nanomaterial consisting of CMC and MWCNTs are biocompatible and exhibit the high strain sensitivity and low thermal resistance, which make them promising for medical applications as strain and pressure sensors. The authors thank Professors V.M. Podgaetsky and S.V. Selishchev for useful tips. This research was done at the expense of the project of the Ministry of Education and Science of the Russian Federation (agreement 14.575.21.0089, RFMEFI57514X0089).

## Mathematical analysis and STEM observations of symmetrical tilt grain boundaries

K. Inoue<sup>1</sup>, M. Saito<sup>2</sup>, C.L. Chen<sup>1</sup>, M. Kotani<sup>1</sup> and Y. Ikuhara<sup>1,2</sup>

<sup>1</sup>WPI-AIMR, Tohoku University, Sendai, 980-8577, Japan;

<sup>2</sup>Institute of Engineering Innovation, The University of Tokyo, Tokyo 113-8656, Japan

I

Intensive studies have been carried out since several decades ago to unravel complicated structures of grain boundaries (GBs). After the successful formulation of the coincidence-site-lattice (CSL) theory, in which GBs have been classified by the coincidence index  $\Sigma$ , and the higher dimensional CSL theory has been proposed from a mathematical interest and in order for studying quasicrystals as well. GBs of high index are often found to decompose into arrangements of two types of energetically stable sub-structural unit(SU)s with low index. An algorithm to obtain the arrangement of SUs was provided, assuming that the boundary structure can be described by a combination of two delimiting boundaries, and the structure may change continuously, depending on the misorientation between two adjacent grains [1]. Recently, irrational interfaces resulting in quasi-periodic structures have been studied.

It can be shown that the periodicity of SUs in a symmetrical tilt grain boundaries (STGBs) and that of the O-lattice points are closely related to the distribution of irreducible rational numbers and they exactly correspond to each other [2]. This approach can be generalised to describe the structures of STGBs for any misorientation by interpolating the structure in a given precision. We proposed an algorithm to obtain periodical arrangements of SUs in  $\langle 001 \rangle$  STGBs by means of the Farey sequence [3]. This method can be applied to predict the structure of other types of GBs in metals and ceramics so that the minority units, where GB dislocations can be introduced, are maximally separated by utilising the extended Farey diagram [4].

[1] A. P. Sutton and V. Vitek, *Phil. Trans. R. Soc. Lond.*, **A309**, 1–68 (1983).

[2] K. Inoue, M. Saito, Z.W. Wang, M. Kotani and Y. Ikuhara, *Mater. Trans.*, 56(3), 281-287, (2015).

[3] K. Inoue, M. Saito, Z.W. Wang, M. Kotani and Y. Ikuhara, *Mater. Trans.*, 56(12), 1945-1952, (2015).

[4] K. Inoue, M. Saito, C.L. Chen, M. Kotani and Y. Ikuhara, to appear (2016).

**Simultaneous improvement of strength and ductility in ultrafine grained Fe-24Ni martensitic steel through microstructure and grain boundary engineering**

H. Abolfathi, H. Jafarian, A. Eivani, H. Arabi

School of metallurgy and materials engineering, Iran University of science and technology,  
Tehran, Iran

In this paper, microstructure and mechanical properties in a Fe-24Ni lath martensitic steel processed by accumulative roll bonding (ARB) and subsequent annealing was studied. Microstructural observations analysis was carried out by FE-SEM/EBSD. The microstructural analysis indicated that after 6-cycle of the RAB process nano-structure grains having mean grain size below 200 nm is obtained. Furthermore, the starting typical lath martensitic structure transformed to dual phase microstructure consisting of ultrafine and equiaxed ferrite besides austenite. Formation of austenite can be attributed to significant impact of grain refinement on martensite start temperature. Tensile results proved that both the yield strength and uniform tensile elongation improved drastically during ARB process. Improvement of uniform tensile elongation can be attributed to stabilization of austenite by the ARB process.

**Strain distribution in ultra-thin In(Ga)N/GaN quantum wells**

G.P. Dimitrakopoulos<sup>1</sup>, C. Bazioti<sup>1</sup>, Th. Pavloudis<sup>1</sup>, J. Kioseoglou<sup>1</sup>, S. Kret<sup>2</sup>, J. Kozirowska<sup>3</sup>, T. Suski<sup>3</sup>, E. Dimakis<sup>4</sup>, T. Moustakas<sup>5</sup>, Th. Karakostas<sup>1</sup>, Ph. Komninou<sup>1</sup>

<sup>1</sup>Physics Department, Aristotle University of Thessaloniki, 54124 Thessaloniki, Greece

<sup>2</sup>Institute of Physics, Polish Academy of Sciences, Al. Lotników 32/46 02-668 Warsaw, Poland

<sup>3</sup>Institute of High Pressures Physics, UNIPRESS, 01-142 Warsaw, Poland

<sup>4</sup>Helmholtz-Zentrum Dresden-Rossendorf, 01328 Dresden, Germany

<sup>5</sup>Boston University, Boston, MA 02215, U.S.A.

In the field of III-Nitride compound semiconductors, a lot of emphasis is being placed on the effort for growth of ultra-thin pure InN or high In-content InGaN quantum wells (QWs). It has been shown that, through tailoring of the internal polarization, it is possible that such layers exhibit topological insulator properties, making them suitable for applications in spintronics and quantum computing [1]. Two-dimensional electron gas properties and a temperature-independent behavior in the diagonal resistance, indicating the topological nature of the 2DES, were demonstrated in monolayer-thick, nominally InN QWs [2]. At the same time, the internal quantum efficiency of optoelectronic devices can be benefited by the band gap engineering that is feasible by short period In(Ga)N/GaN superlattices (SPSs). However, the stress-strain state of such heterostructures has not been clarified so far, as it may deviate from the conventional biaxial one, i.e. the plane stress state also referred to as ‘tetragonal distortion’. In the present contribution we have considered the interfacial accommodation at SPS samples comprising nominally 1, 2, and 4 monolayer (ML) thick QWs that were grown by molecular beam epitaxy (MBE) on (0001) GaN templates. We have employed high resolution transmission electron microscopy (HRTEM), and high resolution Z-contrast scanning TEM (HRSTEM) in order to correlate the chemical composition with the strain, focusing on the influence of pseudomorphic accommodation on the out-of-plane strain component. Phenomena of interfacial sharpness and indium clustering have also been considered. Experimental observations were analyzed using geometrical phase analysis, peak finding, and Z-contrast quantification. Experimental results were compared to theoretical simulations, in particular, energetic calculations using *ab initio* density functional theory and molecular dynamics with a modified Tersoff interatomic potential. In both cases, deviation from the biaxial stress state of InN was identified for these QWs in agreement with the experimental observations.

[1] M.S. Miao, Q. Yan, C.G. Van de Walle, W.K. Lou, L.L. Li, K. Chang. *Phys. Rev. Lett.* **109**, (2012) 186803

[2] W. Pan, E. Dimakis, G.T. Wang, T.D. Moustakas, D.C. Tsui. *Appl. Phys. Lett.* **105**, (2014) 213503

Acknowledgement: Work partially supported by the Sonata 8 (2014/15/D/ST3/03808) project of the Polish National Science Centre.

**Increased strengthening of UFG austenitic steel produced by combined loading**

M.V. Karavaeva<sup>1</sup>, M.M. Abramova<sup>1,2</sup>, N.A. Enikeev<sup>2</sup>, G.I. Raab<sup>2</sup>, R.Z. Valiev<sup>1,2,3</sup>

<sup>1</sup>Ufa State Aviation Technical University,  
12 K. Marx str., Ufa 450000 Russia

<sup>2</sup>Institute of Physics of Advanced Materials, Ufa State Aviation Technical University,  
12 K. Marx str., Ufa 450000 Russia

<sup>3</sup>Saint Petersburg State University  
7-9 Universitetskaya naberegneya, Saint Petersburg 199034 Russia

Low carbon austenitic steels are known to be not hardened by heat treatment. Therefore, the formation of ultrafine-grained structure by severe plastic deformation (SPD) has a good prospect for increasing the strength of austenitic steels due to the SPD-induced dislocation and grain boundary strengthening. The maximum strength increase is observed after the early SPD stages, and then there is a gradual decrease in the efficiency of hardening [1]. The further increasing of strength can be obtained by the combination of SPD and industrial processing techniques (such as extrusion or rolling) as shown in [2, 3] for the case of pure Ti. This study is devoted to investigation of the microstructure changes and mechanical properties of austenitic steel 08X18H10T after combined strain treatment by equal channel angular pressing (ECAP) and rolling at  $T = 400^{\circ}\text{C}$ . We report on a significant increase of the strength after deformation via "ECAP + rolling" processing route as compared to plain "ECAP" or "rolling" treatment. Increased strength of SPD+rolling austenitic steel due to grain and twin boundary hardening.

The authors gratefully acknowledge the support from the Ministry of Science and Education of the Russian Federation under grant agreement No. 14.583.21.0012 (unique identification number RFMEFI58315X0012).

- [1] R. Z. Valiev, Bulk nanostructured materials: fundamentals and applications / by Ruslan Z. Valiev, Alexander P. Zhilyaev, Terence G. Langdon. 2013, pp. 456. - ISBN: 978-1-118-09540-9.
- [2] D.V. Gunderov, A.V. Polyakov, I.P. Semenova, G.I. Raab, A.A. Churakova, E.I. Gimaltdinova, V.D. Sitdikov, I.V. Alexandrov, N.A. Enikeev, R.Z. Valiev, I. Sabirov, J. Segurado Evolution of microstructure, macrotexture and mechanical properties of commercially pure Ti during ECAP-conform processing and drawing. Materials Science and Engineering: A. 2013. T. 562. C. 128-136.
- [3] V.V. Stolyarov, R.Z. Valiev, Y.T. Zhu, T.C. Lowe. Microstructure and properties of pure Ti processed by ECAP and cold extrusion. Materials Science and Engineering: A. 2001. T. 303. № 1-2. C. 82-89.



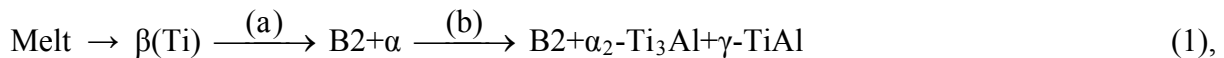
## Phase transformations and ordering in $\gamma$ -TiAl(Nb,Cr,Zr) intermetallic at the high-gradient float zone processing

A.V. Kartavykh, M.V. Gorshenkov, A.V. Korotitskiy

National University of Science and Technology "MISIS", Leninsky pr. 4, 119049 Moscow, Russia

Heat-resistant  $\gamma$ -TiAl based intermetallics are attractive candidates for high temperature structural applications for their low density, specific strength and good creep resistance. Many approaches and techniques are targeted currently to balance strength and ductility of  $\gamma$ -TiAl within the temperature range expanded towards 800-850°C for aerojet turbines design. In the last years, novel  $\gamma$ -TiAl based alloys family, so-called TNM i.e. TiAl(Nb,Mo)-like alloys have been developed [1]. These Al-lean alloys contain a high level of  $\beta$ -stabilizing elements Nb, Mo, Cr, W et al. Such alloying leads to the retaining of a significant amount of  $\beta$ (Ti) phase, or its ordered B2 counterpart within all technologically important domains of phase diagram. Being especially ductile at the elevated temperatures, stabilized  $\beta$ (Ti)/B2 phase plays the positive role in an improvement of performance of TNM alloys. Here we consider the experimental results of structural-phase engineering of Ti-44Al-5Nb-3Cr-1.5Zr (at.%) TNM intermetallic by the high-gradient (300 °C·cm<sup>-1</sup>) induction float zone (FZ) processing.

The phase transformation path of Ti-44Al-5Nb-3Cr-1.5Zr can be simplified as the follow:



where the stage (b) is splintered in turn into two kinetic mechanisms really proceeding in non-equilibrium mode:



On FZ solidification stage the boundary mushy zone layer is affected by the high “pulling” thermal gradient that leads to the axially aligned columnar structure growth of primary  $\beta$ (Ti) *bcc* grains with sole orientation  $\langle 001 \rangle$ . In the course of following solid-state transformations appearing phases generally match the *Blackburn* crystallographic orientation relationships  $\{110\}_\beta \parallel \{0001\}_{\alpha_2} \parallel \{111\}_\gamma$  and  $\langle 111 \rangle_\beta \parallel \langle 11\bar{2}0 \rangle_{\alpha_2} \parallel \langle 110 \rangle_\gamma$ . However, EBSD orientation mapping of FZ-processed microstructure have shown that only some orientations between a parental and born phases can competitively survive under high-gradient thermal impact.

Finally FZ-processing led to the ordered microstructure creation consisting of  $(\gamma + \alpha_2)$  axially-aligned lamellar colonies of submicron lamellae thickness, separated by minor seam-like  $\gamma$ -granular interlayers, and the least intergranular quota of stabilized  $\beta$ (Ti)/B2 phase according to the volumetric ratio of sub-structural constituents  $(\gamma + \alpha_2)/\gamma/\text{B2} = 80:15:5$ .

Specific microstructural adjustment and phase engineering enhances substantially both the ambient and high-temperature mechanical properties of the alloy: yield and ultimate strengths, Young modulus and creep resistance [2]. By this way the thermal limit of  $\gamma$ -TiAl(Nb,Cr,Zr) applicability could be expanded from 750-800°C towards 900-950°C.

*This work supported by the Ministry of Education and Science of Russia, project ID: RFMEFI57514X0042.*

- [1] F. Appel, H. Clemens, F.D. Fischer. *Progress in Materials Science* - in press, doi:10.1016/j.pmatsci.2016.01.001

### **Fe diffusion in Cu-Fe alloys**

A. Rodin, A. Khairullin

Department of Physical Chemistry, NUST MISiS, 4, Leninsky pr-t, Moscow, Russian Federation, e-mail: rodin@misis.ru

The interest to Fe diffusion in Cu is connected with the anomalies which were observed in our previous studies – absence of accelerated GB diffusion in comparison with the bulk [1]. Possible explanation of the result is based on the idea of additional driving force connected with surface energy gradient appeared with Fe concentration gradient at GB. Fe-Cu, as well as Co-Cu, is characterized by increasing of surface and GB energy with increasing of Fe (Co) concentration which is very unusual. At other hand, it was shown that the dependence of surface energy is non-monotonous [2]. That is the reason why diffusion in Cu, preliminary alloyed by Fe, was studied. It was shown that the effect is the same. At other hand the study of Ni diffusion demonstrates that kinetic properties of GB does not change, because the alloying do not effect to Ni GB diffusion parameters.

- [1]. Prokoshkina D., Esin V., Rodin A. Def. and Dif. Forum. V. 323-325 ( 2012). P.171-176.
- [2]. S. N. Zhevnenko J. Phys. Chem. C, 119 (5) (2015), , pp 2566–2571

**Formation of ultrafine-grained structure in TWIP steel during cryo rolling and annealing**

M.V. Klimova<sup>1</sup>, S.V. Zharebtsov<sup>1</sup>, G.A. Salishchev<sup>1</sup>, D.A. Molodov<sup>2</sup>

<sup>1</sup>Belgorod State University, Pobeda 85, Belgorod 308015, Russia

<sup>2</sup>Institute of Physical Metallurgy and Metal Physics, RWTH Aachen University, D-52056 Aachen, Germany

The influence of rolling at 77 and 293K to a true strain  $\epsilon=2.66$  followed by annealing at 200–700°C on formation of ultrafine-grained structure in Fe-0.3C-23Mn-1.5Al TWIP steel was quantified using scanning and transmission electron microscopy. Microstructure evolution at both temperatures of deformation was associated with an increase in the dislocation density and extensive twinning, following by the development of cell or subgrain structure and formation of nanograins. The effect of rolling temperature on twinning and kinetics of microstructure refinement was revealed. Transformation of twin boundaries into arbitrary high-angle grain boundaries due to interaction with lattice dislocations led to the formation of grains/subgrains with the size of 30-50 nm after cryo rolling to strain of 2.66 while new nanograins was not observed during room temperature deformation.

The subsequent annealing resulted in the development of recovered or recrystallized ultrafine-grained microstructure depending on both the deformation temperature and the annealing temperature. The grain growth during recrystallization was accompanied by an increase in the fraction of  $\Sigma 3$  CSL boundaries. The recrystallization onset temperature and the recrystallization kinetics were reduced with a decrease in the temperature of the preceding deformation.

The effect of deformation and annealing temperature on the mechanical properties of TWIP steel was studied.

This work was supported by Russian Foundation for Basic Research (Grant no. 16-38-00550 mol\_a).

**Structure and properties of alumina reinforcement with graphene nanoplatelet obtained by spark plasma sintering**

E.A. Klyatskina<sup>1</sup>, E.G. Grigoriev<sup>2</sup>, A.G. Zholnin<sup>2</sup>, M.D. Salvador<sup>1</sup>, A. Borrell<sup>1</sup>,  
V.V. Stolyarov<sup>2,3,4</sup>

<sup>1</sup>Instituto de Tecnología de Materiales (Universidad Politécnica de Valencia)

<sup>2</sup>National Research Nuclear University MEPhI (Moscow Engineering Physics Institute)

<sup>3</sup>Mechanical Engineering Research Institute of Russian Academy of Sciences

<sup>4</sup>Moscow State University of Mechanical Engineering (MAMI)

Since its discovery, graphene has attracted worldwide attention in the scientific community due to its unique combination of electrical [1], mechanical [2, 3] and thermal [4] properties. Thus, graphene is an ideal second phase in order to improve structure and properties of metals, ceramics and polymers composites materials.

In this work alumina composite reinforced by graphene nanoplatelet (GNP) has been prepared by spark-plasma sintering. Two sizes of  $\delta$ -Al<sub>2</sub>O<sub>3</sub> powders, nanometer and submicrometer, preceded by aluminum oxidation in air plasma jet, were applied to produce composites. The microstructure and mechanical properties of composites are apparently influenced by the addition of GNP. In particular, composite hardness improves notably. Its maximum value reaches 27,4 GPa for a sample fabricated with nanometric powders, which is about 27% higher than the monolithic one. The detailed Raman analysis was found to be very useful to study the graphene orientation in the composite. Eventually the grain morphology in composite is modified by the GNP addition during densification process compared with monolithic alumina structure.

[1] Stankovich S. et al. «Graphene-based composite materials», Nature 442, 282 (2006)

[2] C. Soldano, A.Mahmood, E.Dujardin, Production, properties, and potential of graphene // Carbon48 (2010) 2127–2150.

[3] I.W. Frank, D.M.Tanenbaum, A.M.Vander Zande, P.L.McEuen, Mechanical properties of suspended graphene sheets // J.Vac.Sci. Technol. 6 (2007) 2558–2561.

[4] A.A. Balandiin, S.Ghosh, W.Bao, I.Calizo, D.Teweldebrhan, F.Miao, C.N. Lau, Superior thermal conductivity of single-layer graphene // Nano Lett. 3 (2008) 902–907.

### Grain boundary wetting in Cu-based alloys

O.A. Kogtenkova<sup>1</sup>, A. Korneva<sup>2</sup>, A.B. Straumal<sup>1</sup>, A. Wierzbicka-Miernik<sup>2</sup>, B.B. Straumal<sup>1</sup>

<sup>1</sup>Institute of Solid State Physics Russian Academy of Sciences, Chernogolovka, 2 Academician Ossipyan str., Moscow district, 142432, Russia

<sup>2</sup>Institute of Metallurgy and Materials Science PAN, 30-059 Cracow, Poland

The wetting of grain boundaries by a liquid phase (melt) plays an important role in the materials science. The grain boundary phase transformations can drastically modify the properties of polycrystals. Most important grain boundary phase transformation is the transition from incomplete to complete wetting of a grain boundary by a second phase.

The grain boundary wetting phase transitions in the peritectic system Cu–Co before and after high pressure torsion (HPT) has been studied. The complete and incomplete wetting of Cu/Cu grain boundaries by the Co-containing melt has been studied in Cu–2.2 wt.% Co alloy before high pressure torsion (Fig. 1). Between  $T_{wmin} = 1088$  °C and  $T_{wmax} = 1096$  °C the portion of wetted grain boundaries in the alloy increases with increasing temperature.

The melting process of HPT-treated Cu–2.2 wt.% Co and Cu–4.9 wt.% Co alloys was studied by the differential scanning calorimetry. The position of differential scanning calorimetry peaks showed that melting of ultrafine-grained Cu–Co alloys starts 10–20 °C below bulk solidus line. The thermal effects of melting below bulk solidus line are explained by the grain boundary premelting and permitted to construct the grain boundary solidus line.

The grain boundary wetting in a peritectic system Cu–Co, where the grain boundary wetting layer is depleted by a second component and not enriched like in the conventional cases, has been observed for the first time.

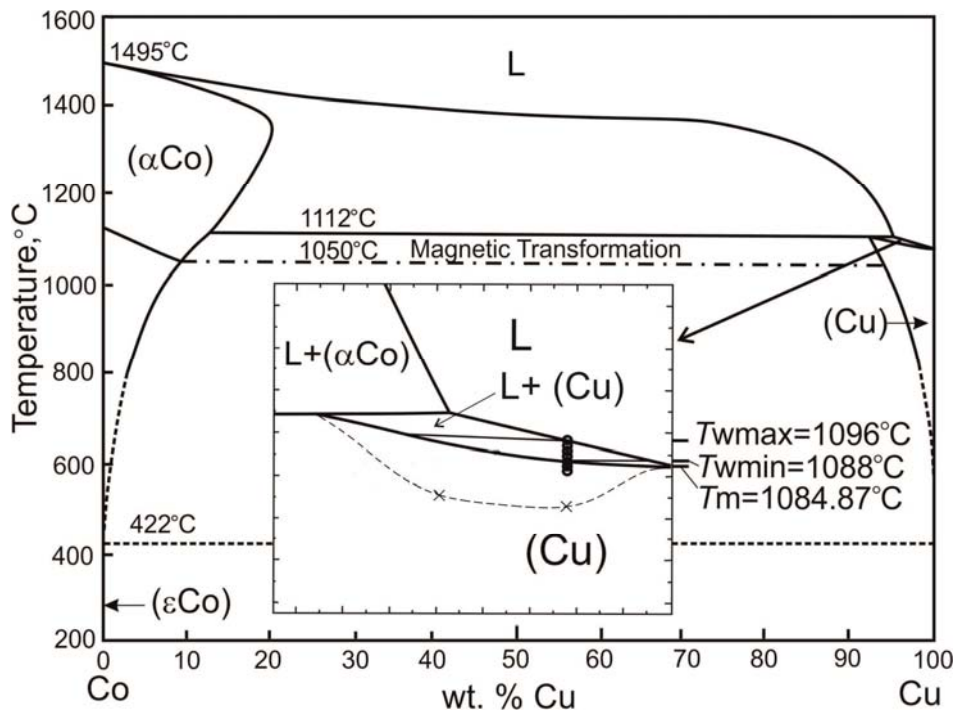


Fig.1. Cu–Co phase diagram with tie-lines of the complete ( $T_{w\text{max}} = 1096^\circ\text{C}$ ) and incomplete ( $T_{w\text{min}} = 1088^\circ\text{C}$ ) phase wetting transition. Solid lines show the phase transitions in the volume. The dotted line indicates the grain boundary phase transitions.

This work was financed by the Russian Foundation for Basic Research (contract 14-08-00972).

**Chemically-driven misfit relaxation in high-alloy content InGaN epilayers**

Ph. Komninou<sup>1</sup>, C. Bazioti<sup>1</sup>, E. Papadomanolaki<sup>2</sup>, Th. Kehagias<sup>1</sup>, T. Walther<sup>3</sup>,  
J. Smalc-Koziorowska<sup>4</sup>, E. Iliopoulos<sup>2</sup>, G.P. Dimitrakopoulos<sup>1</sup>

<sup>1</sup> Physics Department, Aristotle University of Thessaloniki, 54124 Thessaloniki, Greece

<sup>2</sup> Microelectronics Research Group, Physics Department, University of Crete, P.O. Box 2208, 71003 Heraklion-Crete, Greece, and, IESL, FORTH, P.O. Box 1385, 71110 Heraklion-Crete

<sup>3</sup> Department of Electronic & Electrical Engineering, University of Sheffield, Sheffield S1 3JD, UK

<sup>4</sup> Institute of High Pressure Physics, Polish Academy of Sciences, Sokolowska 29/37, 01-142 Warsaw, Poland

The influence of indium concentration on the misfit relaxation processes that take place in high alloy content InGaN thin films was considered. Such films are promising for high efficiency photovoltaics applications. We have considered  $\text{In}_x\text{Ga}_{1-x}\text{N}$  films grown by molecular beam epitaxy (MBE) across the  $x = 0.1-0.6$  compositional range. The films were deposited on (0001) GaN/sapphire templates using the temperature as variable under constant element fluxes, and had thicknesses up to 500 nm. Experimental observations were performed using transmission electron microscopy (TEM), high resolution TEM (HRTEM), scanning TEM (STEM) and energy dispersive x-ray spectroscopy, in combination with high resolution X-ray diffraction (HRXRD). Films grown at lower temperatures exhibited higher alloy contents as a result of reduced indium desorption. Although the reduced growth temperature promoted film mosaicity, they relaxed in a classical manner through misfit dislocation segments. However, upon increasing the growth temperature, indium mobility and segregation at the growth front promoted the compositional pulling phenomenon in response to the misfit strain, thus resulting in compositional grading in the initial stages of growth. In such films, only a small part of the overall misfit was plastically relaxed at the heteroepitaxial interface through misfit dislocations. The relaxation of the residual elastic strain was delayed until a critical thickness was attained for the introduction of multiple basal stacking faults and associated partial dislocations. This resulted in sequestration layering of the films. The sequestration interface was found to constitute a primary source of **a**-type threading dislocations. Further increase of the growth temperature suppressed the film sequestration but led to an alternative strain relaxation mechanism through V-pit formation attributed to preferential indium segregation at the cores of ascending threading dislocations with **c**-type Burgers vector components.

- [1] C. Bazioti, E. Papadomanolaki, Th. Kehagias, T. Walther, J. Smalc-Koziorowska, E. Pavlidou, Ph. Komninou, Th. Karakostas, E. Iliopoulos, G. P. Dimitrakopoulos, *J. Appl. Phys.* **118** (2015) 155301

Acknowledgement: Research co-financed by the EU (ESF) and Greek national funds - Research Funding Program: THALES, project NITPHOTO.

## Long-range atomic order and parameters of special grain boundary in alloys with L1<sub>2</sub> superstructure

E.V. Konovalova<sup>1</sup>, O.B. Perevalova<sup>2</sup>, N.A. Koneva<sup>3</sup>, E.V. Kozlov<sup>3</sup>

<sup>1</sup>Surgut State University, Surgut, pr. Lenina, 1, 628400 Russia

<sup>2</sup>Institute of Strength Physics and Materials Science, SD RAS, Tomsk, pr. Akademicheskii, 2/4, 634021 Russia

<sup>3</sup>Tomsk State University of Architecture and Building, Tomsk, pl. Solyanaya, 2, 634003 Russia

The effect of the long-range atomic order  $\eta$  on the ratio of the general and special grain boundaries in the grain boundary ensemble and on the special boundaries parameters in alloys based on the palladium (Pd<sub>3</sub>Fe) and nickel (Ni<sub>3</sub>Mn, Ni<sub>3</sub>Fe, Ni<sub>3</sub>(Fe,Cr)) with super structure L1<sub>2</sub> was investigated in the paper. The atomic ordering in the studied alloys occurs at the phase transition A1→L1<sub>2</sub>. The different  $\eta$  values in the alloy Pd<sub>3</sub>Fe are achieved by variation of the ordering annealing, in the Ni<sub>3</sub>Mn alloy – by the deviation from stoichiometric composition. The angles of deviation from the theoretical misorientation angles values and rotation axis in coincident site lattice model (CSL) and average value of the relative energy were determined for special boundaries. The values of  $\eta$  were determined by X-ray diffraction (XRD). The grain structure and the parameters of special boundaries were investigated by methods of optical metallography (OM) and scanning electron microscopy (SEM) with using the method of electron backscattered diffraction (EBSD). The relative energy of special boundaries was determined in the triple junctions of grain boundaries using Herring ratio. The average deviation angle of grain boundaries closed to special boundaries from its parameters in the CSL model is reduced at the  $\eta$  increasing in the Pd<sub>3</sub>Fe and Ni<sub>3</sub>Mn alloys. The dependences of the twin boundaries share ( $\delta_{\Sigma 3}$ ) in the special boundaries spectrum from the  $\eta$  are different in the Pd<sub>3</sub>Fe and Ni<sub>3</sub>Mn alloys: in the Pd<sub>3</sub>Fe alloy  $\delta_{\Sigma 3}$  increases and in the Ni<sub>3</sub>Mn alloy  $\delta_{\Sigma 3}$  decreases at the  $\eta$  increasing. This is due to the fact that in alloys with superstructure L1<sub>2</sub>  $\delta_{\Sigma 3}$  depends on the atom mean square displacement:  $\delta_{\Sigma 3}$  decreases at the atom mean square displacement decreasing [1]. In the most of alloys including the Ni<sub>3</sub>Mn alloy experiencing the “superstructure compression” at the A1→L1<sub>2</sub> phase transition the atom mean square displacement decreases. In the Pd<sub>3</sub>Fe alloy the lattice parameter increases with  $\eta$  increasing at the “superstructure compression”. The  $\eta$  increasing is accompanied by atom mean square displacement increasing in the Pd<sub>3</sub>Fe alloy. The dependences of the average relative energy of special boundaries in the alloys with superstructure L1<sub>2</sub> from the  $\eta$  are defined by the dependences of  $\delta_{\Sigma 3}$  in special boundaries spectrum from an atom mean square displacement and by the probability of the grain boundary antiphase boundary (GAPB) superposition to the border plane. The probability increases with the alloy stacking fault energy increasing. The average energy of special boundaries decreases with atom mean square displacement increasing in the alloys Pd<sub>3</sub>Fe and Ni<sub>3</sub>Mn. The special boundary average energy dependences from  $\eta$  are different in the alloys Pd<sub>3</sub>Fe and Ni<sub>3</sub>Mn. In the Pd<sub>3</sub>Fe alloy the special boundary average energy decreases with  $\eta$  increasing. In the Ni<sub>3</sub>Mn alloy the special boundary average energy increases with  $\eta$  increasing.

[1] O. Perevalova, E. Konovalova, N. Koneva, E. Kozlov. *Bulletin of the Russian Academy of Sciences. Physics.* **79** (2015) P. 715.



**EBS and APT study of the reverse transformation mechanism and pseudoelastic behavior in Fe-9.6Ni-7.1Mn martensitic steel under heat treatment**

H.R. Koohdar<sup>1</sup>, M. Nili-Ahmadabadi<sup>1,2</sup>, M. Habibi-Parsa<sup>1,2</sup>, H.R. Jafarian<sup>3</sup>

<sup>1</sup>School of Metallurgy and Materials Engineering, College of Engineering, University of Tehran, Tehran, Iran

<sup>2</sup>Center of Excellence for High Performance Materials, School of Metallurgy and Materials Engineering, College of Engineering, University of Tehran, Tehran, Iran

<sup>3</sup>School of Metallurgy and Materials Engineering, Iran University of Science and Technology, Tehran, Iran

In this paper, a Fe-9.6Ni-7.1Mn (at.%) lath martensitic steel was subjected to study the reverse transformation of martensite to austenite during intercritical annealing. This was carried out at 580 °C in the ferritic-austenitic ( $\alpha+\gamma$ ) dual phase region for 0.48 ks and characterized by means of electron back scattering diffraction (EBS) and atom probe tomography (APT). It was found that under intercritical annealing at 580 °C at a heating rate of 20 °C/s, the reverse transformation takes place through mixed diffusion control mechanism, i.e. controlled by bulk and interface diffusion. Subsequent isothermal ageing after intercritical annealing was also performed at 480 °C for 3.6 ks which resulted in the formation of  $\theta$ -NiMn nano-sized precipitates. The cyclic tensile test results revealed pseudoelastic behavior in the reversely formed austenite after subsequent ageing.

Keywords: Fe-Ni-Mn martensitic steel; Reverse transformation mechanism; Interface; Precipitation; Pseudoelastic behavior.

## The phase transformation in process of contact melting in copper-aluminum system

A.A. Ahkubekov<sup>1</sup>, P.K. Korotkov<sup>1,2</sup>, M.Z. Laypanov<sup>3</sup>, A.R. Manukyants<sup>2</sup>, M.Kh. Ponegev<sup>1</sup>,  
V.A. Sozaev<sup>1,2</sup>, B.M. Khubolov<sup>1</sup>

<sup>1</sup>Kh.M. Berbekov Kabardino-Balkarian State University, Chernyshevskogo, 173, Nalchik, 360004 Russia

<sup>2</sup>North-Caucasus Institute of Mining and Metallurgy (State Technological University), Nikolaeva, 44, Vladikavkaz, 362021 Russia

<sup>3</sup>Karachaevo-Sherkessky State University, Lenina, 29, Karachaevsk, 369202 Russia

Studying of the contact melting (CM) in Cu/Al system plays an important role for development of technology of the contact – reactive soldering, liquid-phase agglomeration micro and the nanopowders Cu and Al, receiving bimetals [1-4]. In the real work an attempt to reveal features of structure of contact layers at contact melting of copper with aluminum of the AMG-2 brand (Structure Mas is made. %: Mg - 1.8-2.8, Mn - 0.2-0.6, Cu - 0.1, Zn - 0.2, Fe - 0.4, Si - 0.4, the rest Aluminum) and aluminum - a lithium alloy (Al - 0.4 at. Li %) is made. Connections med/AMG-2 and copper/Al-Li formed at contact melting are brittle. For example, when receiving a break in system copper/Al-Li in a zone closer to Al-Li to an alloy eutectics with various structures are observed. The break morphology from Cu is characterized by existence of intermetallic phases  $Al_nCu_m$ . These phases, by the sizes  $\approx 40 \times 50 \times 60$  micron, being formed on interphase boundary of Cu/Al, also are, apparently, the reason of embrittlement of the compounds by created at the contact melting (CM).

The processes of phase formations at the contact melting (CM) of thin two-layer films of Cu/Al in vacuum  $10^{-2}$  Pas was studied with help of the raster electron microscope Phenom.

High-purity films were deposited on substrates from optical glass of the S-8 brand by thermal evaporation. It is revealed that on border a two-layer film the Cu/Al-vacuum is observed formation of dendritic structures, and also intermetallic phases. On separate sites of a film it is visible that the eutectic structures mainly formed along of grain boundary (figure 1).

Approximate size of grains  $\sim 40$  microns.

This work was supported by the State Order 3.423.2014/K, project no. 423

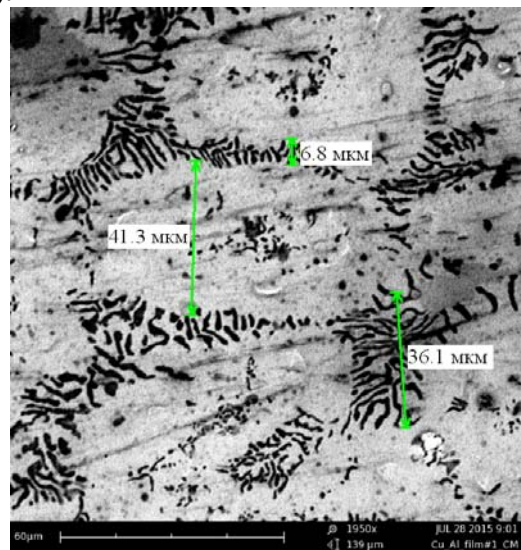


Figure 1. - The photo of granular structure on Cu/Al film, 1950 $\times$

[1] A.A. Ahkubekov, T.A. Orkvasov, V.A. Sozaev. Contact melting of metals and nanostructures on their basis. Moscow: Fizmatlit, 2008, 152p. (Rus).

[2] I.M. Temukuev. *Vestnik KBGU, Ser Fiz* (Nalchik: KBSU) (2000) 5. pp.21-24 (Rus).

[3] P.K. Korotkov, A.R. Manukyants, V.A. Sozaev, M.Kh. Ponezhev, M.Z. Laypanov. *Journal of Surface Investigation: X-Ray, Synchrotron and Neutron Techniques*. 8/4 (2014). 722-725.

[4] A.A. Ahkubekov, S.N. Ahkubekova, T.B. Guppoev, In: *Proceedings of the 12<sup>th</sup> International symposium "Order, disorder and properties of oxides" (ODPO-12), Rostov-na-Donu*. (2009). 1. 196-197 (Rus).

**Annealing-induced indentation recovery in thin Au(Fe) bi-layer films**

A. Kosinova<sup>1</sup>, R. Schwaiger<sup>2</sup>, L. Klinger<sup>1</sup>, E. Rabkin<sup>1</sup>

<sup>1</sup> Department of Materials Engineering, Technion-Israel Institute of Technology, 32000 Haifa, Israel

<sup>2</sup> Karlsruhe Institute of Technology, Institute for Applied Materials, PO Box 3640, 76021 Karlsruhe, Germany

In producing thin films systems for practical application, an understanding of the film morphology evolution upon heat treatment and defects formation is required. Defects on the surface of a metal film can serve as nucleation sites for the holes and thus accelerate the dewetting process and, on the other hand, they can add the fast diffusion paths in the near-surface region and thus promote the healing processes in the material controlled by capillary forces or defects interaction. Here we present the results of defects recovery studies in Au(Fe) bi-layer films modified by nanoindentation, which was employed to inject additional structural defects into the film.

Au(Fe) thin films (48 nm thick Au film on a 2 nm thick Fe underlayer) were deposited on sapphire substrates using electron beam deposition. The Au layer was bi-crystalline, exhibiting a [111] out-of-plane orientation and two twinning-related in-plane orientations. The arrays of nano-indents (array size 100×100 μm) were produced on the film surfaces with a Berkovich tip at applied loads of 0.1 and 0.2 mN. The samples were annealed in a forming gas flow (Ar + 10% H<sub>2</sub>) at 700 °C. We followed the thermally induced morphology evolution of indents after several consecutive heat treatments using optical and atomic force microscopies.

Upon heating, neither lateral growth nor deepening of indents was observed. On the contrary, healing process of indents was thermally initiated. However, it did not result in a totally flat metal surface. The initially triangular imprints evolved to hillocks followed by an adjacent cavity formation. After prolonged annealing, the hillocks dissipated and the cavities deepened. The cavities exhibit an elongated shape with gently sloping edges and a recess in the middle. This fact testifies to a significant contribution of grain boundaries into the cavity formation. We discuss the observed thermo-mechanical behavior in terms of collapse of the dislocation loops generated by the indenter, with concomitant formation of nanopores at the grain boundaries and their subsequent dissolution.

**Mechano-stimulated equilibration of iron microparticles on sapphire**

O. Kovalenko, F.O. Chikli, E. Rabkin

Department of Material Science and Engineering, Technion – Israeli institute of Technology,  
32000 Haifa, Israel

We applied a new method for equilibration of faceted submicrometer Fe particles on sapphire obtained by solid state agglomeration (dewetting) of metal thin film. The method relies on crystalline defects introduced in the particles by the atomic force microscopy-based indentation and tapping by hard diamond tip. The shape changes of individual crystals after plastic deformation followed by a heat treatment were investigated with the aid of Atomic Force Microscopy (AFM) and Scanning Electron Microscopy (SEM), and compared with the changes of the pristine particles.

Over 400 deformed and pristine particles were examined. The shape of deformed particles evolved more readily than the shape of their pristine counterparts, approaching the equilibrium crystal shape. The Winterbottom analysis [1] was applied to 11 deformed particles exhibiting the highest aspect ratio. The resulting value of the work of adhesion ( $W_{ad}$ ) of the Fe(110)/Al<sub>2</sub>O<sub>3</sub>(0001) interface at 880 C ° was calculated assuming that these crystals have reached their equilibrium shape. The obtained value is  $W_{ad} \approx 2.4 J/m^2$ , which is nearly by a factor of two higher than the corresponding value for the molten Fe on sapphire [2].

[1] W.L. Winterbottom, Acta metall. 15 (1967) 303

[2] D. Chatain, I. Rivollet and N. Eustathopoulos, J. Chim. Phys., 83 (1986) 561

**Misfit strain relaxation in the shell of a composite nanowire with a parallelepipedal core**M.Yu. Gutkin<sup>1,3</sup>, S.A. Krasnitckii<sup>1,2</sup>, A.M. Smirnov<sup>2</sup><sup>1</sup> Peter the Great St. Petersburg Polytechnic University, Polytekhnicheskaya 29,  
St. Petersburg, 195251 Russia<sup>2</sup> ITMO University, Kronverkskii 49, St. Petersburg, 197101 Russia<sup>3</sup> Institute of Problems of Mechanical Engineering, Russian Academy of Sciences, Bolshoi 61,  
Vasil. Ostrov, St. Petersburg, 199178 Russia

Nanowires (NWs) and nanoparticles (NPs) have attracted much attention due to their unique electronic, magnetic, optical and catalytic properties which are strongly affected by the presence of various defects. The NWs and NPs, which consist of Au cores and Pd shells, are among the most promising materials for using as catalyst in CO and vinyl acetate oxidation. That is why the structure of such nanostructures is of great interest [1-3]. Experimental observations revealed the presence of multiple stacking faults in truncated octahedral NPs with Au:Pd = 1:1 shells and Au cores. The appearance of stacking faults can be explained by Au diffusion from the core to the shell or by the formation of Shockley partial dislocations accompanied by stacking faults. Based on these observations, we suggest a theoretical model based on the energy approach and describe the possibility of generation of either Shockley partial dislocations associated with stacking faults or perfect dislocations in cylindrical NWs consisting of Au parallelepiped cores and Au-Pd alloy shells. In doing so, we use an analogy between flat interfaces in truncated octahedral core-shell NPs and those in cylindrical NWs with parallelepipedal cores. We analyze the changes on the total energy of the system, which are caused by generation of perfect and partial dislocations by gliding in the shell along the core-shell interface, and calculate the energy barriers characteristic for dislocation appearance in dependence on the core size  $a$  and NW radius  $R$ . For example, it is shown that for  $a = 10$  nm, the barrier value decreases from 2.11 to 0.58 eV/nm for a partial dislocation and from 4.21 to 2.28 eV/nm for a perfect dislocation, with an increase in  $R$  from 7.5 to 11 nm, respectively. This means that in the finest NWs with small shell thicknesses, the generation of partial dislocations is more energetically favorable than the generation of perfect dislocations. However, in thicker NWs with thinner cores, the situation is inverted: for  $a = 7.5$  nm and  $R = 30$  nm, the barrier value is 7.6 eV/nm for a perfect dislocation and 8.7 eV/nm for a partial dislocation. Therefore, the perfect misfit dislocations become more preferable than the partial ones in this case.

SAK and AMS got the support from RFBR project No. 16-32-00521.

- [1] Wang, D., Villa, A., Porta, F., Su, D., Prati, L., *Chem. Commun.* **18** (2006) 1956
- [2] Chen, M., Kumar, D., Yi, C. W., Godman, D. W., *Science* **310** (2005) 291
- [3] Ding, Y., Fan, F., Tian, Z., Wang, Z. L., *J. Am. Chem. Soc.* **132** (2010) 12480

**Multiscale simulation of consolidation phenomena and  
microstructure formation in additive manufacturing**

M.D. Krivilyov, V.A. Ankudinov, G.A. Gordeev, E.V. Kharanzhevskiy

<sup>1</sup>Institute of Mathematics, Informatics and Physics, Udmurt State University,  
Universitetskaya 1, 426034 Izhevsk, Russia

Recent development of lasers has led to numerous new industrial techniques including additive manufacturing. An important fundamental problem in this domain is proper description of underlying physical and chemical phenomena [1] including consolidation and microstructure formation of powders. A multiscale macroscopic-mesoscopic-atomistic approach is developed and employed in the present work which results in a better accuracy of computer simulations on impulse laser melting of metallic powders. This approach has been shown to be a robust tool for numerical simulation of conjugated phase transformations and transport phenomena. The macroscopic analysis reveals that the heating and cooling rates, and solidification velocity in the molten zone are of the order  $10^6$  K/s,  $10^5$  K/s and  $10^{-1}$  m/s correspondingly during impulse laser annealing. Therefore the consolidation of powder occurs as short as in 0.1–1 ms. The analysis of dynamics of the gas-melt interfaces at the mesoscopic level showed the mechanism of coalescence of the molten particles and its dependence on a distance from the surface. At this spatial level important data on the activation energy of viscous flow were extracted to the macroscopic level where the relative density of the powder is calculated as a function of time. The observed conditions of rapid cooling may lead to substantial undercooling of the melt and subsequent phase selection of the metastable phases. The most typical regimes of microstructure formation are analyzed with a conclusion that microsegregation plays moderate role in Fe systems and has a small impact in Ti-base powders. The solidification path is also influenced by a shift [2] in thermodynamic equilibrium of chemical reactions which leads to nontypical phase composition of the sintered material.

- [1] M.D. Krivilyov, E.V. Kharanzhevskii, V.G. Lebedev, D.A. Danilov, E.V. Danilova, P.K. Galenko. *The Physics of Metals and Metallography*, **114** (10) (2013) 799
- [2] M. Krivilyov, E. Kharanzhevskiy, S. Reshetnikov, L.J. Beyers. *Metal. Mater. Trans. B*, 2016, DOI 10.1007/s11663-016-0616-y.

**Crystallization kinetics of metastable cubic solid solutions in nanosized calcia stabilized zirconia precursors upon its thermal evolution**

O.Yu. Kurapova<sup>1,2</sup>, V.G. Konakov<sup>1,2</sup>

<sup>1</sup>Institute of Chemistry, St. Petersburg State University, Universitetskii pr. 26, Peterhof, St. Petersburg, 198504, Russia

<sup>2</sup>Research Laboratory for Mechanics of New Nanomaterials, St. Petersburg State Polytechnical University, Polytechnicheskaya 29, St. Petersburg 195251, Russia

Nanosized stabilized zirconia powders gain much interest both from the theoretical and practical point of view as they are widely used to produce oxygen conducting nanostructured ceramics, ceramic coatings, various composite materials. In this regard, the investigation of crystallization kinetics as well as the relationship between amorphous phase, metastable and stable crystalline solid solutions in stabilized zirconia powders is of particular importance for further fabrication of various advanced materials with desired properties. The use of mild chemistry synthesis techniques gives a unique opportunity to change crystallization kinetics, phase formation mechanisms and control the crystal growth during thermal treatment. As a result significant shift of phase ratio in the final material is observed. Thus the goal of present work was the investigation of crystallization kinetics and phase formation mechanisms in stabilized zirconia in the wide range temperatures and compositions. For the study,  $x\text{CaO}-(100-x)\text{ZrO}_2$ ,  $x=5,9,12,15$  mol.%, was used as a model system. Commercially available salts  $\text{ZrO}(\text{NO}_3)_2 \cdot 2\text{H}_2\text{O}$  and  $\text{Ca}(\text{NO}_3)_2$  were used to prepare 0.1M aqueous solution. 1M ammonium aqueous solution was used as a precipitant. In order to form gels of nanosized hydroxides dilute salt solution was added to ammonium one by drops under defined conditions. Precipitate was filtered, washed until neutral pH and subjected to freeze-drying (20 °C, 0.018 Torr) and freezing in liquid nitrogen. The obtained precursors were annealed at 400-1300 °C for 2 hours. The temperatures and mechanism of phase transformations from amorphous precursor to metastable and stable crystalline solid solution, degree of crystallinity and crystalline growth were controlled by STA

and XRD. In case of freeze drying the phenomena of slow crystallization was observed after treatment at  $\sim 380$  °C during 3 hours and was accompanied by slight exothermal effect exothermic effect on DSC curve. Crystallization kinetics was studied via peak intensity change on XRD patterns. The prolonged exposition at 380 °C resulted in peak intensity increase up to 6200 c.u. Most likely, crystallization process takes place only on particles surface. For all the compositions fast formation of metastable cubic zirconia based solid solution takes place at  $\sim 490$ - $550$  °C and referred to bulk crystallization. According to BET, in the range of  $< 800$  °C phase formation is accompanied by precursor structure change from sponge to globular-type comprised of small crystallites and retarded crystalline growth. In the range from 800 to 1000 °C recrystallization, deagglomeration processes are observed following quasi linear crystalline growth ; 1000-1300 °C baking of agglomerates is observed following recrystallization in case of final compositions (mol.%) 15CaO-85ZrO<sub>2</sub> and 5CaO-95ZrO<sub>2</sub>. Equilibrium phase composition is reached with crystallinity degree of 70-85 %. To summarize, the detailed examination of crystallization processes nanopowders obtained by mild chemistry technique was performed via SEM, BET, X-ray tomography, STA, XRD and PSD-analysis. To summarize, slow crystallization of cubic zirconia based solid solution in zirconia powders, manufactured freeze-drying prior main exothermic effect on DSC curve was studied. The range of cubic zirconia based solid solution stabilization is extended up to 1000 °C comparing to equilibrium phase diagrams due to slow crystalline growth and high powders dispersity. This work was supported by Bortnik fund, UMNİK program (agreement 0020835) and by the special President's scholarship for young scientists (research project CP-1967.2016.1).



**Hard nanocomposite Zr-Si-B-(N) coatings with enhanced wear- and oxidation resistance**

Ph.V. Kiryukhantsev-Korneev, M.V. Lemesheva, I.V. Yatsyuk, D.A. Sidorenko,  
K.A. Kuptsov, A.V. Bondarev, D.V. Shtansky, E.A. Levashov

National University of Science and Technology "MISIS", Leninsky pr., 4, Moscow 119049,  
Russia

Zirconium diboride is a leading material from the family of high-temperature ceramics.  $ZrB_2$  has a very high melting point (3245°C), high thermal conductivity (57.9W/(m·K)), good resistance to thermal shock, low coefficient of thermal expansion ( $5.9 \times 10^{-6} K^{-1}$ ), retention of strength at elevated temperatures and stability in extreme environments, high hardness (22 GPa) and wear resistance. Due to the properties listed above,  $ZrB_2$  based materials are considered as candidates to the protective coatings for different high-temperature applications (turbine and rocket engine components, cutting and stamping tools, leading edges of supersonic flying apparatus etc.). Aim of present work is to develop and study the Zr-Si-B-(N) thin films with enhanced wear- and oxidation resistance.

The Zr-Si-B-(N) films were deposited by DC magnetron sputtering of  $ZrB_2$ -20%Si and 50% $ZrB_2$ -50% $ZrSi_2$  targets in Ar+N<sub>2</sub> (0, 15, and 100% N<sub>2</sub>). The targets were manufactured by means of self-propagating high-temperature synthesis. The structure, chemical and phase composition of films were studied by high resolution transmission and scanning electron microscopy, X-ray diffraction, Raman and infrared spectroscopy, energy-dispersive analysis, and glow discharge optical emission spectroscopy. The films were characterised in terms of their hardness, elastic modulus, elastic recovery, adhesion strength, resistance to cyclic impact loading, friction coefficient, and wear rate. Optical and electrical properties of films were also examined. To evaluate the short- and long-time oxidation resistance, diffusion-barrier properties, and thermal stability, films were annealed in air atmosphere at temperatures 1000-1600°C.

Results obtained show that films deposited at low nitrogen partial pressure consist of nanocrystallites of hexagonal  $ZrB_2$ -phase, 1-3 nm in size and amorphous regions. N-rich films exhibit fully amorphous structure. The maximum hardness 26 GPa, Young's modulus 260 GPa, and elastic recovery 60% were determined for films deposited in Ar-15%N<sub>2</sub>. The addition of nitrogen significantly increased wear resistance in sliding and impact conditions. All films showed good oxidation resistance at 1000°C. Maximal oxidation resistance ( $T_{ox} > 1400^\circ C$ ) was achieved for low-nitrogen Zr-Si-B-(N) films. High protective properties of Zr-Si-B-(N) films are due to formation of dense SiO<sub>2</sub> top-layer reinforced with ZrO<sub>2</sub> nanoparticles which impedes penetration of oxygen into the depth of films.

**Decoration of grain boundary in a monolayer film of C<sub>60</sub> on WO<sub>2</sub>/W(110) surface by static molecules**

S.I. Bozhko<sup>1,3</sup>, E.A. Levchenko<sup>4</sup>, V. Taupin<sup>2</sup>, M. Lebyodkin<sup>2</sup>, C. Fressengeas<sup>2</sup>, O. Lubben<sup>3</sup>,  
K. Radican<sup>3</sup>, V.N. Semenov<sup>1</sup>, I.V. Shvets<sup>3</sup>

<sup>1</sup>Institute of Solid State Physics, Russian Academy of Sciences, Chernogolovka, Ac. Ossipyan str. 2, Moscow district, 142432 Russia

<sup>2</sup>Laboratoire d'Etude des Microstructures et de Mécanique des Matériaux (LEM3) Université de Lorraine/CNRS, 57045 Metz Cedex 01, France.

<sup>3</sup>Centre for Research on Adaptative Nanostructures and Nanodevices (CRANN), School of Physics, Trinity College Dublin, Dublin 2, Ireland.

<sup>4</sup>Department of Physics, Astrakhan State University, Astrakhan 414056, Russia.

The structure of the C<sub>60</sub> monolayers is determined by a competition between the C<sub>60</sub>-C<sub>60</sub> planar interactions and the substrate-monolayer interactions. Intermolecular Van der Waals interaction resulted in self assembling of C<sub>60</sub> into a planar close packed C<sub>60</sub> hexagonal monolayer usually observed in ultrathin films [1]. Substrate-monolayer interaction determines orientation of hexagonal lattice of C<sub>60</sub> on the substrate [2]. Deviations from a spherical shape of C<sub>60</sub> molecule give it rotational degrees of freedom. As a result, rotational phase transition in the film has been established.

The scanning tunneling microscopy investigation of a C<sub>60</sub> molecular layer deposited onto highly anisotropic WO<sub>2</sub>/W(110) surface reveals the existence of two preferential orientations of C<sub>60</sub> grains, inside of grains molecules being self assembled into close packed hexagonal structure. The misorientation between two C<sub>60</sub> domains is accommodated in a tilt boundary by a linear array of molecular structural units (MSU) identified as disclination dipoles, i.e. rotational defects in the hexagonal structure of the layer. In the vicinity of MSUs the hexagonal symmetry of the molecular lattice is broken. Despite STM experiment was performed at temperature above T<sub>C</sub> of rotational phase transition, STM image of individual C<sub>60</sub> in the vicinity of MSU reveals molecular orbital structure, i.e. the rotation of the molecules were suppressed. The distance between static molecule's centers of mass was measured to be about 0.2Å smaller than the same value for rotating molecules far from MSU. Reduction of intermolecular distance for static molecules can be considered as a result of extra pressure. A field theory of Volterra's crystal defects (disclinations and dislocations) was used to construct maps of the elastic energy, elastic strains and stresses induced by the rotational defects over the monolayer. Using realistic elastic constants for the hexagonal fullerene monolayer, the predicted regions of high elastic compression are found to overlap with the regions where the orbital structure of the fullerene molecules is visible, i.e. where their molecular rotation is stopped. Such overlapping is consistent with the idea that apparent stillness of the C<sub>60</sub> molecules is due to lattice compression.

- [1] S. A. Krasnikov, S. I. Bozhko, K. Radican, O. Lübben, B. E. Murphy, S.-R. Vadapoo, H.-C. Wu, M. Abid, V. N. Semenov, and I. V. Shvets // Nano Res. 2011, 4(2): 194-203.  
[2] Bozhko S. I., V. Taupin, M. Lebyodkin, C. Fressengeas, E. A. Levchenko, K. Radican, O. Lübben, V. N. Semenov, and I. V. Shvets // Phys. Rev. B 90, 214106 (2014)

## Intergranular and superficial polyatomic segregation in binary metallic systems

B. Lezzar<sup>1</sup>, O.B.M. Hardouin Duparc<sup>2</sup>, O. Khalfallah<sup>1</sup>, V. Paidar<sup>3</sup>

<sup>1</sup>Mentouri University, LMDM, Constantine, Algeria

<sup>2</sup>École Polytechnique, LSI, CNRS, CEA, Université Paris-Saclay, 91128 Palaiseau, France

<sup>3</sup>Institute of Physics, Academy of Sciences, 18040 Praha 8, Czech Republic

The surface-segregation in a bimetallic alloy strongly modifies the properties vis-à-vis its catalytic properties. The surface excess concentration of one alloying element leads to a sharp change in the behaviour of the alloy compared to its bulk properties.

Surface and interfacial segregation is a continuous subject of numerous studies both experimental and theoretical. After studying the driving forces of segregation at the atomistic level per atomic site at surfaces and at grain boundaries [1-4], we investigate the segregation power of an atomic site when one, or several, neighbouring site(s) are already segregated. We first limit ourselves to the case of binary metallic systems such as for instance Ni(Ag). We study the typical case of the (110) surface [3] and the  $\Sigma=11$  {332} <011> tilt grain boundary which has a rich variety of segregating sites [1-2]. We use Embedded Atom Model potentials of the Finnis-Sinclair family specially adapted to face centred cubic metals and adapted to reproduce their intrinsic stacking fault energies [2-4]. The nature of the mixed parameters between A solute atoms and B solvent atoms is fitted according to formulae developed in [4] on experimental enthalpies of mixing of A within B.

In this study, we examine the effects of segregation of many atoms on the surface in order to compare the multi atomic energies of segregation to those for the monoatomic ones.

- [1] B. Lezzar, O. Khalfallah, A. Larere, V. Paidar, and O. Hardouin Duparc. *Acta Materialia* 52 (2004) 2809
- [2] O. Hardouin Duparc, A. Larere, B. Lezzar, O. Khalfallah, and V. Paidar. *Journal of Materials Science* 40 (2007) 1791
- [3] B. Lezzar, O. Hardouin Duparc, O. Khalfallah, A. Larere, and V. Paidar, *Physical and Chemical News*, 41 (2008) 46
- [4] N.E.H. Djerouni, O. Hardouin Duparc, and O. Khalfallah. *Physics Procedia* 2 (2009) 1359
- [5] V. Paidar, and O. Hardouin Duparc. *International Journal of Materials Research* 100 (2009) 308

## Atomic structure of SiC/SiO<sub>2</sub> vicinal interface

P. Liu<sup>1</sup>, B. Deng<sup>2</sup>, J. Guo<sup>1</sup>, G. Duscher<sup>3</sup>

<sup>1</sup>Key laboratory of interface science and engineering in advanced materials, Ministry of Education, Taiyuan University of Technology, Taiyuan 030024, China

<sup>2</sup>College of Animal Science, South China Agricultural University, Guangzhou 510642, China

<sup>3</sup>Department of Materials Science and Engineering, the University of Tennessee, Knoxville, TN 37996, USA

The SiC/SiO<sub>2</sub> interface is generally considered to be the cause for the reduced electron mobility of SiC power devices. Previous studies have shown a correlation between the mobility and the transition layer width at the SiC/SiO<sub>2</sub> interface. We investigated this interface with atomic resolution Z-contrast imaging and electron energy-loss spectroscopy (EELS), and discovered that this transition region was due to the roughness of the vicinal interface [1]. A through focal Z-contrast image series revealed the 3D structure of the vicinal interface with atomic resolution. The roughness of a vicinal interface consisted of atomic steps and facets deviating from the ideal off-axis cut plane. EELS spectra were interpreted from a chemometrics point of view. SiC/SiO<sub>2</sub> interface was treated as a white multicomponent system and concentrations of chemical species at the interface were quantitatively determined. Results from chemometrics analysis agreed well with the conventional EELS quantification, and confirmed our conclusion that the atomic scale roughness of SiC/SiO<sub>2</sub> vicinal interface is limiting the mobility in the channels of SiC MOSFETs.

- [1] P. Liu, G. Li, Y. K. Sharma, A. C. Ahyi, T. Isaacs-Smith, S. Dhar, J. R. Williams, G. Duscher. *J. Vac. Sci. Technol., A*, **32** (2014) 060603

**Graphene aerogel: synthesis, characterization and properties.**

A.S. Lobach<sup>1</sup>, N.G. Spitsyna<sup>1</sup>, S.A. Baskakov<sup>1</sup>, Y.M. Shulga<sup>1,2</sup>, V.A. Kazakov<sup>3</sup>

<sup>1</sup>Institute of Problems of Chemical Physics, Russian Academy of Sciences, Chernogolovka, Ac. Semenov av. 1, Moscow district, 142432 Russia

<sup>2</sup>National University of Science and Technology MISIS, Leninsky pr. 4, Moscow, 119049 Russia

<sup>3</sup>Keldysh Center, Onezhskaya 8, Moscow 125438 Russia

Graphene aerogels (GA) are a new class of 3D carbon monoliths holding promise for applications as diverse as electrochemical energy storage, drug delivery, pollutant adsorption and tissue engineering. GA consist of entangled single or few layers of graphene, and they partially retain the excellent properties of monolayer graphene such as high electrical conductivity, mechanical strength and surface area.

The starting material for preparation of GA is an aqueous dispersion of graphene oxide (GO). Synthesis GA included process gelation of the GO solution by chemical (NaHSO<sub>3</sub>, H<sub>3</sub>PO<sub>2</sub>+I<sub>2</sub>, ascorbic acid, EDA, PEI) or hydrothermal reduction and result in the formation of reduction GO (RGO) hydrogel. Graphene hydrogel was freeze-dried to produce low density graphene aerogel.

Here we report of the various composition of GA: RGO, RGO+SWCNT, RGO+MWCNT, RGO+humic acid, RGO+humic acid+SWCNT [1,2]. A complex of methods (FTIR, UV-VIS-NIR optical absorption, Raman scattering techniques, scanning electron microscopy, low temperature nitrogen adsorption technique and conductivity measurement was used to prove the chemical structure and to study the properties of the obtained graphene aerogel materials.

The work was supported by the RFBR Grant No. 14-03-00428a.

[1] Yu.M. Shul'ga, A.S. Lobach, S.A. Baskakov et al., *High Energy Chem.*, 2013, **47**(6), 331.

[2] S.A. Baskakov, A.S. Lobach, S.G. Vasil'ev et al., *High Energy Chem.*, 2016, **50**(1), 43.

## **Production of mechanically alloyed nanocrystalline Fe-Cu-Co-Ni binders for superhard materials cutting tools**

P.A. Loginov, D.A. Sidorenko, A.A. Zaitsev, E.A. Levashov

National University of Science and Technology “MISIS”, Leninsky prospect, 4, Moscow, 119049 Russia

Cutting tools based on superhard materials, such as diamond and cubic boron nitride, are widely used in construction industry for precise disassembling of building sections, road surfaces, take-off runways etc. Although the grains of superhard materials are responsible for process of cutting itself, the role of another constituent – metallic binder – is also crucial for obtaining of high performance tools. It is established, that higher the mechanical properties of the binder – better diamond retention in the working layer of the tool and, usually, longer its operating life. The tools with high strength can be used at machining of materials with severe abrasivity. Therefore, upgrading of mechanical properties of the binders can have a significant impact on tool performance.

There are number of well-known approaches for enhancing of binder properties – modification of chemical composition, introduction of dispersion hardening agents (nanoparticles of different kind), application of ultrafine powders. One of the most recent methods used in this area is mechanical alloying (MA) and the structure variation of the initial metallic powder mixtures. In general MA is known as an effective method for production of solid solutions, nanocrystalline and amorphous alloys. Supersaturated solid solutions in non-equilibrium state with improved mechanical properties as to compare with conventional materials can be obtained using MA of immiscible or partially soluble elements.

The work is dedicated to development of a new Cu-Fe-Ni-Co mechanically alloyed (MA) binder composition using planetary ball mills “Activator-2s” and “MPP-1”. Carbonyl Fe, Co, Ni, electrolytic Cu and Cu-Fe-Co-alloy powders were taken in different proportions as initial materials. Three principal types of microgranules with various microstructure were obtained due to high-energy processing under different MA conditions. The 1st type consists of individual strained particles of initial powders. The 2<sup>nd</sup> - is microgranules having lamellar like structure with 1-3  $\mu\text{m}$  layer thick. In the 3rd case mixture contains the coarse grains (up to 100  $\mu\text{m}$ ) chemically uniform granules which composed of supersaturated solid solution fcc-(Ni,Fe,Cu,Co). Pressing and sintering features for all obtained types of microgranules were investigated. Phase compositions of powder mixtures before and after hot isostatic pressing were studied by means of X-ray diffraction analysis. Nanocrystalline structure of hot pressed binder samples was investigated by means of TEM, HRTEM, and EDX.

**Authors** gratefully acknowledge the support from the Russian Foundation for Basic Research (project no. 15-38-70019).

**The elastic properties of the polycrystalline refractory metals at high pressures**

A.V. Lugovskoy, Yu.Kh. Vekilov, O.M. Krasilnikov

National University of Science and Technology MISiS, Leninskiy prospekt 4, 119049, Moscow, Russia

The general method is proposed for the calculation of the  $n$ -order ( $n \geq 2$ ) elastic constants of a loaded crystal in the framework of nonlinear elasticity theory. The two calculations methods are developed for the second and third order elastic constants of crystals with cubic symmetry at hydrostatic compression from the energy – finite deformation and the stress – finite deformation relations. The crystal energy and the mechanical stresses at different deformations are defined in the framework of density functional theory. The second and third order elastic constants in the pressure range 0 – 600 GPa are calculated for the *bcc* Nb, Ta, Mo and W. The effective second and third order Lamé constants for isotropic aggregates of cubic crystals for these metals in the studied pressure range are obtained from the calculated results. The comparison with the experimental data is presented.

## An improved dislocation model of the parent-martensite interface in a NiTi shape memory alloy

X. Ma<sup>1,2</sup>, C.B. Ke<sup>1</sup>, S. Cao<sup>1</sup>, X.P. Zhang<sup>1</sup>

<sup>1</sup>School of Materials Science and Engineering, South China University of Technology, 381 Wushan Road, Guangzhou 510640, Guangdong, China

<sup>2</sup>Department of Mechanical Science and Engineering, University of Illinois at Urbana-Champaign, 1206 W. Green St., Urbana, IL 61801, USA

In the previous topological model (TM) of martensitic phase transformations [1], the rigid body rotation of the parent and martensite crystals with respect to the terrace plane was treated as a free variable, and a range of arbitrary values of the twist angle were used until the resulting habit plane was found to be closest to the experimentally observed ones. However, the defects may not be able to physically present at the exactly required position for a complete coherency strain accommodation. To tackle this problem, a criterion is set out by firstly considering the coincidence of  $\xi_{TM}^L$  and  $\xi_i^L$ , therefore an optimum value of the twist,  $\omega_o$ , can be mathematically deduced by solving the equilibrium equations, so that an energetically favorable and physically available strain-relieving defect network can be obtained [2]. In the present work, the newly developed criterion has been applied to analysis the interface between the B2 cubic parent and the B19' monoclinic martensite crystals in a NiTi shape memory alloy; the defect parameters, i.e., the Burgers vectors, line directions, and dislocation spacings of the interfacial dislocations are quantified via rigorous crystallographic analysis and matrix algorithm based on the Frank-Bilby equation. Consequently, the martensite transformation crystallographic features, e.g., the habit plane index, the orientation relationship and the transformation strain, of the NiTi alloy are determined, the results so obtained are found to be in excellent agreement with those predicted by the well-established phenomenological theory of martensite crystallography (PTMC) [3], as well as experimental observations [4]. In addition, it should be note that the predicted defects are not only able to fulfill the function of completely accommodating the coherency strains arising on the terrace plane, but also capable of reaching the required position at the habit plane by a diffusionless manner.

- [1] R.C. Pond, X. Ma, Y.W. Chai, J.P. Hirth, Chapter 74: *Topological modelling of martensitic transformations*, in *Dislocations in Solids*, F.R.N. Nabarro and J.P. Hirth, eds., Vol. 13, Elsevier, Amsterdam (2007) 225
- [2] Z.Z. Wei, X. Ma, X.P. Zhang. *Phil. Mag. Lett.* **94** (2014) 288
- [3] C.M. Wayman, *Introduction of the Crystallography of Martensitic Transformation*, Macmillan Company, New York (1964) 1
- [4] O. Matsumoto, S. Miyazaki, K. Otsuka, H. Tamura. *Acta Metall.* **35** (1987) 2137



**Role of deformation banding in grain refinement in an aluminum alloy under equal-channel angular pressing**

S. Malopheyev, V. Kulitskiy, M. Gazizov, R. Kaibyshev

Laboratory of Mechanical Properties of Nanostructural Materials and Superalloys, Belgorod State University, Pobeda 85, Belgorod 308015, Russia

The mechanism of grain refinement of an Al-5.4Mg-0.4Mn-0.2Sc-0.09Zr alloy subjected to equal-channel angular pressing (ECAP) with a back pressure (BP) for up to 12 passes via route B<sub>C</sub> at 573K (300 °C) was studied. New grains form through a specific mechanism of continuous dynamic recrystallization (CDRX). The formation of microshear bands (MSB) enclosed by a pair of geometrically necessary boundaries (GNBs) plays a vital role in initiation of recrystallization process. Transformation of the 2D lamellar structure to 3D crystallites occurs through the intersection of primary MSBs by secondary MSBs, mainly. Upon further deformation the GNBs evolve to planar sub-boundaries and then to high-angle boundaries. The formation of primary MSBs is associated with the appearance of texture  $\alpha$ -fiber, and the appearance of a new type of shear texture, which is an axial {112} texture of orientation around the transverse direction accompanies the formation of ultra-fine grains.

**Modelling of granule formation process of titan-magnetite powdered materials by the method of rolling**

G. I. Kelbaliyev, A.N. Mamedov, Q.M. Samedzade, A.M. Qasimova, D.B. Tagiyev

Institute of Catalysis and Inorganic Chemistry ANAS, G.Javid av., 113,  
Baku AZ-1134, Azerbaijan

The construction of complex model of titan-magnetite granule formation of powdered materials in drum granulators taking into account of anisotropy of structure and laminating on surface is considered [1]. It has been noted that granule formation proceeds in some stages depending on relaxation time of embryo formation. On the base of model a graphic interpretation of process of laminating of powder on surface is cited. Rheological model of compact of granules under action of external deformation stresses allowing to estimate the change of porosity and density in time of arrive is presented. The comparison of calculation and experimental results for evolution of distribution of granules on sizes has been presented. The granulation process of titan-magnetite powdered materials is stochastic as far as the prepared granulemetric composition is polydisperse which is determined by uniform completeness of granules depending on drops sizes of binding substance (dispersion character), particles of powder and such phenomena as coagulation and destruction, wear and deformation. At the same time as a result of drum rotation the forming nuclei can also coagulate, which influences on the end granule size. Apparently, with increase of drops size of liquid and nucleus sizes, the probability of formation of granules of large size and large lumps is increased.

1. Kelbaliyev G.I., Samedli V.M., Samedov M.M., (2009). Modeling of granule formation process of powdered materials by the method of rolling. // Powder Technology, v.194, № 1-2, p.87-94.

## **Influence of microstructure evolution on microhardness and electrical resistivity of UFG Al under annealing**

A.M. Mavlyutov<sup>1</sup>, A.S. Bondarenko<sup>2</sup>, M.Yu. Murashkin<sup>2,3</sup>, R.Z. Valiev<sup>2,3</sup>, T.S. Orlova<sup>1,4</sup>.

<sup>1</sup>St. Petersburg National Research University of Information Technologies, Mechanics and Optics, Kronverksky Pr. 49, St. Petersburg 197101 Russia

<sup>2</sup>St. Petersburg State University, Universitetskaya nab. 7–9, St. Petersburg 199034 Russia

<sup>3</sup>Institute of Physics of Advanced Materials, Ufa State Aviation Technical University, K. Marx str. 12, Ufa 450000 Russia

<sup>4</sup>Ioffe Physical-Technical Institute, Russian Academy of Sciences, Politekhnicheskaya ul. 26, St. Petersburg 194021 Russia

Metallic materials subjected to severe plastic deformation demonstrate unique physical and mechanical properties due to ultra-fine grained (UFG) structure and high density of defects [1].

In present work, we have studied the influence of microstructure evolution on microhardness and electrical resistivity of commercial purity Al subjected to severe plastic deformation.

An UFG structure has been obtained by high-pressure torsion (HPT) at room temperature (RT). Then samples were annealed at different temperatures from the range of 90 – 400 °C to create structures with different grain sizes. Characterization of microstructure were carried out using X-Ray diffraction analysis, transmission electron microscopy and electron back-scattering diffraction. The temperature dependence of electrical resistivity in the temperature range from 77 to 300 K was measured by standard four-probe technique with accuracy of 1%. Microhardness was estimated by Vickers method.

It is shown that the microhardness of the coarse grain (CG) material was 205 MPa which increased up to 596 MPa after HPT treatment. It was found that there are no significant decrease in hardness of the UFG material at annealing temperatures below 200 °C. After annealing at 400 °C, no difference in hardness was observed in comparison with initial CG state.

Experimentally obtained decrease in electrical resistivity as a result of annealing at 90 °C indicates an elevated resistivity of grain boundaries in non-equilibrium state. The tunnel model of electrical resistivity of grain boundaries is discussed. The mean width of the potential barriers at grain boundaries in UFG Al was determined. Large value of potential barriers is noted in comparison to the crystallographic width of grain boundaries.

[1] R.Z. Valiev, R.K. Islamgaliev, I.V. Alexandrov. *Prog. Mat. Sci.* (2000) **45** 103 – 189.

**The structure and transport properties of the solid electrolytes based on  
ZrO<sub>2</sub>-Y<sub>2</sub>O<sub>3</sub>, obtained directional crystallization of the melt**

M.A. Borik<sup>1</sup>, V.T. Bublik<sup>2</sup>, S.I. Bredikhin<sup>3</sup>, A.V. Kulebyakin<sup>1</sup>, I.E. Kuricyna<sup>3</sup>,  
E.E. Lomonova<sup>1</sup>, V.A. Mizina<sup>1</sup>, Ph.O. Milovich<sup>2</sup>, S.V.Seryakov<sup>2</sup>, N.Yu.Tabachkova<sup>2</sup>.

<sup>1</sup>Prokhorov General Physics Institute, Russian Academy of Sciences, Moscow, Vavilov Str., 38,  
119991 Russia

<sup>2</sup>National University of Science and Technology "MISiS", Moscow, Leninsky Prospekt 4,  
119049 Russia

<sup>3</sup>Institute of Solid State Physics, Russian Academy of Sciences, Chernogolovka, Ac. Ossipyan  
str. 2, Moscow district, 142432 Russia

Currently, as a solid electrolyte for a solid-oxide fuel cell (SOFC) mainly is used ceramic materials based on ZrO<sub>2</sub>. The grain size distribution, the inhomogeneity distribution components on grain boundaries and in their bulk can influence on electrical properties and stability of the operating conditions SOFC. In contrast to ceramic materials, the influence of these factors can be eliminated at using of single crystals. One problem is the unstability of the characteristics of SOFC at operating temperatures for a long time, which can be due to the phase transformations and recrystallization ceramic at operating temperatures. For the single crystals the stability is determined only by the phase steadiness of the solid solution. The aim of this work was study the influence of the structure on the physical characteristics of the solid solutions ZrO<sub>2</sub>-Y<sub>2</sub>O<sub>3</sub>, obtained by directional solidification.

The crystals ZrO<sub>2</sub> stabilized with yttrium oxide in a wide range of compositions (from 2 to 12 mol.% Y<sub>2</sub>O<sub>3</sub>) were studied. The phase composition, density, physical and chemical properties of the crystals we determined for all concentrations.

The partially stabilized zirconia (PSZ) crystals consist of two tetragonal phases (P4<sub>2</sub>/mnc) with varying degrees of tetragonal at adding Y<sub>2</sub>O<sub>3</sub> in concentrations from 2.5 to 5.0 mol.% Y<sub>2</sub>O<sub>3</sub>. The first tetragonal phase (t) has a ratio  $c/\sqrt{2}a - 1,014-1,015$ , and a second (t') has ratio  $c/\sqrt{2}a - 1,004-1,005$ . The both tetragonal phase have twinned structure, but have different twinned morphology. The concentration of Y<sub>2</sub>O<sub>3</sub> in t and t' phases and the quantitative ratio of the phases in crystals with concentration of yttrium from 2.5 to 5.0 mol.% Y<sub>2</sub>O<sub>3</sub> were estimated. Cubic (Fm3m) phase is formed in crystals above 6 mol.% Y<sub>2</sub>O<sub>3</sub>, in the form of local inclusions. The crystals consist only of the cubic phase beginning with a concentration of 8 mol.% Y<sub>2</sub>O<sub>3</sub>. Conductivity changed nonmonotonic, with increasing concentration of Y<sub>2</sub>O<sub>3</sub>. The existence of two maxima of ionic conductivity at temperatures 800-900°C for compositions ZrO<sub>2</sub> - 3.2 mol.% Y<sub>2</sub>O<sub>3</sub> and ZrO<sub>2</sub> - 8 mol.% Y<sub>2</sub>O<sub>3</sub> was shown. The electrical conductivity decreased with increase the concentration of the stabilizing impurity in crystal above 10 mol.% Y<sub>2</sub>O<sub>3</sub>. The mechanism of the formation of different types of twin structure in crystals ZrO<sub>2</sub>-Y<sub>2</sub>O<sub>3</sub> system was proposed and the bond of these structures with the physical and chemical characteristics of crystals, including the physical properties was shown.

This work was financially supported by RSF (Project No. 16-13-00056)

### **The Portevin–Le Chatelier effect in an AlMg alloy containing precipitates**

A.A. Mogucheva<sup>1</sup>, D.Y. Yuzbekova<sup>1</sup>, D.A. Zhemchuzhnikova<sup>1,2</sup>, T.A. Lebedkina<sup>2</sup>, M.A. Lebyodkin<sup>2</sup>, R.O. Kaibyshev<sup>1</sup>

<sup>1</sup>Belgorod State University, Pobedy str. 85, Belgorod 308015 Russia

<sup>2</sup>LEM3 CNRS UMR 7239, Université de Lorraine, Ile du Saulcy, 57045 Metz CEDEX 01, France

Al-Mg alloys exhibit instability of plastic flow known as the Portevin-Le Chatelier (PLC) effect [1-3]. Minor additions of Sc and Zr to Al-Mg alloys give rise to precipitation of coherent nano-scale Al<sub>3</sub>(Sc,Zr) dispersoids which impart significant strengthening and promote the efficiency of the extensive grain refinement [4-6]. However, the effect of Al<sub>3</sub>(Sc,Zr) dispersoids on the PLC instability is virtually unstudied. Although the literature data testify that the secondary phase can also affect the serration patterns, this question mostly remained beyond the attention of researchers. The objective of this work is to study spatiotemporal behaviors in an Al-Mg alloy containing nanoscale coherent precipitates, with different grain structures, namely, in either a coarse-grained state or with unrecrystallized, partially recrystallized, and fully recrystallized grain structures generated upon severe plastic deformation.

The spatial and temporal characteristics of the PLC instabilities in the investigated 5024 alloy were studied experimentally at room temperature with the aid of high-frequency local extensometry. Tensile tests were carried out on flat specimens at strain rates in the range from 10<sup>-4</sup> s<sup>-1</sup> to 10<sup>-2</sup> s<sup>-1</sup>. It was found that the grain refinement significantly affects the stress serration patterns. At the same time, they mostly belong to well-known types of serrations, A, B, and C (see, e.g., [1-3]). These types are generally believed to be associated with transitions from a quasicontinuous propagation of deformation bands to a hopping propagation and to static bands when the strain rate is decreased. Surprisingly, the propagation mode was found to persist in the entire strain-rate range. Moreover, this observation concerns both the coarse-grained and ultrafine-grained material, in spite of the differences in the characteristic serration patterns. This unusual behavior is discussed in relation with the role of precipitates.

The financial support received from the Ministry of Education and Science, Russia, (Belgorod State University project №14.587.21.0018 (RFMEFI58715X0018)) is acknowledged. The main results were obtained by using equipment of Joint Research Center, Belgorod State University. T. L. acknowledges support by the Center of Excellence “LabEx DAMAS” (Grant ANR-11-LABX-0008-01 of the French National Research Agency).

- [1] J.M. Robinson and M.P. Shaw: Intern. Mater. Reviews., 1994, vol. 39, pp. 113-22.
- [2] M. Lebyodkin, L. Dunin-Barkowskii, Y. Bréchet, Y. Estrin and L. P. Kubin: Acta Mater., 2000, vol. 48, pp. 2529-41.
- [3] H. Halim, D.S. Wilkinson and M. Niewczas: Acta Mater., 2007, vol. 55, pp. 4151-60.
- [4] S. Malopheyev, V. Kulitskiy, S. Mironov, D. Zhemchuzhnikova, R. Kaibyshev, Mater. Sci. Eng. A 600 (2014) 159-170.

## **Deformation –induced wetting processes at phase boundaries in superplastic Pb-Sn eutectic**

F. Muktepavela, R. Zabels

Institute of Solid State Physics, University of Latvia, 8 Kengaraga str, Riga LV-1063, Latvia

The mechanical properties of the interphase boundaries (IB) and phases in the Sn–38wt.%Pb eutectic both in the deformed and annealed state were investigated at room temperature using tensile, micro- and nanoindentation tests. SEM, AFM and optical microscopy were used for the structural investigations. Bimetallic solid phase joints (Sn/Pb) with atomically clean interfaces were obtained by a special method of cold welding at room temperature [1] and were used as a macromodel of the deformed IB. The strength properties of the joints were determined by the shear test. The local hardness and elastic Young's modulus of the individual grains and the development of grain boundary sliding (GBS) were studied on the atomically clean surfaces and on the real surfaces of Pb-Sn eutectics using micro- and nanohardness testers.

It was found that the deformation of the alloy is localized at the Pb/Sn interphase boundaries and occurs by grain boundary sliding (GBS) accompanied by fast diffusion processes under the action of the capillary forces on the Pb/Sn IB. During severe plastic deformation the lattice dislocations are continuously absorbed by GBs increasing the GB energy. As a result, the complete wetting of such non-equilibrium GBs by the second solid phase appears. This deformation-induced process takes place due to the wetting of Sn with Pb. Diffusion accommodation processes are facilitated by the low values of the Pb/Sn interphase energy ( $0.07 \text{ J/m}^2$ ), the tin's overlaying with lead is thermodynamically favourable because the condition  $\gamma_{\text{GB}} > 2 \gamma_{\text{IB}}$  is satisfied. Processes are also kinetically allowed due to the relatively high homologous temperature ( $> 0.5T_m$ ). It was shown the differences in the structural investigations of GB wetting in the Sn–Pb system both in equilibrium conditions (by melt) and during continuous strain.

From the results of micro- and nanoindentation measurements obtained on the atomically clean surfaces it follows that in the deformed state near surface layer has very small hardness. This could be related to the intensive deformation-induced diffusion mass transfer processes at the all free surfaces of the grains.

In the annealed eutectic both the Sn and Pb phase are strengthened and the relaxation processes occur mainly at the IB. The IB in the annealed Sn–Pb eutectic act as barriers to the motion of dislocation ensemble when the size of the plastic zone is comparable to the grain size and lower the hardness values due to the development of GBS when more grains are involved in the process of deformation. Nanoindentation testing allowed us to trace the change in the values of the elastic Young's modulus ( $E$ ) at different stages of the indenter displacement. The obtained values of the nanohardness and elastic modulus evidence that the IBs in the Sn–Pb eutectic have to be considered as a separate quasi-phase with its own properties. This work has been supported by the National Research Program IMIS2

[1] F. Muktepavela and J. Maniks. Def. Diff. Forum, **216-217** (2003) 169-176.

## Parameters of localized states in two-dimensional gallium monosulfide

S.N. Mustafaeva<sup>1</sup>, M.M. Asadov<sup>2</sup>

<sup>1</sup>Institute of Physics, Azerbaijan National Academy of Sciences, pr. H. Javid 131, Baku, AZ1143 Azerbaijan

<sup>2</sup>Institute of Catalysis and Inorganic Chemistry named after M. Nagiyev, Azerbaijan National Academy of Sciences, pr. H. Javid 113, Baku, AZ1143 Azerbaijan

According to  $T$ - $x$  diagram of the system Ga–S two compounds GaS and Ga<sub>2</sub>S<sub>3</sub> are creating. Gallium monosulfide melts congruently at  $1235 \pm 5$  K. GaS single crystals are layered wide-gap semiconductors with a rather high dc- resistivity [1]. GaS-based materials, combining interesting electrical and optical properties, are potential candidates for use in various transducers, light modulators, and information storage units. The layered GaS single crystals used for our study were grown by the Bridgman method and have hexagonal structure with lattice parameters:  $a = 3.58 \text{ \AA}$ ,  $c = 15.47 \text{ \AA}$  at room temperature. The bulk sample, which is used in the experiments, was prepared by splitting the single crystal along the cleavage plane and hence the resultant surface was mirror-like without any mechanical treatment. It is revealed that GaS single crystals exhibit a variable-range hopping conduction along a normal to their natural layers at temperatures  $T = 140\text{--}238$  K in a dc- electric field. Estimates are made for the density of states near the Fermi level ( $6.2 \times 10^{19} \text{ eV}^{-1} \text{ cm}^{-3}$ ) and their energy spread (0.08 eV), the average jump distance (46 Å), the activation energy of the hopping conductivity (0.07 eV) and the concentration of trapping states ( $5 \times 10^{18} \text{ cm}^{-3}$ ) responsible for the hopping dc-conductivity in GaS single crystal. Ac-electric and dielectric properties of the GaS single crystals were studied in a broad frequency range. The nature of dielectric losses and the hopping mechanism of charge transport in the GaS crystals were established, and the parameters of localized states in the forbidden gap of studied crystals have been evaluated from ac-electrical measurements.

[1] S.N. Mustafaeva, M.M. Asadov, *Inorganic Materials*. **25**, 212 (1989).

**Atomistic simulation of shear deformation at bcc-Fe grain boundary and effect of Cr<sub>23</sub>C<sub>6</sub> precipitation**

K. Nakamura, T. Kumagai, T. Ohnuma

Central Research Institute of Electric Power Industry, Nagasaka, 2-6-1, Yokosuka, Kanagawa, Japan

Nucleation of the creep void under long-time high temperature creep is dominated by plastic deformation and vacancy condensation near grain boundaries (G.B.s). Once creep voids nucleate, they grow by vacancy diffusion along G.B.s and coalescence of neighboring voids forms micro-crack along grain boundaries. In the case of the commercial heat resistant steels, fine precipitates are utilized to inhibit dislocation motion. However, it was revealed that creep voids nucleate at interfaces between parent phase and precipitated carbides on G.B.s [1]. Thus, vacancy formation energy and theoretical tensile stress at representative  $\alpha$ -Fe G.B. and  $\alpha$ -Fe/V<sub>4</sub>C<sub>3</sub> interface has been investigated [2]. In order to understand the microscopic deformation mechanism of the heat resistant steels, estimation of the temperature dependence of the critical shear stress to induce the slip deformation at the G.B. must be essential. Therefore, in this study, classical molecular dynamics (MD) simulations were utilized to investigate the temperature and tilt angle dependence of shear deformation behavior at  $\alpha$ -Fe G.B.s. By performing Parrinello-Rahman MD simulation, shear stress was gradually applied along the G.B. plane. Shear deformation at  $\langle 001 \rangle$  axial  $\alpha$ -Fe grain boundaries was found to accommodate the grain boundary migration. The critical shear stress to induce the grain boundary migration decreased as increasing temperature and MD simulation time, because G.B. migration is thermally activated process. Tilt angle dependence of the critical shear stress could be successfully explained by the classification of the structure units at G.B.s. In addition to the pure  $\alpha$ -Fe G.B., the effect of the G.B. precipitation on the critical shear stress was also investigated by using our developed Fe-Cr-C ternary bond order-type interatomic potential [3]. Cr<sub>23</sub>C<sub>6</sub> precipitation on the  $\langle 001 \rangle$  axial  $\alpha$ -Fe G.B.s was found to increase the critical shear stress as shown in Fig. 1. Strengthening of the critical shear stress was verified by the theoretical equation to consider the increase of the shear strength by the ordered precipitates [4]. Moreover, it was confirmed that shear deformation mechanism at the Cr<sub>23</sub>C<sub>6</sub> precipitated  $\langle 001 \rangle$  axial  $\alpha$ -Fe G.B.s was the same as pristine G.B.s.



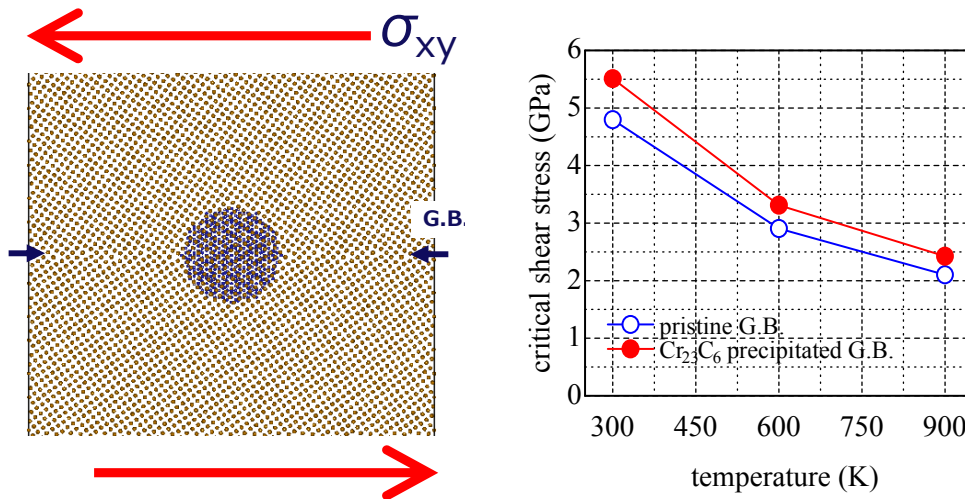


Fig. 1 Atomistic model of  $\text{Cr}_{23}\text{C}_6$  precipitated  $[001]\{0\bar{1}6\}$   $\Sigma 37$  G.B. and temperature dependence of the critical shear stress

- [1] K. Nakamura and T. Ogata, J. Soc. Mater. Sci., Japan, 60, 102 (2011)
- [2] K. Nakamura, T. Ohnuma and T. Ogata, J. Mater. Sci., 46, 4206 IIB2010 (2011)
- [3] T. Kumagai, K. Nakamura, S. Yamada and T. Ohnuma, J. Appl. Phys., 116, 24431 (2014)
- [4] P. Guyot, Phil. Mag., 24, 190 (1971)

## **A new method for calculation of thermodynamics characteristics of grain boundaries and triple junctions in nanocrystalline metals**

A.G. Lipnitskii, I.V. Nelasov

Belgorod State University, 85, Pobedy St., Belgorod, 308015, Russia

The Gibbs energy, enthalpy and entropy of grain boundaries and their triple junctions present significant fundamental interest in the context of thermodynamics of nanocrystalline (nc) materials. However, the traditional analysis of the experimental or computer simulation data for establishing the thermodynamics characteristics uses models of the geometric structure of grain boundaries and triple junctions in nc materials [1], which can lead to systematic errors. We develop a new method of calculating the characteristics of the grain boundaries and the triple junctions in the nc materials using the excess of the thermodynamics property (the Gibbs energy, enthalpy or entropy) of the nanocrystalline state with respect to the crystalline counterpart. The developed method is free from any model assumptions about the geometry and the structure of the intergranular region except it consists of grain boundaries and their triple junctions. As an application, the grain boundaries and triple junctions enthalpies in nanocrystalline copper and titanium modeled using the embedded atom method and the nanocrystalline selenium obtained by partial crystallization of the amorphous state were calculated. We have established that the relative contribution of the triple junctions in the excess enthalpy of the nanocrystalline state in metals is higher than the calculated values obtained using the composite model of nanocrystalline materials.

[1]. Caro A., Swygenhoven H. *Phys. Rev. B* **63** (2001) 134101

## The structure and properties of the interfaces CPAA/phosphate

A.S. Neustroev, V.M. Chernov, D.A. Zakharyevich

Chelyabinsk State University, Chelyabinsk, Br.Kashirinykh str. 129, 454001, Russia

We report the results of our studies on composites polyantimonic acid ( $\text{H}_2\text{Sb}_2\text{O}_6 \cdot n\text{H}_2\text{O}$ )/ $\text{MeH}_2\text{PO}_4$  (Me = K, Na) synthesized by precipitation of phosphate from solution on the surface of insoluble polyantimonic acid. The composites exhibit sharp peak in compositional dependence of proton conductivity when the volume fraction of the phosphate is close to 15% (up to 0.14 S/cm at 25°C) [1,2]. This value is by 1.5 orders of magnitude higher than the conductivity of pure polyantimonic acid. The peak has been assigned to the fast proton transport in interfacial regions of composites; corresponding concentration is the percolation threshold for interfacial continuous cluster. The X-ray phase analysis indicates partial substitution of protons in  $\text{H}_2\text{Sb}_2\text{O}_6 \cdot n\text{H}_2\text{O}$  by alkaline ions, i.e. the ion-exchange reaction between components takes place during synthesis and the composition of the precipitate is shifted towards phosphoric acid. Pulsed NMR studies revealed that there are three modes of proton dynamics in composites at room temperature, two of which relate to the pure components, and the third is the fastest and could be assigned to interface protons. Furthermore, their contributions are composition and temperature-dependent, such that at  $T > 80^\circ\text{C}$  only the fastest component persists. Also, phase transition occurs in composites at  $\sim 80^\circ\text{C}$ , which is not accompanied by mass change. Based on these data we assume that the interface is in liquid-like state, its composition close to phosphoric acid, and 'luqified' zone expands at heating. The proposed explanation could help to understand conduction mechanism in different phosphate-based composites, and the composites studied could serve as a model for the development of new proton conductors for phosphoric acid fuel cells.

- [1] Zakharyevich D.A., Neustroev A.S. *Mater. Res. Soc. Symp. Proc.* V. 1256E (2010), 1256-N16-42.
- [2] Neustroev A.S. Zakharyevich D.A. *Russian Journal of Electrochemistry*, Vol.51, No.5 (2015)

**Conditions for the formation of atomic complexes in grain boundaries.**

V. Nikulkina, B. Bokstein

National University of Science and Technology MISiS, Moscow, Russia

Grain boundary diffusion (GBD), being order of magnitude faster than diffusion within the grains, plays a key role in a mass transport in metallic alloys at mediate temperatures between 0,4 – 0,7 matrix melting temperature.

When solute diffusion is studied, the triple product  $P = s\delta D_b$  ( $s$  is enrichment coefficient,  $\delta$  is grain boundary (GB) width and  $D_b$  is GBD coefficient) is usually obtained. The important role in GBD the atomic interaction with GB and between atoms plays. The result of the first one is a grain boundaries adsorption (GBA) and second – formation of atomic complexes  $B_2$ , AB, etc. type. Both processes have not been adequately studied, especially the process of atomic complexes formation and its effect on GBD.

The analysis of thermodynamic calculations [1, 2] and computer modeling [3 - 5] pointed to the next important conditions of atomic complexes formation:

1. Low solute solubility;
2. The existence of chemical compound in a system;
3. Slow bulk diffusion.

From this point of view, the Cu-Sn system, in which processes of the bulk diffusion have been studied thoroughly, to be choiced as a basic, we can expect the strong effect on GBD of Sn in Cu from the addition of such impurity as iron (see the table 1).

Table 1 - Comparison of the possible influence of different impurities on GBD of Sn in Cu.

System: matrix-solute	Sn solubility at 900 K [6]	Chemical compounds from the Sn side [6]	$D_{900K}$ , m <sup>2</sup> /sec
Cu-Sn	~ 15 at. %	$\beta$ - Cu <sub>3</sub> Sn, nonstoichiometric	$1 \cdot 10^{-15}$ [7]
Ag-Sn	~ 11 at. %	$\epsilon$ - Ag <sub>4</sub> Sn, nonstoichiometric	$6,8 \cdot 10^{-15}$ [8]
Fe-Sn	~ 3,5 at. %	FeSn <sub>2</sub>	$2,6 \cdot 10^{-18}$ [9]

From these data we can see a very slow Sn diffusion in Fe, low solubility and the availability of stoichiometric chemical compound.

#### References

- [1] Bokstein B.S., Esin V.A., Rodin A.O. Phys. Met. and Metallography, 109 (2010) 1
- [2] Esin V.A., Bokstein B.S., Acta Mat. 60 (2012) 5109
- [3] Briant C.L. Met.Trans. 21A (1990) 2339
- [4] Mendeleev M.I., Rodin A.O., Bokstein B.S. Def. and Dif. Forum, 309-310 (2011) 223
- [5] Itckovich A., Mendeleev M., Bokstein B., to be published
- [6] Mehrer H., Diff. in Solid Metals and Alloys, Landolt-Börnstein, New Serial III, 26 (1990)
- [7] Fogelson R. L., Ugay Ya. A., Akimova I.A. Fiz. Met. Metalloved, 37 (1974) 1107
- [8] Tomizuka C.T., Slifkin L.M. Phys. Rev., 96 (1954) 610
- [9] Hennesen K., Keller H., Viehhaus H. Scr. Metall., 18 (1984) 603

**The effect of grain boundary state on the mechanical properties and corrosion resistance of ultra-fine grained titanium alloys Ti-4Al-2V**

A.V. Nokhrin<sup>1</sup>, V.N. Chuvil'deev<sup>1</sup>, V.I. Kopylov<sup>1,2</sup>, A.M. Bakhmetyev<sup>3</sup>, N.G. Sandler<sup>3</sup>,  
P.V. Tryaev<sup>3</sup>, N.A. Kozlova<sup>1</sup>, N.Yu. Tabachkova<sup>4</sup>, A.S. Mikhaylov<sup>3</sup>, M.K. Chegurov<sup>1</sup>,  
A.V. Piskunov<sup>1</sup>, E.S. Smirnova<sup>1</sup>

<sup>1</sup> N.I. Lobachevsky State University of Nizhny Novgorod, Nizhny Novgorod, Gagarina av. 23,  
903950 Russia

<sup>2</sup> Physical-Technical Research Institute of National Academy of Science of Belarus, Minsk, Ac.  
Kuprevicha str. 10, 220141 Belarus

<sup>3</sup> JSC "Afrikantov OKBM", Nizhny Novgorod, Burnakovskii proezd 15, 603074 Russia

<sup>4</sup> National University of Science and Technology MISiS, Moscow, Leninskii av. 4, 119049,  
Russia

Commercial titanium alloy Ti-4.73%Al-1.89%V) was selected as object for this investigation. The ultra-fine grained (UFG) structure in the alloy was produced by Equal Channel Angular Pressing (ECAP) method. The strain rate was 0.4 mm/s; ECAP temperature was 723-748 K. In the initial state (before ECAP), the structure of the alloy was characterized by non-homogeneous grain-size distribution. In the structure of the alloy meet the area with fine-grained and coarse-grained (CG) structure. The average grain size in different areas varies from 5-10  $\mu\text{m}$  (area I) to 50-100  $\mu\text{m}$  (area II). EDX analysis shows the presence in the alloy structure two types of grain boundaries (GB) – GB of  $\alpha$ -Ti and single GB with high concentrations of vanadium (up to 10-16 wt.%). The average macro-elasticity limit  $\sigma_0$  and yield stress  $\sigma_y$  are 420 and 620 MPa, respectively. The tensile strength ( $\sigma_s$ ) and elongation ( $\delta_{\text{max}}$ ) to failure were 730 MPa and 28%, respectively. The average grain size for alloy after ECAP  $\sim 0.5 \mu\text{m}$ . GB with a high concentration of vanadium was not detected. With increasing the ECAP cycles number N from 1 to 4, macro-elasticity limit  $\sigma_0$  increases to 750 MPa, and  $\sigma_y$  grows to 1020-1050 MPa. Alloy after ECAP has high plasticity ( $\delta_{\text{max}}=47.5-50\%$ ) and high tensile strength  $\sigma_s \sim 1000-1050$  MPa. The hot salt intercrystalline corrosion (ICC) tests in coarse-grained materials show that the average depth of ICC is  $L_{\text{cor}}= 500-600 \mu\text{m}$  (test time - 500 h). Summary of results of testing on the hot salt ICC shows that the alloy structure is observed two types of corrosion defects. First - this is the defects, the width of which is small, and the average distance between them is close to the average grain size of the alloy in the region I. Depth of defects of this type ICC does not exceed 100  $\mu\text{m}$ . Secondly, in region II, it ICC defects, the depth of which is 500-700  $\mu\text{m}$ . The volume fraction of this ICC defects does not exceed 5%, which is close to the volume fraction of GB with a high content of vanadium.

The analogous tests of UFG alloy show that character of corrosion process does not change and the corrosion is mainly developed along GB. However, the depth of corroded layer ( $L_{\text{cor}}$ ) in UFG alloy does not exceed 100-150  $\mu\text{m}$ . It can be unambiguously argued that grain refinement has led to visible reducing the intensity of corrosion process. It is shown that the cause of improving the corrosion resistance of Ti-Al-V alloy is the change in the concentration of vanadium at the GB during ECAP. During high-temperature ECAP, together with formation of new GB, there is a diffusion redistribution of vanadium atoms in these GB. In this case, because of an evident increasing about two orders the total GB area, the vanadium concentration at GB is became lower up to about two orders of value. However, due to the greater purity of such GB, the electrode potentials difference of GB and of GB bulk should be reduce and, consequently, their resistance to corrosion should increase.

## The effect of grain growth on sintering of ultrafine-grained tungsten carbide with high hardness and fracture toughness

A.V. Nokhrin<sup>1</sup>, V.N. Chuvil'deev<sup>1</sup>, Yu.V. Blagoveshchenskiy<sup>2</sup>, M.S. Boldin<sup>1</sup>,  
N.V. Sakharov<sup>1</sup>, N.V. Isaeva<sup>2</sup>, S.V. Shotin<sup>1</sup>, N.V. Trushin<sup>1</sup>, E.S. Smirnova<sup>1</sup>

<sup>1</sup> N.I. Lobachevsky State University of Nizhny Novgorod, Nizhny Novgorod, Gagarina ave. 23,  
903950 Russia

<sup>2</sup> A.A. Baykov, Institute of Metallurgy and Material Science of RAS, Russian Academy of  
Science, Moscow, Leninskii ave. 49, 119991 Russia

This paper provides an overview of Spark Plasma Sintering (SPS) [1, 2] of tungsten carbide, which is an advanced technology for high-rate sintering of powder materials by applying mechanical pressure to the powder compact and heating it using a pulsed direct current.

Spark Plasma Sintering studies of the high-rate consolidation of pure tungsten carbide WC nanopowders have been carried out. As the initial materials, we used nanopowders of tungsten carbide prepared by plasma-chemical synthesis [3] from tungsten oxide and carbon in the reducing gas jet and subsequent low-temperature furnace synthesis. The powders differed by particles size ( $R_0$ ) and by volume fraction ( $f_v$ ) of tungsten monocarbide ( $\alpha$ -WC) particles. The variation in the particle size of tungsten carbide and the content of monocarbide  $\alpha$ -WC in the synthesized charge was done by varying the plasma temperature as well as the temperature and time of furnace synthesis. As an initial materials were used tungsten carbide powders, produced by plasma-chemical synthesis and annealed at the low temperature in hydrogen (series №1:  $R_0=46$  nm,  $f_v=83.5\%$ ; series №2:  $R_0=55$  nm,  $f_v=91.7\%$ ; series №3:  $R_0=63$  nm,  $f_v=93.6\%$ ; series №4:  $R_0=113$  nm,  $f_v=83.5\%$ ; series №5:  $R_0=72$  nm,  $f_v=100\%$ ; series №6:  $R_0=80$  nm,  $f_v=100\%$ ). To compare was used tungsten monocarbide powder by «H.C. Starck» ( $R_0=112$  nm). Spark Plasma Sintering was conducted on «Dr.Sinter model SPS-625» at the temperature ranging from 1400 to 1950 °C, at the heating rate ( $V_h$ ) from 25 to 2400 °C/min. The influence of the initial size of the WC nanoparticles and modes of their heating the density, structural parameters, and mechanical properties of tungsten carbide are studied. Samples of high-density nanostructured tungsten carbide with high hardness (up to 31-34 GPa) and fracture toughness (4.3-5.2 MPa m<sup>1/2</sup>) are obtained. It is found that the effect of accelerating tungsten carbide nanopowder sintering under conditions of high-rate heating is associated with the acceleration of diffusion along grain boundaries in the sintered material. It is shown that the nonmonotonic dependence of the optimal sintering temperature on the initial grain size  $R_0$  is caused by a change in grain-boundary diffusion coefficient in conditions of abnormal grain growth. It is found that the size of abnormally large grains in spark plasma sintering depends on the volume fraction of particles of the non-stoichiometric phase.

[1] Tokita M. Spark Plasma Sintering (SPS) Method, Systems, and Applications (Chapter 11.2.3). In Handbook of Advanced Ceramics (Second Ed.). Academic Press. 2013. P. 1149-1177.

[2] Munir Z.A., Anselmi-Tamburini U., Ohyanagi M. *Journal of Materials Science*. **41** (2006) 763-777.

[3] Isaeva N.V., Blagoveshchenskiy Yu.V., Blagoveshchenskaya N.V., Mel'nik Yu.I., Samokhin A.V., Alekseev N.V., Astashov A.G. *Russian Journal of Non-Ferrous Metals*. **55** (2014) 585-591.

**Determination of electrical conductivity structure of  $ZrO_2$ - $HfO_2$ - $Y_2O_3$  and  $ZrO_2$ - $In_2O_3$ - $Y_2O_3$  solid electrolytes by impedance spectroscopy**

N.N. Novik<sup>1,2</sup>, V.G. Konakov<sup>1,2</sup>, O.V. Glumov<sup>1</sup>, S.N. Golubev<sup>3</sup>

<sup>1</sup>Institute of Chemistry, St. Petersburg State University, Universitetskiy pr. 26, Petrodvorets, St. Petersburg, 198504, Russia

<sup>2</sup>Research Laboratory for Mechanics of New Nanomaterials, Peter the Great St. Petersburg Polytechnic University, Polytechnicheskaya 29, St. Petersburg, 195251, Russia

<sup>3</sup>Scientific and Technical Center "Glass and Ceramics", 9 linia V.O. 20 lit A, St. Petersburg, 199004, Russia

Ternary zirconia based systems can serve as alternative electrolyte materials to traditionally used yttria stabilized zirconia (YSZ) ceramics for fuel cells and gas sensors fabrication. However, third oxide introduction to YSZ could lead to both phase composition shift and intragranular, and intergranular structure change in the final ceramics. The conductivity of  $(92-x)ZrO_2-xHfO_2-8Y_2O_3$  ( $x=5,15,20$ , mol%) and  $(100-2,25x)ZrO_2-1,25xIn_2O_3-xY_2O_3$  ( $x=4,8$  mol%) ternary solid electrolytes was studied by impedance spectroscopy. XRD revealed cubic fluorite-like solid solution stability for all compositions except  $82ZrO_2-10In_2O_3-8Y_2O_3$ . Arrhenius curves were plotted both for inter and intragrain conductivity. The activation energies of conductivity were calculated. One can see that at low hafnia content the activation energy values of intergranular and intragranular conductivities are close to each other, it is likely because grain boundaries are discontinuous. The difference between activation energies of components of conductivity increases with the increase of hafnia content at the same sintering conditions. Brick layer model was used to calculate conductivity features. At a temperature above 500°C the ionic conductivity of all investigated systems is higher than that for 8YSZ ceramics [1]. It is referred to mixed ion-electron conductivity that is common for  $91ZrO_2-10In_2O_3-8Y_2O_3$  ceramics. Such nature of conductivity is due to indium oxide segregation to grain boundaries. The investigated ceramics exhibiting the ionic conductivity can be recommended as solid electrolyte materials for fuel cells, oxygen sensors and similar devices manufacturing, that operate at extremely high temperatures because of high thermal stability and in aggressive environments whereas ceramic compositions with mixed conductivity can be used as fuel cell anode material.

[1] N.N. Novik, V.G. Konakov and I. Yu. Archakov. Rev. Adv.Mater. Sci. 40 (2015) 188-207



**Liquid metal inside boundaries wetting processes in polycrystalline copper based systems**

A.A. Novikov<sup>1</sup>, A.L. Petelin<sup>1</sup>, E.A. Novikova<sup>1</sup>, A.I. Plokhikh<sup>2</sup>, N.A. Volsky<sup>1</sup>

<sup>1</sup>National University of Science and Technology «MISIS», Leninskiy Pr. 4, Moscow, RU-119049, Russia

<sup>2</sup>National University of Science and Technology «MISIS», Leninskiy Pr. 4, Moscow, RU-119049, Russia

The present work contains the experimental investigations of grain boundary liquid metal channels formation and the processes of common melt front movement in copper based polycrystalline samples. There were defined the morphological peculiarities and the average rates of liquid grain boundary net spreading into the polycrystalline structure. The comparative experiences of the liquid metal layer boundaries grooving in Cu-Nb multilayer system were carried out.

## Magnetoplastic effect in Cu-Be metal alloys

J.V. Osinskaya, A.V. Pokoev

Samara State Aerospace University, Samara, 443086, Russia

Earlier authors [1] had been established the steady effect of appreciable microhardness increase of beryllium bronze BrB-2 after ageing in the constant magnetic field (CMF) which it is possible to carry to version of magnetoplastic effect (MPE) in metal alloys. In the present work the brief review of some new data about influence of Ni alloying additives on the kinetics of artificial ageing processes of binary Cu-Be-alloys in CMF is given. The alloys ageing regimes were chosen on the basis of the available published data [2] and results of the earlier conducted investigations of the aging process of the BrB-2 alloy in the CMF [3]: 30 minutes annealing at the constant temperature of 800 °C, water hardening at 20 °C, ageing in vacuum  $\sim 10^{-3}$  Pa at the temperature 350 °C during 10-120 min in the CMF with the intensity of 7 kOe.

The analysis of the received experimental data shows that 1) imposing of CMF always leads to a «negative» MPE by  $\sim 35$  %; 2) increase in Ni additive to the alloy from 0.4 up to 1.0 wt. % leads to a disproportionate increase in microhardness of Cu-Be alloy; 3) Ni-addition presence in the alloy results in the lowering of the average size of coherent dispersion blocks and heightening of the relative microdeformation and dislocations density; 4) the reason of the MPE occurrence and «magnetic memory» [4] in Cu-Be alloys is the atomic reorganization of atoms at the phase formation stage under the artificial ageing in CMF.

- [1] J.V. Osinskaya, A.V. Pokoev. *Fizika i Himiya Obrabotki Materialov*. No 3 (2003), p. 18. (in Russian).
- [2] R.L. Tofpenez. *Razuprochnyayushchiye processy v stareyushchikh splavakh*. Nauka i tekhnika, Minsk 1979. (in Russian).
- [3] Yu.V. Osinskaya and A. V. Pokoev. *The Physics of Metals and Metallography*. Vol. 105, No. 4 (2008), p. 356.
- [4] R.B. Morgunov, A.L. Buchachenko. *Journal of Experimental and Theoretical Physics*, Vol. 109 (2009), p. 434.

**Influence of faceting on migration of  $\{1\ 0\ -1\ 2\}$  twin boundaries in hcp metals**

A. Ostapovets<sup>1</sup>, J. Buršík<sup>1</sup>, R. Gröger<sup>1</sup>, A. Serra<sup>2</sup>

<sup>1</sup>Central European Institute of Technology - Institute of Physics of Materials (CEITEC IPM),  
Academy of Sciences of the Czech Republic, Žitkova 22, 61662 Brno, Czech Republic.

<sup>2</sup>Department of Civil & Environmental Engineering, Universitat Politecnica de Catalunya,  
Jordi Girona 1-3, 08034 Barcelona, Spain

Recent experimental observations show that  $\{10\bar{1}2\}$  twin boundaries in hcp metals are frequently faceted. The most important facet are represented by basal-prismatic interface, i.e. basal plane in twin coincides with prismatic plane in matrix or vice versa. The objective of our work is to investigate the influence of faceting on the strain produced by deformation twinning. Several facet configurations, which were observed in experiments, will be analyzed. It is shown that the migration of basal-prismatic facets, terminated by opposite disclinations, along a straight  $\{10\bar{1}2\}$  twin boundary produces ordinary twinning shear. On the other hand, joining conjugate twins gives rise to BP facets terminated on the parent twin boundaries by identical disclinations. In this case, the strain produced by the migration of BP facets is tetragonal and can be considered as an average between the strains produced by the individual conjugate twins.

**The effect of spark plasma sintering temperature on the composite structure of Ti/TiB**

M.S. Ozerov, M.V. Klimova, S.V. Zhrebtsov

Belgorod National Research University, Belgorod 308015 Russia

Microstructure and mechanical properties of TiB - reinforced titanium matrix composites produced by the spark plasma sintering were studied. TiB - Ti composites were synthesized by chemical reaction between  $\text{TiB}_2$  and Ti during the SPS process at  $850^\circ\text{C}$  ( $\alpha$ -Ti) and  $1000^\circ\text{C}$  ( $\beta$ -Ti) at 40 MPa for 15 min. Chemical compositions with 10 wt.%  $\text{TiB}_2$  amount were used. The effect of the temperature on the structure, morphology, interphase boundaries and mechanical properties of composite were investigated. The synthesized TiB with orthorhombic structure with needle-shaped morphology was distributed rather uniformly in the titanium matrix. It was shown that TiB particles grow along the [010] direction like hexagonal prism with (100), (101), and (10-1) planes. It is known that orientation relationships between Ti and TiB whiskers is described as  $(001)_{\text{TiB}} \parallel (110)_\beta$ ;  $[010]_{\text{TiB}} \parallel [-111]_\beta$  and  $(100)_{\text{TiB}} \parallel (100)_\alpha$ ,  $[0-11]_{\text{TiB}} \parallel [011]_\alpha$ , which is consistent with the Burgers OR for alpha and beta phases in titanium. But matching of lattices of alpha Ti and TiB in the case of its formation in beta matrix and further cooling to room temperature has not been studied previously. Features of the TiB/ $\alpha$ -Ti orientation relationship after the  $\beta \rightarrow \alpha$  phase transformation were discussed. The energy of (semi)coherent  $\alpha$ /TiB interphase boundary  $(10-10)_\alpha \parallel (100)_{\text{TiB}}$  possesses the lowest energy of  $2.7 \text{ J/m}^2$ , while non-coherent  $\alpha$ /TiB boundary  $(0001)_\alpha \parallel (010)_{\text{TiB}}$  (normal to the growth direction) had the highest energy of  $4.1 \text{ J/m}^2$ .

## Nonequilibrium columnar grain boundaries in the coating TiAlN

O.B. Perevalova, V.P.Sergeev

Institute of Strength Physics and Materials Science, SD RAS, Tomsk, pr. Academicheskii, 2/4,  
634021 Russia

The problem of thermal stability of magnetron coatings TiAlN remains relevant, although the addition of aluminum to TiN coating increased its thermal stability. It was found [1] that the thermal stability of the magnetron coating TiAlN increases at the substrate pretreatment by titanium ions. It is known [2], that the heat resistance of the coatings is determined by the type and magnitude of the elastic macrostresses. Thermal stability increases with compressive macrostrain increasing. The paper task is to investigate the TiAlN coatings grain structure, the state it's grain boundaries, and their influence on the coating macrostresses and heat resistance. For this purpose the investigation of the magnetron TiAlN coatings microstructure was studied before and after thermal cycling. The TiAlN coatings are differed by the presence of the ion beam titanium substrate pretreatment. The methods of X-ray diffraction (XRD), transmission electron diffraction microscopy (TEM) and scanning electron microscopy (SEM) with energy analysis were used. It was found that the magnetron TiAlN coatings consist of the two-syllable. The layer adjoined to the substrate has the TiN phase microcrystalline structure. The grains are equiaxed with sizes equal 70 nm. The layers thickness is not more than 150 nm. The second layer has the  $Ti_{1-x}Al_xN$  phase columnar grain structure with boundaries arranged perpendicular to the substrate. The  $Ti_{1-x}Al_xN$  phase has FCC structure of the NaCl type. The columnar grains transverse dimensions are in the range of 20-100 nm depending on titanium ion beam pretreatment presence. The  $Ti_{1-x}Al_xN$  phase grain structure has texture 200. Analysis of the 200 X-ray line profile shows that the  $Ti_{1-x}Al_xN$  phase grain crystal lattice parameter and, consequently, titanium and aluminum concentration are inhomogeneous. The ionic pretreatment of the substrate enhances the coating inhomogeneous. The  $Ti_{1-x}Al_xN$  phase columnar grains consist of domains differed by crystal lattice parameter. It leads to elastic microstresses formation. The columnar grain boundaries are nonequilibrium. Also it leads to the elastic microstresses formation. The bending extinction contours existence proves presence of the elastic microstresses [3]. The microstresses decreases with an increasing of the columnar grains transverse dimensions exponentially. In the coating without substrate treatment the columnar grains transverse dimensions increases from 20 nm to 100 nm with distance increasing from the coating-substrate interface. In the coating with substrate treatment the columnar grains transverse dimensions equal to 20 nm and don't change with distance increasing from the coating-substrate interface. The pretreatment leads to the elastic stresses increasing as microstresses in the coating columnar grains as compressive macrostresses. The elastic compressive macrostresses in the coating surface layers depend on microstresses in the coating columnar grains and nonequilibrium their borders.

[1] Akulinkin A., Shugurov A., Panin A., Sergeev V., C.H.Cheng. AIP Conference Proceedings 1683, P. 020001 (2015).

[2] Tabakov V.P., Chihranov A.V. Wear resistant coating of cutting tools worked in continuous cutting condition. Ul'janovsk: Izd-vo UIGTU, 255P. (2007). (In Russian)

[3] Valiev R.Z., Aleksandrov I.V. Nanostructured materials produced by intensive plastic strain. Moscow: Logos, 2000, p.272 (In Russian).

## **Crystallization kinetics of Al-Y system under high pressure torsion**

E.A. Pershina, G.E. Abrosimova, A.S. Aronin, D.V. Matveev

Institute of Solid State Physics, Russian Academy of Sciences, Chernogolovka, Ac. Ossipyan  
str. 2, Moscow district, 142432 Russia

Al-RE and Al-Ni(Fe)-RE (RE - rare earth element) amorphous systems are well known for their outstanding mechanical properties and low specific weight. These alloys demonstrate even higher characteristics in the state when the amorphous phase is partially crystallized. This significantly expands the range of their application. Recently severe plastic deformation (SPD) has been applied as a new promising approach for obtaining such structural state in Al-based alloys.

The main advantage of SPD-methods is that the nanocrystalline structure can be obtained even for the alloys, for which it is unattainable by conventional heat treatment. Despite numerous studies of the SPD-induced crystallization in the amorphous alloys, the deformation mechanism has not been clearly formulated yet. In particular, it is not established if either a local temperature rising or a significant change of free volume is the main cause of the crystal's nucleation and growth during the deformation.

Usually amorphous systems are multicomponent. We used binary Al<sub>90</sub>Y<sub>10</sub> amorphous alloy in the present study regarding it as a model system. The aim of this work was to compare diffusion coefficient of Al in nondeformed and deformed areas of the material and to determine whether the increase of free volume during the deformation is sufficient to ensure nucleation and growth of Al nanocrystals.

Differential scanning calorimetry and Kissinger method were used to obtain activation energy of the alloy in the as-cast state. Activation energy of crystallization in the state after the deformation was estimated by TEM structure analysis. Considering this difference and assuming that no heating occurred during the deformation process, the effective diffusion coefficient of the SPD-deformed Al<sub>90</sub>Y<sub>10</sub> alloy was determined. The obtained value is lower than that required for the nanocrystal formation. It was suggested that the crystal precipitation during the deformation process is caused both by structural changes of the amorphous matrix and temperature increase. According to our estimation the temperature during the deformation of Al<sub>90</sub>Y<sub>10</sub> alloy was increased locally up to 300<sup>0</sup>C.

This work was supported by Russian Foundation for Basic Research (projects №№ 14-42-03566, 16-03-00505, 16-32-00786).

**Model description of grain boundary diffusion processes in nano- and microcrystalline solid systems**

A.P. Petelin, A.A. Novikov, I.V. Apykhtina

National University of Science and Technology «MISIS», Leninskiy Pr. 4, Moscow, RU-119049,  
Russia

The simple model of grain and phase boundaries diffusion into polycrystalline solid system with nano- and micro grain dimensions is proposed. There are considered different types of diffusion regimes which are realized by definite correlations between volume and grain boundary diffusion lengths and average grain sizes.

## The model of interface amorphization in inorganic eutectics and composites

V.S. Pervov<sup>1</sup>, A.A. Petrov<sup>1,2,3</sup>, N.V. Kireeva<sup>3</sup>

<sup>1</sup>Kurnakov Institute of General and Inorganic Chemistry RAS, Leninsky prosp. 31, Moscow 119991 Russia

<sup>2</sup>Moscow Institute of Physics and Technology, Dolgoprudny, Insitutsky per. 9, Moscow region, 141701 Russia

<sup>3</sup>Frumkin Institute of Physical Chemistry and Electrochemistry, Leninsky prosp. 31, Moscow 119071 Russia

We propose a theoretical model that is capable of interpreting the amorphization effects of interphase boundaries (interfaces) in inorganic composites and eutectic alloys. A Two-dimensional binary system is chosen. The components are represented as jammed packings of hard disks (types A and B), which diameters ( $d_A$  and  $d_B$ ) are associated with component incommensurability. To estimate the amount of amorphization we used the theory of “excess volume” (excess area as a two-dimensional approximation for jammed packing of incommensurate disks) [1]. The excess area dependence on both disk incommensurability  $I$  ( $I=d_B/d_A$ ) (Fig.1(a)) and disk concentration (quantity ratio)  $Q$  ( $Q=[A]/([A]+[B])$ ) (Fig.1(b)) were determined. Amorphization effects have a significant impact on properties of nanostructured composites and eutectic alloys and have to be also taken into account when some ceramic materials for electrochemical energetics are developed [2]. They can also explain some properties of intercalation compounds and inorganic suprastructures of the “host-guest” type [3].

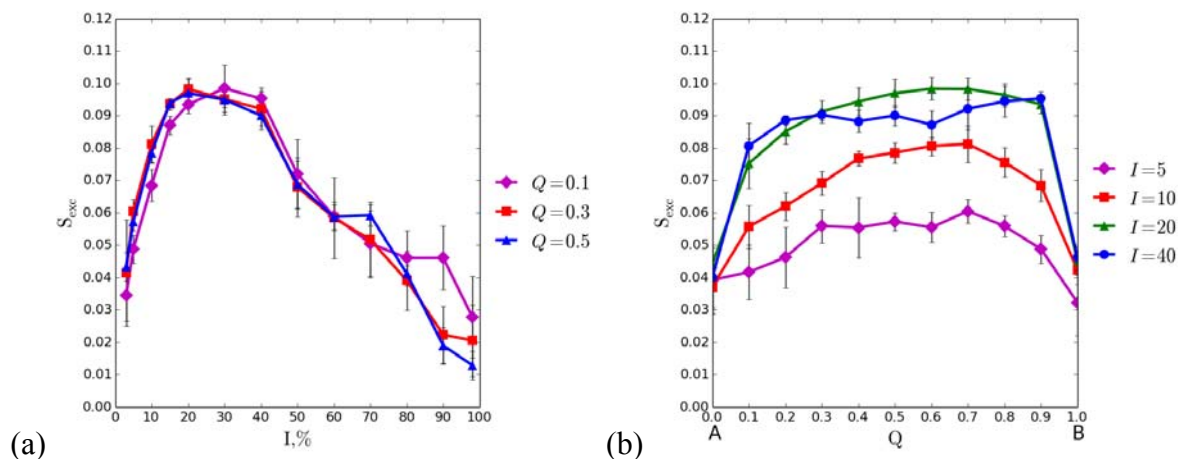


Fig.1 Excess area  $S_{exc}$  vs. (a) disk incommensurability  $I$  and (b) disk concentration  $Q$

The work was supported by the Russian Foundation for Basic Research (projects 14-03-00223 and 14-29-04084) and by President Grand for Support of Young Russian Scientists (MK-1003.2014.3)

- [1] V.N. Chivildeev. Non-equilibrium grain boundaries in metals. Fizmatlit Moscow, 2004. — 304 p. [in Russian]
- [2] J. Maier. *Chem. Mater.* **26** (2014) 348
- [3] V.S. Pervov, E.V. Makhonina, A.E. Zotova, N.V. Kireeva, I.-M. Kedrinsky. *Nanotechnologies in Russia.* **9** (2014) 347



**Precipitations at grain boundaries in stainless steel 304 during long thermal ageing and their effect on fracture mechanisms under dynamic loads**

S.N. Petrov, B.Z. Margolin, O.Yu. Prokoshev

Central Research Institute of Structural Materials «Prometey», 49 Shpalernaya str., St. Petersburg, 191015, Russia

Structural analysis has been performed on grain boundaries of SS 304 subjected to 170000hrs thermal ageing at temperatures up to 550°C peculiar to operation conditions in heat-exchangers of nuclear power plant BN-600. Thereafter the structure changes and their effects on mechanical properties have been revealed.

Chromium carbides Cr<sub>23</sub>C<sub>6</sub> and  $\alpha$ -ferrite, depleted in Cr and Ni, have been shown to be the main secondary phases which appear on grain boundaries, although some phase enriched with Ni, Mn and Si has been found there as well.

A notable distinction has been revealed between chromium carbides precipitated at grain boundaries and at twin boundaries as follows. While plate-like particles are typical for the latter case, mostly globular carbides are detected on the grain boundaries. This effect is seemingly due to the orientation relationship that is provided on both planar sides of particles situated on a twin boundary. Since such carbides reduce the impact toughness, the treatment temperature (700°C) has been found that results in their dissolution and, hence, the toughness restoration, whereas the globular carbides have lesser effects on mechanical properties.

The above-mentioned disappearance of carbides at twin boundaries results in an about double increase of impact toughness insofar as the mechanism of brittle inter-phase rupture is no longer actual.

**Analytical indentation for studying microstructure constituents**

M.I. Petrzhik, P.A. Loginov, E.A. Levashov

National University of Science and Technology «MISiS», Leninskiy pr. 4  
Moscow 119049 Russia

One of advantages of nanoindentation tester is a possibility to impress very fine in size imprints (one micron and less) with the same scale extreme precision to positioning thereof. This makes possible to study the interfaces like coating/substrate, inclusion/matrix etc. at multiphase and micro composite materials. In this presentation the experimental results on mechanical properties of individual microstructure constituents (Young modulus, hardness, elastic recovery etc.) of some advanced materials will be shown and discussed. The obtained data are base for simulation of mechanical behavior and design of novel materials [1].

**Effect of Fe<sub>3</sub>O<sub>4</sub> nano particles on strength and grain size of aluminum matrix composite fabricated via accumulative roll bonding (ARB) process**

B. Pirouzi, E. Borhani

Department of Nano technology, Nano material Science group, Semnan University, Semnan, Iran

In this work, a new nanostructured Al-Fe<sub>3</sub>O<sub>4</sub> composite was manufactured using accumulative roll bonding (ARB) process at room temperature. Uniform distribution of nano sized Fe<sub>3</sub>O<sub>4</sub> particles between layers of composite were improved by increasing the number of ARB cycles. At primary cycles, the presence of nano particles caused to produce discontinuity between layers and then decreased and porosity declined by increasing ARB cycles. Moreover, tensile strength increased by increasing ARB cycles and reached to 198 MPa after 8 cycles. On the other hand, the presence of Fe<sub>3</sub>O<sub>4</sub> nano particles influence the microstructural characteristics of aluminium. During the fourth cycles, nano particles increased dislocation density (calculated by XRD) and raised stored energy which acts as a driving force for continuous recrystallization during ARB process. The results shows, in Al-0.1%Vol Fe<sub>3</sub>O<sub>4</sub>, the dislocation density increased to  $5.7 \times 10^{12} \text{ m}^{-2}$  after 4 cycles and then decrease to  $1.97 \times 10^{12} \text{ m}^{-2}$  after 8 cycles. The grain size aluminium calculated by Williamson-Hall and Rietveld method were 115 nm and 198 nm, respectively.

**Magnetic behavior of Co doped Cu–Ni powder compositions prepared by mechanical alloying, annealing and pressing**

D.A. Podgorny<sup>1</sup>, A.B. Akinin<sup>2</sup>, A.S. Bykov<sup>1</sup>, A.V. Druzhinin<sup>1</sup>, A.A. Rodin<sup>1</sup>

<sup>1</sup>National University of Science and Technology "MISiS", Moscow, Leninsky Prospect. 4,  
119991 Russia

<sup>2</sup>Research Institute of Goznak, Moscow, Mytnaya Street 19, 115162 Russia

Powder composition in Cu-Ni-Co system which ensure certain magnetic response of the finally stamped product was chosen. The problem included necessity to avoid Co dissolution in Cu and Ni as well as intermediate phases formation with reduced magnetic properties. The composite with given porosity (analog of cast cupronickel, Cu : Ni – 70 : 30) was produced by mechanical alloying of micro-sized powders Cu and Ni powders by adding 1,5 – 2,5 wt % of Co with following compacting. Magnetic properties were measured during all stages of the treatment: primary powder product compacting, annealing and pressing. The magnetic susceptibility value was measured by Quantum Design PPMS system, grain size and Co distribution were estimated by Ulvac JSM-6480LV SEM, phase composition by Rigaku Miniflex XRD. It was shown that compacting and afterward powder product annealing led to Cu-based solid solution formation with dramatic (3-5 times) decreasing of magnetic properties.

The chemical and phase composition of interphases were investigated with the use of Physical Electronics AES PHI-680.

The effect of mechanical mixing and grain boundary diffusion on the solid solutions structure and the magnetic properties change were studied. Also the effect of particles morphology, their structure and composition was analysed.

**Particularities of luminescence in oriented scintillation nanocomposites  
from organic phosphors and inorganic nanoparticles**

A.P. Pokidov, N.V. Klassen

Institute of Solid State Physics, Russian Academy of Sciences, Chernogolovka, Ac. Ossipyan  
str. 2, Moscow district, 142432 Russia

Our team has developed scintillation composites based on mixtures of inorganic nanoparticles and organic phosphors. These new kinds of scintillators possess unique combination of big capture ability for gamma quanta, nanosecond decay time of light emission and high light yield comparable to the best inorganic scintillators. These record characteristics are achieved by super-fast transfer of the excitation energy from heavy inorganic particles absorbing X-Rays to organic phosphors emitting scintillation light. Usually organic scintillators have low radiation hardness resulting in decrease of light yield, optical transparency and mechanical strength during relatively short working time. The composite scintillators demonstrate manifold increase of radiation hardness due to intermolecular fixation of polymers by nanoparticles.

Orientation of polymer molecules by means of plastic deformation (they are aligned during slow extension of the films) increases effective area of the transfer of the excitations from nanoparticles to the organic phosphors via benzene rings. Studies of influence of orienting and non-orienting deformation treatment on X-Ray luminescence of the composites revealed different redistributions of the light emission spectra. Non-orienting deformation results in significant increase of slow inorganic luminescence and slight decrease of fast organic luminescence. On the other hand orienting plastic deformation of the composite films by means of slow extension increases the both components: either organic or inorganic luminescence. These results are explained by presence of three channels of recombination of electron excitations created in inorganic nanoparticles by absorption of X-Ray quanta. The main channel is connected with the fast transfer to the organic phosphors with subsequent fast light emission. Another channel is connected with slow light emission of the inorganic scintillator itself. The third channel means non-radiation recombination of inorganic excitations by the transfer of their energy to high frequency molecular vibrations of hydrogen bonds connected with the nanoparticles. Non-orienting deformation destroys significantly these weak hydrogen bonds resulting in significant amplification of the inorganic light emission. This deformation destroys partially strong bond of the nanoparticles with the benzene rings of organic molecules, but the decrease of their luminescence is much weaker. Moreover the orienting deformation increases the fast X-Ray luminescence of the organic phosphors, revealing the improvement of the energy transfer from the nanoparticles to the phosphors. We attribute this improvement by better adjustment of the benzene rings to the nanoparticles and increase of effective area of the energy transfer by means of the orienting deformation. One more way of the increase of the fast scintillation light yield of the scintillation composites is connected with preparation of the composites with micro-periodical distribution of the density and refraction index analogous to photonic crystal. This structural ordering can result in optimized selective direction of scintillations directly to the photodetector.

### **Micromechanisms of magneto-plastic effect in metal alloys**

J.V. Osinskaya<sup>1</sup>, A.V. Pokoev<sup>1</sup>, S.V. Divinski<sup>2</sup>, R.B. Morgunov<sup>3</sup>, B.B. Straumal<sup>4</sup>

<sup>1</sup>Samara State Aerospace University, Moscow Highway, 34, Samara, 443086, Russian Federation

<sup>2</sup>Institute of Materials Physics, University of Münster, Wilhelm-Klemm-Str. 10, 48149, Münster, Germany

<sup>3</sup>Institute of Problems of Chemical Physics, Russian Academy of Sciences, Academician Semenov avenue 1, Chernogolovka, Moscow district, 142432, Russian Federation

<sup>4</sup>Institute of Solid State Physics, Russian Academy of Sciences, Chernogolovka, Ac. Ossipyan str. 2, Moscow district, 142432, Russian Federation

A phenomenon of remarkable changes of properties of plastic solids under action of a constant magnetic field of a rather low intensity (1-10 T) was called as a magneto-plastic effect (MPE). The understanding level of the MPE's physical nature in solids is determined by our knowledge of elementary atomic and electron-spin processes of plastic deformation on the basis of microcosm laws. The data on MPE in metallic alloys, which is induced by ageing in magnetic fields, are rather limited and controversial. At the same time, the MPE in metallic alloys represents a considerable interest from a point of view of atom-spin micromechanics and practical application in modern manufacture technologies of nanomaterials with required properties.

The mechanisms of MPE were experimentally investigated in model Cu-Be alloys with different contents of Be and Ni and the maintenance of the total amount of other magnetic impurities below than 0.05 wt.% [1]. Particularly, the following materials were examined: 1) beryllium bronze BrB-2 (a technical alloy); 2) the binary Cu-Be alloys (prepared from high purity materials with the Be concentration ranging from 0.5, 1.0, 1.6, 2.7 up to 3.0 wt.%); and 3) the triple Cu-2 wt. % Be-Ni alloys with Ni content ranging from 0.4 to 1.0 wt. %. The possible micro-mechanisms of MPE are comprehensively discussed including the effect of nickel. It is shown that MPE acts as a tool for studying the type and properties of obstacles (impurity atoms, spin clusters, nano-sized precipitates of intermetallic phases, impurity segregation at interfaces with atomic and magnetic ordering) for moving dislocations.

[1] J.V. Osinskaya, A.V. Pokoev. Magneto-plastic Effect in Cu-Be Alloys with Ni Additives. Def. Diff. Forum Vol. 363 (2015), p. 186.

**Structure and antibacterial characteristics of B- and Ag-doped TiCaPCON films**

V.A. Ponomarev, A.N. Sheveyko, I.V. Sukhorukova, D.V. Shtansky

National University of Science and Technology “MISiS”, Leninsky prospect 4, Moscow  
119049, Russia

Enhanced osteointegration of Ti implants can be achieved by surface modification, for instance, by deposition of films. Our previous studies have demonstrated that TiCaPCON films are biocompatible and bioactive. Implant-related bacterial infections during surgery remain a serious problem. To overcome this problem, the TiCaPCON films were doped with well known bactericidal elements, such as B and Ag. Films were deposited by simultaneous magnetron sputtering of composite TiC-CaO-Ti<sub>3</sub>PO<sub>(x)</sub> and TiB<sub>2</sub> targets (produced by self-propagating high-temperature synthesis) or by simultaneous magnetron sputtering of TiC-CaO-Ti<sub>3</sub>PO<sub>(x)</sub> target and ion sputtering of metallic Ag target. The as-deposited TiCaPCON-based films contained either 1-4 at.% of Ag or 7-15 at.% of B. The structure of films was studied using XRD, SEM-EDS, TEM, GDOES and FTIR. In addition, the rates of Ag ion release were studied and electrochemical measurements were performed. Doping with Ag resulted in the formation of Ag nanoparticles (NPs), 5-10 nm in size, on the film surfaces. Electrochemical tests demonstrated that enhanced antibacterial activity of the films was achieved due to the dissolution of these NPs resulting in intensive Ag ion release into the physiological solution. In the case of B-doped films, the formation of nanocrystalline structure with crystallite size of about 5 nm was observed. As was revealed by XRD and TEM, the film contained two main phases, namely Ti(C,N) and TiB<sub>2</sub>. The film surface analysis using FTIR revealed the presence of boron oxides and hydroxides, which are believed to provide antibacterial characteristics. Thus our study has demonstrated that by a proper choice of the alloying element it is possible to provide a strong bactericidal effect without compromising other biological characteristics.

## Configurable Size of Silicon Photonics via Neural Network for Maximizing of the Photon Absorption

A. Poulou<sup>1</sup>, M.Poulos<sup>2</sup>

<sup>1</sup> Department of Materials Science and Engineering, University of Ioannina, Greece

<sup>2</sup> Laboratory of Information Technologies, Ionian University, Corfu, Greece

Nanophotonic circuits permit for recognizing complex optical functionality on a chip and enable the assembly of functional devices with many optical modules in a scalable manner [1]. A recent trend in the field of silicon photonics is toward the miniaturization of silicon-on-insulator (SOI) waveguides to sub wavelength dimensions [2]. The geometry of the waveguide offers high lateral optical confinement. Schematic of the silicon waveguide cross-section is sketched in Figure 1. The principle of waveguide symmetry violation consists in realizing a trench in the silicon waveguide core by using a single-trench photoresist mask and etching depressed to the desire depth. In particular, the SOI waveguide proposed here is characterized by an overall width  $W$  height. The single trench width ( $t_w$ ) and high ( $t_h$ ), while the parameters indicated as “ $a$ ” and “ $b$ ” in Figure are ranged proportional regarding to parameter  $W$  [3].

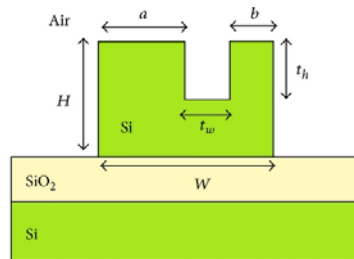


Figure 1. The geometric parameters of a typical Silicon Photonics

The above geometric parameters  $\vec{p} = [H, w, t_h, t_w, a, b]$  play an important role for absorption issues. In particular, the certain goal in the nowadays research is to maximize the absorption efficiency of the above device [4, 5, 6]. However, this configuration consists of an empirical testing and the certain goal is achieved with a non-computational procedure. In this study, a data mining technique is proposed in order to associate the absorption efficiency of a silicon device (see Figure 1) with the parameters which are described of vector  $\vec{p}$ . The value absorption which corresponds in the geometric parameters of vector  $\vec{p}$  is calculated with simulation way using Finite-Difference Time-Domain Method. These manual associated values are used in order to train a well fitted Elman Neural Network [6].

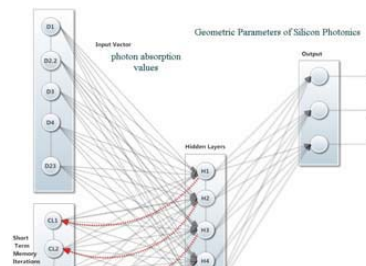


Figure 2. The architecture of the Elman Neural network



Thus, we trained as input vectors the photon absorption values and the other hand as target vectors we considered the vectors  $p$ . The suggested architecture of the neural network is depicted in figure 2. Finally, in the testing procedure using the Sigmoid Function we test max values of the photon absorption and we obtain the candidate vector  $p$ . In this way, if it is possible a weight association between the photon absorption values and the vectors  $p$  to be achieved

- [1] M. Antelius, K. B. Gylfason, and H. Sohlström. *Optics express*, vol. 19, no. 4, pp. 3592–3598 (2011).
- [2] K. Yamada, *Silicon Photonics II*, Springer, pp. 1–29 (2011)
- [3] B. Troia, F. et. all *Advances in Optoelectronics*, vol. 2014 (2014)
- [4] M. Pohl, “Ultrafast Optical Phenomena in Magneto-Plasmonic Crystals and Magnetically Ordered Materials,” Technische Universität Dortmund, Germany, 2014.
- [5] J. B. Schneider. *School of electrical engineering and computer science Washington State University*.—URL: [\(http://www.Eecs.Wsu.Edu/~schneidj/ufdtd/\(request data: 29.11.2012\)\)](http://www.Eecs.Wsu.Edu/~schneidj/ufdtd/(request+data:29.11.2012)) (2010).
- [6] M. Lipson. *Lightwave Technology, Journal of*, vol. 23, no. 12, pp. 4222–4238 (2005)
  
- [7] M. Poulos, T. Felekis, and A. Poulou, *Journal of Medical Hypotheses and Ideas*, in press (2016)

**Defect and precipitates in silicon after high temperature diffusion of zinc and quenching**

V.V. Privezentsev<sup>1</sup>, V.V. Saraykin<sup>2</sup>, M.P. Shcheglov<sup>3</sup>, V.N. Sokolov<sup>4</sup>, M.S. Chernov<sup>4</sup>,  
L.G. Bulygina<sup>4</sup>

<sup>1</sup>Institute of Physics & Technology, Russian Academy of Sciences, Moscow, Nakhimovskiy prosp., 34, Moscow 117218, Russia

<sup>2</sup>Research Institute of Physical Problems, Zelenograd, Moscow 124460, Russia

<sup>3</sup>Ioffe Institute, Politekhnikeskaya ul., 26, St.Petersburg 194021, Russia

<sup>4</sup>Faculty of Geology, Moscow State University, Leninskie Gory, Moscow 119998, Russia

In Si doped by Zn during high-temperature diffusion annealing with the subsequent quenching the defects with  $\mu$ -sizes have been observed [1-3]. They were vacancy type and connected with Zn precipitates settling at dislocations or grain boundaries. In present communication we reported about Zn mapping by secondary ion mass-spectrometer (SIMS) and visualization 3D using the X-ray (XR) computer  $\mu$ -tomography in such material.

Wafers of n-type CZ-Si were doped by Zn at temperature 900°C and 1200°C correspondently with subsequent quenching. The virgin n-type of conductivity was not changed, and Zn concentration were made  $N_{Zn}=1\times 10^{14}$  and  $1\times 10^{16}\text{cm}^{-3}$  according to Zn solubility in Si.

For investigation it was employed CAMECA IMS-4f SIMS. For visualization Zn precipitates was used the XR computer  $\mu$ -tomography TDM-1000H-II (Yamato Scientific Co.)

There were obtained Zn and  $Zn_2$  dimmers concentration distribution mapping on a Si surface. From them analysis follows, that sizes of Zn precipitates and  $Zn_2$  clusters make tens  $\mu\text{m}$  for both samples. For both samples in the region of  $0.1\mu\text{m}$  the specified Zn/ $Zn_2$  ion current relations close to a value of 50 for a metal Zn. It testifies [4] about decomposition of Zn solid solution in Si and metal Zn precipitation.

During the visualization the 3D-models of sample XR absorption and 2D cross-section of these volumes were obtained. There were detected the light spots with a size of about  $3\mu\text{m}$  and more. A lighter tone corresponds to increased x-ray absorption, which depends on the density and impurity atomic number, i.e. these spots correspond to zinc precipitate.

[1] E.B. Yakimov, V.V. Privezentsev. *J. Mater. Sci.: Mater. Electron.* **19** (2008) S277.

[2] K.D. Scherbachev, V.V. Privezentsev. *Phys. B: J. Cond. Matter* **404** (2009) 4630.

[3] V.V. Privezentsev. *Crystall. Reps.* **58** (2013) 963.

[4] V.V. Saraykin, A. Trifonov. *Surf. Interface Anal.* **49** (2008) 486.

**Estimations of grain-boundary surface tension in elemental solids**

S.I. Prokofjev

Institute of Solid State Physics, Russian Academy of Sciences, Chernogolovka, Academician  
Ossipyan str. 2, Moscow district, 142432 Russia

The empiric correlations estimating the surface tension of liquid-like grain boundary in elemental metals, semimetals and semiconductors at melting temperature, and the temperature coefficient of the grain-boundary surface tension are proposed. The well-known empiric expressions relating a grain-boundary surface tension of pure metals and their surface tensions in solid and liquid states at melting temperature are validated using derived correlations. Obtained correlations can be useful to estimate averaged surface tension of high-angle grain boundaries in pure metals at high enough homologous temperature.

**Grain boundaries as a source of ZnO magnetic properties**

S. Protasova<sup>1,4</sup>, B. Straumal<sup>1,2</sup>, A. Mazilkin<sup>1,2</sup>, P. Straumal<sup>3</sup>, E. Goering<sup>4</sup>, G. Schütz<sup>4</sup>,  
B. Baretzky<sup>2</sup>

<sup>1</sup>Institute of Solid State Physics, Russian Academy of Sciences, 142432 Chernogolovka,  
Russia

<sup>2</sup>Karlsruher Institut für Technologie (KIT), Institut für Nanotechnologie, 76344  
Eggenstein-Leopoldshafen, Germany

<sup>3</sup>Baikov Institute of Metallurgy and Materials Science, Moscow 117991, Russia

<sup>4</sup>Max-Planck-Institut für Intelligente Systeme, Heisenbergstrasse 3, 70569 Stuttgart,  
Germany

It is known that grain boundaries can play an important role for different kinds of materials properties. We have demonstrated earlier [1] that the presence of ferromagnetic properties in zinc oxide is in a good correspondence with the amount of grain boundaries in the material, i.e. the samples are ferromagnetic if only the specific grain boundary area is higher than a definite threshold value. One of the possible reasons for ferromagnetism is considered to be the defects of the oxygen sites in the ZnO lattice [2]. X-ray photoelectron spectroscopy was used to clarify the state of oxygen in the investigated ZnO samples. The results obtained testify that in the ferromagnetic ZnO samples oxygen has an additional bound energy in comparison with non-ferromagnetic ones. Appearance of the additional oxygen peak in XPS spectra can be explained by the presence of the areas both deficient and excessive by the oxygen content.

Authors thank the Russian Foundation for Basic Research (contracts 15-03-04220) for the financial support.

[1] B.B. Straumal, A.A. Mazilkin, S.G. Protasova, A.A. Myatiev, P.B. Straumal, G. Schütz, P.A. van Aken, E. Goering, and B. Baretzky, Grain-boundary induced high  $T_c$ -ferromagnetism in pure and doped nanocrystalline ZnO, *Phys. Rev. B.* **79**, 205206 (2009).

[2] T. Dietl, A ten-year perspective on dilute magnetic semiconductors and oxides, *Nature Mater.* **9**, 965–974 (2010).

**The dynamics of dislocation wall generation in metals and alloys under shock loading**M. Yu. Gutkin,<sup>1,2,3</sup> E. A. Rzhavtsev<sup>1</sup><sup>1</sup> Peter the Great St. Petersburg Polytechnic University, St. Petersburg, Russia<sup>2</sup> Institute of Problems of Mechanical Engineering, Russian Academy of Sciences,  
St. Petersburg, Russia<sup>3</sup> ITMO University, St. Petersburg, Russia

The study of microstructural changes in metals and alloys during plastic deformation is one of fundamental problems in the physics of strength and plasticity [1-3]. In recent years, an effective tool in theoretical modeling of the severe plastic deformation processes has become the approach of 2D discrete dislocation-disclination dynamics (the D<sup>4</sup>-approach) which describes the collective behavior of straight dislocations interacting with partial disclinations [4-6]. This approach can also be used for modeling the grain fragmentation in polycrystalline metals and alloys under shock compression [7, 8]. In view of highly nonequilibrium conditions of shock wave propagation, we assumed that at the boundaries of the simulation box, which model the subgrain boundaries in a metallic grain under shock compression, there were some jumps of misorientation angles. For tilt boundaries, the jump points are effectively described in terms of partial wedge grain-boundary disclinations. These disclinations can capture the dislocations of opposite signs gliding nearby within the subgrain and make them to form new dislocation walls – fragment boundaries. This process, in fact, represents the physical mechanism of fragmentation within pre-existing subgrains in shear bands in metallic materials under shock loading. If in the process of modeling, the distance between two dislocations of opposite signs becomes less than a critical distance, it is considered that the dislocations are annihilated. To simulate the motion of dislocations, we used the 2D D<sup>4</sup>-approach. In doing so, we took into account two new features as compared with our earlier works [7, 8]. First, we accounted for the temperature increase in the shear bands and used it

for calculating the local drag coefficient  $\beta$ . Second, we considered the fact that on the subgrain boundaries, at the place of newly generated dislocations, new opposite-sign dislocations appear. Such dislocations create their own stress fields and strongly affect the dynamics of all dislocations in the simulation box. As a result, our new 2D D<sup>4</sup> computer model clearly demonstrated the subgrain fragmentation. In comparison to results of previous works [7, 8], the modification of the boundary conditions made a significant impact on the final microstructure in the case of both fine and coarse initial subgrains. We obtained stable dislocation structures similar to those observed in experiments [9, 10] and showed that the typical shock duration is enough to complete the fragmentation process within the initial subgrain, and the necessary stress magnitude (0.5 GPa) well agrees with experiments [9, 10].

- [1] R.Z. Valiev, T.G. Langdon. *Prog. Mater. Sci.* 51 (2006) 881.
- [2] A.P. Zhilyaev, T.G. Langdon. *Prog. Mater. Sci.* 53 (2008) 893.
- [3] Y. Estrin, A. Vinogradov. *Acta Mater.* 61 (2013) 782.
- [4] K.N. Mikaelyan, M. Seefeldt, M.Yu. Gutkin, et al. *Phys. Solid State* 45 (2003) 2104.
- [5] S.V. Bobylev, M.Yu. Gutkin, I.A. Ovid'ko. *Acta Mater.* 52 (2004) 3793.
- [6] G.F. Sarafanov. *Phys. Solid State* 50 (2008) 1868.
- [7] M.Yu. Gutkin, E.A. Rzhavtsev. *Trudy SPbGTU, No. 515* (2013) 82.
- [8] E.A. Rzhavtsev, M.Yu. Gutkin. *Scripta Mater.* 100 (2015) 102.
- [9] Yu.I. Meshcheryakov, A.K. Divakov, et al. *Tech. Phys. Lett.* 36 (2010) 1125.
- [10] Yu.I. Meshcheryakov, A.K. Divakov, et al. *Mater. Phys. Mech.* 11 (2011) 23.

## On the size dependence of the melting heat of metal nanoclusters

V.M. Samsonov, N.Yu. Sdobnyakov, S.A. Vasilyev, D.N. Sokolov

General physics department, Tver State University, Sadovii per., 35, Tver, 170002 Russia

The size dependence of the melting heat of transition metal nanoclusters (*Ni*, *Au*, *Cu* and *Ag*) was investigated using two alternative methods of computer simulation (isothermal molecular dynamics and Monte-Carlo, see table 1). A more detailed investigation was carried out for *Au* and *Cu* nanoclusters in a wide range of their size (see table 2). It has been shown that the melting heat decreases under decreasing the nanocluster size and, in an approximation, tends to the linear dependence on the particle inverse radius.

Table 1. Values of melting temperature  $T_m$ , heat of melting  $\Lambda$  and entropy of melting  $\Delta S_m$  for the transition metal nanoclusters ( $N = 1000$ ) obtained on the basis of molecular dynamic results. Data for macroscopic values of the melting temperature used in our calculations are presented in [1].

Metal	$T_m, K$	$\Lambda$ , kJ/mol		$\frac{\Lambda}{\Lambda^{(\infty)}}$	$\Delta S_m$ , J/(mol·K)	$\frac{\Delta S_m}{\Delta S_m^{(\infty)}}$
		Computer simulation	Experiment, $\Lambda_m^{(\infty)}$ [1]			
<i>Ni</i>	1453	7.2	17.6	0.41	4.96	0.49
<i>Au</i>	921	4.8	12.6	0.38	5.21	0.55
<i>Cu</i>	1261	5.3	13.0	0.41	4.20	0.44
<i>Ag</i>	1063	5.3	11.3	0.47	4.99	0.54

Table 2. Evaluation of critical size for nanoclusters *Au* and *Cu*, corresponding  $\Lambda^* = 0$ .

Metal	Method	$R_{ch}$ , nm	$N_{ch}$
<i>Au</i>	MD	1.05	270
	MK	0.65	129
<i>Cu</i>	MD	0.62	72
	MK	0.45	21

Support of Ministry of Education and science of RF (project No. 3.2448.2014/K) and of RFBR (grant No. 16-33-00742) is acknowledged.

[1] *Fizicheskie velichiny: Spravochnik (Physical Quantities. Handbook)*, Moscow: Energoatomizdat, 1991.

## Thermodynamic approach to size dependence of melting temperatures of thin films

V.M. Samsonov, N.Yu. Sdobnyakov, D.N. Sokolov

General physics department, Tver State University, Sadovii per., 35, Tver, 170002 Russia

In [1] we obtained the next formulas for a free and supported film, respectively:

$$\frac{\Delta T}{T_m^{(\infty)}} = \frac{2(\sigma_s - \sigma_l)}{\rho_l^{(\infty)} \lambda_m^{(\infty)} h}, \quad \frac{\Delta T}{T_m^{(\infty)}} = \frac{\sigma_s + \sigma_{ss'} - \sigma_l - \sigma_{ls'}}{\rho_l^{(\infty)} \lambda_m^{(\infty)} h}. \quad (1)$$

In the above formulas  $\Delta T = T_m^{(\infty)} - T_m$  is the difference between the macroscopic melting temperature  $T_m^{(\infty)}$  and the melting temperature  $T_m$  of the film of thickness  $h$ ,  $\rho_l^{(\infty)}$  is the density in the bulk liquid phase,  $\lambda_m^{(\infty)}$  is the macroscopic value of the specific heat of melting,  $\sigma_s$  and  $\sigma_l$  are surface tensions of the solid substrate and melt, correspondingly,  $\sigma_{ss'}$  is the interfacial tension at the boundary between the crystalline area of the film and the substrate,  $\sigma_{ls'}$  is the interfacial tension at the melt-substrate boundary. As reliable values of  $\sigma_{ss'}$  and  $\sigma_{ls'}$  are, as a rule, not known, in [1] the effect of the solid substrate on  $\Delta T$  was taken into account via a correction term added to Eqs (1) and expressed via the uniparticle potential of the substrate. In this connection the term of the substrate can be expressed as the difference between energies of adhesion of the film in liquid  $W_l$  and solid  $W_s$  states. The energy of the adhesion of the liquid film will be approximately equal to the energy of the adhesion of liquid to the same substrate. Besides,  $W_l$  relates to the equilibrium contact angle  $\theta_e$ :  $\cos \theta_e = 2W_a / W_c = W_a / \sigma_l$ , where  $W_c = 2\sigma_l$  is the cohesion energy. Eqs (1) can be rewritten as

$$\Delta T / T_m^{(\infty)} = \left[ 2(\sigma_s - \sigma_l) + \sigma_l \cos \theta_e (1 - \rho_s^{(\infty)} / \rho_l^{(\infty)}) \right] \left\{ \rho_l^{(\infty)} \lambda_m^{(\infty)} h \right\}^{-1}. \quad (2)$$

$T_m(h)$  of copper (upper curve) and tin (lower curve) films shown in Fig. 1 were calculated for the case of the solid substrate presented by the same metal under assumption on a primary skin-layer of the thickness 1 nm. According to Fig. 2, the forms of the size dependences of  $T_m$  for copper and tin on a carbon substrate are principally different.

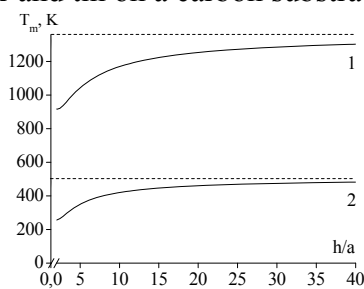


Fig.1:  $T_m(R)$  for copper (curve 1) and tin (curve 2) films on the same metal.

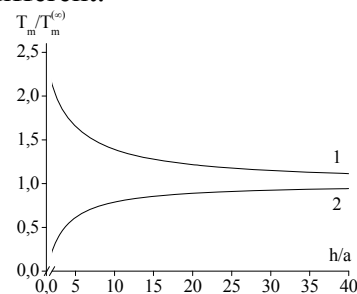


Fig. 2:  $T_m(R)$  of copper (curve 1) and tin (curve 2) films on the carbon substrate.

Obviously, the effect of the growth of the melting temperature under decreasing the film thickness result from a noticeable difference between the values of the surface tension of copper and carbon as well as under effect of the interfacial boundary.

Support of Ministry of Education and science of RF (project No. 3.2448.2014/K) and of RFBR (grant No. 16-33-00742) is acknowledged.

[1] Samsonov V.M., Sdobnyakov N.Yu., Bembel A.G., Sokolov D.N. *Physiko-khimicheskie aspekti izucheniya klasterov, nanostruktur i nanomaterialov.* **4** (2012) 257.



**Molecular dynamic study of crystalline and amorphous metal film formation by condensation on cooled metal substrate**

A.G. Bembel, S.A. Vasilyev, V.M. Samsonov

General physics department, Tver State University, Sadovii per., 35, Tver, 170002 Russia

Our computer program makes it possible to simulate the process of the island film formation, including the epitaxial growth on single crystal faces. For this purpose, the atomic beam of definite energy, density and cross-section is directed to the substrate, precipitates on it with the following relaxation (annealing) or quenching of the forming island film. A comparative study of Ag and Au films formation was carried out under the same deposition conditions on Ni (100) face at 300k with the following quenching at the high cooling rate (1010 K/s) up to the helium temperature (4K). Such a quenching rate and so low temperatures are used in direct experiments to obtain amorphous metal films using the condensation on the cooled substrate. It has been found that even at so high cooling rates the Ag beam condensation results in a crystalline film formation. The result obtained agrees with the experimental fact that neither via the melt quenching no by means of the vapor condensation on cooled substrates the amorphous films/particles of some pure (single-component) metals (including Ag) have not been obtained. At the same time, the Au atom beam under the same conditions forms an amorphous island film. Fig. 1 demonstrate the radial distribution function (RDF) for the final states of Ag and Au films, respectively. As one can see, RDF for the Au film has one-two well resolved maxima whereas for the Ag film RDF has several well resolved maxima which agrees in general with Kobeko's criterion formulated in 50th for bulk amorphous phases.

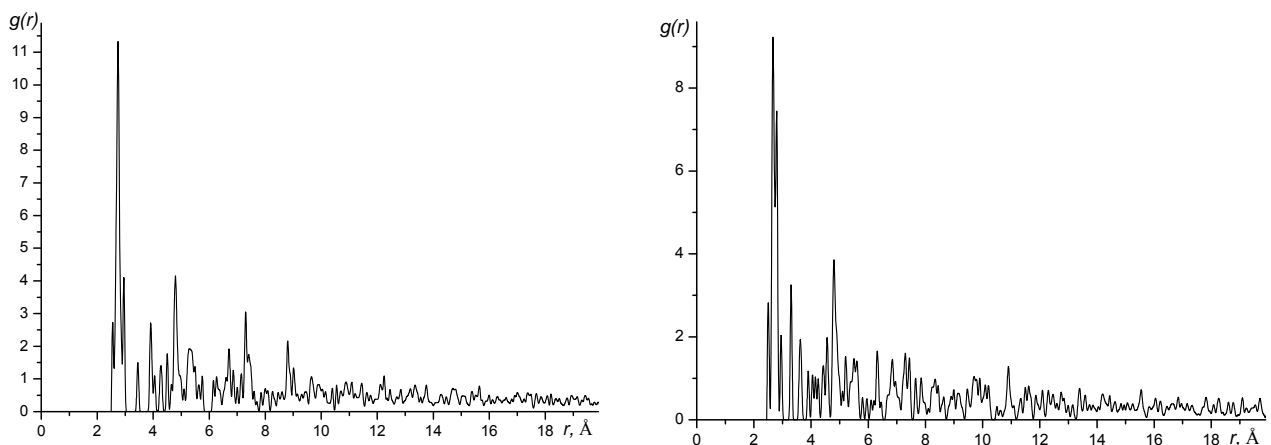


Fig.1. RDF for the Ag and Au films on Ni (100) face, respectively

Support of Ministry of Education and science of RF (project No. 3.2448.2014/K) and of RFBR (grant No. 16-33-60171) is acknowledged.

## **Nonlinear optical properties of composite biosolders based on single-walled carbon nanotubes**

M.S. Savelyev, A.Y. Gerasimenko, L.P. Ickitidze, V.M. Podgaetsky, S.A. Tereshchenko

National Research University of Electronic Technology - MIET, bld. 1, Shokin Square,  
Zelenograd, Moscow, Russia, 124498

In this study, we have conducted research of composite biosolder (CS) based on single-walled carbon nanotubes (SWNT) type of SWCNT-90A and bovine serum albumin (BSA), which can be used for laser welding of biological tissue. At the same time, influence of laser radiation under CS can cause a change of liquid into solid phase, what provides high strength of welding seam and the necessary conditions for the regeneration of these tissues. For the preparation of CS it is very important to provide a stable aqueous dispersion medium SWCNT/BSA (0.3 wt.% SWNTs, 25 wt.% BSA), and also development of a model of interaction of the laser radiation not only causing but also not causing nonlinear effects in the substance. Phenomenological approach based on the radiation transfer equation was used to simulate the process of such interaction. In the experiments for approbation of the model, solid-state Nd:YAG laser LS-2147 (LOTIS TII) with linear polarization of the laser radiation in the horizontal plane and a pulse duration of 16 ns was used. As a result, it was found that the process of attenuation of laser radiation lower than the threshold power density (intensity) of about  $10 \text{ MW} \cdot \text{cm}^{-2}$  can be described by a constant absorption coefficient  $\alpha$  in the range of  $0.5\text{-}2 \text{ cm}^{-1}$ , with the layer thickness CS  $\sim 0.2 \text{ cm}$ . Such intensity is not capable to cause irreversible processes in substance without long-term exposure to this radiation. However irreversible processes in CS even from the effects of a single pulse occur after exceeding the threshold intensity in several times. For studied CS, threshold value of the intensity of  $\sim 10 \text{ MW} \cdot \text{cm}^{-2}$ , the nonlinear absorption coefficient of  $\sim 1 \text{ cm} \cdot \text{MW}^{-1}$  were obtained. Knowing the nonlinear optical parameters of the substance allows to determine the energy of the laser radiation that has been absorbed by this substance. As a result, it becomes possible to control the process of forming of the CS. A high temporal stability of dispersion is obtained and there is no agglomeration of nanotubes. Thus, these studies demonstrate the ability to control the process of forming of a CS from the aqueous dispersion with SWCNT/BSA in laser welding of biological tissues.

The authors thank Professor S.V. Selishchev for useful tips. This work was provided by the Ministry of Education and Science of the Russian Federation (Agreement 14.575.21.0044, RFMEFI57514X0044).

**Discontinuous creep and spatio-temporal dynamics of deformation bands in an Al-Mg alloy**

A.A. Shibkov, M.F. Gasanov, M.A. Zheltov, A.E. Zolotov, V.I. Ivolgin

Tambov State University, Tambov, Internationalnaya str. 33, 392000 Russia

Many structural Al-based alloys, and Al-Mg alloys, in particular, exhibit an intermittent plasticity on the macroscopic scale also known as the Portevin-Le Chatelier (PLC) effect which is associated with repetitive stress drops related with the nucleation of the bands of localized plastic deformation in tests with a constant imposed strain rate. In the current work we reveal discontinuous creep in commercial AlMg6 alloy used in aerospace industry. This phenomenon manifests itself as ‘strain bursts’ during creep tests, where the creep curves contain macroscopic strain jumps in the magnitudes of several percent. The experimental investigation employs the measurements of the load and strain sensors synchronized with a high-speed video camera to capture the deformation band nucleation and evolution [1]. Unexpectedly, an individual strain burst is found to generate a complex jerky load response which consists of a number of stress drops (similar to the PLC effect) due to inertia of the ‘specimen – creep machine’ mechanical system. Each stress drop is associated with a fast evolution stage of a single deformation band which takes the shape of a widening neck in a flat specimen. We have established that the main mechanism responsible for the development of the strain burst is a multiplication of the deformation bands, when the boundary of each band generates the secondary band and so on. It is shown that when the initial specimen length increases the intermittent load response exhibits a tendency to the state of self-organized criticality [2]. We found that the time-periodic stress oscillations in form of a limit cycle can be spontaneously generated in short-time range during dynamical regime of type A. This study was supported by the Russian Science Foundation, project no. 15-12-00035.

[1] A.A. Shibkov, A.E. Zolotov, M.A. Zheltov, M.F. Gasanov, A.A. Denisov. *Phys. of the Solid State*. **56** (2014) 881.

[2] A.A. Shibkov, A.E. Zolotov, M.A. Zheltov, A.A. Denisov, M.F. Gasanov. *Phys. of the Solid State*. **56** (2014) 889.

## The electric current-induced suppression of the Portevin - Le Chatelier effect in Al-Mg alloys

A.A. Shibkov, A.A. Denisov, M.A. Zheltov, A.E. Zolotov, M.F. Gasanov

Tambov State University, Tambov, Internationalnaya str. 33, 392000 Russia

The direct current-induced suppression of the Portevin - Le Chatelier (PLC) effect has been revealed and investigated in Al-5wt.% Mg and Al-6wt.% Mg alloys during tensile tests at a constant strain rate. Suppression of the PLC effect by direct electric current manifests itself as an increase in the critical strain  $\varepsilon_c$  for the onset of serration flow with increasing current density exceeding a certain critical value  $j_c$  which depends on the weight content of Mg in Al-Mg alloy [1]. The current density range in which the transition from a jerky tensile curve to a smooth one occurs is found to depend on the type of PLC instabilities apart from the testing temperature and an imposed strain rate. The obtained results show that the observed suppression of jerky flow by electric current is not directly associated with Joule heating per se of the whole sample. Suppression of jerky flow by direct current is accompanied by an increase in the flow stress. It is shown that the critical plastic strain and the current-induced hardening increase with increasing both the current density and the weight content of Mg in Al-Mg alloys. We assume that this effect is related to the suppression of dynamic strain ageing due to a change in the mobility of impurity ions Mg caused by electromigration. Another possible scenario is that the current-induced dissolution of small precipitates (GP zones) can result in the suppression of the jerky flow within the framework of the precipitation model of the inverse behavior of critical strain for the PLC effect [2]. The new phenomenon of current-induced suppression of PLC serrated deformation can be used to develop a technology of electric current treatment of metals to increase the lifetime of commercial alloys of the Al-Mg system.

This study was supported by the Russian Science Foundation, project no. 15-12-00035.

[1] A.A. Shibkov, A.A. Denisov, M.A. Zheltov, A.E. Zolotov, M.F. Gasanov. *Mat. Sci. Eng. A.* **610** (2014) 338.

[2] A.A. Shibkov, M.A. Zheltov, A.E. Zolotov, A.A. Denisov, M.F. Gasanov. *Cryst. Rep.* **60** (2015) 895.

## High-temperature carbonization of humic acids and graphene oxide composite: a porous hybrid carbon material

Y. M. Shulga<sup>a,b</sup>, S. A. Baskakov<sup>b</sup>, Y. V. Baskakova<sup>b</sup>, V. M. Martynenko<sup>b</sup>, A. S. Lobach<sup>b</sup>, S.A.Vasiliev<sup>b</sup>, Y. M. Volkovich<sup>c</sup>, V. E. Sosenkin<sup>c</sup>, N. Y. Shulga<sup>a</sup>, Y. N. Parkhomenko<sup>a</sup>

<sup>a</sup>National University of Science and Technology MISIS, Leninsky pr. 4, Moscow 119049, Russia

<sup>b</sup>Institute of Problems of Chemical Physics, Russian Academy of Sciences, Chernogolovka 142432, Moscow Region, Russia

<sup>c</sup>A.N. Frumkin Institute of Physical Chemistry and Electrochemistry, Russian Academy of Sciences, Leninsky pr. 31, Moscow 119071, Russia

Humic acids (HA) extracted from peat and HA derived carbon (HADC, carbonized at 900 °C in inert atmosphere) has been studied by solid-state nuclear magnetic resonance (NMR) spectroscopy with magic angle spinning, differential scanning calorimetry (DSC), thermogravimetric analysis (TGA), Raman spectroscopy and the method of standard contact porosimetry (SCP). Mass spectrometry was also used for analysis of gases released upon heating of the samples. At low temperature heating (150 °C) HA release primarily CO<sub>2</sub> and H<sub>2</sub>O. At higher temperatures, HA decomposes to CO and low molecular weight hydrocarbons. The composite of HA with graphene oxide (HA+GO) derived carbon (DC) has been prepared using carbonization of HA+GO in an inert atmosphere at 900 °C. Small agglomerates of carbon with sharply defined edges have been obtained because of carbonization of HA, and the composite of HA+GO forms only a large aggregates at the same condition. The values of specific surface area of HADC and (HA+GO)DC are 173 and 474 m<sup>2</sup>/g, respectively. The value of specific surface correspond to the area of all pores (S<sub>pore</sub>) is equal to only 3 m<sup>2</sup>/g in the case of HADC. In the case of the (HA+GO)DC, S<sub>pore</sub> is equal to 237 m<sup>2</sup>/g.

**The fabrication of a protective  $\text{CuMn}_2\text{O}_4$  spinel coating on ferritic stainless steel used as solid oxide fuel cell interconnects**

Z. Ranjbar-Nouri, M. Soltanieh, S. Rastegari

Center of Excellence for High Strength Alloys Technology (CEHSAT)

School of Metallurgy and Materials Engineering, Iran University of Science and Technology,  
Tehran, Iran

At high temperature and long operating time of solid oxide fuel cells (SOFC), ferritic stainless steels face with some problems such as overgrowth and spallation of the surface oxide and cathode poisoning due to chromium evaporation. In the present work in order to improve the above problems, the protective/conductive  $\text{CuMn}_2\text{O}_4$  spinel coating was created on the AISI-430 ferritic stainless steel by means of pulse electrodeposition and subsequent heat treatment. So that at first the copper was applied on the substrate from a sulfate bath with an average current density of  $48 \text{ mA/cm}^2$  and a deposition time of 4 min. Then manganese was electrodeposited on top of the copper layer from a sulfate bath with an average current density of  $125 \text{ mA/cm}^2$  and a deposition time of 8 min. In the pulse electrodeposition of Cu and Mn the duty cycle and frequency were 80% and 100 Hz, respectively. Then to convert the metallic layers to spinel and also to evaluate its prevention of outward diffusion of Cr, oxidation was carried out at  $750^\circ\text{C}$  in air for 24 h and 100 h. Microstructural evaluation of samples cross section by scanning electron microscope (SEM) equipped with EDS indicated that the  $\text{CuMn}_2\text{O}_4$  spinel layer acted as a barrier to outward diffusion of Cr effectively and the amount of Cr in the coatings surface was zero. Also coating layer had good adhesion to the substrate. By studying of samples oxidation in air for 0.5, 10 and 120 min at  $750^\circ\text{C}$ , the results indicated that at the beginning of the oxidation of the Cu-Mn metallic coating, manganese was quickly oxidized to MnO and  $\text{Mn}_3\text{O}_4$ . Gradually, the MnO and  $\text{Mn}_3\text{O}_4$  disappeared and  $\text{Mn}_2\text{O}_3$  was formed and the copper was oxidized to CuO. Finally, spinel phase of CuO and  $\text{Mn}_2\text{O}_3$  was formed.

## Grain boundary segregation and contact melting of metals

K.M. Elekoeva, Y.N. Kasumov, V.A. Sozaev

North-Caucasus Institute of Mining and Metallurgy (State Technological University),  
Nikolaeva, 44, Vladikavkaz, 362021 Russia

We recognize four general mechanisms of contact melting (CM): diffusion, adhesion, segregation, and a one associated with dimensional effects [1, 2]. CM is intertwined with surface properties of components of a solid solution. It is well known that the lower the surface energy of an element, the lower its melting point; that is why the elements with the lower surface energy (and thus the lower melting points) are adsorbed, primarily, (segregate) on grain boundaries (GB) and outer surfaces. This can affect both the rate and the temperature of CM [3]. Degree  $x^0$  to which adsorption centers are populated by impurity atoms (at  $x \ll 1$ ) on a surface or along GBs is described by the Langmuir–Maclean isotherm (see, for instance, [4]), or the Zhukhovitskii isotherm [5]. As is shown in [3], the rate of CM  $\langle v \rangle \sim \ln x^0 / (1 - x^0) \sim \Delta\sigma = \sigma_1 - \sigma_2$  ( $\sigma_1, \sigma_2$  being the surface energies of compounds) which indicates the importance of the segregation mechanism of CM.

Therefore, one has to account for the segregation mechanism along with the diffusion mechanism of CM: for polycrystalline samples, impurities accumulate, due to the grain boundary segregation, along the grain boundaries and, by diffusing along the latter, result in the formation of triple eutectics with lower temperatures of CM and double eutectics at boundaries; thus, the rate of CM increases. We shall note that there is indirect indication on the relation found by us between the rate of CM and the limiting solubility  $x_{\text{lim sol}}$  of impurities in a metallic matrix, which is, in turn, associated with the grain boundary segregation [6].

This work was supported by the State Order 3.423.2014/K, project no. 423.

1. A.A. Akhkubekov, T.A. Orkvasov, V.A. Sozaev *Kontaktnoe plavlenie metallov i nanostruktur na ikh osnove* (Contact Melting of Metals and Nanostructures on Their Base), Moscow: Fizmatlit, (2008).
2. A.Yu. Gufan, A.A. Akhkubekov, M.\_A.V. Zubkhadzhev, Z.M. Kумыков, *Bull. Russ. Acad. Sci.: Phys.* (2005). vol. 69. no. 4. pp. 632–638.
3. A. A. Akhubekov, S. N. Akhubekova, K. M. Elekoeva, R. A. Musukov, and V. A. Sozaev *Bulletin of the Russian Academy of Sciences. Physics.* (2014). Vol. 78. No. 4. pp. 281–284.
4. B.S. Bokshstein, L.S. Shvindlerman *Preprint of Institute of Solid State Physics of the USSR Acad. Sci.*, Chernogolovka. (1978).
5. A.A. Zhukhovitskii, *Zh. Fiz. Khim.*, (1943). vol. 17. nos. 5–6. pp. 313–317; (1944). Vol. 18. nos. 5–6. pp. 214–238.
6. E.D. Hondros, M.P. Seah, *Int. Metallurg. Rev.* (1997). vol. 22. no. 12. pp. 261–303.

**Surface modification of BN nanostructures by Cu and Al in microwave plasma**

A.E. Steinman<sup>1</sup>, A.T. Matveev<sup>1</sup>, A.M. Kovalskii<sup>1</sup>, K.L. Firestein<sup>1</sup>, I.V. Sukhorukova<sup>1</sup>, D. Golberg<sup>2</sup>, D.V. Shtansky<sup>1</sup>

<sup>1</sup>National University of Science and Technology "MISIS", Leninsky prospect 4, Moscow, 119049, Russia

<sup>2</sup>National Institute for Materials Science (NIMS), Namiki 1-1, Tsukuba, Ibaraki 3050044, Japan

In recent years BN nanostructures have found many useful applications due to unique combination of mechanical, physical and chemical properties. Main interest was attracted by BN nanotubes, but other BN structures – nanospheres, nanoparticles and graphene-like nanopetals –can also be utilized in different fields, such as biomaterials for drug delivery systems, reinforcing phases in composite materials and as catalysts. Realization of these applications requires modification of nanostructure surfaces using different metals. Thus we developed a method and an experimental setup for modifications of BN nanostructures with various metals using microwave plasma treatment. In particular, dosing, cooling and collecting systems were designed. For plasma generation Ar and N<sub>2</sub> gases were used. Simultaneous introduction of metals and diverse BN nanostructures in various temperature zones of a reactor resulted in their modification with Cu and Al. These metals were deposited on BN nanostructures in a form of continuous and discontinuous (islet-like) coatings. Then modified BN nanostructures were studied using scanning and transmission electron microscopy, EDX-analysis, Raman and infrared spectroscopies. The obtained hybrid (Metal/BN) nanomaterials can find valuable applications in various fields thanks to the newly acquired properties after the regarded surface modifications.



## **Microstructure evolution of Ag films at annealing**

V.G. Sursaeva, A.B. Straumal

Institute of Solid State Physics, Russian Academy of Sciences, Chernogolovka, Ac. Ossipyan str. 2, Moscow district, 142432 Russia

Different types of microstructure evolution kinetics in thin metal films at annealing were experimentally observed. Depending on the grain size and temperature four microstructure change scenarios were observed. 1. There is almost no grain growth; this stage is an incubation period. The observed incubation period of the grain growth is generated by the vacancy grain growth inhibition 2. Grain growth goes on according to a linear law, where the triple junction inhibition plays the defining role. 3. An intensive grain growth by a parabolic law, where an important role belongs to the grain boundary motion. The deviation of the grain growth from the parabolic law is a result of the microstructure inhomogeneity of the film. 4. The diffusive mobility of the atoms is high at high temperature. Consequently the surface diffusion leads to the growth of thermal grooves and grain growth deceleration. The film loses continuity at the grain agglomerates boundaries and breaks up into islands. The discovered holes growth incubation period at the film annealing is comparable by size to the grain growth incubation period. The coincidence of these experimental values allows the authors to assume that the inhibition nature of the grain growth and the hole growth is the same.

The fact that the microstructure of the silver film is stable at temperatures lower than 300°C and at 500°C the stability remains only 30 minutes is a potentially useful result.

The authors thank the Russian Fond for Basic Research for financial support of the research in the framework of a RFBR project (№14-42-03556)

## Kinetic properties of grain boundary ridges in Zn

V.G. Sursaeva, A.B. Straumal

Institute of Solid State Physics, Russian Academy of Sciences, Chernogolovka, Ac. Ossipyan str. 2, Moscow district, 142432 Russia

The development of the microstructure of a polycrystal during grain growth is subject to the influence of numerous factors that, directly or indirectly, affect the motion of the grain boundaries involved in the minimization of the free energy of a solid. Since a polycrystal is a natural topological network comprised of grain boundaries and their junctions, the properties of these elements can influence the evolution of the microstructure because the migration of a single grain boundary entails necessarily the concomitant motion of the other elements. Consequently, a slower migration rate of any element will impact the general development of the grain structure. Although these elements are the only features of a grain structure required to satisfy all topological constraints of a polycrystal, it is well known that due to the anisotropy of grain boundary properties other microstructural features can emerge. For instance, grain boundary facets are commonly found in the microstructure of metallic materials. In recent investigations it was shown that facets and the intersection between them, i.e. ridges, can affect grain boundary migration if their kinetics is different from that of the grain boundary. In this study, we investigated the effect of the grain boundary ridges on grain boundary migration.

The migration of single  $[10\bar{1}0]$  tilt boundaries was previously investigated by us in detail. While the phenomena of non-activated motion of high angle grain boundaries has been disclosed on special  $[11\bar{2}0]$  tilt boundaries in zinc. The  $[10\bar{1}0]$  tilt grain boundaries migration shows an activated motion character. Therefore it is obvious to assume that the kinetic properties of grain boundary ridges formed by segments of  $[10\bar{1}0]$  and  $[11\bar{2}0]$  tilt grain boundaries will differ. It was experimentally observed that at the  $[11\bar{2}0]$  tilt grain boundary migration by half loops the form of the ridges is asymmetrical. The grain boundary loop mobility changes from  $1.36 \cdot 10^{-10}$  to  $4.33 \cdot 10^{-10}$  m<sup>2</sup>/s in the temperature interval from 360°C to 400°C. The grain boundary ridges activation enthalpy formed by a  $[11\bar{2}0]$  tilt grain boundary segment is  $H=0.47$ eV. At the  $[10\bar{1}0]$  tilt grain boundary migration in the form of a half loop the form of the ridges is symmetrical. The grain boundary loop mobility changes from  $3.98 \cdot 10^{-10}$  to  $1 \cdot 10^{-8}$  m<sup>2</sup>/s in the temperature interval from 340°C to 410°C. The grain boundary ridges activation enthalpy formed by a  $[10\bar{1}0]$  tilt grain boundary segment is  $H=1$ eV.

The authors acknowledge the financial support from the Russian Foundation for Basic Research (contract 16-03-00248).

**The structure and thermoelectric properties of low-temperature thermoelectric materials obtained by Spark Plasma Sintering**

V.T. Bublik<sup>1</sup>, I.A. Drabkin<sup>2</sup>, V.B. Osvenskiy<sup>2</sup>, V.P. Panchenko<sup>1,2</sup>, Yu.N. Parkhomenko<sup>1,2</sup>, A.I. Sorokin<sup>2</sup>, N.Yu. Tabachkova<sup>1</sup>

<sup>1</sup>National University of Science and Technology “MISiS”, Moscow, Leninsky Prospekt 4, 119049 Russia

<sup>2</sup>State Scientific-Research and Design Institute of Rare-Metal Industry "Giredmet" JSC, Moscow, B. Tolmachevsky lane, Building 5-1, 119017 Russia

Semiconductor thermoelectric materials are widely used in generators, refrigerators, thermostats, conditioners and other devices. The basic energy characteristics of the thermoelectric devices are defined by thermoelectric efficiency. The creation of nanostructured materials is one way to increase thermoelectric efficiency. However, the causes of increase in the thermoelectric efficiency  $ZT$  in materials, obtained by pressing of nanopowders, are still unclear. There is no clear understanding of whether the  $ZT$  growth is associated with effects within the grains due to a large number of defects generated during grinding and pressing nanopowder, or with the influence of grain boundaries. The most common point of view is the phonon scattering at the grain boundaries in nanostructured samples occurs stronger than the scattering of electrons, due to the thermal conductivity at nanostructuring reduce quickly then electrical conductivity. However, the comparison of the means free path of electrons and phonons with grain sizes do not confirm this point of view.

In this work we used the method of spark plasma sintering (SPS) powders for obtaining bulk nanostructured thermoelectric material based on  $\text{Bi}_{0,4}\text{Sb}_{1,6}\text{Te}_3$ . Milling was carried out in high-energy ball mill. The research of the material structure was carried out by X-ray diffraction and transmission electron microscopy. All the effects of the influence of the nanostructure on the processes of charge carriers motion should increase with decreasing temperature due to growth of the mean free path within the grain and when mean free path

comparable with the size of the grain. Therefore, the temperature dependences of the electrical conductivity and the Hall effect were measured.

We showed that recrystallization of the initial grains occurred in the process of sintering. The crystallite growth and reduction of surface defects occurred with increasing of sintering temperature up to 400 °C. The concentration of charge carriers did not show significant changes, it means own surface defects are not electrically active (neutral). The grain size reached to several microns at the sintering temperature of 400 °C. A large number of nano-sized grains appeared in the structure at 450 °C. The composition of the nano-grains matched the composition of the sample. For samples annealed at 400 °C the mobility of charge carriers at 15 K was higher than the mobility in samples annealed at 450 °C. The number of new grains significantly increased at 550 °C, and they increased in size. This process did not accompany changes in the concentration of holes, that means the nano-grains appeared due to healing of some own neutral defects, and not necessarily point defects and located within or on the large grains boundaries. These results suggest that there are other (high temperature) self-organizing processes of formation of nanostructures based on redistribution of nonequilibrium intrinsic point defects besides well-known low temperature. The contribution of grain boundary scattering of phonons in the increase of the figure of merit ( $Z$ ) at room temperature is not dominant because it should be considered an essential role of point defects in the bulk of the grains.

This work was supported by RFBR (Project No. 15-03-09089\_a)

## **Effect of dynamic recrystallization mechanism on grain boundary assemblies in austenitic stainless steel**

M. Tikhonova, R. Kaibyshev, A. Belyakov

Laboratory of Mechanical Properties of Nanostructured Materials and Superalloys, Belgorod State University, Pobeda, 85, Belgorod 308015, Russia

The microstructure evolution associated with the development of dynamic recrystallization was studied in a high nitrogen austenitic stainless steel subjected to hot working. The hot working was carried out by compression at temperatures from 800°C to 1100°C under a strain rate of  $10^{-3} \text{ s}^{-1}$ . The structural investigations were carried out on the sample sections parallel to the compression axis using Nova Nano SEM 450 scanning electron microscope equipped with an electron backscatter diffraction (EBSD) analyzer incorporating an orientation imaging microscopy (OIM) system.

The relationship between the grain/subgrain size and flow stress can be expressed by power law functions with different grain size exponent depending on deformation conditions. The grain and subgrain size exponents of about -0.7 and -1.0, respectively, were obtained for discontinuous dynamic recrystallization under hot working conditions. These dependencies lead to the fraction of high-angle boundaries being a function of the flow stress. Namely, the fraction of high-angle boundaries in dynamically recrystallized structures should decrease with a decrease in the flow stress. The effect of processing conditions on the grain boundary misorientation distribution and fraction of special boundaries in discontinuously dynamically recrystallized structures is discussed in detail.

**An epitaxial alumina–carbon coating for improving the electrochemical performance of  $\text{LiNi}_{0.4}\text{Mn}_{0.4}\text{Co}_{0.2}\text{O}_2$  cathode material**

V.V. Volkov, E.V. Makhonina, A.E. Medvedeva, Yu.A. Politov

N.S. Kurnakov Institute of General and Inorganic Chemistry, Russian Academy of Sciences,  
31 Leninsky pr., Moscow, 119991 Russia

There is a great demand for energy storage in the world due to increasing usage of portable electronic devices, the need to balance fluctuations of the energy source output, and quick rise of new electric vehicles. For these reasons Li-ion batteries (LIBs) have become the subject of extensive studies for general LIBs performance and extended lifetime improvements. One of the key components in LIBs improvement process is the active cathode element such as positive electrode material. Here we describe a new type of the surface modification for advanced cathode  $\text{LiNi}_{0.4}\text{Mn}_{0.4}\text{Co}_{0.2}\text{O}_2$  material used to improve the LIB electrochemical performance. Such layered  $\text{LiNi}_{0.40}\text{Mn}_{0.40}\text{Co}_{0.20}\text{O}_2$  compound was synthesized from simple precursors followed by the surface coating with mixed alumina–carbon film by means of simple soft chemical route.

For the first time, we get an experimental diffraction evidence that the alumina coating can create a thin epitaxial layer on basal  $\{001\}$  facets of mentioned above cathode grains, whereas side-view grain's facets, like  $\{010\}$ , remain free from the crystalline  $\alpha\text{-Al}_2\text{O}_3$  film, thus leaving them easy for Li-ion diffusion into the LIB cathode structure. Our conclusions follow from local electron diffraction analysis suggesting that the alumina film can create a natural epitaxial interface structure promoted by a good “ $a \times \sqrt{3}$ ” type of lattice matching for host  $\text{LiNiO}_2$  grain and guest  $\alpha\text{-Al}_2\text{O}_3$  film structures.

An additional amorphous carbon film facilitates a better electron conductivity of the coating layer and prevents the loss of the electrical contact between cathode grains in the course of battery cycling. Electrochemical tests have revealed that the mixed alumina-carbon coating applied on  $\text{LiNi}_{0.40}\text{Mn}_{0.40}\text{Co}_{0.20}\text{O}_2$  grains can stabilize their surface structure and improve both cycling performance and rate capability for cathodes on this basis in comparison with pristine and/or pure alumina coated  $\text{LiNi}_{0.40}\text{Mn}_{0.40}\text{Co}_{0.20}\text{O}_2$  cathode material.

This work was supported by the Russian Foundation for Basic Research, project no. 14-29-04094.

**Modeling of the X-ray line profile at diffusion carbonization of iron sample**A.V. Pokoev, V.V. Volkov

Samara State Aerospace University, Moscow Highway, 34, Samara, 443086, Russian Federation

A diffraction scattering pattern at the X-ray characteristic radiation on the crystal lattice of a polycrystal alloy contains different information about the interior structure and impurity concentration (carbon) distribution in the base lattice crystal (iron, steel) after the isothermal annealing. Numerical methods application allows simulation of the X-ray line profile (XRLP) by the alloy lattice parameter variations, caused for example by the diffusion penetration of carbon into steel.

In the present work the modeling algorithm is developed and approved, allowing prediction of the diffusion zone parameters at carbonization with the help of the simulated XRLP. It is shown, that depth of the X-ray analysis under certain conditions allows to receive the information on the diffusion zone sizes in the layers considerably exceeding the depth of semi-absorption layer in the sample. For the prompt data analysis the program is developed which allows to compare the experimental data on carbonization with the results of the XRLP forecasting and to correct them accordingly.

- [1] V.V. Volkov, A.V. Pokoev. Certificate about the state registration of the computer program №2015614323 «DiffProfile», 15.04.2015 . (in Russian)

**The accelerated diffusivity along layer boundaries in multilayer metal materials**

A.I. Plokhikh<sup>1,a</sup>, A.L. Petelin<sup>2,a</sup>, N.A. Volsky<sup>2,b</sup>, A.A. Novikov<sup>2,b</sup>

<sup>1</sup> Bauman Moscow State Technical University, 2-aya Baumanskaya 5/1, Moscow, RU-105005, Russia

<sup>2</sup> National University of Science and Technology «MISIS», Leninskiy Pr. 4, Moscow, RU-119049, Russia

In this work the diffusion penetration ability of layer boundaries in multilayer materials was investigated. The boundary diffusivity for Ni layer boundary diffusion into Cu-Nb multilayer system was determined. The difference between grain boundary diffusivity of Ni in Cu and layer boundary diffusivity in researched system was proved to be low.



**Development of a non-aqueous acetonitrile-based electrolyte for double-layer symmetric supercapacitors with low temperature operational limit down to  $-60\text{ }^{\circ}\text{C}$** 

O.V. Zaitseva<sup>1,2</sup>, S.V. Stakhanova<sup>1</sup>, R.R. Galimzyanov<sup>1</sup>, A.T. Kalashnik<sup>1</sup>, M.V. Astakhov<sup>1</sup>

<sup>1</sup>National University of Science and Technology “MISIS”, 119049, Leninskiy prospect 4,  
Moscow, Russia

<sup>2</sup>TEEMP LLC, 127276, Botanicheskaya street 14, Moscow, Russia

Supercapacitors (EDLCs) or electrochemical capacitors are electrochemical devices which store energy within the electrical double-layer formed between electrodes with high surface area (usually based on activated carbons) and an electrolyte solution, leading to higher energy density compared to conventional electric capacitors.

Today an objective is to achieve stable functioning of supercapacitors and batteries at extremely low temperatures primarily for use in avionics and spacecraft, as well as for Extreme North applications. The development of organic electrolytes able to operate efficiently in EDLCs down to  $-70\text{ }^{\circ}\text{C}$  is required. To meet the objective, it is necessary not only to prevent electrolyte freezing at these temperatures, but also to achieve suitable electrical conductivity (no less than  $5\text{-}10\text{ mS/cm}$ ), maintaining relatively low electrolyte viscosity and sufficient concentration of an ionogen in the solution. One way to achieve the goal is to formulate multi-component solvent systems, in which suitable co-solvents with low melting temperatures are mixed with a base solvent that usually have high dielectric constant.

In this study, acetonitrile (AN) was used as a base solvent. Electrolytes based on AN can operate down to  $-40\text{ }^{\circ}\text{C}$ . Ethyl acetate (EA) was chosen as a co-solvent, which has lower melting point compared to AN, as well as low viscosity. The concentration of the co-solvent varied from 15 to 60 vol%. All considered multi-component electrolytes remain in liquid form

down to  $-60\text{ }^{\circ}\text{C}$ ; the lowest melting temperatures (below  $-65\text{ }^{\circ}\text{C}$ ) are achieved with 20-35 vol% of the co-solvent. Moreover, electrolytes with this formulation have the highest electrical conductivity in the whole working temperature range (Fig. 1).

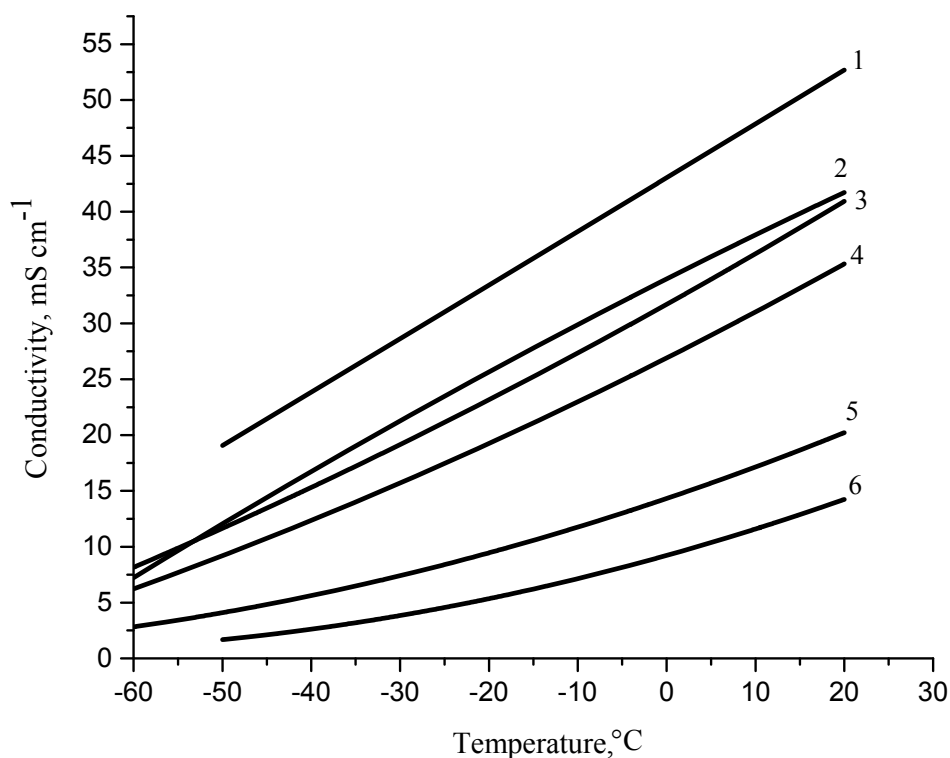


Fig. 1. Electrolyte conductivity vs. temperature for the electrolytes studied: 1M  $\text{Et}_3\text{MeNBF}_4$  in AN (1); 1M  $\text{Et}_3\text{MeNBF}_4$  in mixture AN:EA 85:15 (2); 1M  $\text{Et}_3\text{MeNBF}_4$  in mixture AN:EA 75:25 (3); 1M  $\text{Et}_3\text{MeNBF}_4$  in mixture AN:EA 65:35 (4); 1M  $\text{Et}_3\text{MeNBF}_4$  in mixture AN:EA 50:50 (5); 1M  $\text{Et}_3\text{MeNBF}_4$  in mixture AN:EA 40:80 (6).

Electrochemical characterizations of multi-component electrolytes in EDLCs was investigated using cyclic voltammetry and galvanostatic charge-discharge methods at  $20\text{ }^{\circ}\text{C}$  and  $-50\text{ }^{\circ}\text{C}$ . It was shown that usage of multi-component electrolytes does not decrease specific capacity and performance characteristics of EDLCs and facilitates their stable functioning at temperatures below  $-50\text{ }^{\circ}\text{C}$ .

**Evolution of structure and properties of nanostructured oxide film on the surface of zinc powders during diffusional galvanizing**

D.A. Zakharyevich<sup>1</sup>, R.G. Galin<sup>2</sup>, S.V. Taskaev<sup>1</sup>, Zh.M. Zhumagulova<sup>1</sup>

<sup>1</sup>Chelyabinsk State University, Chelyabinsk, Br. Kashirinykh str. 129, 454001 Russia

<sup>2</sup>LLC „Vika-GAL“, Molodogvardeitsev str. 7, 454001 Russia

Nanostructured zinc oxide attracts huge interest of researchers due to wide range of possible applications, mainly in the field of microelectronics. However, nanostructured zinc oxide is currently used in more traditional and matured application - diffusional galvanizing based on technology by R.G. Galin [1]. The nanostructured oxide layer on the zinc particles' surface plays important role in improving the efficiency of the process. First, it isolates metal cores of the particles thus preventing their sintering and adhesion to the steel surface even at 600°C. Also, this layer contains pores with a diameter of few nanometres, which provide enhanced vapour pressure due to the capillary effect. During the galvanizing process, the powders, being in contact with steel surface at elevated temperature, lose zinc from the metal core and get enriched with oxygen and/or iron, which induce changes in its properties and behaviour and affect the process. Here we present the results of our studies of zinc powders with nanostructured oxide on the particles' surface used in the process of diffusional galvanizing by means of XRD, DSC, TEM and magnetometry. Fresh powders exhibit phase transition at  $T=315^{\circ}\text{C}$ , its thermal effect is too small to be assigned to zinc or oxide and decreasing for powders after galvanizing. It is found that the powders acquire magnetization when iron content is about 2 wt. %, although they contain no magnetic phases detectable by XRD. After magnetic separation, magnetic fraction was separated into fractions by sizes, which were examined separately. It was found that the room-temperature dependence of magnetisation on iron content is non-monotonous. Temperature dependence of magnetisation was obtained with rather surprising result, it is also non-monotonous and exhibit apparent para- to ferromagnetic transition at heating. Possible explanations of the results are discussed in the report.

- [1] R.G. Galin. Modified zinc powder. *Russian patent* 2170643. B22F1/02, C23C10/28. Published 20.07.2001.

**Deformed polycrystalline copper/Cu-Zn-Al<sub>2</sub>O<sub>3</sub> coating interface after cold gas dynamic spray process**

S.N. Zhevnenko<sup>1</sup>, I.S. Gershman<sup>2</sup>

<sup>1</sup>National University of Science and Technology “MISIS”, Leninsky pr. 4, Moscow, 119049, Russia

<sup>2</sup>Joint Stock Company Railway Research Institute 107996, Moscow, 3rd Mytischinskaya str. 10, Russia

Recovering locally worn contact wires for electric railroad transport is a very important problem. Recovery process should not lead to recrystallization of the deformed contact wire. Cold gas dynamic spray technology seems to be suitable as a recovery method for severely deformed copper. During the spray process a carrier gas (normally air) is heated up to 500°C. This technology allows spraying layers with thickness up to few millimeters at a high spray rate.

We analyzed the interface between copper and 30Cu + 40Zn + 30Al<sub>2</sub>O<sub>3</sub> coating after cold gas dynamic spray at gas temperatures 400°C and 500°C. We used EBSD and EDX methods for recrystallization establishment and distribution of coating components. EBSD shows absence of new growing grains. EDX indicates uneven distribution of components of the sprayed coating. Higher temperature leads to oxidation of Zn and decreases the adhesive strength.

This study was carried out with financial support of Russian Science Foundation (Co. 15-19-00217)

**Temperature dependence of allowable angular range for near-special boundaries**

A.A. Zisman<sup>1,2</sup>, V.V. Rybin<sup>1</sup>

<sup>1</sup>St.-Petersburg State Polytechnic University, 29 Politekhnicheskaya str., St.-Petersburg  
195251, Russia

<sup>2</sup>Central Research Institute of Structural Materials „Prometey“, 49 Shpalernaya str., St.-  
Petersburg 191015, Russia

Concept of special boundaries is based on the coincidence site lattice (CSL) specified by  $\Sigma$  parameter that equals unity in a uniform crystal (no boundary) and increases when the coincidence becomes poorer. An enumerable set of CSL, however, covers only an infinitesimal fraction of possible disorientations; hence actual boundaries with special physical properties have near-special rather than special disorientations and involved angular ranges  $2\Delta\theta_B$  around the latter are finite. The widely used Brandon's estimate for  $\Delta\theta_B$  [1] suggests that allowable angular deviations  $\delta < \Delta\theta_B$  are accommodated by grain boundary dislocations (GBD) i.e.  $\delta \approx b_{gb}/h$  where  $h$  and  $b_{gb}$  are their spacing and magnitude of Burgers vector, respectively. This is quite similar to low-angle boundaries made of lattice dislocations where the maximum allowable angle corresponds to *contiguous cores* of constituent defects. At the same time, unlike lattice dislocations on the background of perfect crystal, discrete GBD belong to the DSC lattice (inverse to CSL), which manifests itself only until a certain absolute temperature  $T_\Sigma$  [2,3]. Accordingly, both the GBD and related  $\Delta\theta_B$  are no longer actual above this temperature whereas at  $T < T_\Sigma$  Brandon's criterion wants for a relevant temperature dependence. Even if the latter is insignificant at low  $T$ , the problem remains challenging as a fraction of near-special boundaries found with Brandon's criterion at room temperature depends on their preferential *formation* at notably higher  $T/T_m$  ( $T_m$  is the crystal melting point).

Limitations ( $T < T_{\Sigma}(\Sigma)$  or  $\Sigma < \Sigma_{max}(T)$ ) on physical influence of DSC lattice have been previously evaluated in terms of atom oscillations at the boundary [2,3], Fig.1. In the present paper the same approach is employed in order to follow gradual delocalization of GBD cores with increasing temperature and their eventual merging when the DSC lattice loses influence. Dimensions of GBD core are derived with the Peierls-Nabarro model while allowing for specific stiffness of grain boundary matter and, finally, temperature-dependent angular intervals for near-special boundaries are represented by level lines in  $\Sigma$ - $T/T_m$  map (Fig.2).

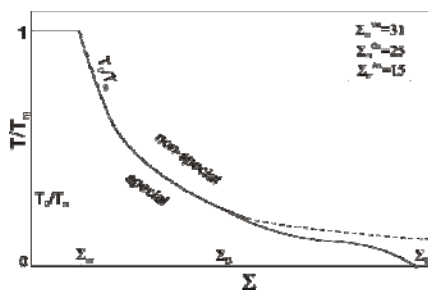


Fig.1.  $\Sigma$ - $T$  domain of *physically* special boundaries [2,3].  $T_m$  and  $T_D$  are the melting point and Debye's temperature, respectively.

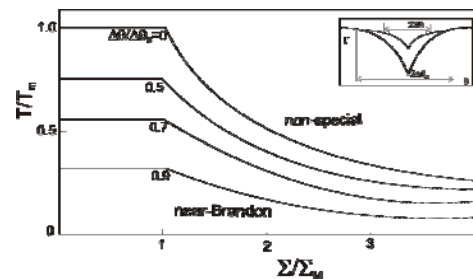


Fig.2. Level lines for normalized angular deviations from a special disorientation, which save special properties of the grain boundary.

- [1] D.G. Brandon. *Acta Metall.* **14** (1966) 1479-1484.
- [2] A.A. Zisman, V.V. Rybin. *Poverkhnost' No.7* (1982) 87-90 (in Russian).
- [3] A.A. Zisman, V.V. Rybin. *Physics of Metals and Metallography* **68** (1989) 264-270 (Eng. Transl. from Rus. *Fizika Metallov i Metallovedenie*).

## **Modeling grains misorientation distribution in polycrystalline materials**

N.Yu. Zolotarevsky<sup>1,2</sup>, E.A. Ushanova<sup>2,3</sup>, V.V. Rybin<sup>1,2</sup>

<sup>1</sup>Institute of Applied Mathematics and Mechanics, Saint-Petersburg Polytechnic University,  
Saint-Petersburg, 195251 Russia

<sup>2</sup>Mechanical Engineering Research Institute of the Russian Academy of Sciences, Nizhnii  
Novgorod, 603024 Russia

<sup>3</sup>Central Research Institute of Structural Materials “Prometey”, Saint-Petersburg , 191015  
Russia

Polycrystalline structure of metals and alloys forms during complex multistage process. This process, in addition to primary crystallization from liquid phase, may include phase transformations and various kinds of deformation and recrystallization, which proceed under subsequent plastic or/and thermal treatments. As it was shown recently [1], the origin and the crystallographic features of the polycrystalline state can be deduced by way of analysis of misorientation distribution function. According to this approach, the misorientation distribution is represented in the form of linear superposition of partial distributions, each of which corresponds to the boundaries of a specific physical nature. Then, using computer modeling the fractions of the boundaries of different nature in the overall structure are determined from the best fit of the computed distribution to the experimental data.

Earlier this approach was used for the analysis of copper, both in recrystallized state and after dynamic deformation realized under condition of explosive welding [1]. Its application allowed, in particular, to determine the contribution of deformation twinning to the structure formation within the narrow interface zone of the explosive joint. In the present work the structure of low-carbon steel obtained after high temperature treatment, recrystallization in austenite state and subsequent phase transformation to polygonal ferrite under cooling was studied. The emphasis is on so called inter-variant boundaries, which misorientation are predetermined by orientation relationship between parent austenite and ferrite, in particular, on their crystallographic characteristics and their contribution to the overall structure of steel.

[1] V. V. Rybina, N. Yu. Zolotarevskii, E. A. Ushanova. *Technical Physics*, 59 (2014) 1819–1832.

ISBN 978-5-93121-396-5

Издательство ООО «ПКЦ Альтекс»

Москва

Печать цифровая. Тир. 250 экз.